Spatio-temporal Urban Climate Variability & UHI Analysis, the case of Addis Ababa City, Ethiopia

PhD Candidate:

Esubalew Nebebe Mekonnen

A Dissertation Submitted to the Office of Graduate Program of the Ethiopian Institute of Architecture, Building Construction and City Development (EiABC), Addis Ababa University

Presented in Fulfillment of the Requirements of Degree of Doctor of Philosophy (Urban and Regional Planning)

Addis Ababa, Ethiopia

July 2024

Spatio-temporal Urban Climate Variability & UHI Analysis, the case of Addis Ababa City, Ethiopia

PhD Candidate:

Esubalew Nebebe Mekonnen

Supervisors:

Dr. Ephrem Gebremariam and Dr. Aramde Fetene

A Dissertation Submitted to the Office of Graduate Program of the Ethiopian Institute of Architecture, Building Construction and City Development (EiABC), Addis Ababa University

Presented in Fulfillment of the Requirements of Degree of Doctor of Philosophy (Urban and Regional Planning)

Addis Ababa, Ethiopia

July 2024

Approval Sheet

Ethiopian Institute of Architecture, Building Construction and City Development (EiABC), Addis Ababa University Office of Graduate Program.

This is to certify that the monograph is prepared by Esubalew Nebebe Mekonnen, titled Spatio-temporal Urban Climate Variability & UHI Analysis, the case of Addis Ababa, Ethiopia. It is submitted in fulfilment of the requirements of the Doctor of Philosophy (Urban and Regional Planning) complies with the regulations of the University and meets the accepted standards with respect to originality and quality.

Approved by examiner board:

Name		Signature	Date
Dr. Ephrem Gebremariam	(Supervisor)	_____	_____
Dr. Aramde Fetene	(Supervisor)	_____	_____
Dr. Hayal Desta	(Internal Examiner)	_____	_____
Dr. Ermias Teferi	(External Examiner)	_____	_____
Dr. Mulugeta Maru	(Chairperson)	_____	_____

Dr. Dagnachew Adugna (Graduate Program Director) _____ _____

Abstract

Climate variability significantly impacts global environmental conditions, with developing countries like Ethiopia experiencing adverse consequences. This study broadly covered the spatio-temporal urban climate variability and UHI analysis of Addis Ababa, Ethiopia. Grid meteorological datasets consisted of monthly precipitation, maximum, and minimum temperature extending from 1981 to 2018, with a spatial resolution of 4x4 km, obtained from the National Meteorology Agency. Auxiliary data was obtained from the Ethiopian Geospatial Institute. Coefficient of variation (CV) and standardized anomaly index (SAI) were used to examine the rate and amplitude of temperature and rainfall dynamics. A geostatistical model, ordinary kriging, was employed to spatially interpolate both rainfall and temperature datasets. Mann-Kendall (MK), Modified Mann-Kendall test (MMK), Sen's Slope (SS) estimator, Principal Component Analysis (PCA), and T-test were employed to determine the significant level, trends, and dimensions at monthly, annual, seasonal, and decadal levels. To scrutinize the rate of surface temperature anomalies caused by land use dynamics, Landsat 5^{TM} (1985), Landsat $8^{OLI/TIRS}$ (2020), and Digital Elevation Model (DEM) were employed. An object-oriented supervised classification with maximum likelihood methods was performed. The Mono-window algorithm, spectral radiance, brightness temperature (BT), and land surface emissivity (LSE) were computed to estimate the land surface temperature (LST). Geospatial technologies, "R" programming, JMP, and origin software were utilized. The findings of the study revealed that the monthly, annual, and seasonal temperatures increased significantly except in the months of January and September. The decadal extreme maximum temperature has exorbitantly risen by 2.7 °C. Moreover, the average decadal maximum and minimum temperatures increased by 1.88 °C and 1.72 °C, respectively. The highest temperature occurred during the spring (*Belg*) season. The PCA analysis results divulge that the first two PCAs account for 90% of the temperature variations. Conversely, the annual, *Kiremt* (main rainy) and *Belg* seasons' rainfall displayed low to moderate variability with CV < 20% and CV < 30%, respectively. The *Bega* season's variability was extreme, with a CV > 70%. In contrast, the decadal rainfall variability was very low (CV<10%). From October to March there was extreme inter-monthly variability rainfall with a CV>100%. The trends of rainfall decreased in all months and seasons, except *Kiremt* and the months of May, June, and September. However, none of the changes were statistically significant (P>0.05). Regarding LST, the built-up area proliferated significantly from 195 km^2 (37.5%) in 1985 to 326.3km^2 (62.8%) in 2020. The average maximum LST increment was detected on built ups, rose by 2.68°C, while bare land grew by 2.64°C. This implied that the land cover dynamics contributed to the increasing trend of the mean LST from 27.2°C in 1985 to 29°C in 2020. Addis Ketema, Arada, Kirkos, and Lideta sub-cities experienced the utmost increase in LST, ranging from 2.79 °C to 4.72 °C. In conclusion, this study offers an indispensable insight into the fluctuation of temperatures, precipitation, and warming tendencies observed in Addis Ababa. The findings underscore the pressing need for the implementation of climate adaptation strategies and policy measures.

Keywords: Addis Ababa; climate variability; Geospatial; spatio-temporal; Mann-Kendall, PCA, Ethiopia

Acknowledgments

First praise to the almighty God for giving me the courage, patience, endurance, and strength to reach this milestone.

First and foremost, my heartfelt gratitude goes to my supervisors, Dr. Ephrem Gebremariam and Dr. Aramde Fetene, for accepting me to work under their supervision, for their unceasing support, spurring, mentorship and considerateness during the last five years of study period. Without their proper follow-up, guidance, and supervision this work would not have reached this level. I would also like to express my appreciation to the Ethiopian Metrological Agency for providing pertinent climate data and the Ethiopian Space Science and Geospatial Institute for administrative data.

Moreover, I am also greatly indebted to my former instructors Professor Abebaw Yirga and Dr. Shimeles Damene for their relentless encouragement and unwavering support. I would also like to extend my appreciation to my colleagues and friends: Dr. Eden Atsebeha, Dr. Liku Workalemahu, Mr. Kibrom Hailu, Melat Solomon, Mr. Hamde Ibrahim, Mr. Berhanu Tsegaye, Mr. Getinet Besha, Brook Tafesse, and Esayas Yirga for their friendship and good words of encouragement during my PhD journey.

Table of Contents

List of Figures

List of Tables

Acronyms and Abbreviations

AAO: Addis Ababa Observatory

AEZ: Agroecological zone

BT: Brightness temperature

CC: Climate Change

CRGE: Climate-Resilient Green Economy

CV: Coefficient of Variation

DEM: Digital Elevation Model

GHG: greenhouse gas emission

ETM: Enhanced Thematic Mapper

GIS: Geographic Information System

FAO: Food and Agriculture Organization

IPCC: Intergovernmental Panel on Climate Change

LST: land surface temperature

LULCC: Land Use Land Cover Change

MLCM: Maximum Likelihood Classifier

MK: Mann-Kendall

MMK: Modified Mann-Kendall

MoH: Ministry of Health

NMA: National Meteorological Agency

NAPA: National Adaptation Program of Action

NDVI: Normalized Difference Vegetation Index

NDBI: Normalized Difference Built-up Index

ND-GAIN: Notre Dame Global Adaptation Initiative

NOAA: National Oceanic and Atmospheric Administration

PCA: Principal Component Analysis

RS: Remote Sensing

SAI: Standardized anomaly index

STA: Standardized temperature anomaly

SDGs: Sustainable development goals

SRTM: Shuttle Radar Topography Mission

TM: thematic mapper

TIR: Thermal infrared

UN: United Nations

USAID: United States Agency for International Development

UNDP: United Nations Development Program

USGS: United States Geological Survey

USGCRP: US Global Change Research Program

UHI: Urban Heat Island

UNFCCC: United Nations Framework Conventions on climate change

WMO: World Meteorological Organization

CHAPTER ONE: INTRODUCTION

1.1. Background

Climate change is defined as an alteration in the conditions of climate variables. It can be detected using statistical tests such as modifications to the mean and variability of its characteristics that endure for a considerable amount of time, usually decades or more (IPCC, 2001; Hegerl et al., 2007). It alters the patterns of precipitation and temperature and occurs as a result of internal natural processes or external forces like variations in solar cycle, volcanic eruptions, and human-caused modifications to the atmosphere's composition (IPCC,2014c). Climate change and variability are global threats to humanity (Adger et al., 2003; IPCC, 2013b; Belay, 2016). It is among the various development challenges of 21st century (Brien & Leichenko, 2000; Bewket et al., 2015). A recent report estimated that approximately 3.3 to 3.6 billion people across the world live in contexts that are highly vulnerable to extreme climate conditions (IPCC, 2023a).

The extent of climate change adverse effects varies greatly across regions, nations, and socioeconomic groups (IPCC, 2007a). However, the impacts become more apparent and pressing in developing countries (Akponikpe et al., 2010; Tessema et al., 2013). Particularly, countries in tropical and sub-tropical regions are disproportionately affected (Stern, 2007; Ayalew et al., 2012). Scientific evidence indicates that humans are responsible for warming the climate (Forster et al., 2007; IPCC, 2021; IPCC, 2023). In this regard, IPCC (2018) noted that anthropogenic factors have caused a 1.0 °C increase in global temperature above pre-industrial levels, in a range from 0.8 °C to 1.2 °C. Global warming is likely to reach 1.5 °C between 2030 and 2052, if it continues at the current rate. Under extreme emission scenarios of shared socioeconomic pathways (SSP5-8.5) the global temperature estimated to increase in the range from 1.3 to 1.9 °C in the near term, ranging from 2021 to 2040 and in the long term, 2041 to 2060, with an increase of 1.9 to 3 °C (IPCC, 2021c). Factors such as unsustainable energy usage, land use change, changes in people's ways of living, changes in patterns of consumption and production, and increase in greenhouse gas emissions for a century have substantially contributed to human-induced climate change (IPCC, 2013c; IPCC, 2022).

Africa is highly susceptible to climate change induced impacts (UNEP, 2013; IPCC, 2022). Sub-Saharan Africa is one of the global hotspots of climate change, and East Africa is a region least covered by climate change studies (Pauleit et al., 2015; Adeniyi, 2016). Nonetheless, the continent's contribution to global greenhouse gas emissions (GHG) is much smaller (UNEP, 2013). Burundi, Kenya, Sudan, and Tanzania are seriously afflicted by the adverse impacts of climate change (Mwangi & Mutua, 2015; Hassaan et al., 2017). Similarly, countries such as Kenya, Ethiopia, and Somalia are highly vulnerable to climate related environmental shocks and stresses caused by natural disasters and anthropogenic factors (Wilby & Dawson, 2013).

Climate change is manifested by changes in frequency, intensity, duration, and timing of extreme weather events (IPCC, 2012a). It also resulted in urban flooding, water scarcity, diminishing agricultural productivity, and loss of biotic resources (United Nations, 2009). Climate variability and change is expected to have a significant ripple effects on the world's ecosystems and communities (Adger et al., 2003; IPCC, 2007a). These challenges include land cover change, biodiversity loss, ecosystem disturbance, and exacerbated climate change (Defries et al., 2010; Seto et al., 2012; The World Bank Group, 2015).

Urbanization is a global phenomenon. In 1950 the global population living in urban areas constituted 30%, in 2018, it grew to 55%, and in 2050, it is estimated to reach 68% (UN-Habitat, 2022). Unplanned urban development due to rapid population growth amalgamated with accelerated urbanization resulted in expansion of cities towards the outer periphery areas, subsequently resulted in environmental challenges on multiple frontiers (Griggs et al., 2013; Wigginton et al., 2016). Africa is experiencing rapid population growth, especially in the east and west (UNECA, 2022). Over the next couple of decades, 2.5 billion people will live in the cities of Africa and Asia (United Nations, 2014). By 2030, the fastest rates of population growth ($\geq 4\%$) will be witnessed in sub-Saharan Africa (World Bank Group, 2017).

Climate change would affect all sectors (IPCC, 2001b, 2023a). Extreme weather events such as heavy rain, flooding, and cyclonic storms significantly affect the densely populated city centers compared to less populous areas (Simone et al., 2011). Particularly, poor people are exposed to the consequences of climate change due to their living conditions (Huq et al., 2007). It would pose

a major challenge to cities in developing countries, providing even the most basic services to their inhabitants would be unimaginable (UN-Habitat, 2011). The negative repercussions of climate change would be very severe for the urban poor (Cochrane & Costolansk, 2013). Added stress through increasing heat waves is threatening the health of vulnerable community groups such as poor residents, the elderly, women, the infirm, communities living on the margins of society, and very young children (World Bank, 2011; Rosenzweig et al., 2011).

Ethiopia is frequently mentioned among the countries highly exposed to the adverse effects of climate change and variability (Thornton et al., 2006; Conway & Schipper, 2011). It is also a major development challenge for the country (World Bank, 2010). This is because the country is primarily reliant on subsistence agriculture and natural resources, limited use of mechanized irrigation, and low adaptive capacity (Collier et al., 2008; Conway, 2009; Matewos, 2019; World Bank, 2010; 2021). Local studies ascertained the vulnerability of the country to the impacts of climate change and variability (FDRE-NAPA, 2007).

Cities in developing countries are on the front lines of climate change impacts. The impacts include increase in extreme weather events, flash flooding, increase air temperature, water scarcity, and public health concerns (IPCC, 2001b). Climate variability in cities could result in economic losses, service interruptions, and a negative impact on well-being of the people (IPCC, 2023a). In the capital city of Addis Ababa, increased heatwaves and high temperatures due to climate change is observed. Recent studies noted that there has been an increase of rainfall intensity in the city that led to flash flooding (Addis et al., 2023).

Several studies were carried out on climate variability and change in different parts of the country with an emphasis on temperature and rainfall trend analysis, and adaptations option, among others Bewket & Conway (2007b); Conway & Schipper (2011) & Alemayehu et al. (2020a) can be mentioned. With respect to the study area context, most of the previous studies focus on statistically downscaling of climate variables using global circulation model and present and projected climate change in Addis Ababa city at different time scale conducted by (Feyissa et al. 2018a, 2018b; Arsiso et al., 2018). Additionally, climate change vulnerability assessment of Addis Ababa sub-cities by (Feyissa et al., 2018b). Moreover, temperature trend analysis of two

meteorological stations that is Bole and Entoto stations (Alemu & Dioha, 2020a). However, limited research is available with respect to the study area context particularly with the focus of climate variability and trend analysis using time series grid meteorological data and land use land cover change (LULCC) impacts on urban heat island effect in both spatial and temporal context covering the whole Addis Ababa city. Hence, this study broadly investigated the spatial-temporal urban climate variability and urban heat island effect analysis of Addis Ababa city, Ethiopia.

1.2. Statement of the Problem

Climate change and variability are worldwide phenomena (IPCC, 2014c). Its impacts varied and complex across regions (Short & Farmer, 2021). It is one of the most contentious and undisputed environmental challenges Addis et al. (2023) evolved into a life threatening global environmental concern (IPCC, 2021b; Tyfield & Yuille, 2022). It continue to be pervasive, rapid, and intensifying across the globe (IPCC, 2023a). Extreme events due to variation in climate and weather have emerged as a key natural hazard of the 21st century (IPCC, 2013a; Dastagir, 2015). Its impact is diverse and globally witnessed (IPCC, 2022a). Watson et al. (2001) and Romero (2008) reported that one of the biggest threats to civilization that is rapidly becoming apparent is climate change.

IPCC (2014a) in its synthesis report indicated that since the 1950s warming of the climate system has been unequivocal and many observed changes have occurred. Over the last century, the average global temperature has increased by 0.74 °C and by the end of this century, it will increase from 1.1 to 5.8° C and the rainfall patterns will also change (IPCC, 2012b). Climate related extreme events are ramped-up in frequency and amplitude as a result of anthropogenic activities, and the consequence is increasing as urbanization spreads, urban centers, and infrastructure expands (Mcphillips et al., 2018). Climate change manifests through rising temperatures, increasingly erratic precipitation, public health concerns, severe floods, disruptions of agricultural production, and droughts (IPCC, 2014c; Adenle et al., 2017; 2021b).

Africa is considered to be a region highly prone to the impacts of climate change (Porter et al., 2014; IPCC, 2014g; Pauleit et al., 2015; Niang et al., 2017). Its economy reliant on rain-fed agriculture and among the region's most sensitive to climate variability and change (IPCC, 2014b). Cook et al. (2013) in their review, indicated that 97% of the published literature on climate supports the position that climate change is happening and largely human caused. In the same vein, IPCC (2023a) noted that human activities through the emission of greenhouse gases caused global warming and affected every corner of the globe.

World cities house more than half of the world's population and industries (United Nation, 2014). Developing countries comprised most of the world's urban population (Satterthwaite, 2008b). Reports exhibited that cities are highly prone to extreme weather events (Mcphillips et al., 2018;

Kron et al., 2019; Short & Farmer, 2021). The World Bank (2009) underscores that climate change and variability are key development issues in sub-Saharan African countries. As a result, Africa's urban areas and cities face twin risks from climate variability and change, which are inextricably linked to urbanization (World Bank, 2009; 2011). Climate change is one of the future challenges of cities in Africa (Mosha, 2011). There are few studies available regarding the past, present, and future patterns of climate extremes in the Great Horn of Africa (Aming et al., 2014).

Ethiopia is vulnerable to climate variability impacts because large segments of its population are poor and dependent on rain-fed agriculture (NAPA, 2007; Oxfam, 2017). The growth and transformation of the country are lagging behind because of climate variability, uncertainty, and change (Dinku et al., 2011). Nearly 90% of Ethiopia is highly subjected to severe climate stress, and almost all of the nation's agriculture is dependent on precipitation (Pacillo et al., 2021). Asaminew (2013) explained that Ethiopia's average annual temperature has been rising by 0.37° C every ten years for the past forty years.

Urbanization resulted in the conversion of natural land cover surfaces into built-ups, and this subsequently resulted in an exponential increase in the built environment, which ultimately led to changes in the underlying urban climate (Mills et al., 2010; Feyisa et al., 2014). With the effect of global warming, cities become warmer, while urbanization aggravates the process through urban heat island generation (Kumar, 2021). Urbanization and climate change have negatively impacted the quality of life, economies, and social stability of people (UN-Habitat, 2011a). In most developing countries, urbanization has brought a general environmental transformation, from clearing of vegetation to reduction in wild life habitat and open spaces leading to rapid development of infrastructure, resulting in a warmer of urban environment (Rushayati et al., 2016; Sari, 2021).

Cities suffer from urban heat island (UHI) effect which is manifested as temperature differ between urban and rural areas (Oke, 1982). UHI is typically characterized by increase in temperature at surface, sub-surface, or in the atmosphere as opposed to its rural counterparts (Manatsa et al., 2008; Kotharkar et al., 2020). Rising air temperature and the UHI phenomenon intensify urban environmental and human health concerns while adding burdens to urban systems as a whole

(Kotharkar et al., 2020). Surface characteristics, building envelope, thermal, and radiative parameters, and anthropogenic variables, all have an impact on the urban microclimate (Kotharkar et al., 2019; Short & Farmer, 2021). UHI is mainly controlled by urban geometry like building orientation, which largely influence air ventilation, solar radiation access, and cooling potential (Unger, 2004; Ali-Toudert & Mayer, 2007). Similarly, Akbari et al. (2016) indicated urban characteristics largely determine the intensity of UHI in cities, such as synoptic conditions, local meteorological features, the type of urban materials and the presence (or lack) green areas. Cities are highly impacted by climate change, such as heat waves, flooding, heavy rains, and storms (Adenle et al., 2017; Wolfram et al., 2019).

Mounting of temperature in urban areas created inconvenient living conditions (Rushayati et al., 2016; Cardoso et al., 2017; Amorim, 2020). The existence of harsh weather conditions would have an impact on city livability, particularly for the poor and marginalized (Short & Farmer, 2021). One of the critical ecological and societal challenges of urbanization among the Africa's cities is the effect caused by urban heat island (Simwanda et al., 2019). Cities in the tropics are characterized by recurrent temperature extremes caused by climate change and the UHI effects (Patz et al., 2000). Data on climate change in cities in sub-Saharan Africa is inadequate (Short & Farmer, 2021). While, its effects are intensifying, adaptation measures are too sluggish, which is referred to as "slow city-quick climate change" (Short & Farmer, 2021).

The challenges induced by climate change and variability is more pronounced in cities (Addis et al., 2023). It adversely affects all economic sectors IPCC (2001b; 2023a), posing unique challenges to the environment (Sibiya et al., 2022). Previous studies reported that climate change has had a significant impact on Addis Ababa city, including flash floods, heavy rain, drought, heat waves, and landslides (Jalayer et al., 2013; Worku, 2017; Arsiso et al., 2017a; Feyissa et al., 2018a; Alemu & Dioha, 2020a; Jemberie & Melesse, 2021). Consistently, climate change-related impacts including drought, severe rain, and high temperature, have social and economic consequences for the residents of Addis Ababa city (Rolkier & Worku, 2015).

High rates of urbanization, rapid population growth, expansion of built-up area, less green area coverage, and accelerated land use changes have been the major factors that aggravate climate

change in the city (Moges et al., 2013; Worku, 2017; Arsiso et al., 2017a; Arsiso et., 2018). Studies reported that due to climate change impacts, Addis Ababa is highly vulnerable to flooding. This is because of rapid urban sprawl in the city and poor urban flooding management (Jemberie & Melesse, 2021). The effect of climate change on the natural environment and urban system of Addis Ababa could be among the most serious and represents a good study area to explore (Worku, 2017).

Numerous studies have been carried out pertaining to climate change and variability with respect to Addis Ababa city. For example, a study by Cochrane & Costolanski (2013) emphasized on climate change vulnerability and adaptability the case of Addis Ababa. The study has shown that positive adaptation measures have been observed in some selected areas of the city, however, maladaptive measures have increased vulnerability. Similarly, Moges et al. (2013) examined the historical changes in rainfall extremes of Addis Ababa Observatory (AAO) and Addis Ababa Bole (AAB) stations. The result revealed that the AAO signified an increasing trend in its extreme rainfall events. Another study on flood risk and vulnerability of Addis Ababa due to climate change and urbanization was done by suing SWAT model (Birhanu et al., 2016). The result found that there was a 10% and 25% increase in peak flow due to climate change and urbanization, respectively.

Moreover, climate change and urbanization have impacts on surface water supply and demand in Addis Ababa (Arsiso et al., 2017b). The finding indicated that the projected population of Addis Ababa city will be about 7 million by the year 2039, with a growth rate of 3.3%. In addition, the results of climate projections for surface water supply under RCP 4.5 and RCP 8.5 scenarios showed that between 2023 and 2039 there will be a decrease in the reservoirs at Legedadi/Dire and Gefersa. Moreover, intermingling climate change adaptation strategies with urban planning and landscape design of Addis Ababa City was conducted by (Worku, 2017). The result revealed that integrated climate change adaptation options in urban planning and landscape design at the city, sub city, neighborhood, project and building level will enhance the sustainability of the city. Furthermore, Alemu & Dioha (2020) conducted trend analysis of temperature data in Addis Ababa using Bole and Entoto stations. The study found that there was a tendency for temperature increment at Bole station as compared with Entoto.

On top of that, Feyissa et al. (2018), climate change vulnerability assessment of Addis Ababa sub-cities using IPCC vulnerability assessment index. The results indicated that the ten sub-cities were found at different levels of vulnerability. The exposure and sensitivity were highest for Addis Ketema, Arada, and Lideta. While the adaptation and mitigation were the highest for Bole, Gulele, and Arada sub-cities. The same authors have done downscaling of future temperature and precipitation extremes in Addis Ababa under climate change scenario. The results unveiled that the maximum temperature increases were in the range of 0.9 °C (RCP4.5) in 2020 to 2.1 °C (CGCM3A2) in 2080 at Addis Ababa Observatory. The minimum temperature is projected to increase by 0.3 °C (RCP4.5) in 2020 and 1.0 °C in 2080 (CGCM3A1B).

Generally, in Ethiopia, both the rural and urban areas are seriously afflicted by the adverse effects of climate variability and change. The intensity of the problem is more pronounced in rural settings of the country. However, recently, cities have been facing similar encounters. Despite its importance, climate change and variability knock-on effects in Addis Ababa are still not adequately researched. In this regard, previous studies conducted by Feyissa et al. (2018a); Worku, (2017a) underscore that climate change and variability studies with respect to urban centers are not extensively available. Many of the studies undertaken mainly focused on climate change and variability with respect to hydrology aspects, flood risk management, adaptation strategies, vulnerability issue, and downscaling of future temperatures and rainfall.

Most of the previous research focused on comparison using meteorological station data between Addis Ababa Observatory and Bole station or Entoto (Moges et al., 2014; Birhanu et al., 2016; Feyissa et al., 2018a; Alemu & Dioha, 2020b). To the best of the researcher's knowledge, there are inadequate studies that are directly related to this study with respect to Addis Ababa, using time series grid data over the past 38 years (1981-2018). In addition, this study is a comprehensive work that addresses the issue of climate change and variability at monthly, annual, seasonal, and decadal time scales, spatially covering the whole Addis Ababa city. Therefore, the research is mainly intended to identify the discrepancy in relation with prior research and display the magnitude of climate change trends and associated environmental impacts on urban systems. The paper would contribute a valuable input in filling the theoretical and practical gaps in the literature on climate studies, trend analysis, and provide a new perspective by intermingling machine

learning with geospatial technologies and urban scenarios. Hence, this study emphasized analyzing the spatial-temporal urban climate variability and change in Addis Ababa over the last approximately four decades (1981-2018).

1.3. Objectives of the study

1.3.1. General objective

The main objective of the study is to analyze the spatial-temporal urban climate variability dynamics and trends, and land use land cover change impacts on city's urban heat island effect across space and time in Addis Ababa city, Ethiopia.

1.3.2. Specific objectives

- To analyze the propensity of rainfall pattern and degree of change over the last 38 years (1981-2018) in both spatial and temporal aspects;
- To examine the extent and magnitude of temperature anomalies, and monotonic nature of change across the observation period;
- To investigate the rapidly growing influence of land use land cover change on the city's urban heat island effect;

1.4. Research questions

- What were the extent and magnitude of change in precipitation in the city over the last 38 years (1981-2018) in both spatial and temporal scale across different seasons and identify the seasons where the rate of change was significant?
- What were the rate and degree of change in maximum and minimum temperature in Addis Ababa city ranging from 1981 to 2018? What was the monotonic trend of the change?
- What changes have occurred in LST in Addis Ababa due to LULCC over the study period between 1985 and 2020?

1.5. Significance of the study

The study's goal was to investigate Addis Ababa's climate variability and change both in space and time, between 1981 and 2018. It is known that Ethiopia launched the Climate Resilient Green Economy (CRGE) strategy, aims to safeguard the nation against the negative ramifications of climate change and develop a green economy strategy that reaches middle-income status by 2025. In this perspective, this study would contribute valuable input towards the realization of this

ambitious goal. In addition, the research is a very comprehensive piece of research that has clearly shown climate variability tendencies and trends over the past 38 years which would be useful for policymakers and decision-makers to take the necessary proactive measures and pursue more sustainable and climate resilient development paths.

Moreover, the findings of the study would be useful for policymakers, researchers, and educators by providing a body of knowledge in the area of concern and updated information on the city's climate dynamics. This would subsequently contribute to the efforts of intervening and mitigating the negative repercussions of climate change and variability on the residents of Addis Ababa city. On top of that, understanding the climate patterns is crucial for effective urban planning, urban agriculture, and water resource management in the city. Knowledge of the spatial and temporal characteristics of rainfall and temperature over the past approximately four decades would help the city administration, planners, researchers, and stakeholders to have accurate information on the city's climate dynamics.

The study is very detailed work that critically addressed temperature, rainfall variability, and UHI analysis. Hence, knowing the dynamic nature of rainfall and temperature, across space and time, would be useful to identify the perspectives, gaps of different actors, and responsible stakeholders involved in climate change-action responses, and crucial for an effective implementation of adaptation mechanisms, designing tailored policies, building climate resilience strategies, and planning prior preventive mechanisms.

1.6. Scope of the research

The primary goal of the research was to investigate Addis Ababa's spatio-temporal climate variability analysis and the magnitude of change both in space and time in the period 1981 - 2018. The study's geographic scope is delimited to Ethiopia's capital city of Addis Ababa, Ethiopia. Administratively, it covered all 11 sub-cities of the city. The study mainly addressed questions such as what the climatic conditions were in Addis Ababa during the past approximately four decades (1981-2018). What was the rate of change in precipitation, maximum, and minimum temperature, and were there any noticeable upward or downward trends. The research analyzed the monotonic change in precipitation and temperature (Tmax and Tmin) on monthly, annual,

seasonal, and decadal time scales. In addition, the study also encompasses the magnitude of change in urban heat intensity across time and space and its interplay with land use land cover dynamics in Addis Ababa sub-cities.

1.7. Limitation of the study

The study was intended to analyze climate variability and change in Addis Ababa with the use of time series meteorological data with a time span of sixty years (1960-2020). However, the meteorological agency did not have complete data within the required time frame. Therefore, the researcher opted to use the available climate data that extends from 1981-2018. But this did not have an impact on this research. The other challenge was related to access to licensed software like ArcGIS Pro. It would have been better if the University offered licensed software for selected PhD students. Particularly, for those students largely depends on the use of Geospatial technologies.

1.8. Structure of the dissertation

This dissertation is compartmentalized into five chapters. Chapter one consisted of background, statement of the problem, general and specific objectives, detailed research questions, significance of the research, scope of the study, limitations, and structure of the dissertation. Chapter two covered: different related literature pertaining to the concept of climate change and variability, drivers of climate change, land use land cover change implications on climate change and UHI, urban heat island effects in cities, theories on climate change, climate change and variability resulting emission of CO2 and published articles in the area of investigation were extensively reviewed and presented as empirical studies. Topics related to each objective were reviewed in detail. Chapter three includes: a description of the study area, data sources, and methodologies employed to achieve the respective specific research objectives. Chapter four largely addresses results and discussions. The results of all the objectives were presented in detail. Finally, chapter five includes synthesis, conclusion, policy recommendations, and future research directions.

CHAPTER TWO: LITERATURE REVIEW

2.1. Concept of climate change and variability

Weather is the changing state of the atmosphere characterized by temperature, wind, precipitation, clouds, and other weather-related factors. While climate refers to the average weather conditions in terms of the mean and variability over a certain time span in a certain geographic area (IPCC, 2001a; Skinner & Murck, 2011). Climate is defined as average weather or more rigorously as the statistical description in terms of the mean and variability over several decades (WMO, 2005; IPCC, 2007b, 2021a; Goosse et al., 2008; Kedir et al., 2013;). Climate change refers to a statistically significant variation in either the mean state of the climate or in its variability, persisting for an extended period (typically decades or longer) National Oceanic and Atmospheric Administration [NOAA], 2018). Climate change is when these averaged conditions start to change and its causes can be either natural or human activities (AMCEN, 2011; IPCC, 2002). It is related to the changes in rainfall patterns and variability, increased extreme weather events, and rising temperatures (Asfaw et al., 2018a; IPCC, 2021a). Variations in climate depend on factors such as latitude, distance from the sea, vegetation coverage, nature of topography, and other geographical factors (IPCC, 2001a).

The concept of CC has emerged in the first few decades of the twenty-first century as a means of presenting the complexity, interdependencies, and difficulties of human existence through new institutions, vocabularies, and imaginaries (Hulme, 2017). CC is the state of the climate that can be identified using statistical tests by changing the mean and/or the variability of its properties that persists for decades (Hegerl et al., 2007; Goosse et al., 2008; IPCC, 2012, 2014b). ADE (2010) conceived that climate change is one of the most challenging threats to sustainable development in Africa. Although its contribution to global greenhouse gas emissions [GHGs] is insignificant, less than 4%.

Climate variability refers to the variations in the mean state and other statistical parameters of the climate on both temporal and spatial scales (IPCC, 2014c). Climate variability can be thought of as the way climatic variables (temperature and precipitation) differ from some average state, either above or below the average value (IPCC, 2007; Mukheibir & Ziervogel, 2007). Climatic variability

refers to the types of changes in temperature, rainfall, and the occurrence of extreme events that impact various sectors (UNFCCC, 2007). The impacts of climate change also include increased water scarcity as a result of persistent drought (Kupika et al., 2018). Precipitation and temperature are the two fundamental factors in climate sciences and hydrology which determine the extent and amount of climate change and variability (IPCC, 2007a). The global climate is changing at an unprecedented rate, having a negative impact on people's welfare everywhere on earth. The situation is especially acute in developing nations, where a significant section of the population is largely dependent on agriculture due to the negative effects of climate change on those countries' livelihoods (Tessema et al., 2013).

The climate of Africa is among the most variable in the world (Pauleit et al., 2015). Regionally, East African countries like Burundi, Kenya, Sudan, and Tanzania are badly hit by the impacts of climate change. Ethiopia is often cited as one of the examples of countries highly vulnerable to the impacts of climate change (Conway, 2009; Conway & Schipper, 2011). Under all assessed emission scenarios, the IPCC (2014b) predicts a rise in surface temperature over the twenty first century. The global average temperature expected to rise by 0.15 to 0.3 °C per decade (IPCC, 2007a).

2.2. Climate change and variability impact in urban areas

Health and biodiversity are among the many aspects of the urban environment that could be impacted by climate change (Reacher et al., 2004). More than half of the world's population lives in urban areas, which are also the epicenter of the climate change crisis. Cities are particularly vulnerable to the effects of climate change in developing countries. These impacts include rising air temperatures, an increase in extreme weather events and flooding and public health concerns. The economy and human well-being are both impacted by climate change, which puts urban residents' possessions and means of subsistence at risk. The impoverished, elderly, women, children, and the marginalized communities are the most susceptible to these effects (World Bank, 2010; Rosenzweig et al., 2011a; Short & Farmer, 2021). With increased urbanization, it will be more crucial than ever to comprehend how climate change is affecting metropolitan areas. There is emerging evidence that urban areas, with their expanding populations, face challenges because

of climate change. Climate change could make it more difficult for cities to offer even the most basic services to their residents (UN-Habitat, 2011).

The negative effects of climate change on the urban poor will have significant ripple effects in the national and global spheres (Cochrane & Costolansk, 2013). Urban centers that will be more at risk are areas where extreme weather conditions such as heavy rain, storms, droughts, heat-waves etc. are widespread (Romero, 2011). The rate of urbanization in Sub-Saharan Africa is increasing (FAO, 2011). Twenty-eight out of the world's 34 megacities are located in developing countries (AACPPO, 2017). Addis Ababa counts for 25% of the country's urban population and it is one of the fastest growing cities in Africa (World Bank Group, 2015). Cities in developing countries such as Ethiopia are highly susceptible to extreme climate change (Hallegatte et al., 2011). Urban poor's' are more vulnerable to climate shocks (Parikh et al., 2014; Stein & Moser, 2014).

2.3. Drivers of climate variability and change

Climate change is triggered by both natural and man-made activities and processes that influence the Earth's energy budget (IPCC, 2013b). Anthropogenic activity and, to a lesser extent, those of natural origin are drivers of climate change (Krissansen-Totton & Davies, 2013). In general, climate change drivers directly or indirectly contribute to GHG emissions (Blanco et al, 2014). Scholars make a distinction between ultimate or underlying factors and proximate drivers. Activities that are closely linked to the emission of greenhouse gases are known as proximate drivers and the things that drive those proximate drivers are known as underlying or ultimate drivers (Blanco et al, 2014). The monsoons and tropical conventions are two local processes that control the seasonal and regional patterns of rainfall and temperature (Conway, 2009). Greenhouse gas emissions are regarded as the principal causes of climate change (Rogelj & Schleussner, 2019).

Scientific evidence shows that the use of fossil fuels is the main source of global CO_2 emissions (Rehman et al., 2021). The increase in energy demand in urban areas has an impact on resource structure which results in environmental degradation (Nguyen et al., 2022). Studies have shown that carbon dioxide emissions pose a serious threat to the environment (Adedoyin et al., 2020). A rising ratio of CO_2 emissions leads to a threat to environmental quality and hence to climate change (Nguyen et al., 2022).

Climate change is largely attributed directly or indirectly to human activities (IPCC, 2007; Clark et al., 2016). Human activities continue to significantly affect Earth's climate through an increase in greenhouse gases, small airborne particles, and the reflectivity of the earth surface (Taylor et al., 2020). ADF-VII (2010) noted that numerous countries in Africa are situated in regions with warm, mostly dry climate. The continent has extensive marginal areas with poor soils and inconsistent rainfall across the continent. Second, most African economies dependent on climate sensitive sectors. Thirdly, because of widespread poverty, weak social and economic infrastructures, conflicts, a lack of institutional and human capacity, and insufficient financial and technological resources, the continent is ill-equipped to adapt to the direct and indirect effects of climate change. Due to its geographic location, topography, and limited capacity to adapt, the country is highly vulnerable to the negative repercussions of climate change (Bewket & Conway, 2007b; Gebreegziabher et al., 2011; Mengistu et al., 2014).

Fahey et al. (2017) found three important results of physical drivers of climate change. These are: caused by human activities. These factors, known as radioactive forcing's, include changes in greenhouse gases, small airborne particles (aerosols), and the reflectivity of the Earth's surface. Second, aerosols caused by human activity play a profound and complex role in the climate system through radiative effects in the atmosphere and on snow and ice surfaces and through effects on cloud formation and properties. Third, the interconnected Earth–atmosphere–ocean system includes a number of positive and negative feedback processes that can either strengthen (positive feedback) or weaken (negative feedback) the system's responses to human and natural influences. Urbanization and pollution are examples of non-climate drivers that have the potential to directly or indirectly affect systems by affecting climate variables like albedo and soil moisture regimes. Land-use and land-cover changes are examples of socioeconomic processes that impact multiple systems (IPCC, 2007a).

2.4. Theories on climate change and variability

There are around ten theories that contend with climate change. These are: Anthropogenic Global Warming (AGW), Clouds Albedo and Cosmic Rays, Human Forcing's, Greenhouse Effects, Ocean outgassing of CO_2, Ocean Currents, Planetary Motion, Volcanic activity, Biological and Chemical Processes and Solar Variability (Bast, 2010b; Sidiropoulos, 2023). Of the various

theories, anthropogenic global warming, greenhouse effects and human forcing are very much related to this study. The theory of anthropogenic global warming depends on greenhouse emissions and noted that during the industrial revolution period due to human activities greenhouse gases were added to the atmosphere through burning of fossil fuels. As a result, the CO_2 concentration in the atmosphere increased which is responsible for the observed global warming.

In addition, the theory argues that man-made CO_2 is responsible for extreme weather, flooding, global warming, droughts etc. AGW pointed out that human emissions of greenhouse gases, predominantly carbon dioxide (CO_2), methane (CH_4), and nitrous oxide (N_2O), are the major factors causing a catastrophic rise in global temperatures. This theory claims that humans are responsible for the adverse effects global climate change (Bast, 2010). Similarly, human activities, such as burning of fossil fuels and deforestation have altered the global climate resulting in increased temperature and alter the amount, intensity, distribution of precipitation, and sea level rising (Hadgu et al., 2015). In line with this, scientific evidence indicates that anthropogenic factors are the major contributors to the prevailing global climate change (Forster et al, 2007; Conway & Schipper, 2011). The intergovernmental panel on climate change (IPCC) underscore that how human induced climate change has already caused widespread harm to societies all around the world (IPCC, 2022b).

The other theory is the theory of human forcing, also linked with this study. According to this theory, the human influence on climate is not caused by greenhouse gas emission. Rather activities such as clearing of forests, irrigating deserts, and building cities. It is deforestation that deters plants from sequestrating CO_2. in cities such as concrete, asphalt, buildings and roads that largely absorb the incoming solar radiation and re-emit thermal energy. Consequently, this would result in rise in temperature in cities (Sidiropoulos, 2023).

Contrary to climate change theories, conspiracy theories that cast doubt on the existence, causes, and consequences of climate change continue to abound (Biddlestone et al., 2022). These conspiracy theories assume that climate change is a hoax and accusations of systematic scientific bias and fraud. They believe that global warming was invented by global elites as part of a sinister plot to create a New World Order (Lillo & Ferguson, 2018; Linden et al., 2021).

2.5. The climate of Ethiopia

Ethiopia is a country of heterogenous topography with a diverse climate (Gleixner et al., 2022). Ethiopia's climate is mostly determined by the seasonal movement of the Intertropical Convergence Zone (ITCZ), which is influenced by the complex topography, the sun's location in relation to the earth, and the atmospheric circulation (Beltrando & Camberlin, 1993; Adaptation Partnership, 2012). Ethiopia has a varied climate, with the lowlands experiencing semiarid desert conditions and the southwest experiencing humid and warm conditions. The distribution of mean annual rainfall reaches its maximum of greater than 2000 mm across the highlands of the southwest and its minimum is less than 300 mm over the lowlands of the Southeast parts of the country. In the highlands, the mean annual temperature is less than 15 °C, whereas in the lowlands, is more than 25 °C. Concerning rainfall distribution, there are three main seasons in Ethiopia: *Bega*, which lasts from October to February and is dry; *Belg*, which lasts from March to May and is a short rainy season; and *Kiremt* (June to September): long rainy season accounts 50-80% of the annual rainfall (NMSA, 2001; Seleshi & Zanke, 2004; Ministry of Environment and Forest, 2015). The mean annual temperature for Ethiopia to be 22.6°C, with monthly temperatures ranging between 20.9°C (December) and 23.9°C (April). Rainfall can range between 0 mm to over 4,000 mm annually and mean annual precipitation is 815.8 mm for the latest climatology, 1991–2020 (World Bank Group, 2021a). Overall, Ethiopia is considered largely arid, but exhibits a high variability of precipitation (USAID, 2016).

Ethiopia's climate is generally divided into three zones: 1) the alpine vegetated cool zones (Dega) with areas over 2,600 meters above sea level, where temperatures range from near freezing to 16 °C; 2) the temperate (Woina-Dega) zones, where much of the country's population is concentrated, in areas between 1,500 and 2,500 meters above sea level, where temperatures range between 16°C and 30°C; and 3) the hot Kola zone, which encompasses both tropical and arid regions and has temperatures ranging from 27°C to 50°C (World Bank Group, 2021b).

Ethiopia's climatic systems can be categorized using a variety of methods, including as the traditional, Koppen, Throw-weight, rainfall regime, and agroclimatic zone categorization systems (Admassu e al., 2010). The conventional and agro-ecological zone (AEZ) classification schemes

are the most widely used. Based on the traditional classification, primarily depend on temperature and altitude. Based on this classification, Ethiopia has five climatic zones as indicated in Table 1.

Table 1: Traditional Climatic Zones and their Physical Characteristics

Traditional Climatic Zones	Altitude (m)	Rainfall (mm/year)	Average annual temperature (^{o} C)	Area share (%)
Wurich (cold to moist, upper highlands)	3200 plus	900 – 2200	<11.5	0.98
Dega (cool to humid, highlands)	2,300 – 3,200	900 – 1,200	11.5-17.5	0.94
Weyna dega (cool sub-humid, mid-lands)	1,500 – 2,300	800 – 1,200	17.5 - 20	26.75
Kola (warm semi-arid, lowlands)	500 – 1,500	200 – 800	20.0 – 27.5	52.94
Berha (hot arid, desert)	< 500	Below 200	>27.5	9.39

Source: Dejene (FAO), 2003

2.6. Climate change/variability Trends at globally, regional, and local context

Global annual average temperature has increased by more than 0.7 °C for the period 1986 – 2016 relative to 1901 – 1960 (Vose et al., 2012). The global average temperature has increased by 0.74 °C in the last century and is projected to increase with 1.1-5.8 °C by the end of this century and the rainfall patterns will change with an increased frequency of extreme events (IPCC, 2012b). Regionally in East Africa, research show that in countries such as Burundi, Kenya, Sudan, and Tanzania have been severely impacted by the effects of climate change in recent decades (Mwangi & Mutua, 2015; Hassaan et al., 2017). Other studies projected that there is an increase in temperatures across Eastern Africa, with Ethiopia potentially experiencing temperature increases that range from less than 2.5 °C to greater than 3 °C by the 2040s, with greater rates of warming likely to take place in western and northern Ethiopia (Daron, 2014). Conway & Schipper (2011)

described that the rainfall behavior in Ethiopia shows no marked emergent changes and future climate projections show continued warming but very mixed patterns of rainfall change.

United Nations Development Program (UNDP) country profile shows that the mean annual temperature has increased by 1.3 °C between 1960 and 2006, an average rate of 0.28°C per decade. The increase in temperature in Ethiopia has been most rapid between July - September [JAS] at a rate of 0.32°C per decade. The mean annual temperature is projected to increase by 1.1 to 3.1°C by the 2060s, and 1.5 to 5.1°C by the 2090s. Under a single emissions scenario, the projected changes from different models span a range of up to 2.1°C. Regarding precipitation, the same source described that the strong inter-annual and inter-decadal variability in Ethiopia's rainfall makes it difficult to detect long-term trends. There is not a statistically significant trend in observed mean rainfall in any season in Ethiopia between 1960 and 2006. Decreases in July-September [JAS] rainfall observed in the 1980s have shown recovery in the 1990s and 2000s (McSweeny et al., 2012).

National Adaptation Program of Action [NAPA], 2007) reports on the variability and trend of the mean annual minimum temperature and yearly rainfall recorded nationwide between 1951 and 2006. During this time, the average annual temperature has increased by roughly 0.37°C every decade, although the trend analysis of annual rainfall across the nation has stayed relatively stable. A report by Federal Democratic Republic of Ethiopia, Ministry of Health [MoH], (2015) signifies that though Ethiopia`s contribution to the global warming is negligible over the last decades, the temperature is increased at about 0.2°C per decade. The increase in minimum temperatures is more pronounced with roughly 0.4°C per decade.

The mean annual temperature in the country will increase in the range of 1.7-2.1°C by 2050 and in the range of 2.7-3.4°C by 2080. However, precipitation over much of the country remained stable; it showed a 15-20% decreasing trend in the eastern and southeastern semi-arid and arid regions with increased frequency of drought. On the other hand, other areas of the country experienced increased precipitation, causing an increase in the frequency of floods. Even with reduced emission, warming is predicted to persist in Ethiopia throughout all seasons and geographic areas. According to Conway & Schipper (2011), the multi-model average indicates

warming in all four seasons and all places. By the 2020s, Ethiopia is expected to experience an annual warming of 1.2 °C, with a range of 0.7-2.3 °C (2050s: 2.2 °C, range 1.4-2.9 °C).

2.7. Land-use land cover changes implications on climate change & urban heat island (UHI)

Land use is described as how land is used by people and their habitats, typically with an emphasis on land's functional role in economic activities, whereas land cover is a physical feature of the Earth's surface (IPCC, 2000; Mariye et al., 2022). Land cover refers to the observed biophysical cover of the earth's surface, while land use reflects man's activities on the land with their intentions (Lambin & Geist, 2006; Prakasam, 2010). Land use and land cover (LULC) dynamics has become a concern of the 21st century with the dramatic implication for human survival and driving forces for global environmental change with impact on livelihoods (Verburg et al., 2015; Elias et al., 2019).

Human activities influence climate change by altering the distribution of ecosystems and their associated fluxes of energy (Dale, 1997). The most significant anthropogenic influences on climate are greenhouse gas emissions and changes in land use such as urbanization (IPCC, 2001c; Pielke et al., 2002). Human activities predicted to influence land use land cover and climate in the future (IPCC, 2014f). Changes in land-cover patterns can directly impact energy and mass fluxes. For example, when large areas of forests are cleared, reduced transpiration results in less cloud formation, less rainfall, and increased drying. Simulations of the deforestation of Amazonia indicate that evapotranspiration and forests would be replaced by either desert or pasture (Dickinson, 1991). Increased albedo and its subsequent effects on climate also result from changes in land-surface characteristics.

Land-use change is also one of the important factors in the climate change cycle and the relationship between the two is interdependent; changes in land use may affect the climate whilst climatic change will also influence future land-use. Climate change and land use affect each other (Dale, 1997). Changes in land cover can alter the reflectance of the earth's surface and induce local warming or cooling; generally, as albedo increases, surface temperatures decline (Wicaksana & Rachman, 1979; Dale, 1997). Land cover changes can occur in response to both human and climate influences. Demand for new settlements, for example, frequently results in the irreversible loss of

natural and working areas, which can cause localized changes in weather patterns, temperature, and precipitation (Kalnay & Cai, 2003; Hale et al., 2006; Pielke et al., 2007).

LULCC contributes to climate change in Ethiopia (Hailemariam et al., 2016). The significant fluctuations in LULC observed in Ethiopia during the previous decades are mostly attributable to population pressure, resettlement programs, climatic change, and other human- and nature-induced driving forces (Regasa et al., 2021). The same source further explained that in Ethiopia very rapid changes of LULC is observed because of population pressure, resettlement schemes, climate change, and other human and natural-induced driving forces. Anthropogenic activities are the most significant factors adversely changing the natural status of the Ethiopian landscape (Marchant et al., 2018). When a considerable portion of the natural land cover is changed by surface built-up, it traps the incoming solar radiation during the day time and re-radiates at night due to a decrease in albedo (Babazadeh & Kumar, 2015). Studies reported that urban centers are warmer than their surrounding countryside leading to an increase in urban heat island (Mohan et al., 2012; Babazadeh & Kumar, 2015). Urban heat island is an anthropogenic phenomenon resulting from the distinct surface modification caused by human settlement in urban areas (Arsiso et al., 2018).

Over the last one decade, the population of Addis Ababa dramatically increased, subsequently resulted in expansion of cities to the outer periphery areas and areas covered by forest, natural vegetation, and green spaces were eventually transformed into built-up surfaces (Moisa et al., 2022). Urbanization is one of the main causes for the alteration in urban land use and land cover change and resulted in drastic changes in vegetation proportion and local climate (Ullah et al., 2020). The most common impacts of land use land cover change is the increase in land surface temperature as compared to the surround peri-urban areas (Zhou & Wang, 2010a). The conversion of urban land use land cover into impervious surfaces was the root cause for the increase of land surface temperature in urban areas (Moisa & Gemeda, 2022). Related studies described that land use land cover is among the factors that trigger land surface temperature change (Balew & Korme, 2020a).

Urbanization and reduction of vegetation are the primary causes for land surface temperature change (Chao et al., 2020; Mensah et al., 2020; Moisa et al., 2022). A study conducted by Moisa

et al. (2022) on the impact of urban land use change on land surface temperature of Addis Ababa using a satellite image for the year 1991^{TM}, 2005^{ETM+} and $2021^{OLI/TIRS}$. The built-up area increased from 96.6 km^2 (18.3%) in 1991 to 277.2 km^2 (52.6%) in 2021. The study concluded that due to the rapid conversion of land use land cover change eventually contributed to the mean LST of the city by 8.3 °C. The result also further explained that higher LST was recorded in the built-up land use class and areas where there is scattered vegetation cover.

Similarly, urbanization driven land use land cover change influences on UHI carried out by (Arsiso et al., 2018). The study used satellite images of two points of time, 1986 and 2011 to detect the change in LST across time. The built-up escalated by 121.88 km^2 over the observation period. The thermal gradient increases from 1.44 °C at the city center (Addis Ketema, Arada, Lideta, and Kirkos) to 0.21 °C at the peripheral parts (Gulele, Bole, Nefasilk-Lafto, Kolfe-Keraniyo, and East of Yeka sub-cities) of the city. Moreover, a recent study focusses on the effects of vegetation dynamics nexus land surface temperature in Addis Ababa (Worku et al., 2021a). The study was done using landsat images of 1985^{TM} and $2015^{OLI/TIRS}$. The research has shown clearly the influence of vegetation in lowering the ambient surface temperature. The study concluded that in the center of the city where there is high impermeable surface and low vegetation coverage, the land surface temperature augmented by 3-8 °C from 1985 and 2015.

In a nutshell, the reduction of vegetation coupled with built environment immensely contributed to the proliferation of land surface temperature in the city. Many of the previous research unveiled that the rapid increase of city's population followed by high rate of urbanization consequently resulted in expansion of cities to outskirt sub-urban areas, in effect the proportion of vegetation and forest coverage through time would decline and rather impervious surfaces such as building, asphalt, concrete etc. dominantly cover the urban built environment. These surfaces transform the radiant energy received from the sun into kinetic energy and are typically characterized by high storage of thermal energy and emit this energy towards the atmosphere in the form of longwave radiation during dusk. The thermal energy released from the surface, some of it would escape to space and some of it would be absorbed by the greenhouse gases such as Carbon dioxide (CO_2), Methane (CH_4), Nitrous oxide (N_2O), Ozone (O_3) in the atmosphere and reradiated back to the surface. This would cause an increase of surface and atmospheric temperature.

The reduction of blue and green spaces positively influences the land surface temperature (LST). While the presence of plants/vegetations largely absorbs CO_2 from the atmosphere for photosynthesis. In addition, the presence of vegetation largely impacts the surrounding environment through cooling effect, shading, and increase the rate of evapotranspiration. Furthermore, plants also play a pivotal role in CO_2 sinking through carbon sequestration, as plants store in their leaves. Literature underscore that examining climate change without considering urban land use patterns excludes the interaction between climate change and the UHI and could result in underestimating future increases in urban temperatures, both mean and extreme values (Dia & Beaudelaire, 2021).

2.8. Urban heat island effect in cities

Urban heat island (UHI) is defined as the difference in spatially averaged surface temperatures between urban and surrounding rural (Pongracz et al., 2006). Compared with rural areas and city peripheries of central Addis Ababa tends to have higher air and surface temperature due to the UHI effect (Worku, 2017b). The intensity of urban heat island concentration can be influenced and decrease by weather conditions such as wind speed and high cloud coverage (Grimmond, 2006; Fernando, 2015). On the other hand, UHI can be further intensified in the presence of high pressure or anticyclone systems and the escalation of population density in cities further amplified the intensity of UHI (Morris & Simmonds, 2001; Kuttler et al., 2007; Arsiso et al., 2018). UHI present at any latitude, may occur during the day or night as it is a function of local thermal balance. The degree of UHI increases during the clear days, it is affected by rainfall and sea breeze winds (Santamouris, 2015).

Rapid population growth is the fundamental causes for the widespread of urbanization in the Sub-Saharan countries (Abebe et al., 2019; Koroso et al., 2021; Croix & Gobbi, 2022). Rapid urban expansion and growth in Sub-Saharan African countries continue to be a major challenge (Njoh, 2003; Satterthwaite, 2017). Over the last three decades, Ethiopia has undergone tremendous urbanization (Koroso et al., 2021). The most apparent impacts of urbanization is increase in land surface temperature (LST) in urban areas (Pongracz et al., 2006; Zhou & Wang, 2010). Understanding urban landscape conversions and interactions between natural phenomenon and

human activities is important for proper land and climate change management (Pringle et al., 2012).

Anthropogenically induced changes in the energy balance in urban centers have a significant effect on temperature, which has been termed the Urban Heat Island (UHI) effect. The energy balance can also change as a result of land surface changes that included variations in the albedo, thermal aerodynamic properties, hydrology, and morphology of the surface (Kifle, 2003). As development continues in the Ethiopian capital city, Addis Ababa, natural habitats are being converted to non-vegetated covers, which results in the development of urban heat island (UHI) (Warkaye et al., 2018). In the same vein, Worku (2017) indicated that Addis Ababa has become vulnerable to climate change impacts such as flooding, drought, and UHI effects over the recent years than it was in the past. The increasing intensity of heat waves is becoming an important health concern for policymakers (WHO, 2013).

For Addis Ababa City, this phenomenon has caused air temperature in the central city that are up to 5 ^{o}C higher than the surrounding areas (Worku, 2017). With the expected increase in the urban population in the next two decades the UHI would also be expected to increase further. Additional empirical and quantitative studies are required to investigate the overall impact of the increase in UHI on the local weather of the city. Particularly studies should focus to analyze the impact and the evolvement of UHI in relation to land-use, forest cover, and the gradual growth of heavy industries, and the resulting air-pollution (Kifle, 2003). Urbanization is the direct cause for the increasing trends of UHI (Moisa et al., 2022).

Due to significant population expansion, Addis Ababa City, Ethiopia's capital city, has suffered urban agglomeration (Terfa et al., 2019). Consequently, the vegetation around the city is converted to impervious surfaces (Teferi & Abraha, 2017a). The city of Addis Ababa is one of the most densely populated cities in Africa (Moisa & Gemeda, 2021a). Expansion of built-up area replacing the agricultural and grass land in the peri-urban areas of the city is very common phenomenon (Kassa et al., 2012). Addis Ababa is one of the fastest growing cities in Africa (Feyissa et al., 2018a). However, the impact of this rapid rate of urbanization on the city environment and livelihoods are very limited and little understood (Kassa et al., 2012; Terfa et al., 2019).

Rapid population growth, if not managed properly, can often result in serious negative environmental and socioeconomic impacts such as urban heat islands, air pollution, traffic congestion, reductions in green space, habitat losses, insufficient infrastructure and services, and inefficient resource utilization (Arsiso et al., 2018; Sahana et al., 2018; Shen et al., 2019). Surface temperature and urban heat island have increased in the city from time to time as the built-up area has expanded and plant cover has declined (Teferi & Abraha, 2017b; Samson et al., 2018). Given the rapid rate of urbanization coupled with the lack of adequate available studies in African cities in general and the low efforts to understand and mitigate the impacts resulted from climate change due to accelerated land use/land cover change in cities like Addis Ababa (Arsiso et al., 2018). Recent studies indicated that the population of Addis Ababa over the last one decade have increasing significantly consequently the vegetation cover and other land uses have been converted rapidly (Moisa et al., 2022). Subsequently, this would have a serious impact on the city's thermal environment.

2.9. Climate change and variability resulting from CO_2 emissions

Greenhouse gases such as CO2, CH4, N2O, and O3 are naturally occurring in the atmosphere and play an irreversible role in regulating global temperature. However, after the industrial revolution the proportion of these greenhouse gases in the atmosphere rose significantly mainly due to burning of fossil fuel (Sidiropoulos, 2023). The same source further elucidated that the increase in concentration of CO2 is responsible for the observed change in global warming. Global warming of 1.5 °C and 2 °C will be exceeded during the 21st century unless deep reductions in CO2 and other greenhouse gas emissions taken place in the coming decades (IPCC, 2021c). The increasing concentration of carbon dioxide (CO2) in the atmosphere has become a significant environmental challenge in the recent years as it contributes immensely to global warming (Nunes, 2023). More than half of the world's population, consumes 75% of global energy, and generates 80% of global greenhouse gas emissions (Duren & Miller, 2012; Short & Farmer, 2021). Globally, approximately 70% of anthropogenic GHG emissions emanate from fossil CO2 emissions and cities (Hopkins et al., 2016). Supporting this argument, Satterthwaite (2008a) denoted that cities are the by far the largest contributor for emissions of greenhouse gas ranging from 75 to 80%.

Urbanization, agriculture, industrial work, and greenhouse effects are the leading causes of the climatic changes and responsible for the increase in Carbon dioxide (CO2) and temperature on the surface of the earth every year (Kabir et al., 2023). CO2 is one of the potent greenhouse gases and plays a major role in escalating global temperature. Deforestation, fossil fuel combustion, agricultural practices, and increase of cement production were the primary drivers for the increase of atmospheric CO2 (West & Marland, 2002; Nunes, 2023). Due to the increasing concentration of CO2 and global warming, the earth surface temperature has been increasing and resulted in various disorders in the environment (Kabir et al., 2023). To limit global emission of greenhouse gases, the Kyoto protocol came into being as a binding commitment drafted in 1997. The protocol aimed to stabilize emission of gases particularly from fossil fuels utilization and other sources through reforestation and afforestation mechanisms (Anderson, 1998).

Comparatively, developing countries have small share of global greenhouse gas emissions, although their contribution is increasing recently (Mulusew & Hong, 2024). Africa's contribution to global greenhouse gas emissions is the least. However, they are the most susceptible to climate variability and change induced impacts (Sarkodie & Strezov, 2019). In this regard, the contribution of Ethiopia to regional and global greenhouse gas emissions is insignificant (Mulusew & Hong, 2024). Ethiopia also pledged to limit its annual net emissions to 126 Mt CO2e or lower by 2030 (FDRE, 2023). Generally, Ethiopia's transport sector GHG emission was the highest 6,647,656 tCO2e in 2014 and grew by 27% in 2015 and further escalated by 48 %, reached to the level of 12,544,346 tCO2e in 2016. Road transport alone accounted for the 96% of the transport emission and as compared to regional cities Addis Ababa city was the leading emitter of GHG (FDRE Ministry of Transport, 2017). Data drawn from the report of Addis Ababa City Administration and C40 Cities (2020) indicate that the contribution of greenhouse gas emissions of Addis Ababa city from the various sectors including energy, transport, and waste for the year 2016 was 14,479,133 tCO2e. The largest emissions come from the transport sector followed by waste and building energy. This has to do with the sharp increase of impervious surfaces in the city of Addis Ababa resulting from clearing of forest for the purpose of infrastructure development and expansion of roads and built-up surfaces.

2.10. Empirical Evidence

From climate change perspective, there are multiple studies covering different parts of the country. However, available research with the focus on cities/urban environments is limited. Since Addis Ababa is the subject of discussion, only a few studies have been conducted addressing climate change and variability. For example, a comparison study by Moges et al. (2014) examined the extreme rainfall variability of the Addis Ababa Observatory and Addid Ababa Bole stations from 1951 to 2000 using quantile perturbation method. The findings of the study revealed that there was an increasing tendency of extreme rainfall event at Addis Ababa Observatory as compared to Bole station. Moreover, downscaling of future temperature extreme scenarios with the focus of Addis Ababa was conducted by (Feyissa et al., 2018). The study statistically downscaled daily maximum and minimum temperature in 30-year intervals by taking Entoto and Addis Ababa observatory station. The result signified that the maximum temperature increases were in the range of 0.9 °C (RCP4.5) in 2020 to 2.1 °C (CGCM3A2) in 2080 at Addis Ababa Observatory. The minimum temperature is projected to increase by 0.3 °C in 2020 and 1.0 °C in 2080.

Similarly, Feyissa et al. (2018) conducted a study with the focus of mapping Addis Ababa's climate vulnerability hotspots. The result revealed that Addis Ababa sub-cities experienced varying degrees of climate variability and change. The study concluded that Addis Ketema, Arada and Lideta sub-cities had the greatest exposure and sensitivity indexes for climate risk. While the adaptive capacity is the highest in Gulele, Bole and Arada sub-cities. On top of that, Arsiso et al. (2018) emphasize indications of present and projected climate change at the urban scale in Addis Ababa City. The result unveiled the rainfall anomalies under RCPs scenarios are wet in the 2030s, 2050s, and 2080s. Both the minimum and maximum temperature anomalies under RCPs are successively getting warmer during these periods. The projected changes show a general increase in rainfall and temperatures, with strong variability in rainfall during rainy seasons.

Moreover, Alemu & Dioha (2020) carried out research in Addis Ababa by taking temperature data from two main meteorological stations, i.e., Entoto and Bole. The result of the study signified that there was a significant increase in the average annual temperature for Bole station. Furthermore, from an administrative and climate governance perspective, Addis et al. (2023) accomplished research on factors affecting climate change governance in Addis Ababa. The result emphasizes

that lack of coordination among the different institutions, political will, weak leadership, and financial constraints were the major factors that deterred the effective implementation of good climate governance in the city.

The results of this study are conistent with earlier research, which showed that the decadal average temperature increased by 2.7 °C over the last 38 years (1981-2018). In contrast, there was an increase of 1.88 °C in average maximum and 1.72 °C in the mean minimum tempertaures. In this regard, all the previous research focused on different time periods; however, their findings were conclusively consistent with the results of this research, all highlighted an increase in temperature in Addis Ababa. Their findings were aligned with the findings of this research, which underscores that there was a significant upward trend of maximum and minimum temperatures in the area of concern. As compared with the previous research, this is a very detailed study that examines the change in climate at monthly, annual, seasonal, and decadal levels. In addition, most of the previous studies made a comparison of two different stations. For instance, Addis Ababa and Addis Ababa Observatory stations; Addis Ababa and Bole stations. However, this research was different in its scope and spatial extent. It covered the whole city.

Pertaning with precipitation, For example, Moges et al. (2014) made a comparison study of precipitation between Addis Ababa Bole and Addis Ababa Observatory using data from the second half of 20th century. The result signified that Addis Ababa Observatory showed an increasing trend in extreme precipitation. The trend analysis results of the same study on an annual, seasonal and monthly basis confirmed that there was little or no significant trend observed, which contradicts the findings of this study that there was a significant decline in spring (*Belg*) rainfall and a slight decrease in mean annual rainfall, an increase in *Kiremt* season precipitation. The results were further proved with Mann-Kandall test and Sen's slope estimator.

Similarly, the results of this study stipulated that there was an increase in main rainy (*Kiremt*) season precipitation over the study period. In this regard, the findings of Feyissa et al. (2018a) precipitation projection support this study findings, which revealed that the highest precipitation increase of 20.9% (RCP8.5) in summer by 2080. While the winter season precipitation was anticipated to be an increasing pattern by 2080, which was different from decreasing trend analysis

report of this study. Likewise, Alemu & Dioha (2020b) carried out a trend analysis of temperature difference between Bole and Entoto stations. Methodologically, it has used Mann-Kendall (MK) test, while this research employed the latest package of Modified Mann-Kendall (MMK) and principal component analysis (PCA), and t-test for temperature trend analysis, and spatially covered the whole Addis Ababa city. The authors mainly considered minimum, maximum, and average temperature whereas this study is a more detailed investigation covering monthly, annual, seasonal and decadal levels. The result indicated that a significant increase of minimum, maximum and average temperature in Bole station, which was in agreement with the findings of this research that there was an upward trend in minimum and maximum temperature in the city during the period of concern.

Regarding the urban heat island effect, numerous studies have been conducted in Addis Ababa. For example, Teferi & Abraha (2017b) assessed the UHI spatial patterns and temporal variations in Addis Ababa between 1985 and 2011. The result signified that an intensified urban heat island effect was observed between Addis Ababa and the surrounding area with a difference of 15 K. From urban climate adaptation perspective, integrating climate change adaptation strategies in urban planning and landscape design of Addis Ababa carried out by (Worku, 2017a). The findings of the study revealed that incorporating climate change adaptations and mitigation measures into the planning and design of the city at different scales will enhance the city's resilience in terms of its ability to withstand flood hazards, water supply, and mitigation of the urban heat island effect. Similarly, urban green areas to mitigate the urban heat island effect, the case of Addis Ababa (Warkaye et al., 2018).

The result reflected that the LST increased by 5 °C between 1985 and 2015 and more pronounced surroundings compared with public parks. In addition, Arsiso et al. (2018) conducted a research on the influence of urbanization-driven land use/cover change on climate in the context of Addis Ababa. Analysis has shown that the built-up areas have increased by 121.88 km^2 within the last 25 years. The impact of the urbanization-driven land use/cover change has resulted in a notable nocturnal urban heat island (UHI) as revealed from an average increase in minimum temperature of 1.5°C at the center of the city relative to rural site over the 1960 - 2001 period at the peripheral

parts of the city transecting across the hot (high-density urban) to moderately warm to cool (non-built-up) areas.

Moreover, Worku et al. (2021a) studied the effects of vegetation dynamics on the land surface temperature of Addis Ababa between 1985 and 2015. The study discovered that in the center of the city, the land surface temperature was in the range of 3-8 °C. Furthermore, a recent study by Moisa et al. (2022) focused on the impacts of land use land cover conversion on the urban heat island effect in Addis Ababa. An accelerated land use land cover conversion was found from 1991 to 2021 with a mean LST of 8.3 °C. Although the result is a bit exaggerated and inconsistent as compared with other reports. Additionally, Mulatu & Desta (2023) study focused on a comparison study between traditional and modern residential housing in relation land surface temperature variations and found that the temperature increased by 2.2 °C between 2006 and 2016. The modern residential exhibits higher temperature as compared with the traditional housing.

All the previous studies used different Landsat data to estimate the anomalies of LST across various time spans and different results were obtained. All the studies noted that there was an increase in land surface temperature across the respective study periods. Furthermore, the increase in LST is higher in urban core areas as compared to sub-urban areas. In this case, there was a similarity with the findings of this research. For example, the result of the study demonstrated that the four sub-cities of Kirkos (3.03 °C), Arada (3.81 °C), Addis Ketema (4.72 °C), and Lideta (2.79 °C) experienced the highest increase in land surface temperature during the study periods (1985 - 2020). While the peripheral Yeka Sub-city LST was augmented by 0.55 °C between 1985 and 2020. This shows that consistent with the previous studies, the land surface temperature was very high at the city center and decreased outwardly. Studies underscore that following reduction of vegetation and intensified urban expansion, high LST was observed over the built-up area (Moisa et al., 2022; Teferi & Abraha, 2017b; Worku et al., 2021a). Similarly, in this study, also high mean LST increase was also noticed in the built-up, with an increase of 2.68 °C in the period of concern. The findings of this study are generally in agreement with the earlier research results. All clearly highlighted that the increase in land surface temperature in the various parts of the city, the LST increment was very much amplified in the downtown area.

Literature has indicated that anthropogenic factors are responsible for the observed temperature increase. In relation to this, the last IPCC report noted that human activity is responsible for the rise in mean and extreme temperature trends across Africa (Mcphillips et al., 2018; IPCC, 2022). With respect to the study area, Alemu & Dioha (2020) described that extreme weather changes in Addis Ababa were observed due to changes in climate. The other reasons that could contribute to the rise of the city's temperature over the course of the study period would be largely associated with urbanization. In this regard, Kocabas et al. (2015) explained that globally urbanization has had a significant impact on the climate and environment, exacerbating the effects of climate change in cities. The same source further added that several cities in Africa are exposed to climate variability due to unplanned development, lack of required risk reduction infrastructures, services, and weak urban governance. Supporting this argument, a more recent study noted that the rapid acceleration of urbanization would result in population growth of a cities and this would gradually escalate the UHI intensity (Kamal et al., 2023). However, a number of factors determine the UHI intensity such as topography, urban canopy layers, land use, urban morphology, human activities etc. (Ngarambe et al., 2021; Chen et al., 2022).

Over the last decade, the magnitude of urbanization in Addis Ababa has been very much intensified due to economic development, which led to an unprecedented rate of increase in the urban population in the city. The city accounts for 3.6% of Ethiopia's total population, 18% of the country's urban population lives in Addis Ababa. It has demonstrated a 2.1% yearly rate of population growth (Berhe, 2017). Particularly, the population over the last decade has been increasing alarmingly due to the massive migration of people from regional towns to Addis Ababa mainly due to economic opportunities and political reasons. This reflects the rapid urbanization that has been followed by the city's enormous population growth. Consequently, with population increase and accelerated urbanization many landforms that were covered in dense forest, vegetation, including public spaces, and other natural features, were transformed into built-up areas and industries. In connection with this, studies divulge that the higher the population density and the lower the share of green and blue areas, the higher the intensity of UHI (Akbari et al., 2016). This is largely a contributing factor to the escalation of the city's temperature. As the land gets warmer quickly than the oceans, it releases thermal energy towards the atmosphere. This subsequently contributed to the rise of both surface and air temperatures.

With respect to Addis Ababa, several research have been conducted pertaining to climate change and variability, urban heat island, and land use changes. For example, Bekalo (2009) analyzes urban landuse/landcover change of Addis Ababa using landsat TM and ETM+ acquired, respectively, in 1986 and 2000. It has been found that tremendous changes in landcover occurred over the study period. The findings showed that the built-up area increased to 49% with an annual growth rate around 3.5%. With respect to precipitation, Moges et al. (2014) undertaken a research on the historical changes in extreme precipitation of Addis Ababa Observatory and Addis Ababa bole stations from 1950 to 2000. The findings of the study demonstrated that Addis Ababa Observatory shows remarkably an increasing trend. Feyissa et al. (2018) conducted a study with the focus of mapping Addis Ababa's climate vulnerability hotspots. The result showed that Addis Ababa sub-cities experienced varying degrees of climate variability and change. The study concluded that Addis Ketema, Arada and Lideta sub-cities had the greatest exposure and sensitivity indexes for climate risk. While Bole, Gulele, and Arada sub-city have high adaptation capacity.

The same authors carried out a study on downscaling of future temperature and precipitations extremes in Addis Ababa under climate change scenario, which had a different focus. The study statistically downscaled daily maximum temperature, minimum temperature, and precipitation in 30-year intervals from the second generation of the Earth System Model (CanESM2) and Coupled Global Climate Model (CGCM3) under two Representative Concentration Pathways (RCP) Scenarios (RCP4.5 and RCP8.5) and two Special Report Emission Scenarios (SRES), A1B and A2, to examine future changes and their extremes. The findings demonstrated that the Addis Ababa Observatory experienced maximum temperature rises between 2020 and 2080, ranging from 0.9 °C (RCP4.5) to 2.1 °C (CGCM3A2). It is predicated that the minimum temperature will rise by 1.0 °C in 2080 and 0.3 °C in 2020.

In addition, Arsiso et al. (2018) carried out a research on the influence of urbanization-driven land use/cover change on climate: the case of Addis Ababa. Analysis has shown that the built-up areas have increased by 121.88 km^2 within the last 25 years. This finding is consistent with NDVI images taken over the same period that reveal a decline in vegetation coverage. The impact of the urbanization-driven land use/cover change has resulted in a notable nocturnal urban heat island

(UHI) as revealed from an average increase in minimum temperature of 1.5°C at the center of the city relative to rural site over the 1960 - 2001 period. at the peripheral parts of the city transecting across the hot (high-density urban) to moderately warm to cool (non-built-up) areas.

Moreover, Arsiso et al. (2017a) researched on climate change and population growth impacts on surface water supply and demand of Addis Ababa. The findings of the study noted that with respect to climate, the surface water supply predictions under the RCP 4.5 and RCP 8.5 scenarios indicate that the volume of reservoir at Legedadi/Dire and Gefersa will be decreased in the anticipated years between 2023 and 2039. Further explained that there would be a serious water shortage in the city due to the unmet water demand under the high population development and dry climate of the RCP 4.5 climate change scenario. On top of that, Arsiso et al. (2018) emphasize on indication of present and projected climate change at urban scale in Addis Ababa City. The result unveiled the rainfall anomalies under RCPs scenarios are wet in the 2030s, 2050s, and 2080s. Both the minimum and maximum temperature anomalies under RCPs are successive getting warmer during these periods. The projected changes show a general increase in rainfall and temperatures with strong variability in rainfall during rainy seasons.

Integrating climate change adaptation strategies in urban planning and landscape design of Addis Ababa City was conducted by (Worku, 2017). The findings of the study demonstrate that how climate change adaptation and other response options should be incorporated into urban and landscape design at the city, sub-city/catchment, neighborhood, site and building levels to improve the sustainability of city in terms of resilience to flood risk hazards, water supply, and urban heat island effects. A more recent study done by Alemu & Dioha (2020a) with an emphasis on climate change and temperature trend analysis in Addis Ababa. The investigation relied on temperature variation between Bole and Entoto stations in the city. The result underlines that in Bole station, there is a propensity for temperature increases. This might happen because of climate change which can cause weather extremes in the capital. A more recent study from climate change governance point of view conducted by (Addis et al., 2023). The study reported that climate change is typically characterized by erratic rainfall and increase in temperature with a predominant urban heat wave. The result of the study underlines that lack of coordination, political will and weak

leadership were the major factors that deter the practice and effective implementation of good climate governance in the city.

2.11. Relation between Climate change and UHI

Urban heat island and climate change are very much interwoven, and they are two important critical factors that negatively affect city residents, ecosystems, infrastructure, and the urban system. Climate change increases the risks of natural and human systems (Choi et al., 2021). Their combined impact on the city residents of Addis Ababa has been considerable. As a result of urbanization, the urban population density would increase in the city. There is a high probability of exacerbating the land use changes, and this would subsequently influence the UHI substantially. Generally, there is an intricate interplay between climate change and urban heat islands. The intensification of temperature in the city, would aggravate the urban heat island consequently resulted in local human health concerns, economic, and environmental repercussions. In this perspective, Corburn (2009) indicated that temperature increases resulting from climate change disproportionally impact cities, exacerbating the phenomenon of urban heat islands.

Literature noted that due to the complex relationship between climate change and urban heat island, a combined effort is needed to address the issue at the micro and macroscales in order to accurately analyze the combined effect of both factors and provide a precise picture of the atmospheric conditions in urban areas (Kamal et al., 2023). In a similar manner, the IPCC (2014b) indicated that the impact of climate change on cities is mostly in terms of increases in surface air temperature and heat waves. The occurrence and intensity of UHI in a city are largely determined by factors such as vegetation, level of albedo, built-up areas, and anthropogenic heat emission (Zhou et al., 2014).

Studies reported that the correlation between surface urban heat island and climate change, i.e., air temperature and precipitation, generally differed at macro-climatic conditions not in urban size. In cities with greater variations in vegetation, surface urban heat island is positively correlated with air temperature, while it is negatively correlated with air temperature in cities with relatively small differences in vegetation (Li et al., 2020). With reference to Addis Ababa, the findings of this study displayed that the average maximum and minimum temperatures increased by 1.88 °C and 1.72

°C, respectively, in the study period (1981-2018). While the land surface temperature analysis result reflected an increase of 1.8 °C between 1985 and 2020. Based on the above assumption, it is possible to infer that there is greater vegetation difference within the city as a result a positive correlation found between LST and air temperature. On the other hand, the relationship between precipitation and surface urban heat island indicates that surface urban heat island is more sensitive to precipitation than air temperature. Therefore, the growing influence of global climate change would further aggravate the urban heat island (Corburn, 2009). Understanding the relationship between UHI and air temperature and precipitation would help to become cognizant of the complex relationship between them. However, studies have reported that there is inadequate research, showing the relationship of UHI with the key climate indicators (precipitation and temperature). Thus, this would be a potential research arena for future research domain.

2.12. Implications for sustainable cities from SDGs perspectives

Sustainable development goals (SDGs) involve various natural, social, short, and long-term challenges (Kelman, 2017). Making cities resilient against natural and anthropogenic factors remains a major challenge for developing and developed countries (Guptha et al., 2021). Among the various Sustainable Development Goals (SDGs) established in the United Nations report (United Nations, 2022). SDG11 (sustainable cities and communities) focusses on making cities and human settlements inclusive, safe, resilient, and sustainable, and SDG13 (climate action) mainly intends to strengthen resilience and adaptive capacity for climate related hazards are highly associated with the intent of this study.

Urban heat island effect, related environmental repercussions, climate change and variability induced impacts are a major concern in cities like Addis Ababa. The municipal must pay attention to achieve these development goals and building a more lively, livable, and ecologically sustainable living environment. In relation to this, the Addis Ababa city administration could consider the garden city concept proposed by Gatarić et al. (2019), incorporating into the city's framework for urban planning and design in a way that would allow for the development of new communities surrounded by green spaces. This would have not only ecological advantages but also economic and cultural benefits.

Enhancing various ecosystem services to ameliorate climate resilience in the face of environmental challenges such as urban heat island effect is imperative. It is a known fact that heatwaves in cities affect numerous people across the world and cause irreversible changes in global ecosystems. To reduce the growing impacts of urban heat island effect in cities like Addis Ababa, monitoring the rapid land use changes and its associated impacts would have a paramount importance for sustainable urban growth and management through the implementation of appropriate land use planning and policy measures. Unplanned urban settlement would have a negative repercussion on the natural resources of any developing country (Khan et al., 2021). Overuse of the LULC for a range of political and economic reasons has the potential to diminish land productivity and future use (Tariq & Mumtaz, 2023a). Thus, ensuring well managed urbanization is a key to the shared and sustainable development of the city of Addis Ababa. This can be achieved through efficient and sustainable urban land use planning and management.

CHAPTER THREE: MATERIALS AND METHODS

3.1. Description of the study area

Ethiopia is the oldest independent state, the diplomatic center for Africa, and the second most populous country in Africa with a total population of 105 million in 2017, with annual growth rate of 2.4%. It is estimated that by 2050 the population will be 191 million (Wubneh, 2013; United Nations, 2017; Berhe et al., 2017). Such an increase in population triggers numerous environmental and socio-economic challenges on the city (Worku et al., 2021). Geographically, the city is located at the heart of the nation, 8°50′N to 9°5′N and 38°48′E to 38° 52′E (Figure 2) and covers an area of about 540 km^2 (Teferi & Abraha, 2017; Worku, 2017; Feyissa et al. 2018a; Worku et al., 2021).

Administratively, Addis Ababa is composed of eleven sub-cities, including Yeka, Bole, Arada, Akaki, Nifasilk Lafto, Kolfe Keranio, Lideta, Addis Ketema, Kirkos, Gulele and Lemi-Ksura. The average altitude of the city is 2400 m above mean sea level, and the highest elevation is at Entoto Hill to the north reaching 3200m. This makes Addis Ababa one of the highest-altitude capital cities in the world (Berhe et al., 2017). The city is endowed with three large rivers: the *Kebena*, Little *Akaki*, and Big *Akaki* Rivers, as well as several tiny streams that join to form the Big *Akaki* river near the city's eastern outskirts.

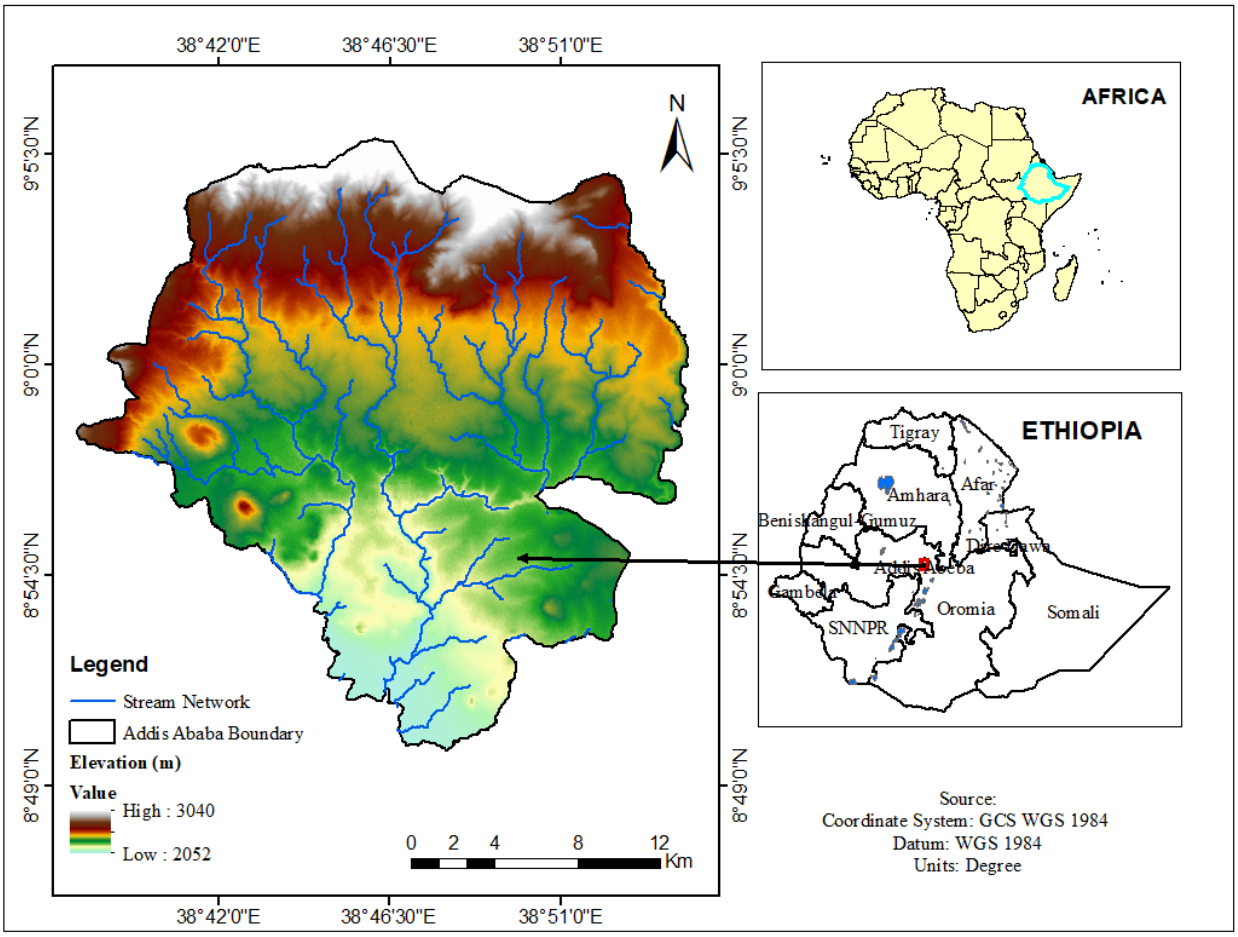

Figure 1: Location map of study area

3.2. Topographic Characteristics

Addis Ababa city is in the central highlands of Ethiopia, with an average elevation of 2600 above mean sea level (m). The altitude range extends from the highest peak at Mount Entoto which is 3041m to 2051 mean above sea level in the lower part of Akaki plain (Feyissa et al., 2018a). The city's terrain is undulating, forming a plateau in the northern, western, and southwestern areas; the mild morphology and flat land areas are characteristics of Bole, Akaki, and the south-western half of the city (Feyissa & Gebremariam, 2018).

3.3. Climate Characteristics of Addis Ababa

3.3.1. Precipitation

The study highlighted that Addis Ababa has a mean annual rainfall of 1150 mm (Figure 3). The mean maximum and minimum annual total rainfall were 1380.23mm and 730.03mm recorded in

the years 1996 and 2014, respectively. The long-term average *Kiremt* (main rainy) season rainfall was found to be 874 mm. The highest and lowest rainfall across the study period were registered in 1996 (1044.91mm) and 1987 (520.16mm). During the *Belg* (Spring) season of the observation period, the average precipitation was 225.2mm. The maximum rainfall occurred in 1987, with a precipitation record of 427.56mm, while the minimum precipitation was 76.77mm of rainfall registered in 1999.

Bega is a dry season where the smallest amount of precipitation is received. The average maximum rainfall received in 1997 was 221.77mm. In 2012, the smallest amount of rainfall, 12.36 mm, was received. The analysis result demonstrated that both the mean annual and seasonal precipitation were highly irregular and lacked a consistent pattern across the study period. In terms of amount and distribution, it was during the *Bega* (dry) season that the minimum rainfall was observed.

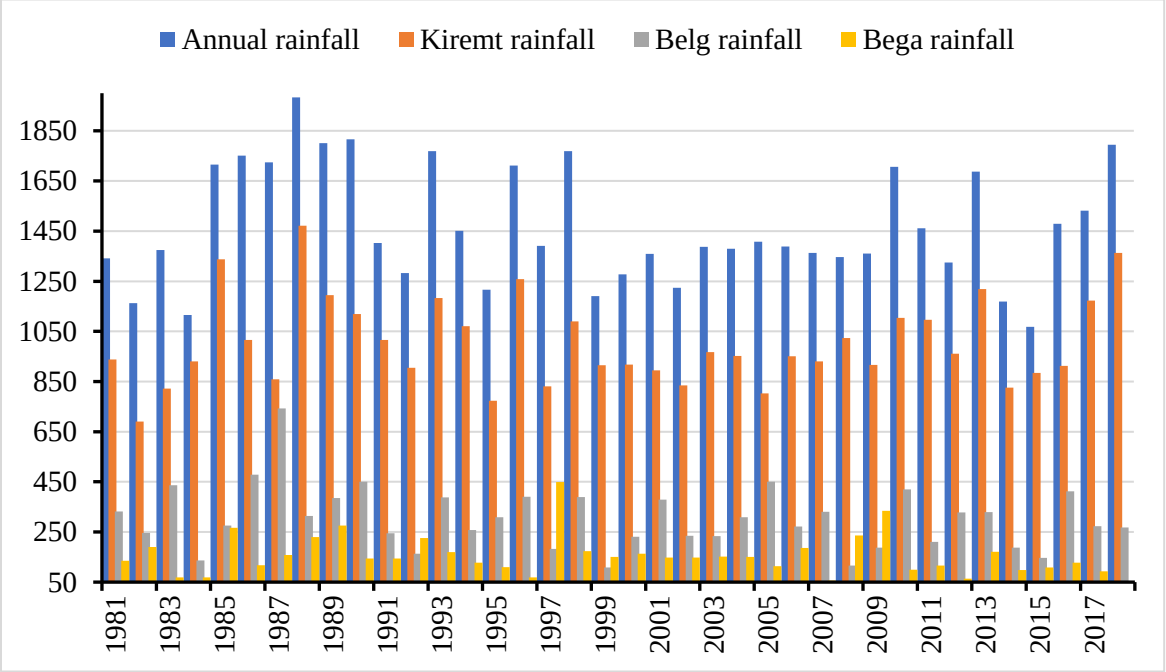

Figure 2: shows the mean annual and seasonal distribution of rainfall over the period of concern (1981-2018).

3.3.2. Maximum Temperature

The study area experienced that the average extreme annual highest and the minimum of maximum temperatures were 29.35 °C and 24.23 °C, respectively, in 2016 and 1986. The seasonal average maximum temperature for *Kiremt* (main rainy season) and *Belg* (spring) seasons occurred in the

same year 2016 with the values of 28.23 °C and 32.92 °C, successively (Figure 4). It was during the *Belg* (spring) season that the highest maximum temperature was recorded in the study period. Correspondingly, the minimum temperature during the *Belg* season was found to be 25.01 °C recorded in 1986. The highest and lowest maximum temperatures during *Bega* season were 29.62 °C (2015) and 23.81 °C (1988), respectively. It was in the same season that the lowest maximum temperature happened across the observation period.

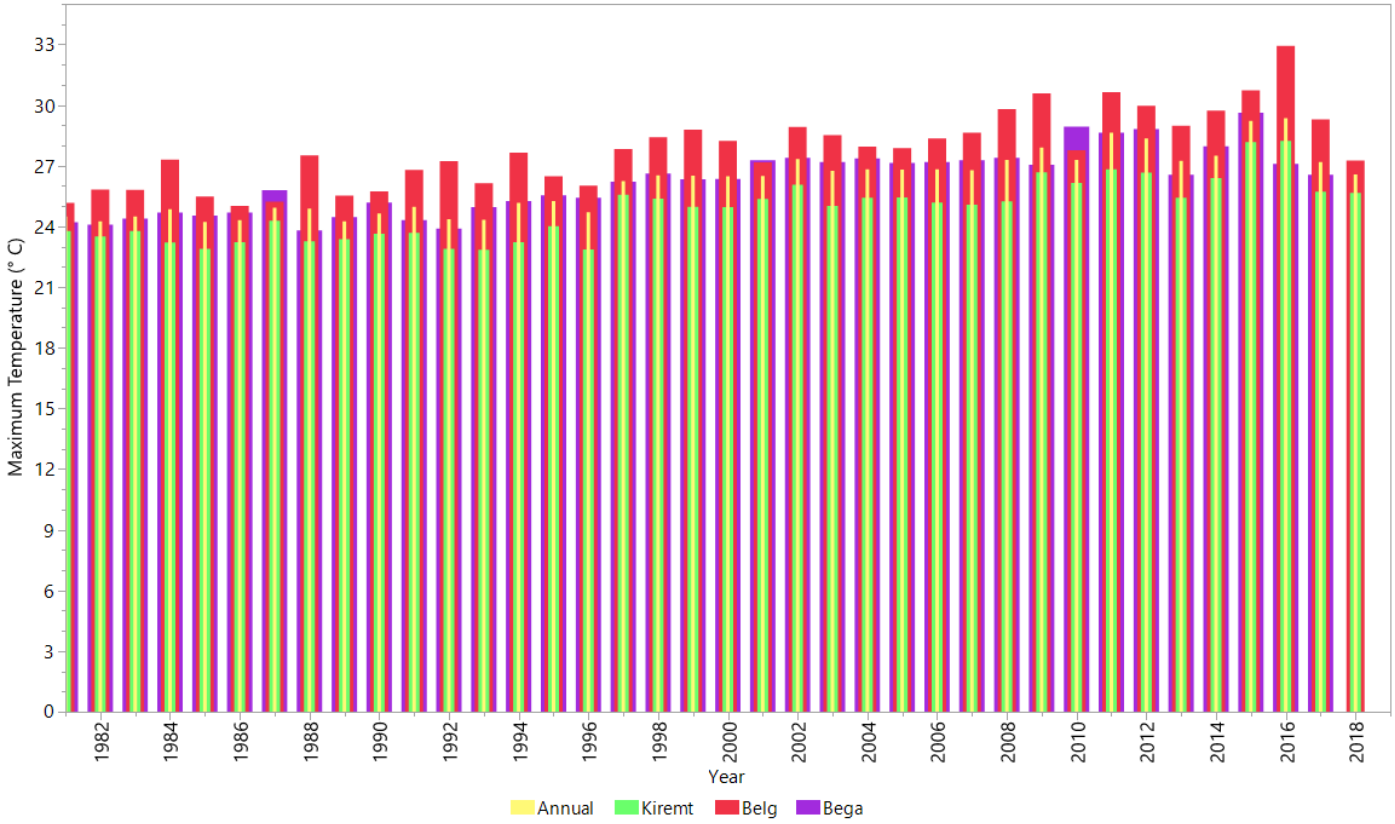

Figure 3: annual and seasonal maximum temperature distribution (1981 and 2018).

3.3.3. Minimum temperature

Figure 5 shows that the minimum temperature lacks a consistent trend in the observation years (1981-2018). The highest minimum temperature for the annual (16.75 °C), *Kiremt* (16.86 °C), and *Bega* (18.28 °C) seasons were registered in the same year of 2007. It was during *Bega* season that the highest minimum temperature occurred. It was in the same season that the lowest minimum (8.77 °C) temperature was recorded in 1986. In a nutshell, the result demonstrated that there was

a escalation of both the minimum and maximum temperatures in the recent observation years of the area of concern.

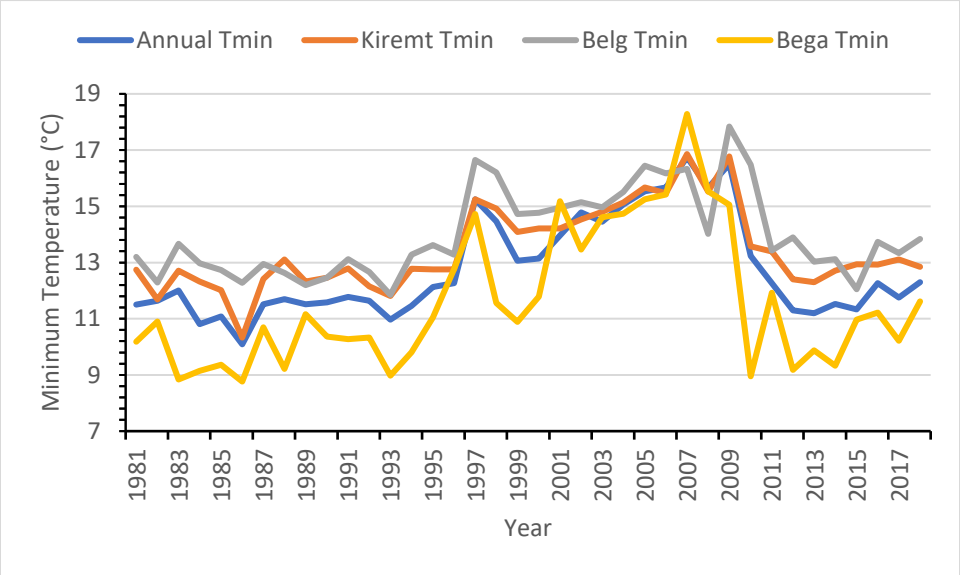

Source: analysis result

Figure 4: annual and seasonal average minimum temperature distribution (1981-2018).

3.3.4. Population and Livelihoods

Addis Ababa is the capital city of Ethiopia and the seat of the African Union (AU) with a population of 3.945 million and a projected population of 5.132 million by 2037 (CSA, 2013). Administratively, the city is classified into 11 sub-cities. Each sub-city is further divided into Woredas, which is the smallest administrative unit. The population density varies among the different sub-cities. Addis Ketema has the highest population density while Akaki-kality sub-city is the least populated. Despite this, all the sub-cities in the downtown have a high population density compared to sub-cities found in peripheral areas (Feyissa et al., 2018b; Woldegerima et al., 2016; Worku, 2017). With a yearly population increasing rate of 2.1%, Addis Ababa's population makes up 3.6% of the country's total population and 18% of Ethiopia's urban population (Berhe et al., 2017).

3.3.5. Soil types of Addis Ababa

As cited in Krauer et al. (2019) National Geospatial Database system for Water and Land Resource Management, the soil of Addis Ababa is classified into four major types, namely Leptosols (LP), Chromic Luvisols, Eutric Nitisols, and Pellic Vertisols. Vertisols is the dominant soil type in the

region which occupies a total area of 287.57 (sq.km) and predominantly found in the eastern, central, and southern parts of Addis Ababa. Euric Nitisols (105.23 sq.km) is the second dominant soil found in the central and North West part of the city (Figure 6). Chromic Luvisols the third largest soil with an area of (97.49 sq.km) mainly found in the northern part of the city. The fourth soil type is Leptosols that constituted the least area (29.79 sq.km).

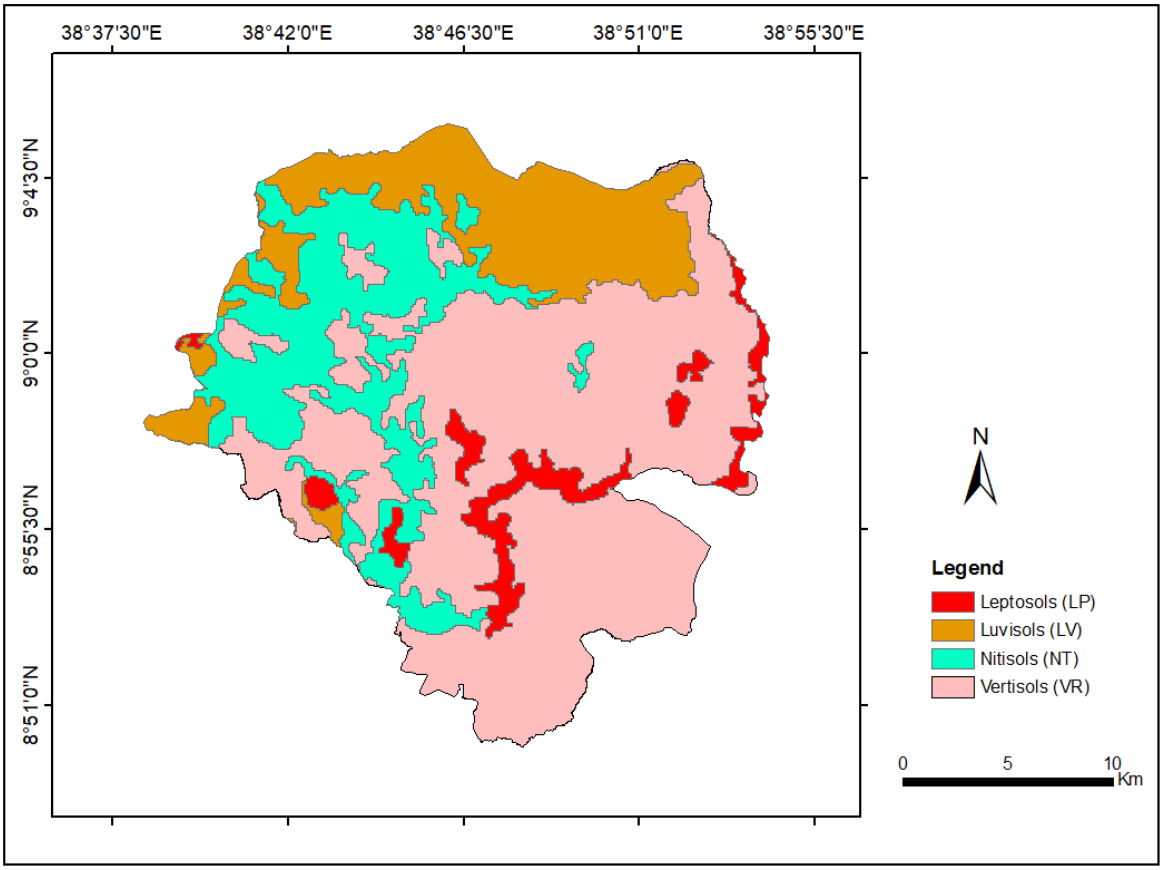

Figure 5: Soil map of Addis Ababa **(**Source: WLRC/CDE: National Geospatial database System EthioGIS-3/Release, 2019).

3.4. Data sources and types

For this study, the data obtained from Ethiopia's Meteorology Agency which consisted of monthly grid rainfall and temperature (Tmax and Tmin) with a spatial resolution 4*4, ranging from 1981 to 2018. Literature noted that temperature and precipitation are the key indicators of climate studies and widely employed to evaluate the degree and extent of change (IPCC, 2007a; Wanyama, 2017). As set by (WMO, 2023) the threshold year for climate studies is 30 years. In this regard, this study satisfied the requirements for climate research since it adheres to the WMO guidelines.

On the other hand, with regard to LST, the most appropriate method for studying the spatial and temporal variations in land surface temperature (LST) is the application of remote sensing data (Li et al., 2013). LST retrieved from remote sensing thermal infrared data widely recognized as an effective method for examining the spatial and temporal patterns of UHIs (Sun et al., 2012; Dissanayake et al., 2019; Liu et al., 2019). In this research, two sets of remotely sensed data; Landsat 5 Thematic Mapper (TM) for 1985 and Landsat 8 Operational Land Imager (OLI/TIRS) for 2020 were used as shown in Table 2 below. The mentioned time frame was considered since this study is highly related to climate studies, considering the minimum threshold years for climate related research and to show the change over a long period of time. The datasets were obtained free of charge from open-source United States Geological Survey (USGS), Centre for Earth Resources Observation and Science (http://earthexplorer.usgs.gov).

Kindu et al. (2013) suggested that cloud-free dry month imageries were utilized to reduce classification gaps between land use classifications caused by seasonal variations. The acquired Landsat images undergo band composite and image preprocessing like image enhancement to increase the interpretability of the image. The processed Landsat scenes that covered the study site were subsequently extracted using the study area boundary. In addition, the Digital Elevation Model (DEM) was also obtained from the same site and used to characterize the relief of the study area. The DEM data was mainly used to show the relationship of land surface temperature with the elevation of Addis Ababa city (Worku et al., 2021b).

Table 2:Satellite image information

Satellite, Sensors	Date	Resolution (m)	Path	Row	Source
L1 Landsat 5 TM (Band 6)	18.01.1985	120, resampled 30	168	54	USGS/ Earth Explorer
L1 Landsat 8 L1, TIRS Band 10	19.01. 2020	100, resampled 30	168	54	
SRTM -1 Arc-Second Global	Digital Elevation (DEM)	30			

3.5. Data quality check: data consistency, accuracy, and missing values

The grid data has been visually examined for completeness, missing values and logical consistency (Huisman & By, 2009). In this study, a total of 120 grid points, including proxy rainfall and temperature (maximum and minimum) were used as inputs to produce the pixel based interpolated surfaces (Figure 7). The calculated mean values were utilized for the unknown position to determine the rainfall and temperature variability and trends across multiple timescales including monthly, annual, seasonal (*Kiremt, Belg,* and *Bega*), and decadal levels. The purpose was to reveal the anomalous trends of change both precipitation and temperature (maximum and minimum) in the investigation period in both space and time (1981-2018). In this study, the grid data was preferred mainly because of several reasons: firstly, the grid datasets were easily accessible and provided comprehensive coverage of the study area. Secondly, ground station data with a reliable and extensive record was limited in availability within the study area. Lastly, the existing station data contained a significant number of missing values (Asfaw et al., 2018b).

In addition, studies unveiled that gridded rainfall and temperature data over Ethiopia is generally in a very good agreement with observation data, hence the dataset is worth of using for regional and global climate changes (Tsidu, 2012). In addition, ancillary data such as administrative boundary of the Addis Ababa City, road network, and river network were obtained from Ethiopian Space Science and Geospatial Institute. To ensure consistency throughout the analysis, all the

datasets were projected to the local coordinate system of the Universal Transverse Mercator (UTM) projection, Zone 37N, and Geodetic datum of Adindan. This projection adjustment aimed to maintain coherence and compatibility among the datasets.

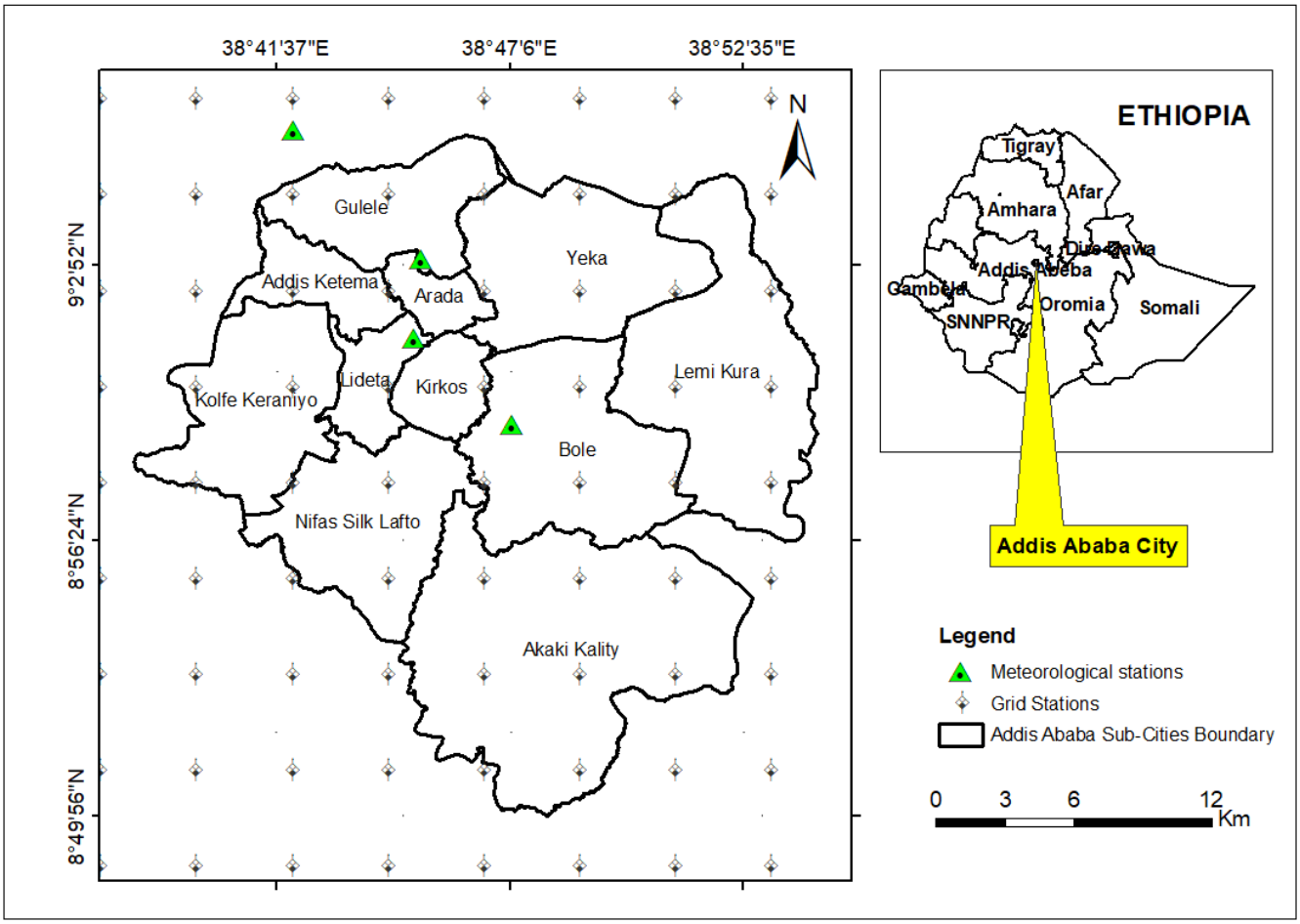

Figure 6: Spatial distribution of grid and meteorological stations in the study area

3.6. Method of data analysis

3.6.1. Geostatistical methods

Measurement and evaluation of the spatially distributed meteorological data have become important in connection with climate-change impact studies (Hofierka et al., 2002). Maps of various climate elements produced by spatial interpolation of point distributed data are frequently used to improve understanding of climate's spatio-temporal variability as well as for various studies of climate impacts on society and ecosystems (Haines et al., 2006). Researchers have evaluated the various methods for interpolation of point climate data. Basically, there are two fundamental interpolation techniques: deterministic and geostatistical (Apaydin et al., 2013;

Verma et al., 2019). The deterministic method is mainly relied on the geometric characteristics of the variables, whereas geostatistical techniques are based on both geometric and autocorrelation of samples (Verma et al., 2019).

Comparatively, geostatistical techniques are preferable over deterministic for spatial data interpolation as it is free from bias (Sluiter, 2009; Ozturk & Kilic, 2016). The basic goal of geostatistical methods such as kriging and cokriging is to interpolate the values for points in areas which have not been sampled, using data from surrounding sampled points (Phillips et al., 1992). Geostatistical models predict the value in un-sampled location and quantifies the uncertainty of the prediction (Yang et al., 2004; Haining et al., 2009; Balding et al., 2012).

Ordinary Kriging is extensively used for geostatistical interpolation method and it is an ideal method that weights the surrounding observed measured points to calculate and predict for the unknown position (Phillips et al., 1992; Hou et al., 2022; Yuan et al., 2022). In several studies, geostatistical methods have been rated superior to deterministic approach (Phillips et al., 1992; Michaud, 1995; Ashraf et al., 1997; Chuanyan et al., 2005; Biernacik et al., 2023). Additionally, it is popular since it enables to use the geospatial autocorrelation between points, distance between points, and spatial variability (Tabios & Salas, 1986; Phillips et al., 1992; Goovaerts, 1999; Piri et al., 2016).

Feyissa et al. (2018) noted that there are five metrological stations in the Addis Ababa city. These are Addis Ababa Observation (AAO), Addis Ababa Bole (AAB), Asko, Entoto, and Sululta stations. Addis Ababa Bole and Addis Ababa Observation are synoptic stations while the remaining are principal and ordinary stations. The same authors noted apart from two stations i.e. Entoto and Addis Ababa Observatory which have a complete dataset over the period of concern.

However, the other stations do not have a data record for the required study period (minimum 30 years). This implies that the availability and distribution of meteorological stations are very limited in Addis Ababa city. In addition, stations are sparsely distributed and most of the station data also suffers from gaps/missing values (Dinku et al., 2014; Hughes, 2006). As a result, the study mainly relied on grid data. In this regard, a possible surrogate would be grid-based estimates of weather

parameters that combine satellite and unevenly distributed ground observations (Joseph et al., 2020). In addition, as literature pointed out that over the test region in, there is no discernable dichotomy between the station data and the combined gauge satellite products, however, in regions with a sparse station distribution, the combined product shows superior quality (Dinku et al., 2014).

Satellite rainfall and temperature estimates are being used widely in place of gauge observations and in comparison to point-based gauge measurements, improved satellite rainfall estimations could truly represent spatial rainfall and temperature variability (Dinku et al., 2007; Belay et al., 2019). Gauge-based gridded temperature and precipitation datasets offer a way to evaluate the climate in areas where there are limited stations (Kursinski and Zeng, 2006; Ahmed et al., 2019). In the same vein, gridded climate datasets are a vital source of climate data when meteorological stations are limited, unevenly distributed, and have large amount of missing data (Hofierka et al., 2002; Asfaw et al., 2018). Moreover, gridded datasets provide long-record data and can improve data integrity because of high spatial coverage that allows data extraction for a large number of locations (Mulugeta et al., 2019). Hence, due to the aforementioned reasons, gridded datasets were widely used in a number of previous studies (Collins, 2011; Wagesho et al., 2013; Addisu et al., 2015; Pingale et al., 2016).

3.6.2. Kriging

In this study, time series gridded precipitation and temperature (maximum and minimum) data were analyzed using kriging techniques (Ryu et al., 2002). This is because kriging provides better estimates than other techniques (Goovaerts, 2000; Webster & Oliver, 2007). Supporting this, a recent study underlines that various interpolation techniques namely: Thiessen polygons, Inverse Distance Weighting (IDW), Thin Plate Spline (TPS), Ordinary Kriging (OK) and ordinary Co-Kriging (CoK) were selected and compared at different time scale. Ordinary Kriging (OK) outperforms other methods (Liu et al., 2022). The Ordinary Kriging is highly reliable and recommended for most climate datasets (Wackernagel, 2003). It is thought to perform better than deterministic interpolation methods such as inverse distance weighted and spline approaches (Kisaka et al., 2015).

Hence, in this research ordinary kriging (OK) was used to analyze time series climate variables data. The equation used in ordinary kriging developed by; Oliver & Webster (1990); Borga & Vizzaccaro (1997); Ryu et al. (2002) is given below (Eq.1)

Eq.1

$$\hat{Z}(_{S_0}) = \sum_{i=1}^{N} \lambda_i Z(_{Si})$$

Where:

$\hat{Z}(_{S_i})$: the value measured at the ith location.

λ_i: a weight unknown for the measured value at the ith location

$(_{S_0})$: the estimation positions.

N: the number of values measured.

With kriging method, the value $\hat{Z}(_{S_0})$ at the point S_0, where the true unknown value is $\hat{Z}(_{S_0})$, is estimated by a linear combination of the values at N surrounding data points. In the Ordinary Kriging, the weight, λ_i depends on a fitted model to the measured points, the distance to the estimation point, and the spatial relationships among the measured values around the estimation location and the Kriging weights are calculated by minimizing the variance (Li & Heap, 2008).

3.7. Spatial-temporal rainfall and temperature variability analysis

3.7.1. Coefficient of variation analysis method

The coefficient of variation calculated from randomly distributed grid data in the research area was used to represent the spatial variability of rainfall and temperature (Abebe et al., 2022). The coefficient of variation (CV) evaluates year-to-year variation in the data series and is represented as a percentage (Eq.2), which is important for determining variance compared to the mean size of observation (Muthoni et al., 2019; Alemu & Bawoke, 2020; Alemayehu et al., 2020; Bayable et al., 2021; Eshetu, 2021):

Eq.2

$$CV = \left(\frac{\sigma}{\mu}\right) * 100$$

Where CV denotes the coefficient of variation, σ is a standard deviation and μ is the mean rainfall/temperature record. The CV evaluates the overall variability of rainfall and temperature record of an area. Based on CV values, rainfall/temperature variability is classified as low (CV<20%), moderate (20<CV<30), high (CV>30), extremely high (CV>40), and extreme (CV>70) (Hare, 2003; Addisu et al., 2015; Eshetu, 2021). In general, a larger CV indicates greater Changes in climate variables, and vice versa (Asfaw et al., 2018b).

As a result, the spatial variability of rainfall and temperature over the research period was investigated, and CV was calculated for seasonal (*Kiremt, Belg*, and *Bega*) and annual rainfall. For that purpose, ArcGIS version 10.8.2 was used, seasonal and annual areal rainfall and temperature variations were analyzed using the conventional kriging interpolation approach.

3.7.2. Standardized anomaly index (SAI) method

Based on long-term mean temperature or rainfall, the standardized anomaly index (SAI) determines which years are wet or dry and looks into the nature of trends (Asfaw et al., 2018; Alemu & Bawoke, 2020). The standardized anomaly index determines the standard deviation between a data value and its mean in standard units. The rainfall and temperature variability index shows how far a rainfall/temperature event differs from the average of the years taken into consideration, expressed in standard deviation (Agnew & Chappell, 2000; Funk et al., 2015). It is also used to evaluate both the frequency and severity of droughts, as well as to assess the extent of wet and dry years in the record (Alemu & Bawoke, 2020). SAI, where positive values indicate above-normal precipitation and negative values imply below normal rainfall (dry) (Muthoni et al., 2019; Anose et al., 2021).

In order to calculate the frequency and intensity of dry and wet years, as well as the cooling (-ve) and warming (+ve) years of the study period, the standardized anomalies index was employed (Bayable et al., 2021). SAI can be calculated using the following equation (Eq.3):

Eq.3

$$\mathrm{SAI} = \frac{\left(\mathrm{X} - \overline{X}\right)}{\sigma}$$

where SAI = standardized anomaly index, X = annual and seasonal mean rainfall and temperature of a particular year, $\overline{X}$ mean annual and seasonal rainfall and temperature over the period of observation, and σ is standard deviation of annual and seasonal rainfall over the period of observation. The drought severity classified based on SAI are extreme drought (SAI < - 1.65), severe drought (- 1.28 > SAI > - 1.65), moderate drought (- 0.84 > SAI > - 1.28), and no (SAI > - 0.84) (Agnew & Chappell, 2000).

3.8. Trend analysis method

3.8.1. Mann-Kendall test

Parametric and non-parametric methods are the two basic tests that are frequently employed in the field of climate science to determine the degree of importance of time series meteorological data (Chen et al., 2007; Orke & Li, 2021). Comparatively, parametric tests are robust approach but the data has to be normally distributed, properties of time series data do not change over time, and statistical independence of the variables is required (Kundzewicz & Radziejewski, 2006).

Mann-Kendall (MK) test is a popular method for determining whether a time series meteorological data is trending downward or upward (Ngongondo et al., 2011; Kiros et al., 2016; Gebremicael et al., 2017; Mohammed et al., 2019; Alemu & Bawoke, 2020). It is a rank based technique, vigorous, and widely applicable for non-parametric tests to identify the patterns in hydro-climate time series (Mann, 1945; Gocic & Trajkovic, 2013; Wasserstein et al., 2019; Wang et al., 2020). Lettenmaier et al. (1994); Sang et al. (2014); and Wang et al. (2019) noted that Mann-Kendall test mostly used to examine the trends in temperature and precipitation data over extended periods of time. The method, which emphasizes ranks of data rather than their actual values, is advised over parametric testing because it is less affected by no data values, irregular data distribution, and outliers (Yue et al., 2002; Huth & Pokorna, 2004; Poudel & Shaw, 2016; Belay et al., 2019; Alemu & Bawoke, 2020).

In this study, Mann-Kendall test and Sen's Slope estimator were used to assess annual, *Kiremt* (main rainy season), *Belg* (smaller rainy or spring season) and *Bega* (dry) season rainfall and temperature distribution for the period from 1981 to 2018 using "R" programming software. When examining whether a trend in climate declining or increasing Mann-Kendall test is the ultimatum

(Ngongondo et al., 2011; Gebremicael et al., 2017; Kiros et al., 2016; Mohammed et al., 2019; Alemu & Bawoke, 2020).

MK is the most commonly utilized and preferred non-parametric test for analyzing time series hydro-climate patterns (Gocic & Trajkovic, 2013; Ahmed et al., 2014; Feng et al., 2016). The World Meteorological Organization (WMO) highly recommends the MK trend test due to its widespread application in trend analysis (WMO, 1966). It is used to confirm if a trend of rainfall/temperature variability is statistically significant or not (Jain & Kumar, 2012). Based on MK test, the null hypothesis (H_o) designates absences of trend in the series, whereas the alternative hypothesis (H_1) describes monotonic (increasing or decreasing) trend in the time series data (Hussain et al., 2015 ; Bayable et al., 2021). It is used to check statistical significance of trend in hydroclimate variables Mann (1945); Yue et al. (2002); Kumar et al. (2010); Shadmani et al., 2012); Yadav et al. (2014); Hu et al. (2020); Wang et al. (2020) and compute the MK statistics S using the following formula (Eq.4):

Eq.4

$$S = \sum_{i=1}^{n-1} \sum_{j=i+1}^{n} Sgn(Y_j - Y_i) \dots\dots J > i$$

Where *n* is the number of datasets; Yi and Yj are the sequential data values on years *j* and *i*, where $j > i$; and Sgn ($yj - yi$) is computed using Eq.5

Eq.5

$$Sgn(yj - yi) = \begin{cases} 1 \ \ if(yj - yi) > 0 \\ 0 \ \ if(yj - yi) = 0 \\ -1 \ \ if(yj - yi) < 0 \end{cases}$$

According to Mann (1945) if the dataset is identically and independently distributed then the mean of S is zero and the variance of S is given by Eq.6:

Eq.6

$$Var(S) = \frac{\mathrm{n}(n-1)(2n+5) - \sum_{i=0}^{m} ti(t_i - 1)(2t_i + 5)}{18}$$

where n is the number of observations, m is the number of tied group (a tied group is a set of sample data having the same value) in the time series; and t_i is the number of observations in the $i^{-}th$ data group. The standard Zs statistics was calculated using the formula below (Eq.7):

Eq.7

$$Z_s = \begin{cases} S + 1/\sqrt{V}ar(S) \text{ for } S < 0 \\ 0 \qquad\qquad for \;\; S = 0 \\ S - 1/\sqrt{V}ar(S) \text{ for } \; S > 0 \end{cases}$$

Test statistics Z_s evaluates the statistical significance of the trend. If Z_s is positive it indicates an upward trend while negative denotes decreasing trend (Al-hasani, 2020). The trend is significant at the 90% confidence level if $|Z_s|$ > 1.65, at the 95% confidence level if $|Z_s|$ > 1.96, and at the 99% confidence level if $|Z_s|$ > 2.58 (Ahmad et al., 2015; Mandale et al., 2017).

3.8.2. Modified Mann-Kendall (MMK) test

The dataset used in the parametric test must have a normal distribution. On the other hand, the non-parametric test needs independent time series datasets and distribution free method (Kundzewicz & Radziejewski, 2006; Sahoo et al., 2021). Because of non-parametric methods are easy to use and simplified nature frequently utilized in trend analysis (Sonali & Nagesh Kumar, 2013). The Modified Mann-Kendall (MMK) test is largely used since it measures both the nature of the trend and level significance (Hamed & Rao, 1998). For temperature trend analysis, MMK is preferred over MK due to its ability to handle datasets with serial correlations (Duhan et al., 2013; Suryavanshi et al., 2014). In this study, the monthly, annual, and seasonal temperature trend for the years 1981 to 2018 was evaluated using "R" package of MMK and Sen's slope estimator test.

MMK and Sen's slope estimator are non-parametric methods widely used for trend analysis of hydroclimatic variables. MMK trend provides the nature of monotonicity time series data along with statistical significance (Pandey et al., 2022a).

According to Signorino & Ritter (1999); Yue et al. (2002); Wang et al. (2020) the MMK statistics S is computed using the following formula (Eq. 8 Eq. 9):

Eq. 8

$$S = \sum_{i=1}^{n-1} \sum_{j=i+1}^{n} Sgn(\mathrm{X}_j - X_i)$$

Eq. 9

$$Sgn(X_j - X_i) = \begin{cases} +1, & if(X_j - X_i) > 0 \\ 0, & if(X_j - X_i) = 0 \\ -1 & if(X_j - X_i) < 0 \end{cases}$$

For a time series x_i that is ranked from $i = 1, 2, \ldots . n$ -1; and *x*j, which is ranked from *j* = *i* + 1, *i* + 2,……,*n*, where *n* is the total number sample points (Zhang et al., 2011). For *n* > 10, *S* follows approximately normal distribution with a mean zero and variance given by Eq. 10

$$E(S) = 0$$

Eq.10

$$Var(S) = \frac{\mathrm{n}(n\ -\ 1)(2n + 5) - \sum_{i=1}^{m} t_i(t_i\ -1)(2t_i + 5)}{18}$$

Where t_i considered the number of ties up to the sample *i*. This (Eq. 10) computation of a variance is original Mann-Kendall test which assumes the autocorrelation among the data points to be insignificant which is actually not the case always (Pandey, et al., 2022b). For this reason, Hamed & Rao (1998) proposed a modified Mann-Kendall (MMK) test where the variance is modified by multiplying a correlation factor to account for the autocorrelation structures for all lags in a datasets. The same source further explained that the modified variance V*(S) is given under Eq. 11 (Swain et al., 2022).

Eq. 11

$$V^*(S) = VAR(S) \cdot C_f$$

where C_f represents a correlation factor by the empirical expression

$$C_f = 1 + \frac{2}{n(n\ -\ 1)(n\ -\ 2)} * \sum_{i=1}^{n-1} (n\ -\ i)(n\ -\ i\ -\ 1)(n\ -\ i\ -\ 2)\rho_i(i)$$

where $\rho_s\ (i)$ the serial autocorrelation in the data series.

The MMK test statistic in Z denoted by Eq. 12 (Swain et al., 2021).

Eq. 12

$$Z_{MMK} = \begin{cases} S - 1 / \sqrt{V^*}(S), & \text{if } S > 0 \\ 0 & if \quad S = 0 \\ S + 1 / \sqrt{V^*}(S) & \text{if } S < 0 \end{cases}$$

where Z_{MMK} follows a standard normal distribution. An upward trend is indicated by a positive Z value, and vice versa. In a two-tailed test, a significant level is also used to indicate an upward or downward trend (Swain et al., 2022).

3.8.3. Sen's slope estimator

Sen's slope estimator was employed to assess the relative efficacy of the MK/MMK test in the analysis of time series climate data (Sen, 1968). It reduced the impact of missing values or outliers on the slope in contrast to the linear regression approach (Bouza-Deaño et al., 2008; Alemu & Bawoke, 2020; Mekonen et al., 2020; Ray et al., 2021). Sen's slope estimator are often used to assess the strength of long-term temporal patterns (Jain & Kumar, 2012; Agarwal et al., 2021). The equation below (Eq. 13) was used to calculate the monotonic trend in climate data using the non-parametric Sen's slope estimator (Sen, 1968; Gelata et al., 2023).

Eq. 13

$$\beta = Median \left(\frac{X_j - X_i}{j - i} \right), \text{ j > i}$$

Sen's slope is denoted by β. β > 0 indicates an increasing trend in the time series. If not, the dataset indicates a propensity to decline during the period of study (Weldegerima et al., 2018). In this study, Sen's slope was used to determine the magnitude of change in precipitation, maximum, and minimum temperatures. The MK/MMK and Sen's slope estimator were chosen and utilized to identify the trends and significance, respectively, because both variables were not normally distributed (Frimpong et al., 2022).

3.8.4. Principal component analysis (PCA)

PCA is a method for reducing a dataset's dimensions, while improving interpretability, and minimizing information loss (Jollife & Cadima, 2016). It is a multivariate statistical technique that is used to analyze correlations and determine the underlying structures of several variables (Ling et al., 2021). PCA is utilized to examine how a particular variable influences climate change Richman & Lamb (1985); Kilmer (2010); Zuśka et al. (2019) and identification the dominant components influencing the particle concentration (Zuśka et al., 2019). PCA is a workhorse for studies of variability in meteorology Reusch et al. (2005) and it has been widely applied to understand, interpret, and reconstruct large and multivariate climate datasets (Walsh, 1978; Mayewski et al., 1997).

The intent of PCA is to reduce the number of variables (Yang et al., 2017; Tadić et al., 2019). In the PCA method, the variance is calculated in relation to all the variables (monthly, annual, and seasonal). The main variable considered in this part of the study was temperature and the variables with the highest correlation coefficients were taken into account (Reusch et al., 2005; Zuśka et al., 2019). The analysis was conducted on a monthly, annual, and seasonal basis from 1981 to 2018.

The two well-known packages in "R" are "princomp" and "prcomp", built PCA using standard deviation and eigen decomposition, respectively. In this study, "prcomp" command was employed (Mayewski et al., 1997; Reusch et al., 2005).

Biplots

The Biplots interpretations are summarized as follows (Gabriel, 1971; Yang et al., 2017; Zgłobicki et al., 2018).

1. Closer points correspond to observations of similar scores in PCs.
2. Elements that are mutually associated have a similar origin.
3. A vector's length can be used to determine its variance.

In PCA analysis, the first component accounts for the largest amount of variation in the overall dataset, while the second component explains for the most variance that remains in the residual dataset (Richman, 1981).

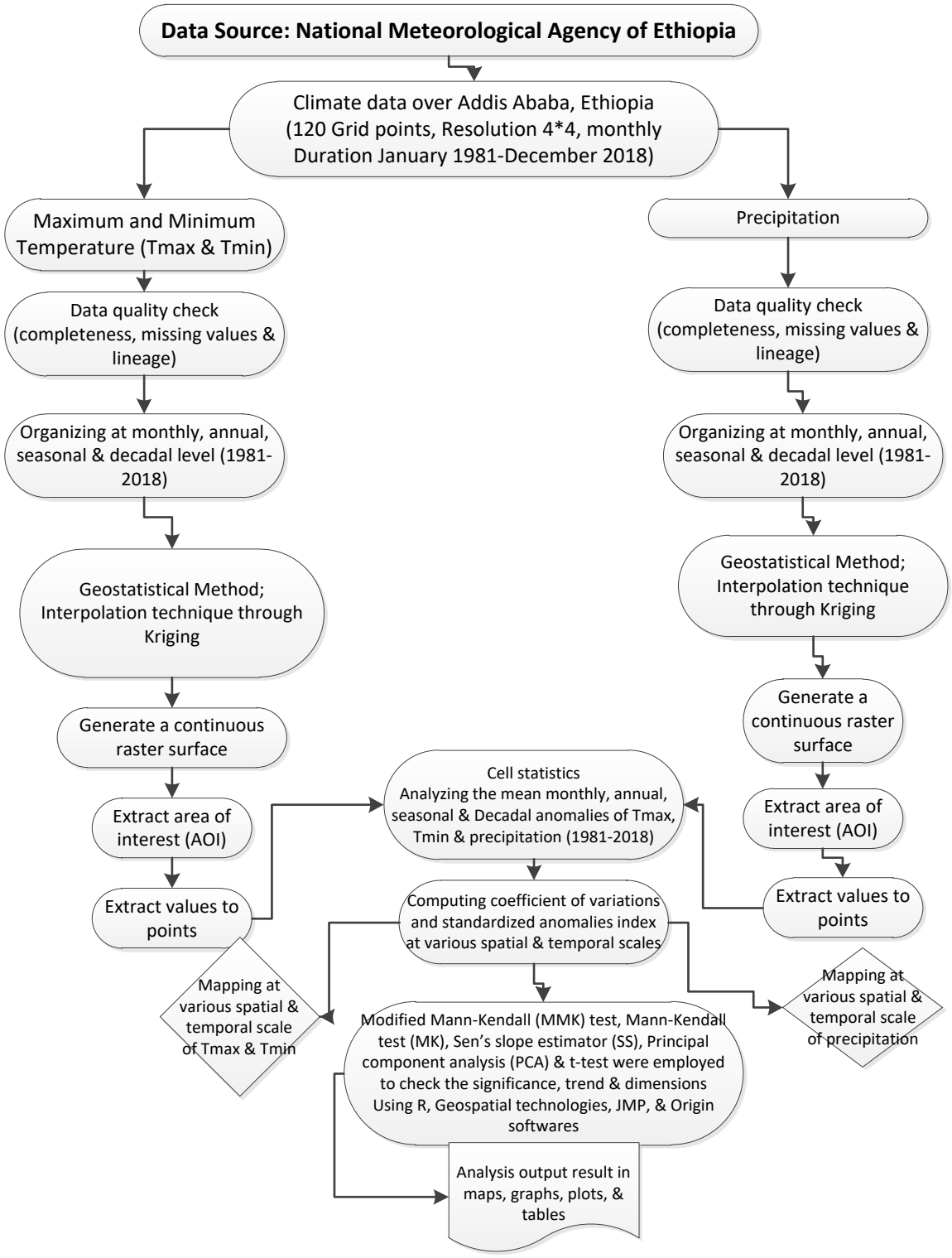

Figure 7: conceptual framework that helps to understand the overall flow of temperature and rainfall trend analysis.

3.9. Methodological flow and statistical analysis of LST extraction

Figure 9 shows the overall methodological flow pursued to analyze the temporal change in and comparison between the LULC and the LST. The scattered plot was constructed using linear regression for the two periods of 1985 and 2020 to correlate LST with NDVI and NDBI. All LST, NDVI, and NDBI pixel values were transformed into points of data (Ranagalage et al., 2017).

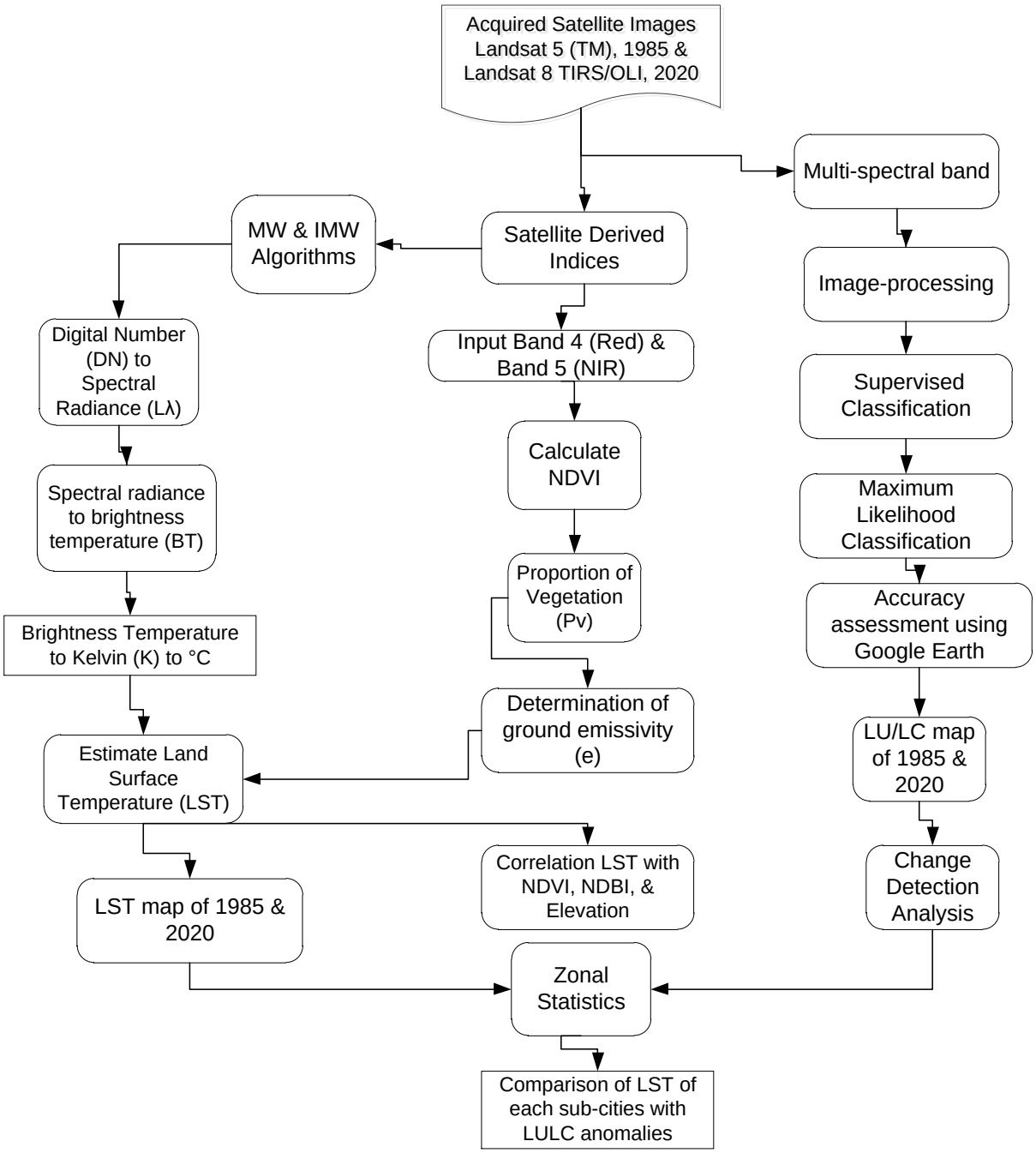

Figure 8: Conceptual framework for land surface temperature extraction.

3.9.1. Data preprocessing

The most appropriate method for studying the spatial and temporal variations in LST is with the application of remote sensing data (Li et al., 2013). LST retrieved from remote sensing thermal infrared data widely recognized as an effective method for examining the spatial and temporal patterns of UHIs (Sun et al., 2012; Dissanayake et al., 2019; Liu et al., 2019). For this study, two sets of remotely sensed data; Landsat 5 Thematic Mapper (TM) for 1985 and Landsat 8 Operational Land Imagery (OLI/TIRS) for 2020. The datasets were obtained from an open-source United States Geological Survey (USGS), Centre for Earth Resources Observation and Science (http://earthexplorer.usgs.gov) free of charge.

Kindu et al. (2013) suggested that cloud-free dry month imageries were utilized to reduce classification gaps between land use classifications caused by seasonal variations. The acquired Landsat images underwent band composite and pre-processing such as image enhancement techniques were applied to enhance the quality of the images for a better interpretation of the analysis result. The processed Landsat scenes that covered the project site were subsequently extracted using the study area boundary. Furthermore, a 30-meter resolution Digital Elevation Model (DEM) from Shuttle Radar Topography Mission (SRTM) of the USGS was downloaded and utilized to describe the research area's relief. The purpose of the DEM data was to demonstrate the relationship with the LST (Worku et al., 2021b).

3.9.2. Extraction of LST

The three important techniques for calculating LST from thermal bands. These are: mono-window algorithm (MWA) developed by Qin et al., (2001), Split window algorithm first discovered by Mcmillin (1975) and Single Channel (SC) developed by (Mcmillin, 1975)(M. Jin et al., 2015; Z.-L. Li et al., 2013). The upgraded method of the mono-window algorithm used to estimate LST from the thermal infrared (TIR) Bands of Landsat-8 improved by Wang et al. (2015). The mono-window algorithm is simpler than the split-window approach, since it only requires two atmospheric parameters i.e. transmittance and mean atmospheric temperature for LST retrieval of Landsat 5TM (Qin et al., 2001; Wang et al., 2015). In the case of Landsat 8 to retrieve LST from thermal bands (Band 10), it requires one additional parameter that is ground emissivity. Landsat 8 brightness temperatures was computed to determine the mean land surface emissivity and subsequently estimate the LST (Naeem et al., 2018; Moisa et al., 2022).

3.9.2.1. LST extraction from Landsat 5

Landsat 5 TM band 6 image was utilized for retrieving temperature for the year 1985 (Sobrino et al., 2004; Yeneneh et al., 2022). To compute land surface temperature (LST), the following steps were applied. The computation of at sensor radiance is a fundamental first step in converting image data from several sensors and platforms into a physically appropriate common radiometric scale (Li et al., 2013). Conversion at sensor spectral radiance ($Q_{cal\ to}\ L_\lambda$).

A. The TM image DNs was converted into thermal spectral radiance using the equation (Eq.14) below (Chander et al., 2009; Wang et al., 2015).

Eq.14

$$L_\lambda = \left(\frac{LMAX_\lambda - LMIN_\lambda}{QCALMAX - QCALMIN}\right) * (QCAL - QCALMIN) + LMIN_\lambda$$

Where:

L_λ = spectral radiance at the sensor's aperture [W/(m^2 sr μm)]

Q_{cal} = Quantized calibrated pixel value [Band 6]

Q_{calmin} = minimum quantized calibrated pixel value corresponding to LMIN$_\lambda$[1]

Q_{calmax} = maximum quantized calibrated pixelvalue corresponding to LMAX$_\lambda$[255]

LMIN$_\lambda$ = spectral at sensor radiance that is scaled to Q_{calmin} [W/(m^2 sr μm)]

LMAX$_\lambda$ = spectral at -sensor radiance that is scaled to Q_{calmax} [W/(m^2 sr μm)]

B. Conversion to At-satellite Brightness Temperature

Brightness temperature (BT) is the actual temperature observed by the satellite under emissivity theory (Chander et al., 2009). The Landsat TM band 6 satellite image was converted from spectral radiance to temperature using Planck's equation (Eq.15) (Tan et al., 2010; Worku et al., 2021).

Eq.15

$$\mathrm{T} = \frac{K2}{Ln\left(\frac{K1}{L\lambda} + 1\right)}$$

Where:

T = At-satellite brightness temperature ($^\circ$K) L_λ = Top of Atmospheric (TOA) spectral radiance Watts/m^2 * rad * μm))$K1$ = Band-specific thermal conversion constant K2 = Band-specific thermal conversion constant.

C. Conversion of degrees Kelvin into Celsius

In order to convert kelvin into Celsius, 273.15 was subtracted from the degrees kelvin value (ESRI, 2014; Kumari et al., 2018).

3.9.2.2. LST extraction from Landsat 8

On the other hand, to extract the land surface temperature from Landsat 8, the listed below steps had been applied.

A. Top of Atmospheric Spectral Radiance Conversion

The digital values of Landsat 8 OLI/TIRS of band 10 images were converted to spectral radiance using (Eq.16) the following algorithm (Abdullah et al., 2019; USGS, 2019). The band data were transformed to reflectance using the reflectance rescaling coefficient provided in the product metadata file. For operational land imagery (OLI) data, the equation (Eq.16) is applied to convert digital number (DN) values to top of atmospheric reflectance (USGS, 2015).

Eq.16

$$\rho\lambda = M_\rho * Q_{cal} + A_\rho$$

Where:

$\rho\lambda$: reflectance

M_ρ : band-specific multiplicative rescaling factor from the metadata (Radinace_Multi_Band_x, where x is the band number)

A_ρ : band-specific additive rescaling factor from the metadata. (Reflectance_Add_Band_x, where x is the band number)

Q_{cal} : quantized and calibrated standard product pixels values (DN)

B. Conversion of radiance to at sensor brightness temperature

The at-sensor brightness temperature is calculated using the assumption that the earth's surface is a black body and incorporates atmospheric effects. The conversion of the brightness temperature from at-sensor radiance is given by (Chander et al., 2009; Ndossi & Avdan, 2016). After converting the digital number to reflection, the TIRS band 10 data should be transformed from spectral radiance to brightness temperature (BT) using the thermal constants listed in Table 3. The equation (Eq.17) below is used to convert the reflectance to brightness temperature (Tan et al., 2010). Landsat 8 has two sensors: Operational Land Imager (OLI) and Thermal Infrared Sensor (TIRS). The TIRS has two thermal bands, Band 10 and 11. However, after the launch of Landsat

8, that was in 2013, Band 11 could not be used because there was a radiance emitted outside the instruments field of view across the focal plane. The stray light effect was roughly 8% higher than the normal thermal radiance received on the band 11 (Montanaro et al., 2014; Gerace & Montanaro, 2017). Therefore, because of this calibration uncertainty, Landsat 8 TIRS of band 11 could not be used (Montanaro et al., 2014; Guha et al., 2018). In this study, only Band 10 Landsat 8 OLI-TIRS image was employed.

Table 3:Satellite data radiance constant value.

Satellite/sensor	Year	K1	K2
Landsat-5/TM	1985	607.76	1260.56
Landsat-8 OLI/TIRS	2020	799.028	1329.2405

Source: respective year metadata.

Eq.17

$$BT = \frac{K2}{Ln\left(\frac{K1}{L_\lambda} + 1\right)}$$

Where: K_1 and K_2 stand for the band-specific thermal conversion constants from the metadata.

C. Conversion to degree Celsius

LST values from Landsat 8 OLI/TIRS were converted to degrees Celsius by subtracting 273.15 from Kelvin (Eq.18) (Kumari et al., 2018; Moisa et al., 2022).

Eq.18

$$LST\ (°C) = LST(K) - 273.15$$

Where:

°C = LST in degree Celsius

K = LST in Kelvin

D. NDVI estimation

Emissivity is the ratio of radiance from a black body at the same temperature to brightness from real-surface materials at that same temperature (Norman & Becker, 1995; Grujić, 2023). The NDVI threshold value was used to estimate emissivity from satellite thermal band data by

characterizing all land surface types (Sobrino et al., 2001; Wang et al., 2015). The visible and near-infrared bands were used to calculate the Normalized Difference Vegetation Index (Huang et al., 2021). The NDVI must be estimated since the amount of vegetation present is a crucial component in estimating LST (Weng et al., 2004; Balew & Korme, 2020a). Calculating the amount of vegetation and emissivity is also essential (Weng et al., 2004; Pettorelli et al., 2005; Bindi et al., 2009; Worku et al., 2021). NDVI was computed using equation (Eq.19).

Eq.19 $$NDVI = \frac{NIR_{Band} - Red_{Band}}{NIR_{Band} + Red_{Band}}$$

Where:

NIR_{Band} is near infrared band reflectance (Band 4 in Landsat 5 and Band 5 in Landsat 8);

Red_{Band} is red band reflectance (Band 3 in Landsat 5 and Band 4 in Landsat 8).

The value of the NDVI spans from -1 to 1. The greater the NDVI value, the denser and heathier the vegetation. Healthy vegetation typically has an index between 0.1-0.75, however for rock, soil, and water bodies are almost always negative (Tan et al., 2010).

E. Proportion of vegetation and Land surface emissivity estimation

Proportion of vegetation (Pv) computed (Eq.21) using NDVI (Carlson & Ripley, 1997; Jimenez-Munoz et al., 2009; Jin et al., 2015; Quintano et al., 2015).

Eq.21

$$P_v = \left[\frac{NDVI - NDVI_{min}}{NDVI_{max} - NDVI_{min}}\right]^2$$

Where $NDVI_{max}$ is a fully vegetated land-covers with the value (0.5); $NDVI_{min}$ is a non-vegetated land-covers value (0.2). Sobrino et al. (2004) and Wang et al. (2015) states that the suggested technique derives the emissivity values from the NDVI while considering several scenarios: if the NDVI < 0.2, the pixel is regarded as bare soil, and the emissivity 1is derived from reflectivity values in the red region with a value 0.964. The same sources further explained that NDVI>0.5, regarded as fully vegetated; an emissivity of 0.986 and if NDVI ≤ 0, the pixel can be regarded as water with LSE of 0.991. Since the land surface emissivity is a proportionality factor that scales

blackbody radiance (Planck's law) to estimate the emitted radiance and also the efficiency of transmitting thermal energy across the surface into the atmosphere, land surface emissivity LSE (ε) is crucial in order to estimate LST (Jimenez-Munoz et al., 2009).

According to Sobrino et al. (2004); Zhihao Qin et al. (2006) indicated that land surface emissivity (ε) was computed based on the following formula (Eq.22).

Eq.22

$$\varepsilon = 0.004 * \rho v + 0.986$$

The calculated radiant surface temperatures was corrected for emissivity using the equation (Eq.23) as suggested by (Chibuike et al., 2018):

Eq.23

$$\text{LST} = \ BT/\{1 + [(w^* \ BT/\rho) * \ln(\varepsilon)\ ]\}$$

Where:

LST is land surface temperature Celsius (°C), BT at satellite brightness temperature in (°C),

λ is the wavelength of emitted radiance, ρ is 1.4348×10^{-2} m k, ε is land surface emissivity.

F. NDBI estimation

One important metric for comprehending urban climate change is the NDBI. The value ranges from -1 to +1, a higher positive value denotes the built-up area, a small positive value indicating bare soils, and a negative value signifies water bodies and vegetation (Ranagalage et al., 2017; Ranagalage et al., 2018; Rousta et al., 2018). The NDBI was retrieved from near-infrared band and mid-infrared bands (MIR) (Li et al., 2017). The NDBI is used to estimate the LST and its correlation with LULC as suggested by (Rousta et al., 2018; Balew & Korme, 2020b). The NDBI is applied to identify the urban built up area with the area of concern as stated in (Eq.20) (Zha et al., 2003; Estoque et al., 2017; Rousta et al., 2018; Simwanda & Murayama, 2018).

Eq.20

$$NDBI = \left[\frac{MIR_{Band} - NIR_{Band}}{MIR_{Band} + NIR_{Band}}\right]$$

Where MIR band represents Band 5 in Landsat 5 and band 6 in Landsat 8, respectively. NIR band represents Band 4 in Landsat 5 and Band 5 in Landsat 8 respectively.

3.9.3. Land use land cover classification.

Land use land cover classification was done with the use of Landsat 5TM and Landsat 8 OLI/TIRS. Using both ERDAS Imagine version 15 and ArcGIS version 10.8.2 An object based supervised classification method with Maximum Likelihood Classifier (MLC) technique was applied to compartmentalize LULC classes into appropriate categories (Hussain et al., 2013; Chen et al., 2012; Ganasri & Dwarakish, 2015; Rousta et al., 2018). Accordingly, the LULC classes in the study area were classified into five major categories: (1) forest, (2) open/bare land, (3) built-up area, (4) waterbody, and (5) cultivated land. The different LULC classes were identified using historical records of Google Earth images, which improved classification accuracy. In essence, classification was carried out between the years 1985 and 2020 with the aim of obtaining data on the rate and magnitude of LULC trend changes during the investigation period and their impact on the UHI/LST.

As Mekonnen et al. (2022) noted a detailed change detection statistical analysis were computed and comparison was made with the analysis output of one image with the corresponding value of the second image. As a result, using the following equation (Eq. 24), the rate of change within the same LULC class and between two time points were calculated and stated in square kilometers (Sq.km) and percentages (%) (Abera et al., 2018).

Eq.24

$$Annual\ rate\ of\ LULCC(\%year^{-1}) = \frac{\frac{A_j - A_i}{A_i}}{t} * 100$$

where LULC = land-use/cover; A_i = area of LULC of year i (previous); A_j = area of LULC of year j (recent); and t = number of years between years i and j.

The LULC classification, statistical analysis, and LULCC mapping were carried out using ERDAS imagine 15 and ArcGIS version 10.8.2. In this regard, Herold et al. (2003) noted that geographic information systems (GIS) and remote sensing (RS) are both extensively employed and acknowledged as potent and successful techniques for identifying spatiotemporal LULC dynamics. Researchers can monitor land-use patterns and process by using remote sensing (RS) to gather valuable multi-temporal data (Lambin et al., 2001). It can also be used to regularly observe long-term large-scale patterns of LULC (Chan et al., 2013). While, Geographical Information

Systems (GIS) provides the capabilities for trend analysis and presenting the analysis output through mapping (Zhang et al., 2019).

3.9.4. Validation of classified LULC maps

The accuracy assessment reflects the true disparity between the classification and the corresponding reference map (Tsutsumida & Comber, 2015). There could be some errors in classified LULC maps generated from remote sensing imagery. As a result, accuracy assessment evaluation was carried out in order to uncover the errors and assure the dependability of the LULC maps created (Merga et al., 2022). To assess the classification's quality, an accuracy assessment was performed using 300 sample points taken from all five LULC classes.

The samples for each LULC class were generated using the create accuracy assessment points method available in the ArcToolbox, under data management tools, and superimposed over Google Earth time series images for the relevant year of LULC maps. For each land use class, 60 sample points were compared with the corresponding classified land use class. In connection to this, Congalton (1991) noted that greater than 250 reference pixels are required to estimate the mean accuracy of a class. As demonstrated in Eq. 25 and 26, the error matrix, overall accuracy, and kappa coefficients were utilized to evaluate a pixel-based LULC classification (Mishra et al., 2019; Moisa & Gemeda, 2021b).

Eq. 25

$$OAC = \frac{\sum Xij}{N} * 100$$

Eq. 26

$$K_{hat} = \frac{(Obs - exp)}{1 - Exp}$$

Where OAC is the overall precision, K_{hat} is the kappa statistics, N is the total number of classes, Xij is the row total, Obs is the accuracy reported in the error classification.

CHAPTER FOUR: RESULT AND DISCUSSION

4.1. Rainfall variability in Addis Ababa

The long-term mean annual rainfall estimates (1981-2018) were divided into five rainfall regime zones: 943-972 mm for regime 1, 973-1010 mm for regime 2, 1011-1160 mm for regime 3, 1,061-1,110 mm for regime 4, and 1,111-1,150 mm for regime 5. Based on the analysis results, the long-term mean annual rainfall estimates in the studied area range between 943 and 1150 mm (Figure 10B, C). The western, partly central, and northern areas of Addis Ababa received the greatest amount of rainfall. In connection with this, rainfall is likewise anticipated to increase over the city over time, but the pace of change is faster in the north than in the south (Arsiso et al., 2018). On the other hand, the southern and southeastern parts of the city received the least rainfall. At sub-city level, Gulele received the highest mean annual rainfall (1120-1150 mm), while Akaki Kality received the smallest (943-972 mm).

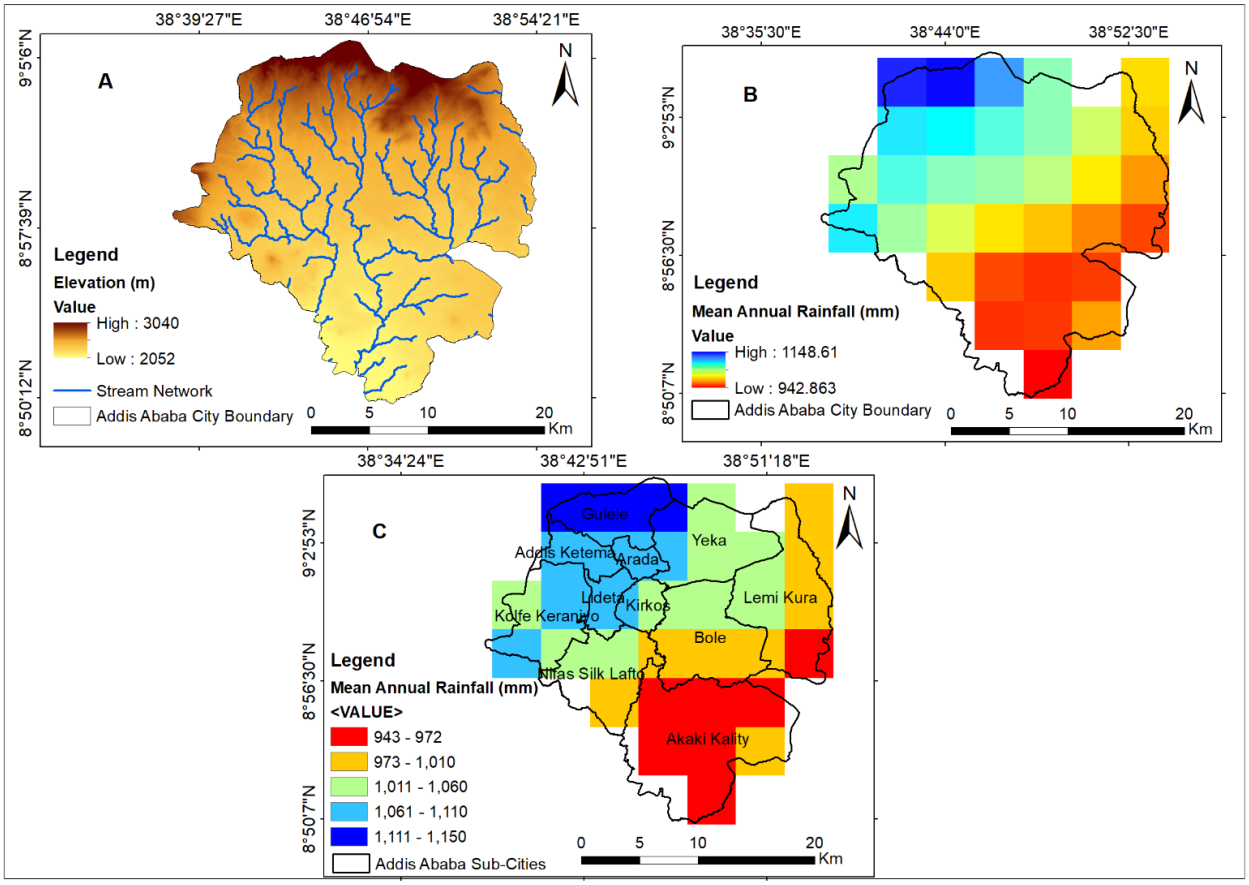

Figure 9: Elevation (A), long-term mean annual rainfall (mm) spatial distributions (B), and long-term mean annual rainfall spatial distributions (C) of Addis Ababa City (1981-2018).

As shown in Figure 10, the maximum rainfall registered in the peak northern edge of Gulele sub-city, while the minimal precipitation occurred in the low elevation southern part of Akaki sub-city. In this case, the result is in line with the findings of Belay et al. (2019) reported that a strong relationship between mean annual rainfall and elevation. In this regard, the findings of the study agree with people's experiences and observations.

4.2. Rainfall distribution across seasons

The spatial distribution of rainfall across the three seasons (*Kiremt, Belg,* and *Bega*) is shown in Figure 11A–C. During the *Kiremt* season (Figure 11A), the north-western part of Addis Ababa City (all parts Gulele, Addis Ketema, and some areas of Arada, Yeka, and Kolfe Keraniyo) received the maximum rainfall (806-874 mm), while the southern part (Akaki Kality sub-city) received the least (675-696 mm). In a similar vein, during the *Belg* season (Figure 11B), the highest rainfall values were recorded in the central parts of Addis Ababa (Kirkos, Lideta, Bole, and Yeka, as well as tiny areas of the Kolfe Keraniyo sub-cities). The analysis results also showed that the lowest rainfall occurred in Akaki and Lemi Kura sub-cities. During the *Bega* (dry) season (Figure 11C), the western and central areas of the city received the highest rainfall. In contrast, the southern parts of Addis Ababa received the least rainfall. *Kiremt* season rainfall was distributed in the same spatial manner as annual rainfall. With the exception of the *Kiremt* season, the southern and southeastern parts of the city received the main rainfall in all the other seasons (*Belg* and *Bega*) (Seleshi & Zanke, 2004).

Hence, it is possible to infer that precipitation and altitude are highly intertwined (Arsiso et al., 2018). In addition, Belay et al. (2019) noted that rainfall is spatially linked with elevation. In this case, elevated areas of the northern and central parts of the city received the maximum precipitation as opposed to less elevated areas of southern Addis Ababa obtained the minimum precipitation.

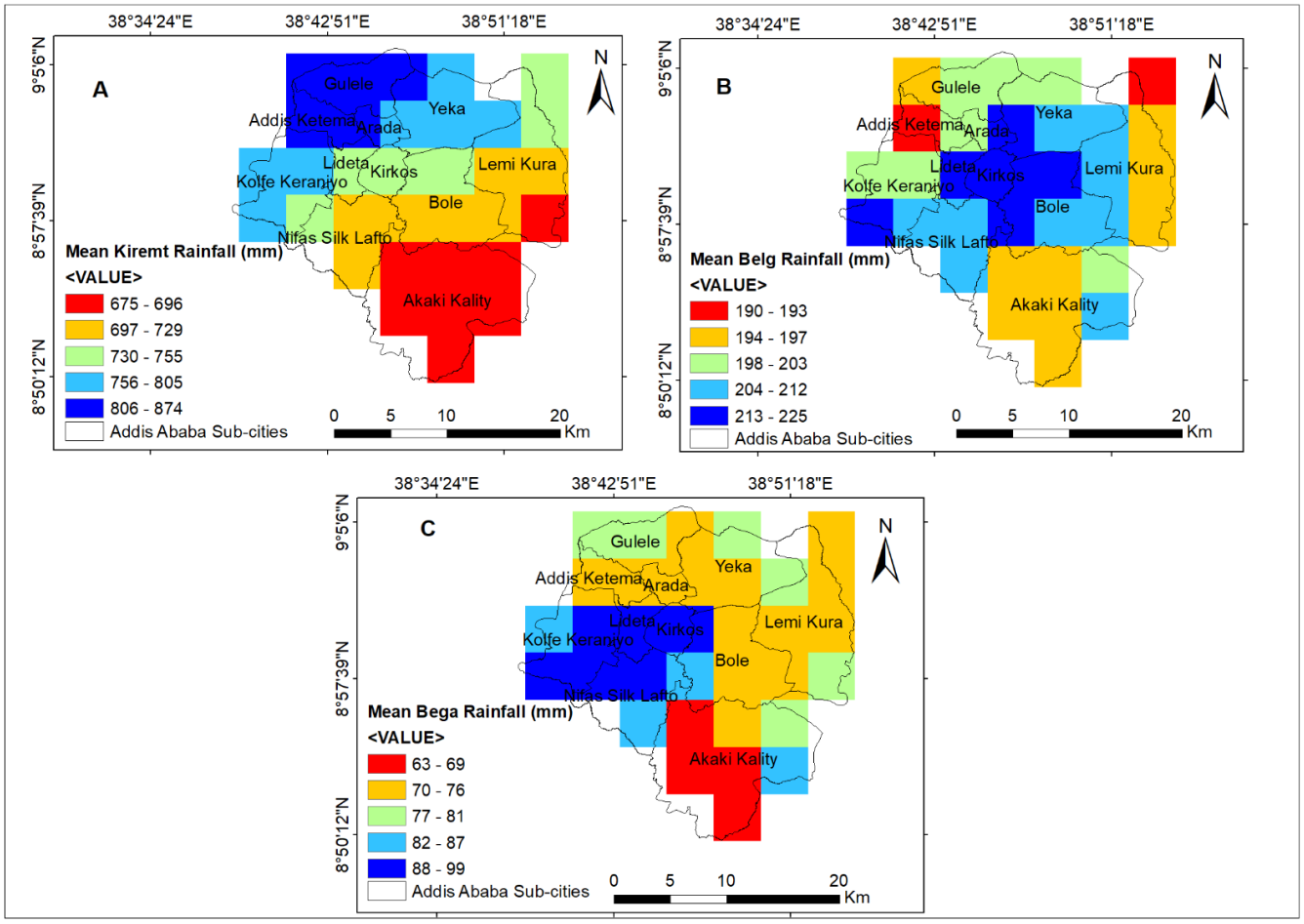

Figure 10: Spatial distributions of Addis Ababa's mean *Kiremt* rainfall (mm) (A), mean *Belg* rainfall (mm) (B), and mean *Bega* rainfall (mm) (C) (1981-2018).

4.3. Coefficient of variation analysis result

Figure 12 depicts the computed coefficient of variation (CV) value at pixel level in annual and seasonal basis (*Kiremt*, *Belg*, and *Bega*) (1981-2018). The highest inter-annual variability of rainfall was observed around the southwestern and northeastern edges of Addis Ababa, with CV > 20.6%. The inter-annual rainfall variability in these areas would affect urban agriculture productivity because it is around the fringes of the city where urban agriculture is largely practiced. While the rest of the entire city (central, southern, and eastern) experienced less inter-annual fluctuation of rainfall with (CV<20.5%), as seen in Figure 14 below. When contrasted with the annual, seasonal rainfall of *Bega* season had the highest inter-annual variability, reaching up to 88.3%. The CV during *Kiremt* season (7.89% < CV < 13.9%) appeared to be relatively stable compared to the other seasons. In connection

with this, previous studies (E.g., Asfaw et al., 2018; Mohammed et al., 2018; Alemu & Bawoke, 2020) reported that less rainfall variability found in *Kiremt* as compared to other seasons in Ethiopia, which is consistent with the result of this study.

The highest CV for *Kiremt* rainfall was witnessed in the southern, north-eastern, and pocket of places in south-western parts of the city. *Belg* rainfall CV (23.2% < CV < 33.7%) was higher than *Kiremt* rainfall, indicating that larger inter-annual variability of *Belg* season rainfall. During this season, the north-eastern and around the edge of western part of the city experienced higher CV. The maximum CV (63.6%<CV<88.3%) occurred during the *Bega* season. During this season, the highest rainfall variability was observed in the western part of the city that extends up to the center including southern and south-eastern areas of Addis Ababa.

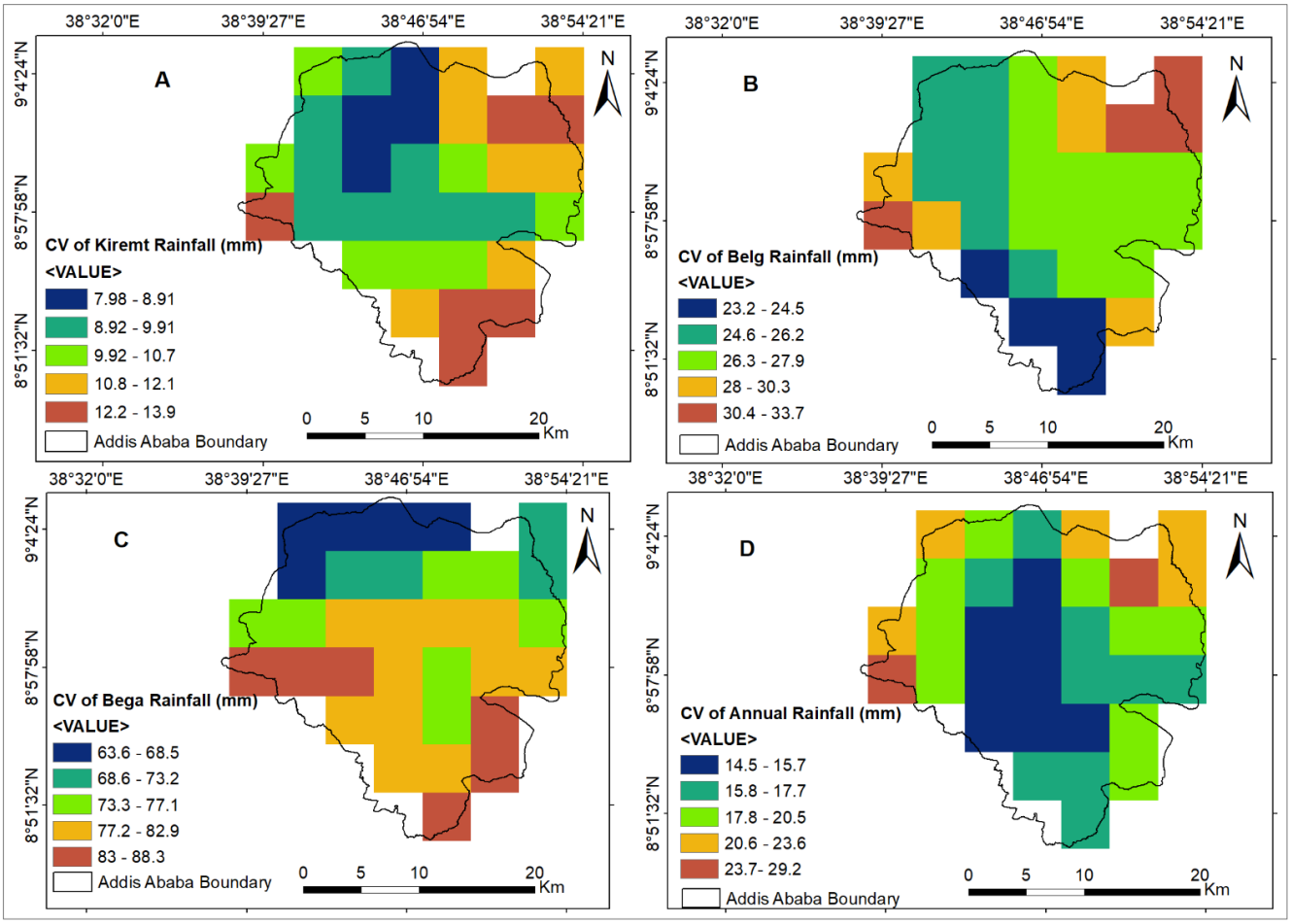

Figure 11: Spatial distribution of CV (%) in *Kiremt* (A), *Belg* (B), *Bega* (C) and annual season rainfall in Addis Ababa City (1981–2018).

4.4. Monthly rainfall variation

Figures 13 and 14 illustrate the long-term mean monthly (January to December) rainfall distribution in the study period. The analysis result showed that the wettest months were June, July, August, and September, which are the main rainy season, while the driest months were November, December, and January. During the months of March, April, and May, little rainfall was recorded which amounted to 67.25 mm, 88.75 mm, and 79.25 mm, respectively. The months with the highest rainfall were July (285.1 mm), August (308.3 mm), and September (144.2 mm).

The smallest amount of precipitation was recorded in December that averaged 6.8 mm. In relation to this, Seleshi & Zanke (2004) and Alemayehu & Bewket (2017) reported that the rainy months in Ethiopia were June, July, August, and September, while the driest months were October through February. In this case, the analysis result agreed with the earlier studies.

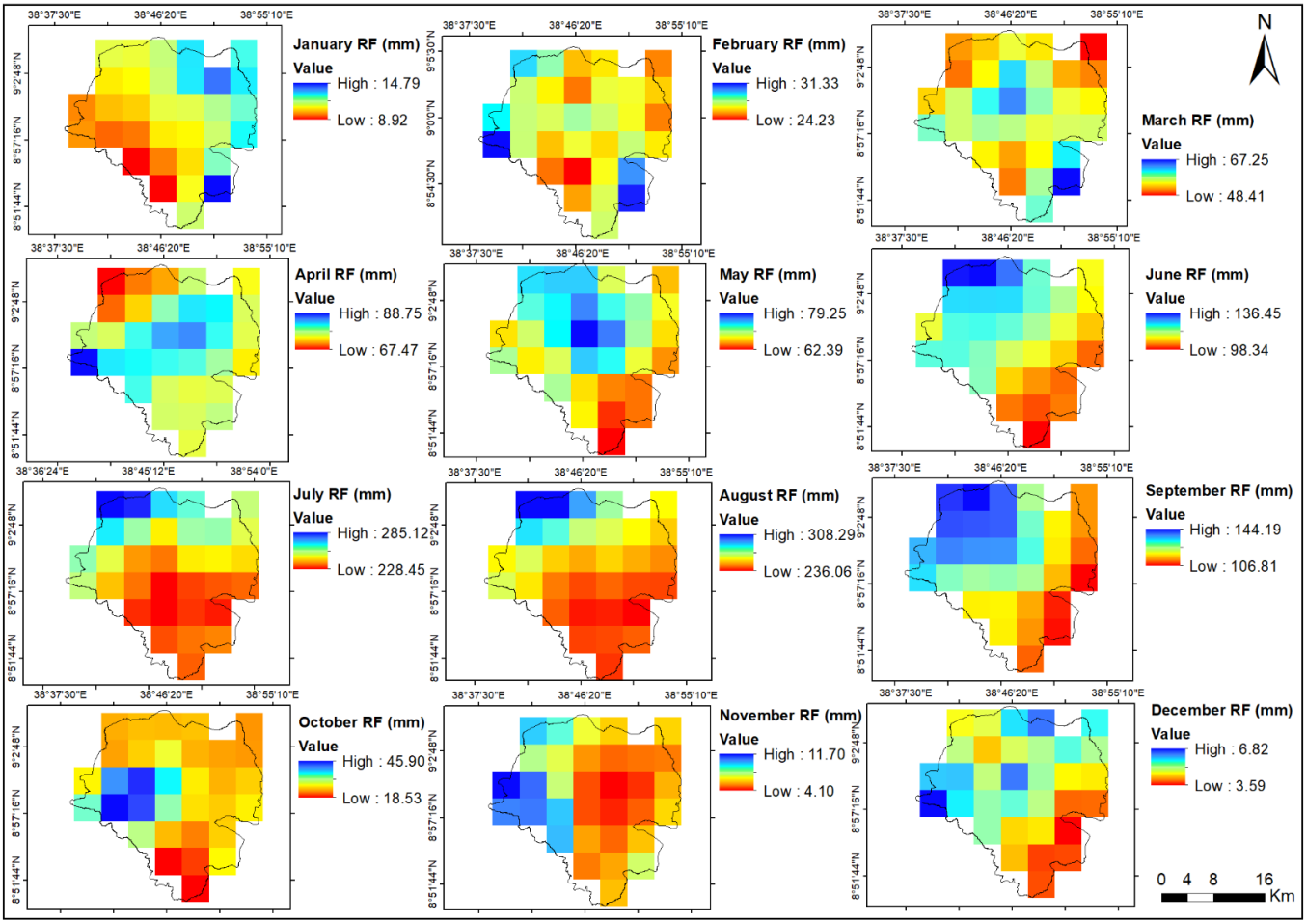

Figure 12: Depicts the spatial distribution of Addis Ababa City's mean monthly rainfall from 1981 to 2018.

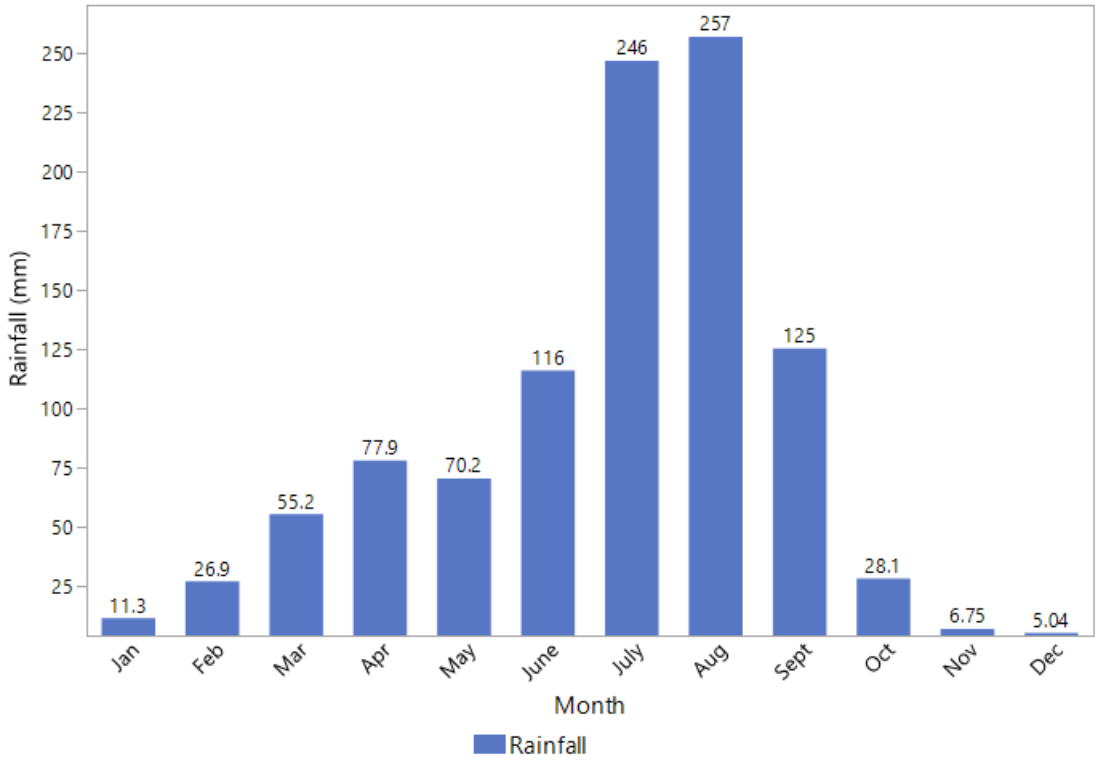

Figure 13: Mean monthly rainfall of Addis Ababa City during 1981-2018 periods.

4.5. Monthly Coefficient of variation analysis result

Figure 15 depicts the spatial distribution of monthly rainfall CV (%). CV greater than 100% show increases in the inter-monthly rainfall variability (Bayable et al., 2021). Based on this assumption, the analysis result demonstrated that there was more inter-monthly variability of rainfall in the research area that extends from October to March, with a coefficient of variation greater than 100%. This signifies that precipitation in those months was extremely variable. Conversely, lower inter-monthly variability happened in the months of July and August. When examining the occurrence of rainfall as Figure 14 and 15 illustrates, June is the onset of the main rainy (*Kiremt*) season while September appears to be the month where the rainfall ceases. In this case, as Figure 15 shows rainfall found to be extremely variable in both months (June and September) since the CV>40%.

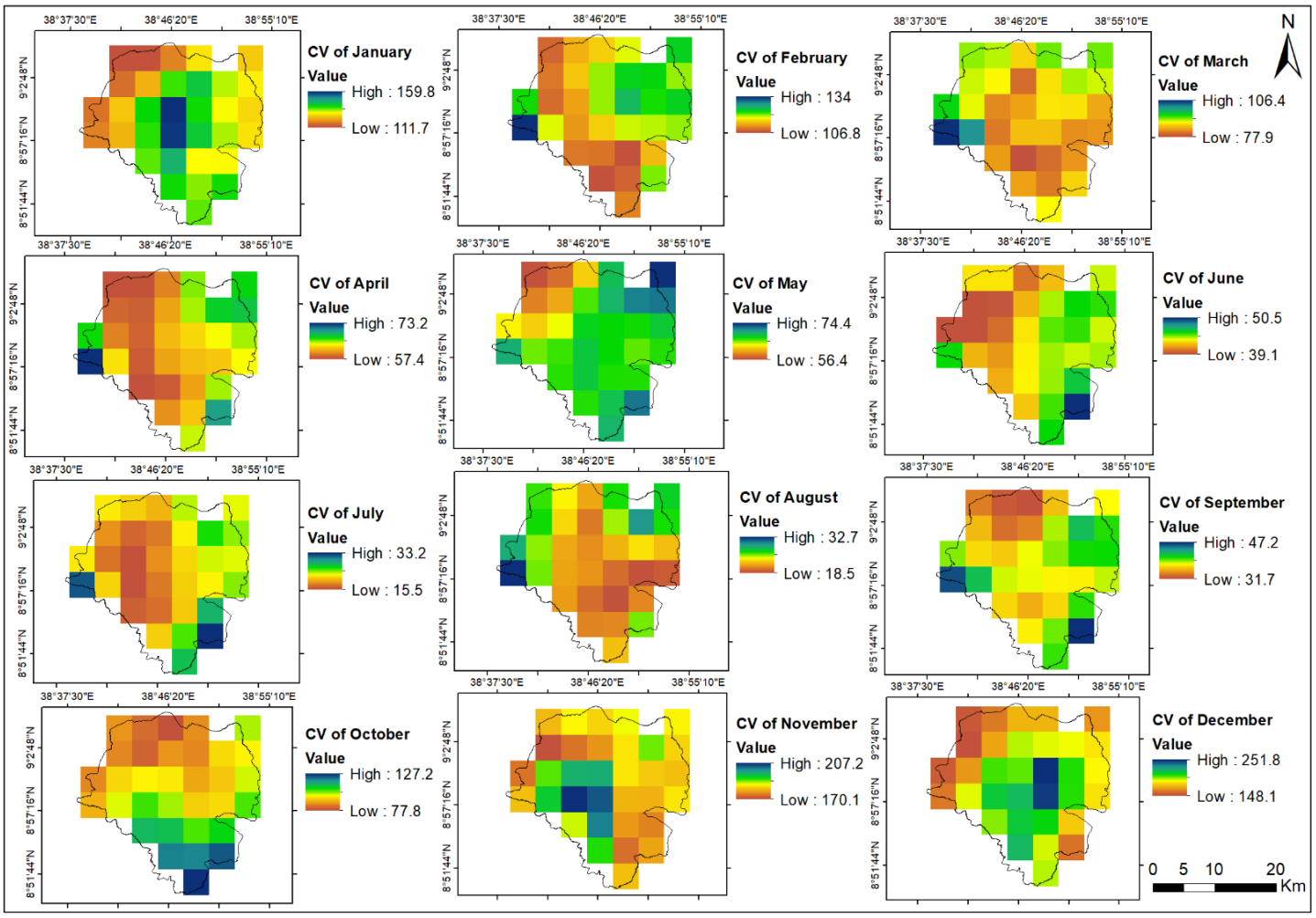

Figure 14: Spatial distribution of monthly rainfall CV of Addis Ababa City (1981-2018).

4.6. Mann-Kendall and Sen's slope test result for monthly, annual, and seasonal

4.6.1. Long-term monotonic trends of rainfall

The Mann-Kendall (MK) test and Sen's slope estimator analysis results of the mean monthly, annual, and seasonal rainfall in Addis Ababa city between 1981 and 2018 are shown in Tables 4 and 5. The positive and negative values reflect an increasing and declining trend in the data, respectively. The statistical analysis results showed a declining trend in rainfall for the months of January (-0.06), February (-0.58), March (-0.51), April (-0.78), July (-0.05), August (-0.02), September (-0.23), and December (-0.02), with a negative Sen's slope value. On the other hand, for the month of May (0.88), June (0.64), and November (0.10) revealed a positive rainfall pattern. A possible explanation for the increase in November rainfall would be associated with the

occurrence of untimely rainfall during this month. On the other hand, the increasing trend of May and June precipitation can be linked with the early onset of *Kiremt* season rainfall.

The degree of anomaly in rainfall trend is greater in the month of May, June, with Sen's slope estimate of 0.88 and 0.64 mm/year, respectively. Nevertheless, for all the months the trends were not statistically significant as the calculated P value was greater than 0.05.

Table 4: MK trend analysis of mean monthly rainfall in Addis Ababa City between 1981 and 2018.

Month	Mean's value	Kendall's tau	S	P-value	Trend	Significant	Sen's slope (mm/year)
January	11.25	-0.11	-79	0.33	Downward	Insignificant	-0.06
February	26.97	-0.21	-146	0.07	Downward	Insignificant	-0.58
March	55.37	-0.12	-83	0.30	Downward	Insignificant	-0.51
April	77.99	-0.13	-89	0.27	Downward	Insignificant	-0.78
May	70.32	0.14	99	0.22	Upward	Insignificant	0.88
June	115.91	0.11	77	0.34	Upward	Insignificant	0.64
July	246.22	-9.96	-7	0.94	Downward	Insignificant	-0.05
August	256.58	-4.27	-3	0.98	Downward	Insignificant	-0.02
September	125.47	-0.06	-43	0.59	Downward	Insignificant	-0.23
October	28.21	-4.27	-3	0.98	Downward	Insignificant	-0.01
November	6.77	0.20	144	0.07	Upward	Insignificant	0.10
December	5.02	-0.13	-91	0.26	Downward	Insignificant	-0.02

Source: statistical analysis in "R" studio

Results of the Sen's slope estimator for mean annual and seasonal (*Kiremt, Belg*, and *Bega*) rainfall showed a negative downward trajectory except for *Kiremt* season with a positive Sen's slope value of 0.22 mm/year (Table 5 and Figure 16). The mean seasonal and annual precipitation was not statistically significant where the computed P value for annual (0.65 mm/year), *Kiremt* (0.66 mm/year), *Belg* (0.17 mm/year) and *Bega* (0.07 mm/year) which is greater than the threshold value of $\alpha = 0.05$.

Table 5: MK trend analysis of mean annual and mean seasonal rainfall (1981-2018) in Addis Ababa City

Seasons	Kendall's tau	S	P-value	Trend	Significant	Sen's slope (mm/year)
Annual Rainfall	-0.05	-37	0.65	Downward	Insignificant	-0.11
Kiremt Rainfall	4.97	3.5	0.66	Upward	Insignificant	0.22
Belg Rainfall	-0.15	-103	0.19	Downward	Insignificant	-0.77
Bega Rainfall	-0.21	-145	0.07	Downward	Insignificant	-0.35

Source: statistical result in "R" studio. P is significant at $\alpha = 0.05$

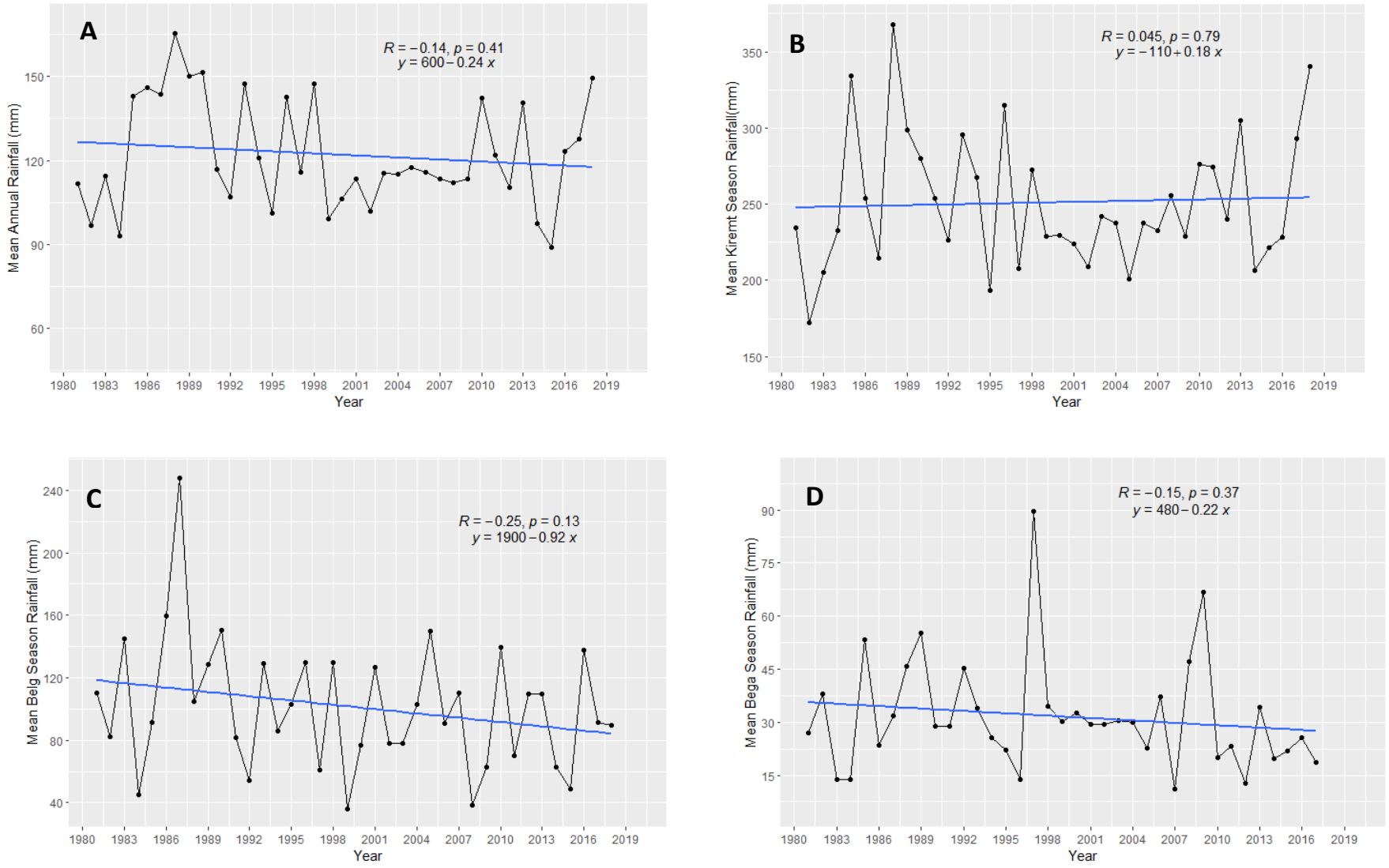

Figure 15: Long term mean annual (A), *Kiremt* (B), *Belg* (C), and *Bega* (D) rainfall of Addis Ababa City (1981-2018). Source: statistical analysis result in"R" studio.

In Ethiopia, geographic location is one of the determining factors for the distribution of precipitation, patterns, intensity, duration, and timing (Belay et al., 2021). Figure 16 demonstrated that the mean annual and seasonal rainfall pattern across the study period varies both spatially and temporally. One year with a slight positive anomaly followed by a negative anomaly. From this, one can infer that precipitation is highly erratic in nature across all seasons of the study period (1981-2018). The analysis result (Figure 16A) stipulated that the mean annual rainfall was slightly decreasing with R^2 value -0.14 across the observation period (1981-2018). Except for *Kiremt* season where the rainfall pattern showed a positive trend with R^2 value of 0.045 and P value of 0.79. Nevertheless, for the other seasons of annual, *Belg*, and *Bega*, the rainfall was decreasing with Pearson value of -0.14, -0.25, -0.15, respectively. As the scatter plot (Figure 16C) divulge that as compared with other seasons, the *Belg* season rainfall have significantly decreased across the study period with R^2 value of -0.25 and P value 0.13. Seleshi & Zanke (2004) noted that higher (lower) frequency of tropical depressions during from November through January followed by abnormally low (high) *Belg* rainfall.

In this case, the analysis result agrees with the MK test result shown in Table 4, where the Sen's slope estimator was positive as a result an upward rainfall trend observed for *Kiremt* season. The increasing trend of main (*Kiremt*) season rainfall could cause flooding and outbreak of human diseases unless proper mitigation and adaptation measures taken (Belay et al., 2021). Likewise, a mounting trend in *Kiremt* rainfall is likely to affect water catchment area of the city (Arsiso et al., 2018). The study's results are consistent with a research by Rosell (2011), which indicated that in Ethiopia's central highlands, there was a tendency of rising annual and *Kiremt* rainfall and decreasing *Belg* rainfall. Similarly, related research carried out in distinct parts of the country reported that there was a declining of *Belg* season rainfall (Alemayehu & Bewket, 2017; Jury & Funk, 2013; Abebe, 2006; Seleshi & Camberlin, 2006; Williams et al., 2012). The reduction of *Belg* (Spring) season precipitation in Ethiopia is caused by atmospheric oceanic interactions that significantly influence the distribution of rainfall in the region (Belay et al., 2021). In addition, the dynamics of global warming caused by El Niño southern-oscillation [ENSO] could affect substantially and decrease the trends of rainfall in East Africa (Matthews et al., 2018). Moreover, it was due to the La Niña effect that decrease rainfall in the *Belg* season in Ethiopia (Orke & Li, 2021). The dynamics of Intertropical convergence zone [ITCZ] over Ethiopia is tele-connected with El Nino occurrences (Seleshi & Zanke, 2004). Further explained that El Nino years are accompanied by below average *Kiremt* rainfall years.

The production of long-maturing crops such as Sorghum and Barley as short-maturing crops like barley depends on the spring season, which locally referred as "*Belg* season" and runs from March to May (National Meteorological Agency [NMA], 2007; NMSA, 2001b). The current variability of *Belg* rainfall in the city makes the season unrealistic for rainfed agriculture compared to the earlier time (Rosell, 2011). *Bulg* season rainfall was very important in Ethiopian agriculture as farmers in considerably area were producing crop using this season rainfall. Consequently, this would highly impact the food security and livelihood sources of the people who relied on urban agriculture as source of living in the study area.

4.7. Inter-annual and seasonal fluctuation of rainfall anomalies

Figure 17 depicted normalized annual and seasonal rainfall anomalies from 1981 to 2018. Both annual and *Kiremt* rains followed a similar pattern during the observation period (Figure 17 A, B). Based on the analysis result, from 1981 up to 1984 both the annual and *Kiremt* season precipitation exhibited a declining trend. Standardized rainfall anomalies (SRA) are positive from 1985 through 1991 for both seasons except a positive anomaly occurred for *Kiremt* season of the year 1987. The year 1988 was the wettest year for the annual and *Kiremt* seasons. From 2004 to 2013, except 2009 a positive annual rainfall anomaly was observed. By contrast, the 1980s were wet compared to the 1990s and 2000s. The standardized annual and *Kiremt* season rainfall anomalies generally showed a decreasing trend in terms of amount and proportion after the year 2001. The MK test result (Table 4), which showed that the P value > 0.05 for all four seasons was statistically insignificant, consistent with the standardized rainfall anomalies result. In Ethiopia the highest yearly rainfall contribution generally comes from *Kiremt* (56%) and is followed by *Belg* (25%) (Alemayehu et al., 2020). During *Belg* season, a negative anomaly was observed in 1982 and 1984, which was followed by a prolonged period of positive anomalies until 1991. Beginning from 1992, the *Belg* season was dominated by negative anomalies i.e. suffered from drier conditions in 1992, 1997, 1999, 2008, 2009, 2014, and 2015 (Figure 17C). In this season, 1999 was assumed to be the driest year while 1987 was the wettest year.

Bega is the driest season in Ethiopia that lasts from October to February (Alemayehu & Bewket, 2017; Seleshi & Zanke, 2004). As the analysis result stipulated (Figure 17D), beginning from the initial year, 1981 that extends to the mid of 1990s, a positive anomaly was observed in *Bega* season except 1982 and 1983. As opposed to this, in the later part of the study period, starting from 2003 to

2018 it was dominated by a negative anomaly. This period (1982-2018) assumed to be the driest decade in comparison with the preceding and 2012 was the driest year in the season.

The findings of the study showed that across the four seasons (Annual, *Kiremt, Belg*, and *Bega*) Addis Ababa experienced a negative anomaly in the year 1984. As the analysis result stipulated that the annual and *Kiremt* rainfall anomaly followed a similar pattern in the observation period. The driest and wettest year for annual and *Kiremt* rainfall was 1982 and 1988, respectively. In Ethiopia when the seasonal rainfall falls from 30% to 50% below normal drought usually occurs (Mera, 2018). Based on the classification of the drought index, the study area had extremes in 1982 and 1984. The years 1999, 2014, and 2015 severe droughts occurred, whereas the year 1997 witnessed moderate droughts. In the remaining years, there was no drought record.

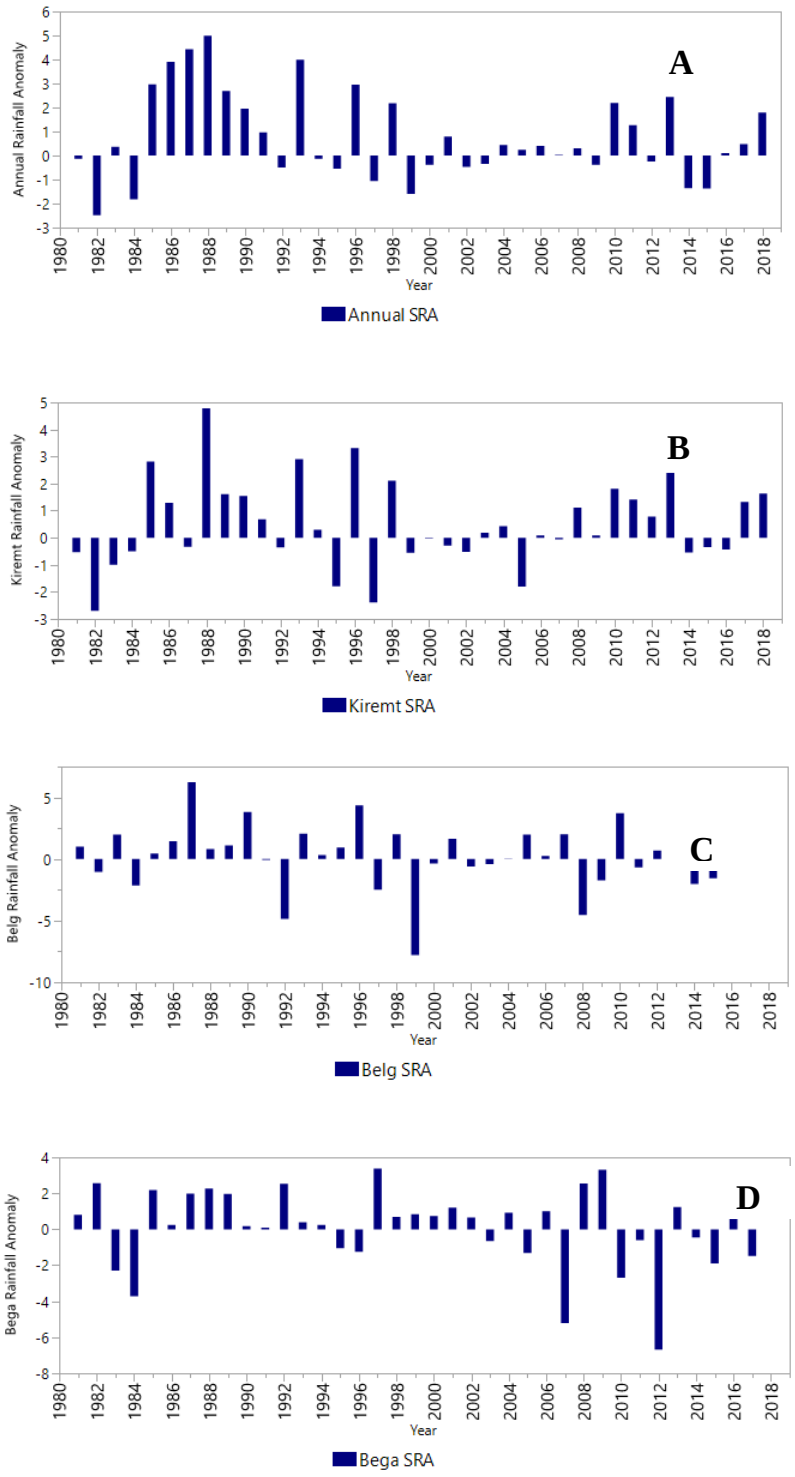

Figure 16: Portrays Annual SRA (A), *Kiremt* SRA (B), *Belg* SRA (C) & *Bega* SRA (D) of Addis Ababa City.

4.8. Rainfall trend at decadal level

Figures 18 and 19 reveal the spatial distribution of rainfall and the coefficient of variation across decades in the study area. The result has shown that, in the first decade (1981-1990), the minimum rainfall was 955.7 mm which was recorded in 1982 and the maximum was 1982.3 mm registered in 1988. For the same period, the mean decadal precipitation was 1267.9 mm, with a standard deviation ±39.9 mm and a coefficient of variation 3.1%. The mean rainfall between 1991 and 2000 was found to be 1167.8 mm in which the minimum and maximum rainfall was 969.9 mm and 1700.9 mm that occurred in 1993 and 1999, respectively. For the same study period, the standard deviation was ±21.2 mm, with a coefficient of variation of 1.92%. The mean decadal rainfall from 2001 to 2010 was 1135.1 mm, with a standard deviation of ±14.6 mm and a coefficient of variation of 1.5%. The minimum and maximum rainfall in this decade were 2002 (1102.8 mm) and 2010 (1416.4 mm). In the last observation period (2011-2018), the area received minimum (992.7 mm) and maximum (1448.2 mm) rainfall in 2015 and 2018, respectively. The average rainfall in the period was 1177.3 mm with standard deviation of ±35.9 mm and 3.6 % coefficient of variation.

Discrepancy in volume, intensity, and distribution of rainfall was recorded in the study area across the observation period across space and time. The Northern and Western part of Addis Ababa city relatively received high amount of rainfall as depicted in Figure 18. Paradoxically, the reverse is true for the Southern part of Addis Ababa where it received the minimum rainfall amount. This has to do with the topography of the country. In this regard, literature underline that the intricate nature the physical landscape play a pivotal role in Ethiopia's climate (Ayele et al., 2016).

Generally, there was a reduction in mean decadal rainfall over time particularly in the first two decades (1981-2000) where the rainfall reduced by 100.1mm. The rainfall amount diminished between 2001 and 2010 by 32.75 mm. However, in the last eight observation years (2011-2018), the mean rainfall was augmented by 42.24 mm. In this regard, the recent IPCC report designated that the global precipitation over land has likely increased since mid of 20th century, relatively faster rate of increase observed since the 1980s (IPCC, 2021c). With the study area context, a study conducted by Arsiso et al. (2018) highlighted that the rainfall anomalies under the two emission scenarios (RCP4.5 and RCP8.5) anticipated to increase in 2030s (2020-2030) in the city. Similarly, Feyissa et al. (2018a) underscore that there will be an increase in precipitation under intermediate (RCP4.5) and high emission scenarios (RCP8.5) in 2080s. The same IPCC report further explained

that urbanization increase the mean and heavy precipitation in cities. As there would be more impervious surfaces which would warm both the surface and atmosphere eventually increase atmospheric humidity, subsequently resulting in more intense rainfall events (Xie et al., 2019; Wang et al., 2020). As the IPCC report suggested, in this study, the possible reasons for the increase of precipitation over the last observation period (2011-2018) caused by an increasing rate of urbanization driven by high population growth in the city which immensely contributed for the slight positive trend of precipitation in the study area. In addition, Arsiso et al. (2018) indicated that there will be a projected precipitation increase in the near future (2020-2030) in Addis Ababa which can be considered as a good indicator for the upward trend of precipitation over the last eight years.

As compared with the mean rainfall of the first decade (1981-1990), the rainfall declined by 90.6 mm. Similarly, as the Table shows that surprisingly the maximum rainfall across the four observation periods has been reduced alarmingly. While the mean minimum precipitation lacks a constant pattern, one decade with a positive anomaly followed by a negative anomaly. It was in the first decade (1981-1990) that the average highest maximum rainfall was recorded with an amount of 1982.3mm and the amount progressively declined in the recent decades. The difference between the first (1981-1990) and last observation (2011-2018) period was 534.1mm rainfall. Overall, it is possible to conclude that the mean decadal and decadal maximum rainfall amount in the four observation periods have been considerably reduced in the study period.

Table 6: maximum, minimum, and mean rainfall distribution across decades.

Rainfall across decades	Maximum rainfall (mm)	Minimum rainfall (mm)	Mean decadal rainfall (mm)	Standard deviation (mm)	Coefficient of variation	Change across decades
1st decade (1981-1990)	1982.3	955.7 mm	1267.9	39.9	3.1%.	- 100.1 mm
2nd decade (1991-2000)	1700.9	969.9 mm	1167.8	21.2	1.92%.	

3rd decade (2001-2010)	1416.4	1102.8 mm	1135.1	14.6	1.5%.	- 32.75 mm
Last observation (2011-2018)	1448.2	992.7 mm	1177.3	35.9	3.6 %	+ 42.24 mm

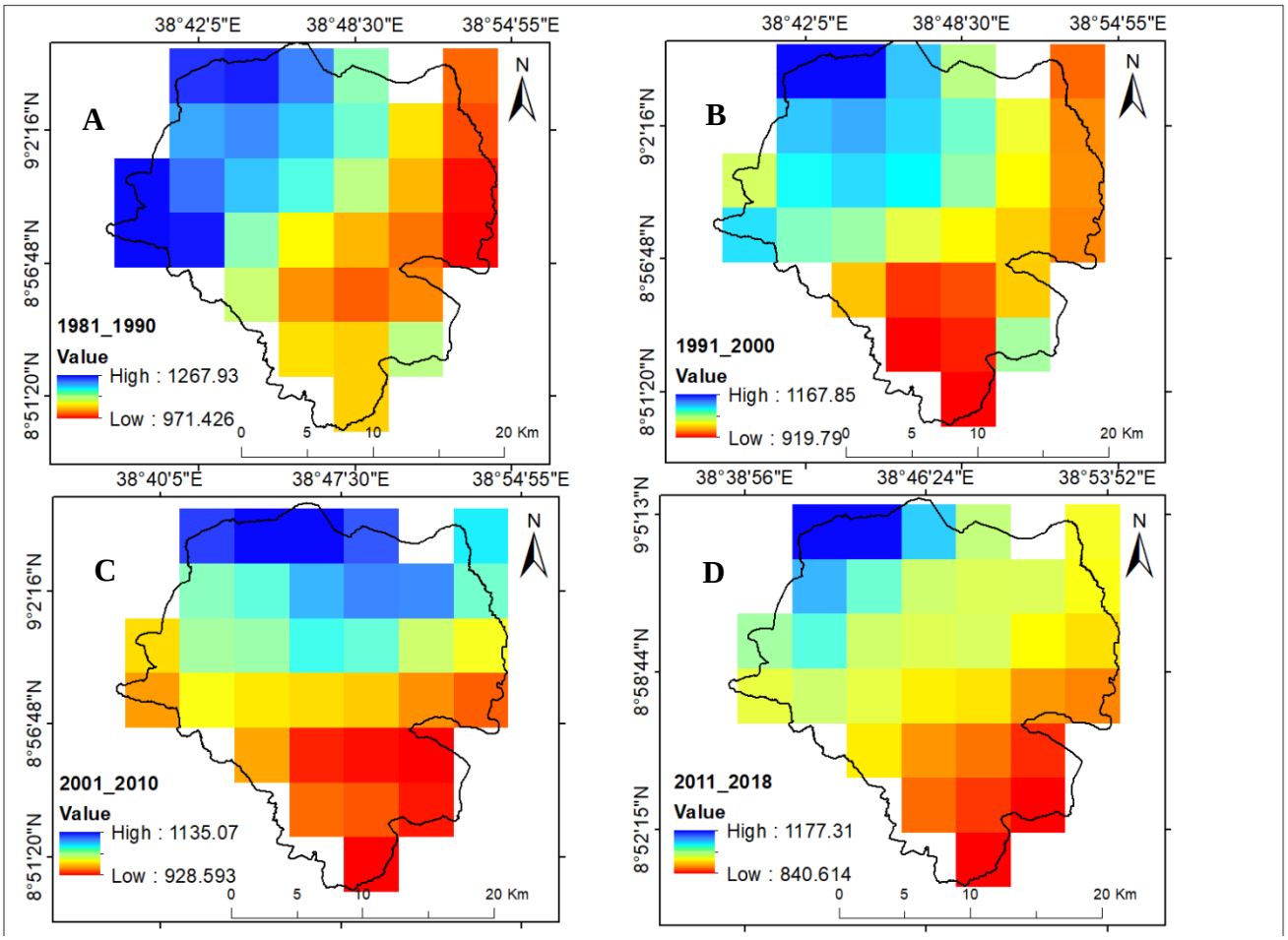

Figure 17: spatial distribution of mean rainfall across decades: A (1981-1990), B (1991-2000), C (2001-2010), and D (2011-2018).

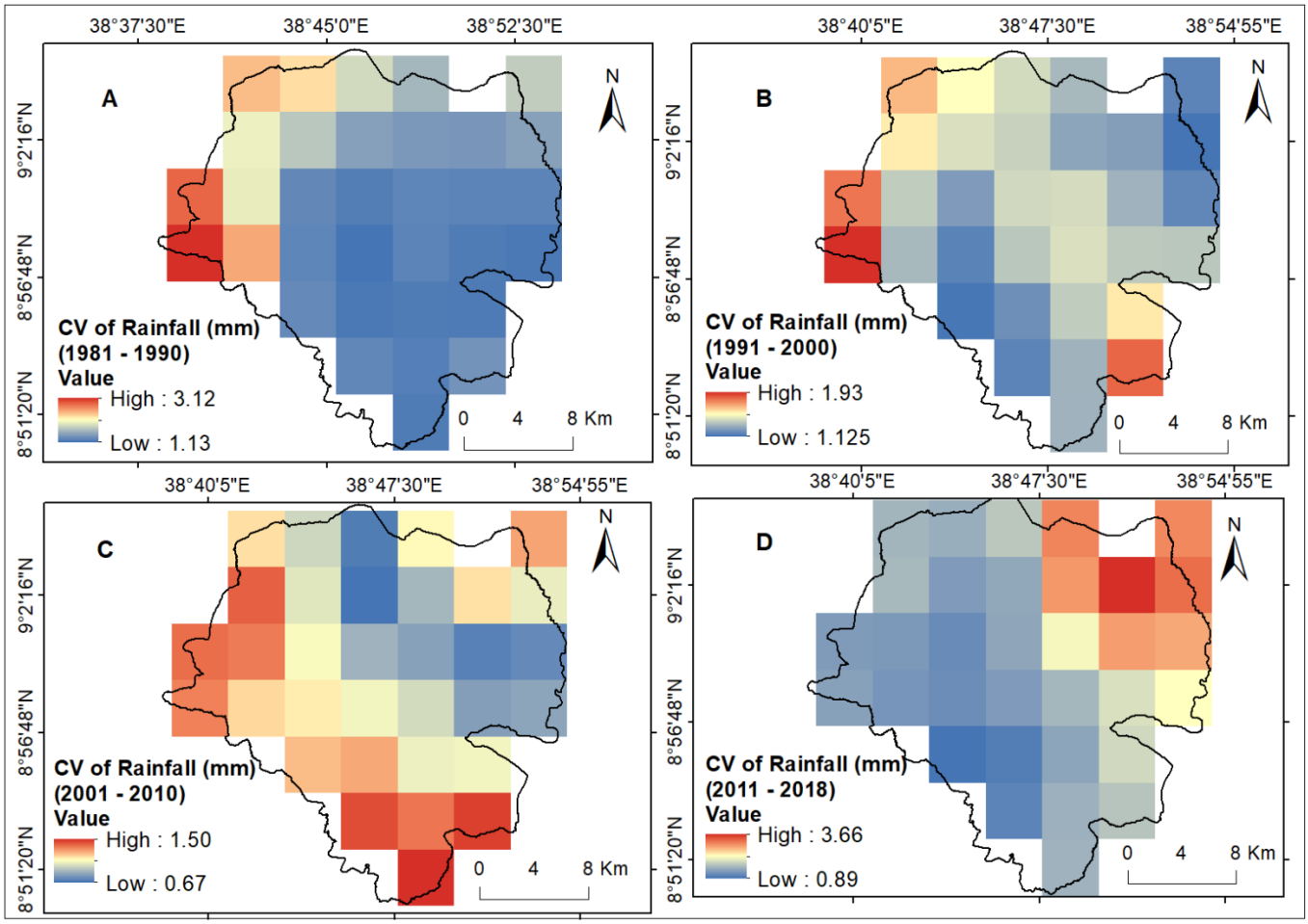

Figure 18: spatial distribution of mean coefficient of variation of rainfall across decades: A (1981-1990), B (1991-2000), C (2001-2010), and D (2011-2018).

4.9. Variability of maximum and minimum temperature in annual and seasonal basis

The mean annual, seasonal maximum, and minimum temperatures in Addis Ababa varied spatially and temporally. The mean annual maximum and minimum temperatures were 25.8 °C and 12.6 °C, respectively (Figure 20A and 21A). Compared to other seasons, the highest maximum temperature, 27.4 °C and minimum temperature, 13.8 °C, were recorded during the Spring (*Belg*) season. Winter (*Bega*) season average maximum and minimum temperature 25.9 °C and 11.4 °C, correspondingly (Figsure 20D and 21D). Main rainy (*Kiremt*) season average maximum temperature found to be 24.5 °C (Figure 20B) and minimum temperature was 13.3 °C (Figure 21B).

The spatial distribution of seasonal average maximum and minimum temperatures (Figure 20 and 21) revealed that the southern part of Addis Ababa was the hottest, where the maximum temperature was recorded. While the northern part of city was the coolest, where the minimum temperature was observed. This is because northern edge of the city is covered by dense forest while the hottest southern was areas with relatively lower elevation. From this it is possible to deduce that temperature and elevation has a direct relationship. It is a universal fact that for every 167m altitude, there is a decrease of temperature by 1 °C. In connection with this, the proximity of Ethiopia to the equator, as well as the intricacy nature of the country's topography has a significant influence Ethiopia's climate, particularly the temperature (AACPPO, 2017; Asefa et al., 2020a). Similarly, physical features such as terrain and sub-basin characteristics typically influence the spatial variability of maximum and minimum temperature (Zegeye et al., 2022).

Among the different seasons, comparatively *Belg* was found to be the hottest. This is because *Belg* season include months of March, April, and May which are the hottest months of the year in the study area and usually it is during this months that the maximum temperature is noticed (Legese et al., 2018). Likewise, Alemayehu and Bewket (2017) summarized earlier researches done in several regions of Ethiopia and found that there was regional and temporal variability of temperature.

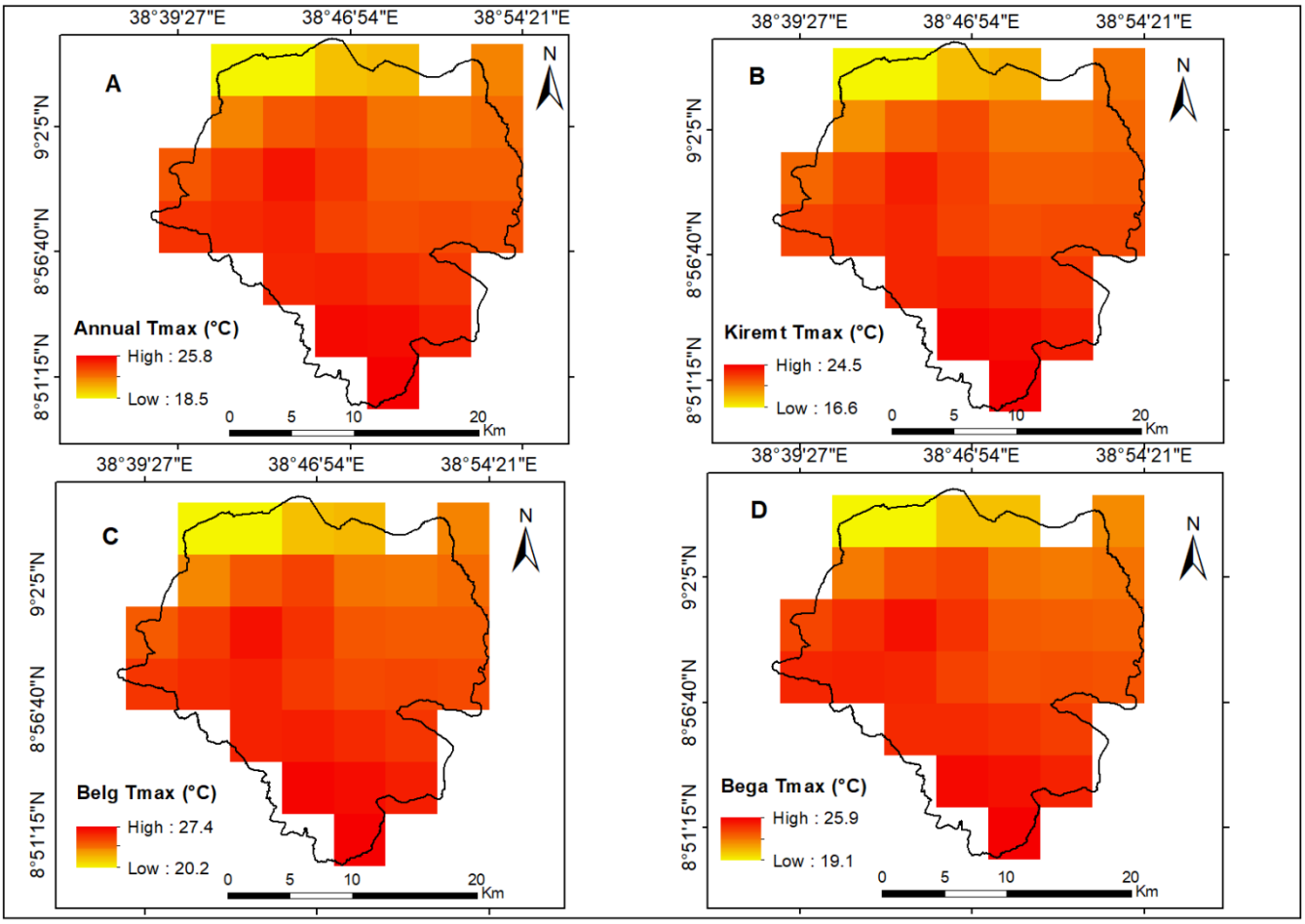

Figure 19: mean annual and seasonal maximum temperature Annual (A), *Kiremt* (B), *Belg* (C) and *Bega* (D) of Addis Ababa (1981-2018).

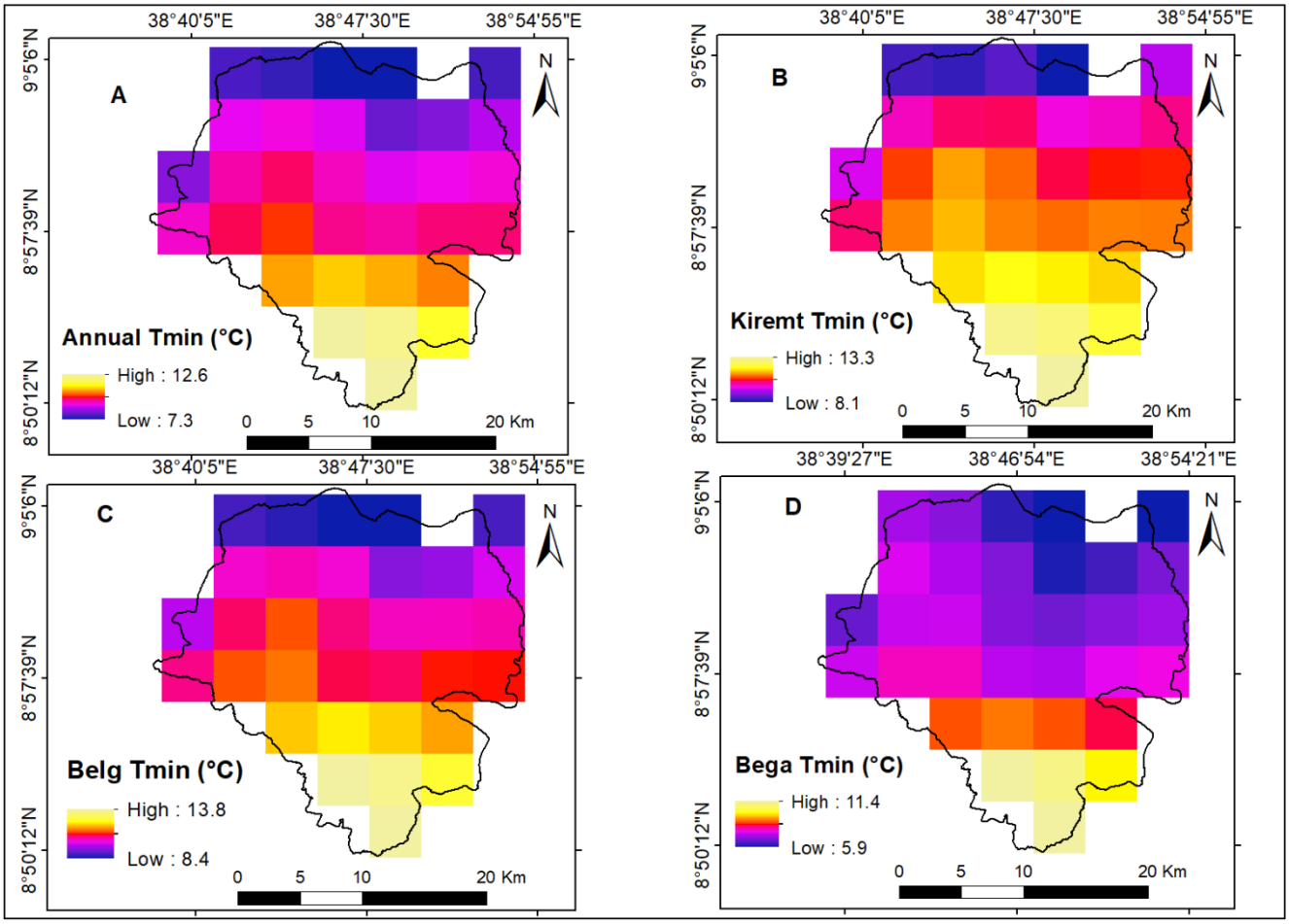

Figure 20: mean annual and seasonal minimum temperature: Annual (A), *Kiremt* (B), *Belg* (C) and *Bega* (D) of Addis Ababa (1981-2018).

4.10. Coefficient of variation in annual, seasonal maximum, and minimum temperature

Across the study period, the annual and seasonal mean maximum temperature coefficient of variation was less variable as CV<10% (Figure 22). The annual CV = 5% and *Belg* season CV = 3% (Figure 22A, C). Likewise, the mean annual and seasonal minimum temperatures have shown low variability (Figure 23). In both observations, the maximum and minimum temperature coefficient of variation, low variability of temperature was observed in *Belg* season, where the value of CV ranges between 2 and 4%. Generally, the average minimum temperature relatively showed higher degree of variability as compared with the maximum temperature in both annual and seasonal time scales as stipulated in Figure 22 and 23.

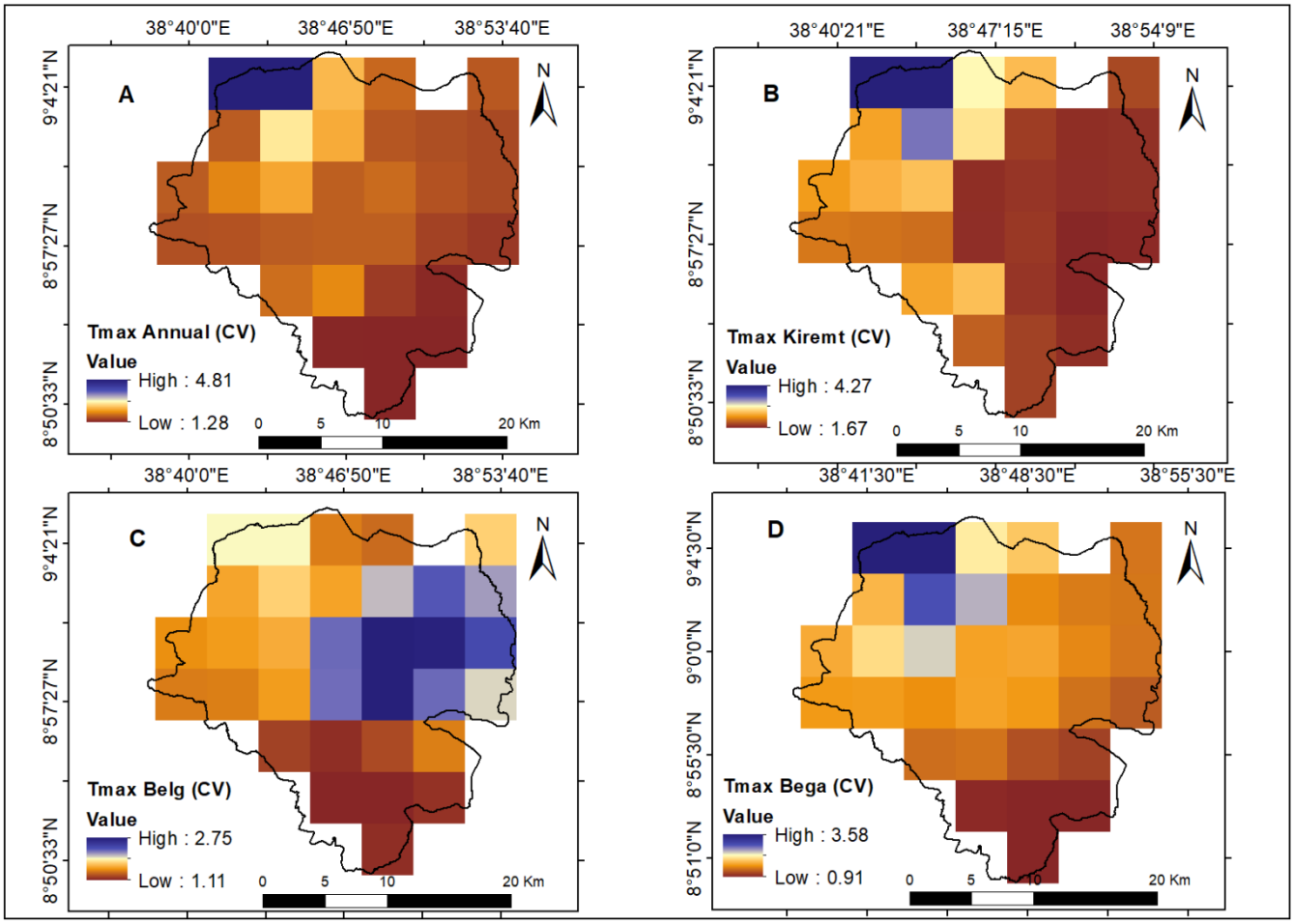

Figure 21: Coefficient of variation of maximum temperature annual (A), *Kiremt* season (B), *Belg* season (C), and *Bega* season (D) over the study period (1981-2018).

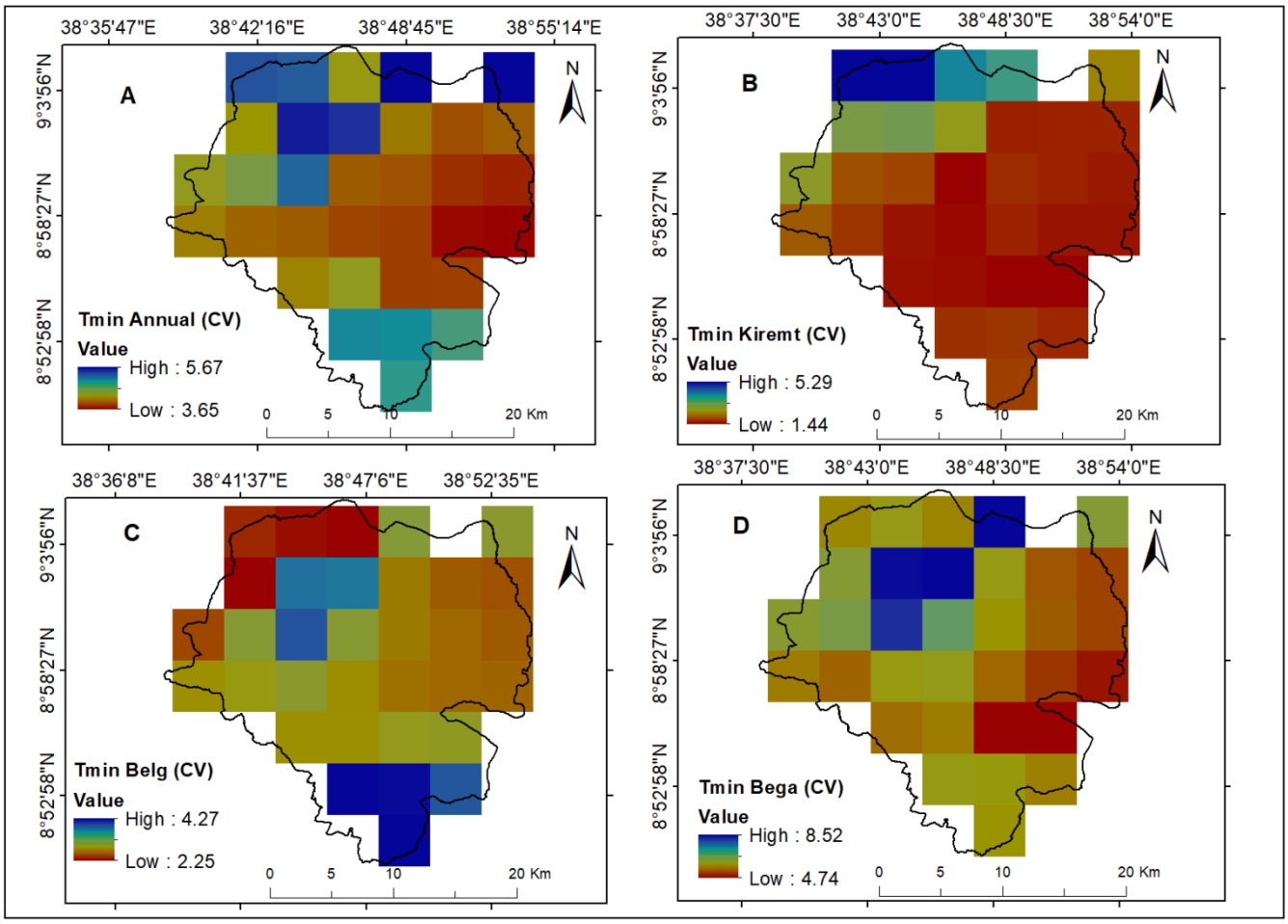

Figure 22: Coefficient of variation of minimum temperature annual (A), *Kiremt* season (B), *Belg* season (C), and *Bega* season (D) in the period of concern (1981-2018).

4.11. Variability of monthly maximum and minimum temperature

The spatial distribution of the average monthly maximum and minimum temperature for the observation period (1981–2018) is shown in Figure 24, 25, and 26. It was in August that the monthly average maximum temperature dropped to its lowest value of 23.37 °C. While in March the monthly average maximum temperature reached its peak of 27.59 °C (Figure 25). Following that, both the high and low temperatures gradually dropped. The highest monthly minimum temperature was recorded in May, 14.33 °C whereas the lowest temperature was registered in December (10.70 °C) (Figure 26).

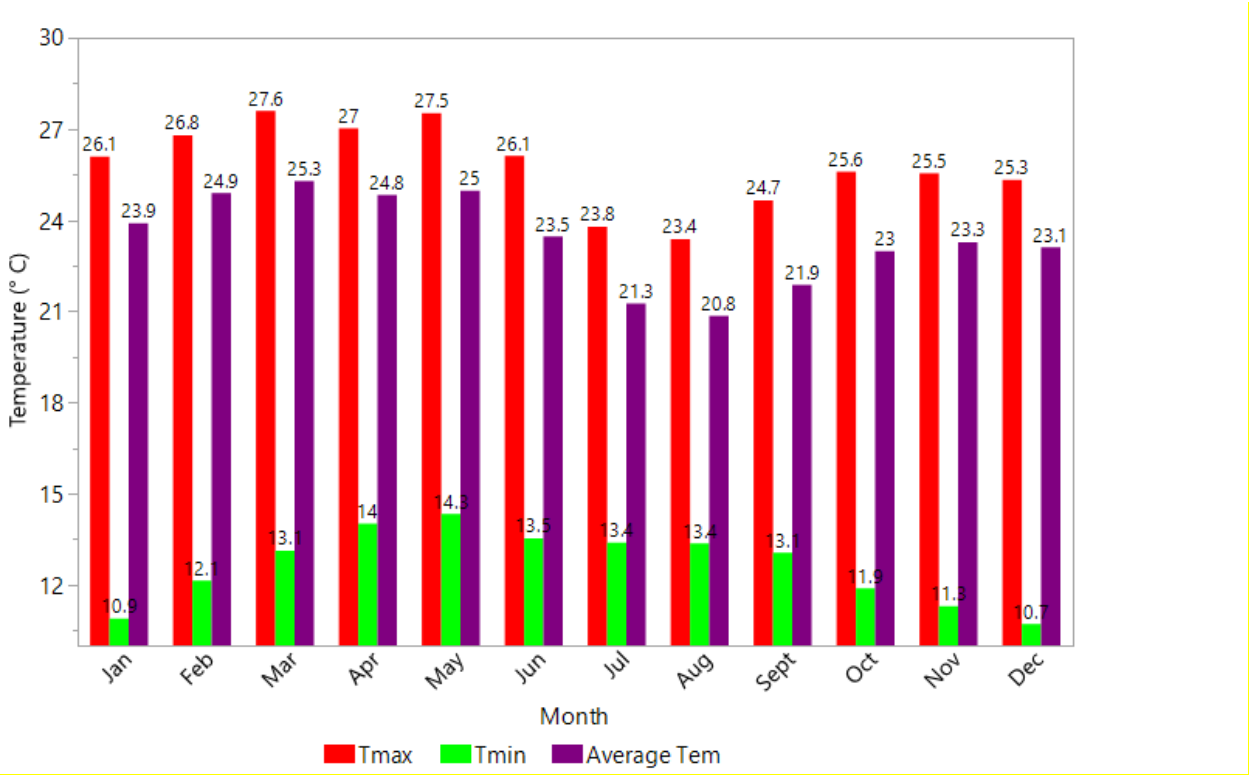

Figure 23: Monthly average temperatures of maximum, minimum, and average for the period from 1981 to 2018.

The highest average monthly maximum temperature was recorded in the months of March (27.59 °C), April (27.03 °C), and May (27.52 °C). Similarly, it was in the months of March (13.12 °C), April (14.01 °C) and May (14.33 °C) that the highest minimum temperature was observed (Figure 25 and 26). During the months of March and December the study area experienced the highest monthly average maximum and lowest minimum temperature, with the value of 27.59 °C and 10.7 °C, respectively. The average maximum temperature dropped to its lowest point in the main rainy (*Kiremt*) season, month of July (23.79 °C), August (23.37 °C), and September (24.65 °C). Similarly, the lowest minimum temperature was registered in the autumn season (October, November, and December).

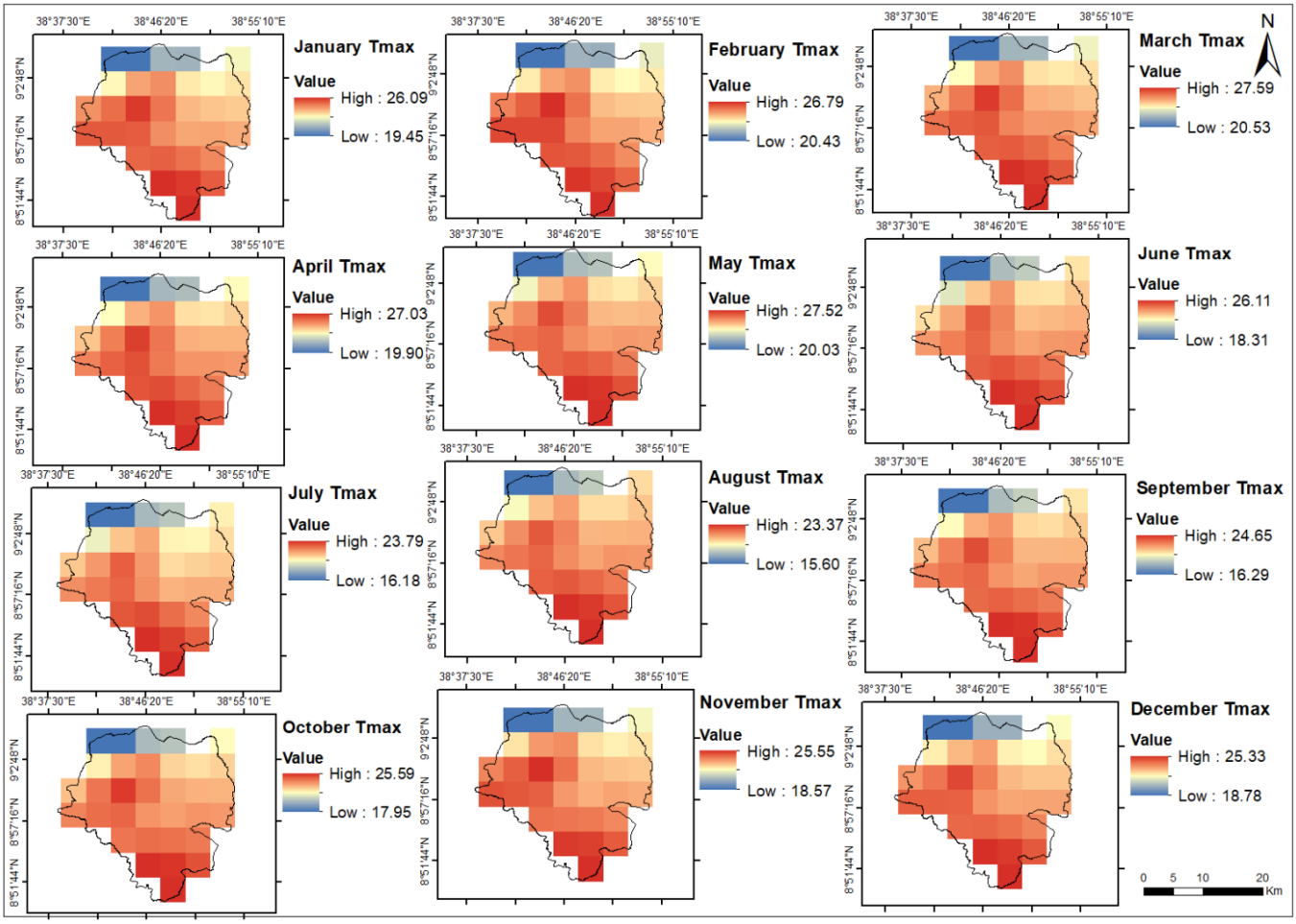

Figure 24: spatial distribution of average monthly (January to December) maximum temperature of Addis Ababa (1981-2018).

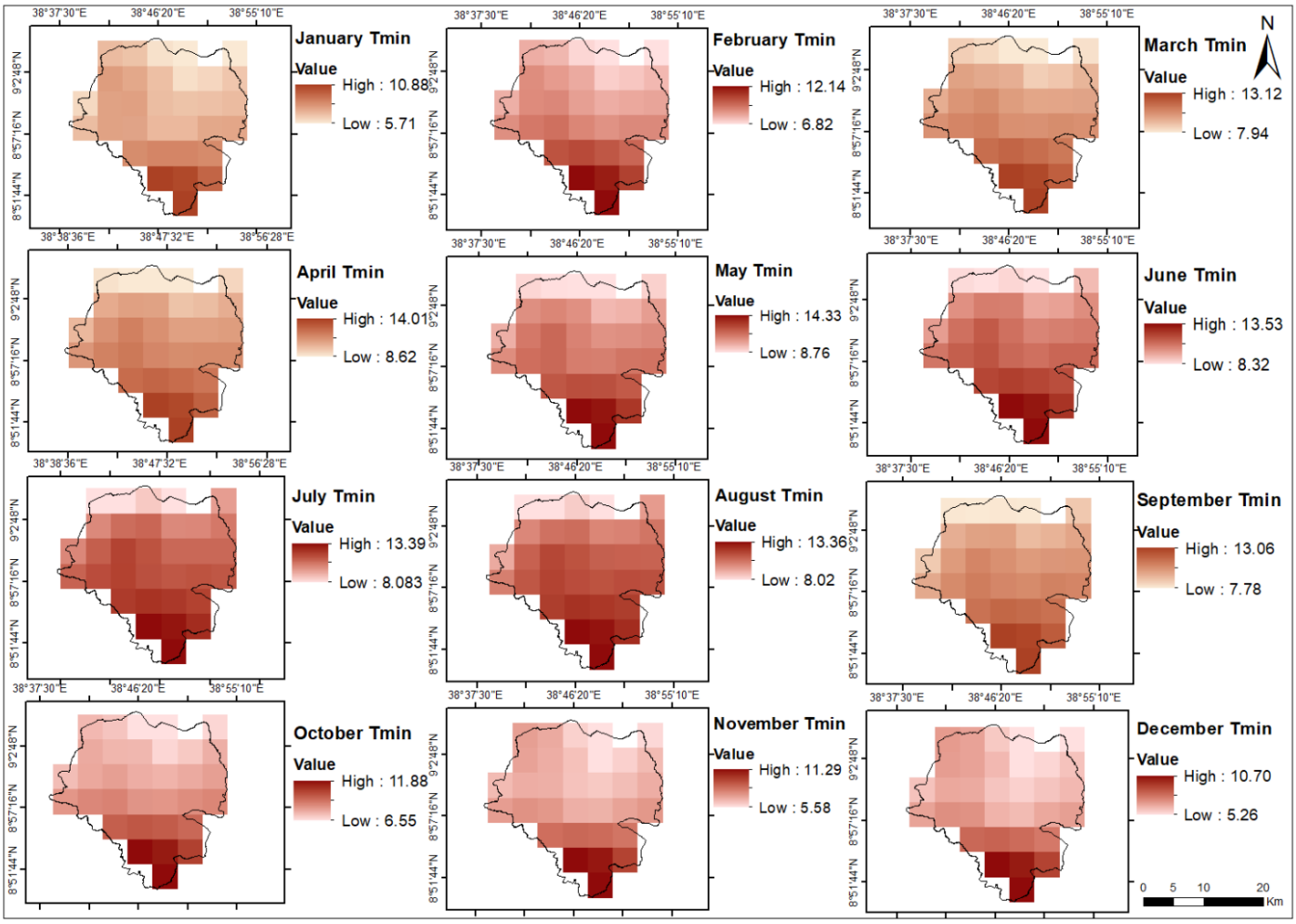

Figure 25: spatial distribution of monthly (January to December) average minimum temperature Addis Ababa (1981-2018).

4.12. Monthly Tmax Tmin Coefficient of variation analysis result

Figures 27 and 28 depicted the average monthly maximum and minimum temperature coefficients of variation analysis result between 1981 and 2018. Overall, the monthly maximum temperature analysis result exhibited a normal variance CV<20% throughout the twelve months. In the same vein, the average monthly minimum temperature demonstrated a minimal variance with a CV<20% from March to September. In October and February, there was moderate variance (CV<30%). It is possible to reach a conclusion that the minimum temperature was relatively more variable compared with the maximum temperature. During the months of November (CV = 30.78%), December (CV = 35.47%), and January (CV = 30.23%), the minimum temperature coefficient of variation was higher. While in

the months of October (CV = 23.35%) and February (CV = 22.22%) was moderately variable. Generally, the minimum temperature variation was higher than the maximum.

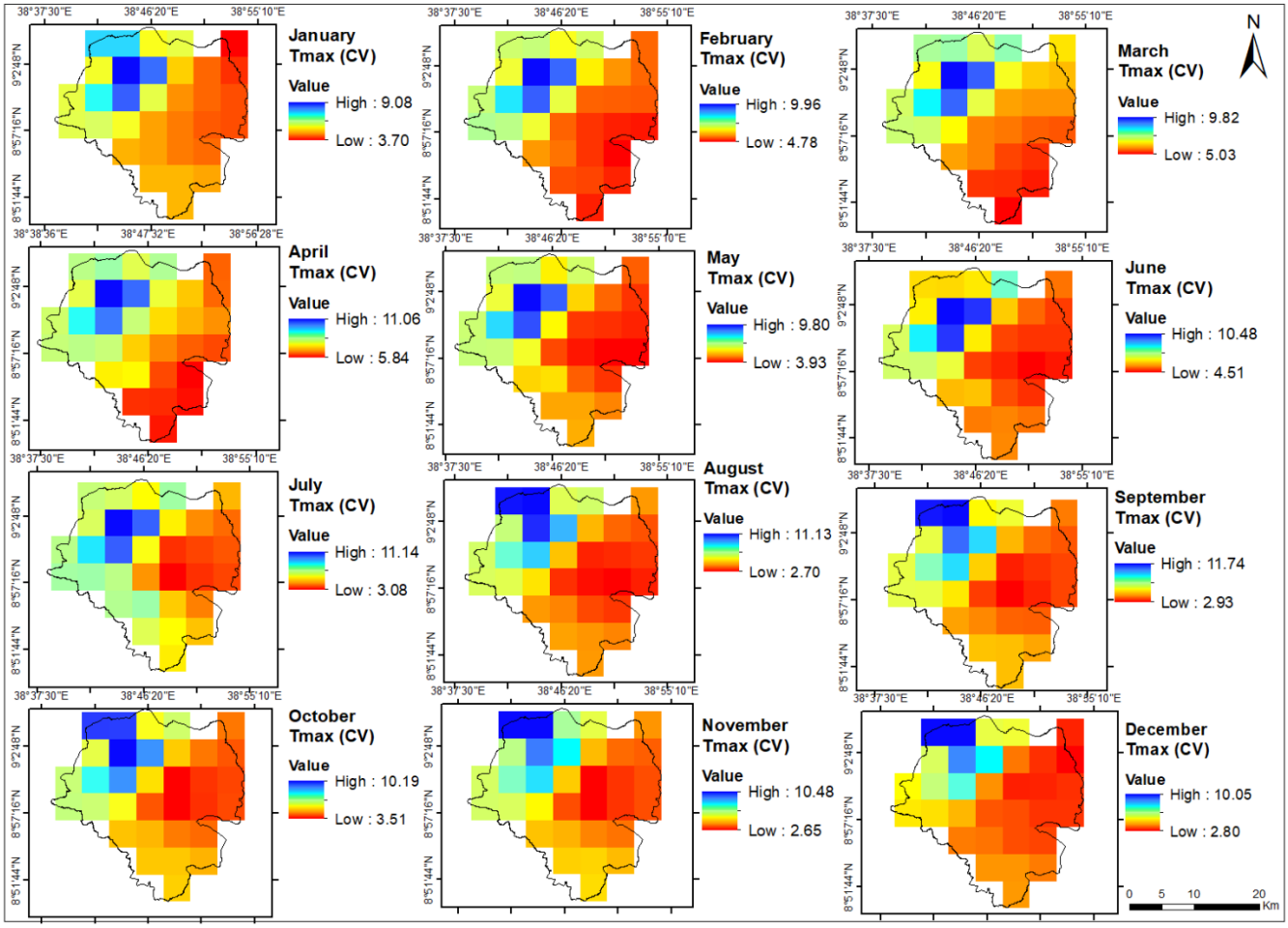

Figure 26: spatial distribution of monthly (January to December) maximum temperature coefficient of variation (CV) of Addis Ababa (1981-2018).

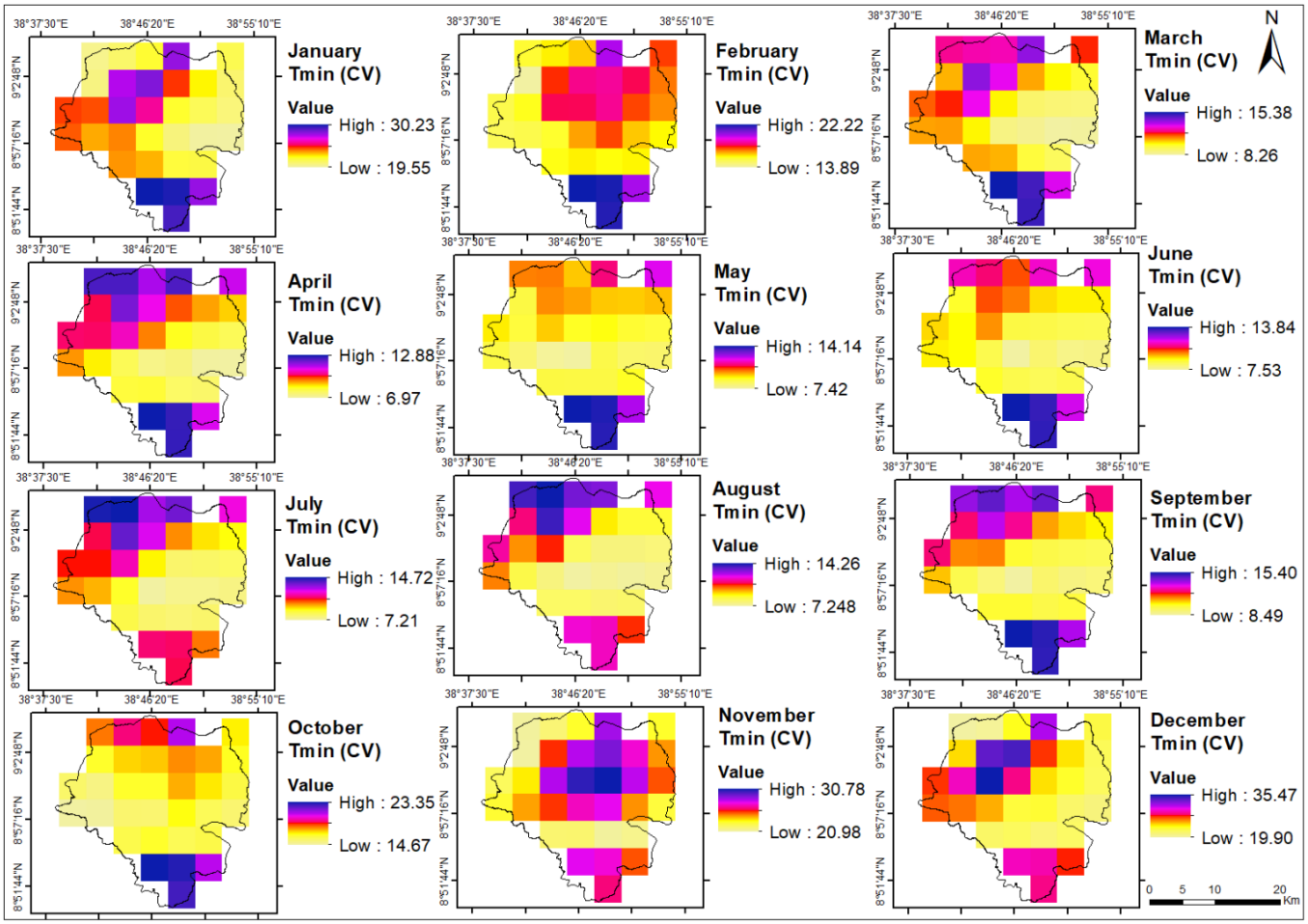

Figure 27: spatial distribution of monthly (January to December) minimum temperature coefficient of variation (CV) of Addis Ababa (1981-2018).

4.13. Standardized anomaly index of maximum and minimum temperature

The annual and seasonal (*Kiremt*, *Belg*, and *Bega*) maximum and minimum temperatures standardized anomaly (STA) index is shown in Figures 29 and 30. The analysis result stipulated that in the last observation period (2011–2018), the maximum temperature warming effect (positive anomaly) was sharply intensified across all seasons (Figure 29) except in *Kiremt* season, where the maximum temperature anomaly was relatively less pronounced. While the warming effect was evident in all the other seasons, the increment of maximum temperature anomalies varies among seasons. In connection with this, the study draws a comparison to previous research in the northern region of Ethiopia, which found a gradual increase in average maximum temperatures between 1983 and 2016. This highlights the long-term nature of the warming trend, spanning several decades (Berhane et al., 2020).

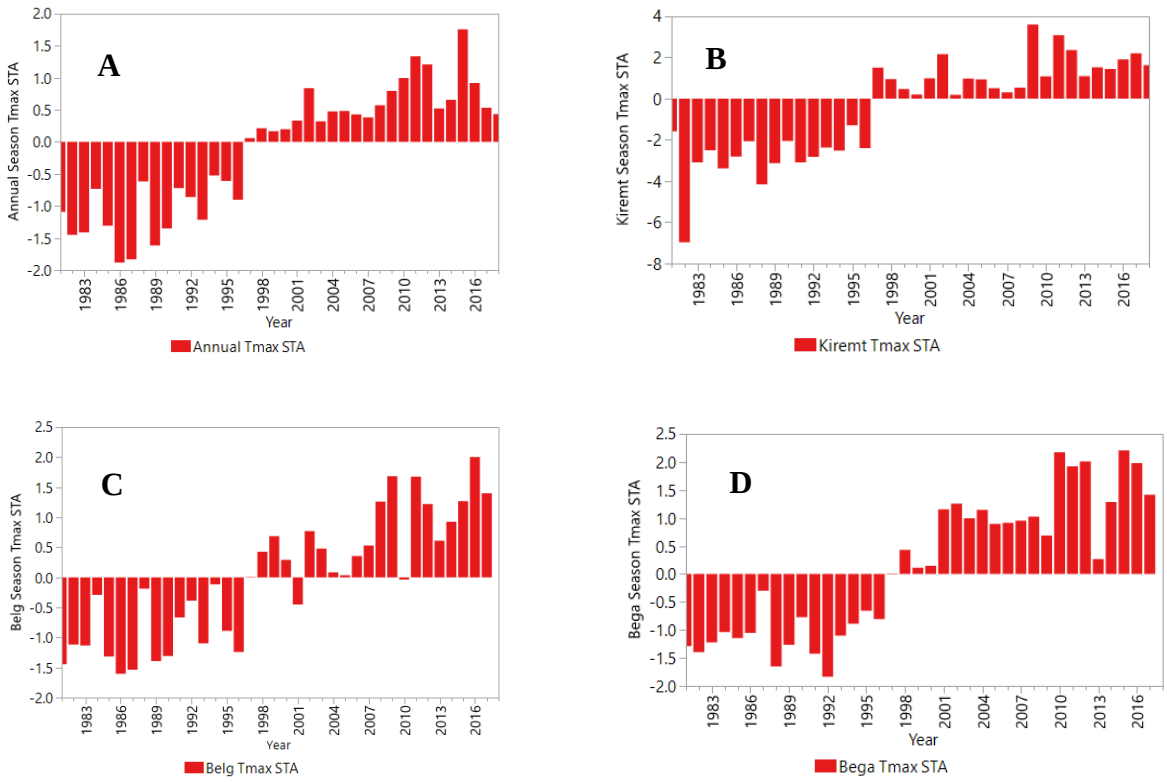

Figure 28: Maximum temperature anomalies for Annual (A), *Kiremt* (B), *Belg* (C), and *Bega* (D) of Addis Ababa (1981-2018).

The analysis findings shown in Figure 30, where the minimum temperature over the last 38 years illustrates how Addis Ababa city consistently experienced both warming and cooling years (Figure 30A-D). The SAI of annual and seasonal minimum temperatures accounts for 65% of warming years and 35% cooling years. The graph (Figure 30A-D) illustrated that the standardized anomaly index betweeen 1981 and 1996 showed a negative anomaly across the four seasons (annual, *Kiremt*, *Belg*, and *Bega*). From 1997 to 2009, a positive anomaly was observed in both annual and seasonal minimum temperatures. However, from 2010 on, a negative anomaly completely dominated the observations. The number of years with negative anomalies was greater than the number of years with positive anomalies. This indicates that Addis Ababa has experienced more dry years than wet years. The findings of the study also designated the 1980s and 2010s as dry years as compared with the 1990s and 2000s, which were wet years.

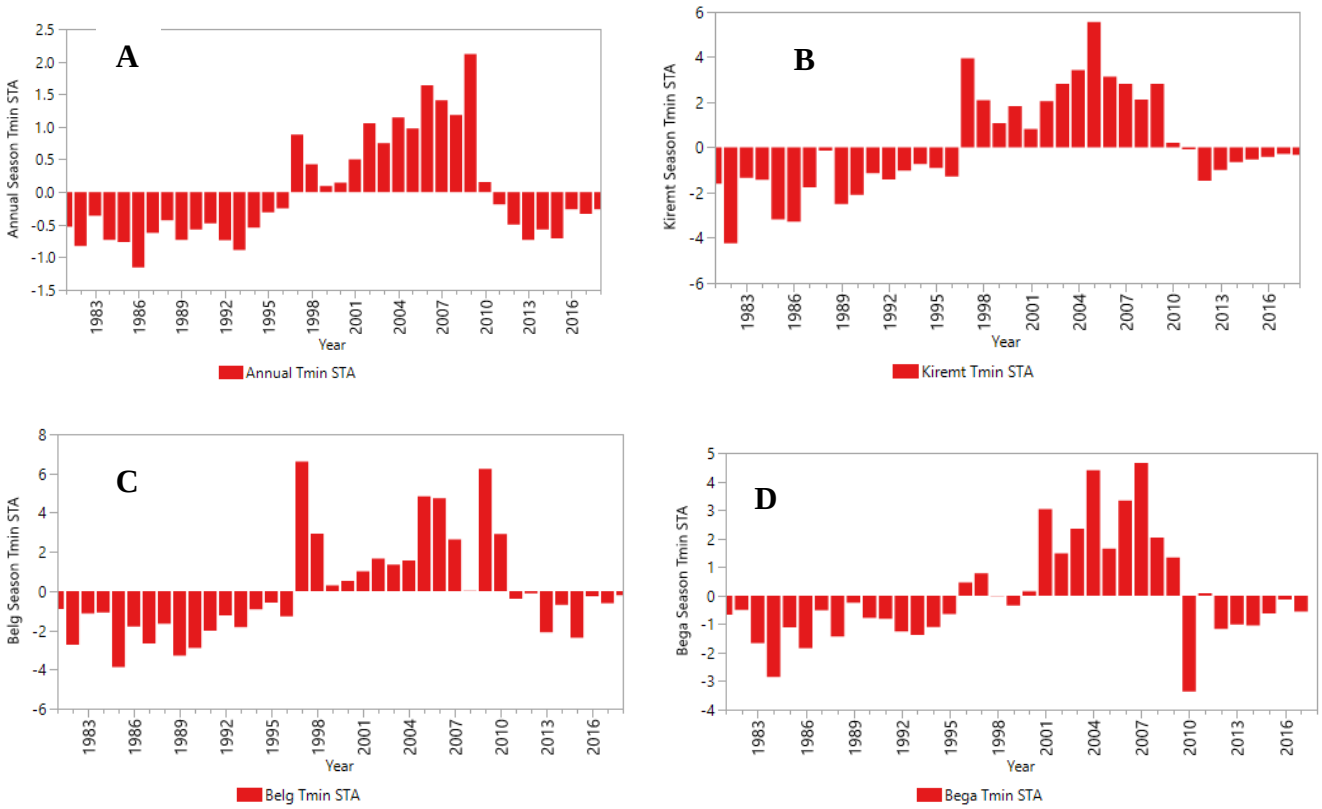

Figure 29: minimum temperature anomalies for Annual (a), *Kiremt* (b), *Belg* (c), and *Bega* (d) of Addis Ababa City (1981-2018).

4.14. Temperature trend analysis

The result obtained from the trend analysis (Figure 31) revealed that there was a positive trend of the average annual, seasonal maximum, and minimum temperature across the observation period (1981-2018). Related studies conducted in southern Ethiopia indicated that significant warming trends of seasonal and annual mean temperatures between 1980 and 2015 (Benti & Abara, 2019). The result of the maximum temperature was statistically highly significant as the calculated p-value = 0.0001, which is lower the threshold significant level (P< 0.05). The same is true for the average annual and seasonal (*Kiremt*, *Belg*, and *Bega*) minimum temperature with the P value was slightly higher than the maximum temperature.

The long term average maximum temperature for annual, *Kiremt*, *Belg*, and *Bega* seasons were 26.16 °C, 24.8 °C, 27.8 °C, and 26.2 °C, respectively. On the other hand, the average minimum temperature for annual (12.77 °C), *Kiremt* (13.4 017 °C), *Belg* (13.99 °C), and *Bega* (11.62 °C). The highest

temperature for both the maximum and minimum temperature was registered during Spring (*Belg*) season. As the scatter plot showed that the rate of increase of the average annual and seasonal maximum temperature by far higher than the minimum temperature. In contrast, the aveage annual and seasonal minimum temperature increment was a moderate one. The linear regression analysis also found that fluctuations in maximum temperature tend to vary with coefficient of determination (R^2) ranging from 0.66 spring (*Belg*) to the 0.80 annual.

Regarding the maximum temperature, the highest average annual minimum and maximum temperature were recorded in 1985 and 2016, with the value of 24.23 °C and 29.35 °C, successively. The highest average annual maximum temperature of *Kiremt* and *Belg* seasons were 28.23 °C and 32.93 °C, correspondingly, both recorded in the same year, 2016. The yearly seasonal average maximum temperature of *Bega* season was 29.62 °C, registered in 2015 (Table 7).

Table 7: average annual and seasonal maximum temperature record

mean annual/seasonal Tmax (1981-2018)	Degree Celsius (°C)	Year
Highest Annual Tmax	29.35	2016
Lowest Annual Tmax	24.23	1985
Highest Kiremt Tmax	28.23	2016
Lowest Kiremt Tmax	22.85	1993
Highest Belg Tmax	32.92	2016
Lowest Belg Tmax	25.01	1986
Highest Bega Tmax	29.62	2015
Lowest Bega Tmax	23.81	1988

Source: ArcGIS statistical analysis result

On the other hand, the minimum temperature average annual, *Kiremt*, and *Bega* seasons temperatures were 16.79 °C, 16.86 °C, and 18.28 °C, consecutively. All occurred in the same year, 2007. While the minimum temperature lowest average value for annual was 10.09 °C, *Kiremt* 10.33 °C, and *Bega*, 8.77 °C, it was registered in 1986 (Table 8).

Table 8: average annual and seasonal minimum temperature record

mean annual/seasonal Tmin (1981-2018)	Degree Celsius (°C)	Year
Highest Annual Tmin	16.75	2007
Lowest Annual Tmin	10.09	1986
Highest Kiremt Tmin	16.86	2007
Lowest Kiremt Tmin	10.33	1986
Highest Belg Tmin	17.84	2009
Lowest Belg Tmin	11.85	1993
Highest Bega Tmin	18.28	2007
Lowest Bega Tmin	8.77	1986

Source: ArcGIS statistical analysis result

Concerning the change in average annual maximum temperature across seasons, the highest temperature change occurred during *Belg* season (Table 7). In this regard, previous studies reported that *Belg* season which includes the months of March, April, and May the warmest months where the maximum temperature is recorded during this season (Zegeye et al., 2022).

It is possible to understand that there was a progressive increasing trend of the average annual and seasonal maximum and minimum temperature across the study period (Table 7 and 8). The results of this study agreed with the previous studies reported that an increasing trend in Ethiopia's annual average, maximum, and minimum temperatures (Asfaw et al., 2018b; Benti & Abara, 2019). Additionally, IPCC (2014b) projections suggested that the global surface temperature is predicted to increase from 0.3 °C to 4.8 °C by the end of the 21st century. Consequently, the increasing temperature in cities like Addis Ababa could result in significant water loss, which has an impact on municipal services and domestic water supplies (Belay et al., 2021).

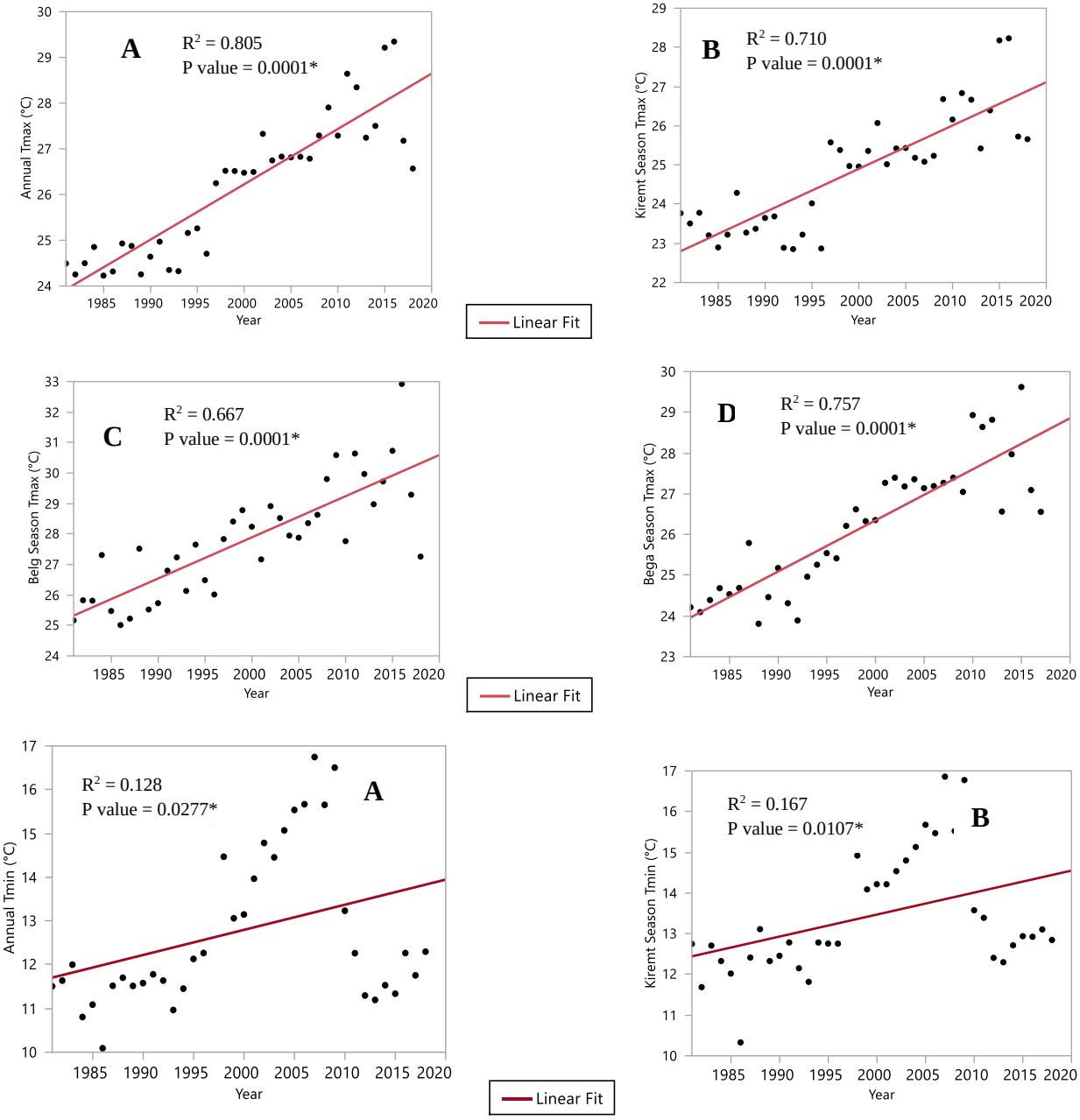
A
R² = 0.805
P value = 0.0001*
Annual Tmax (°C)
Year
B
R² = 0.710
P value = 0.0001*
Kiremt Season Tmax (°C)
Year
Linear Fit
C
R² = 0.667
P value = 0.0001*
Belg Season Tmax (°C)
Year
D
R² = 0.757
P value = 0.0001*
Bega Season Tmax (°C)
Year
Linear Fit
A
R² = 0.128
P value = 0.0277*
Annual Tmin (°C)
Year
B
R² = 0.167
P value = 0.0107*
Kiremt Season Tmin (°C)
Year
Linear Fit

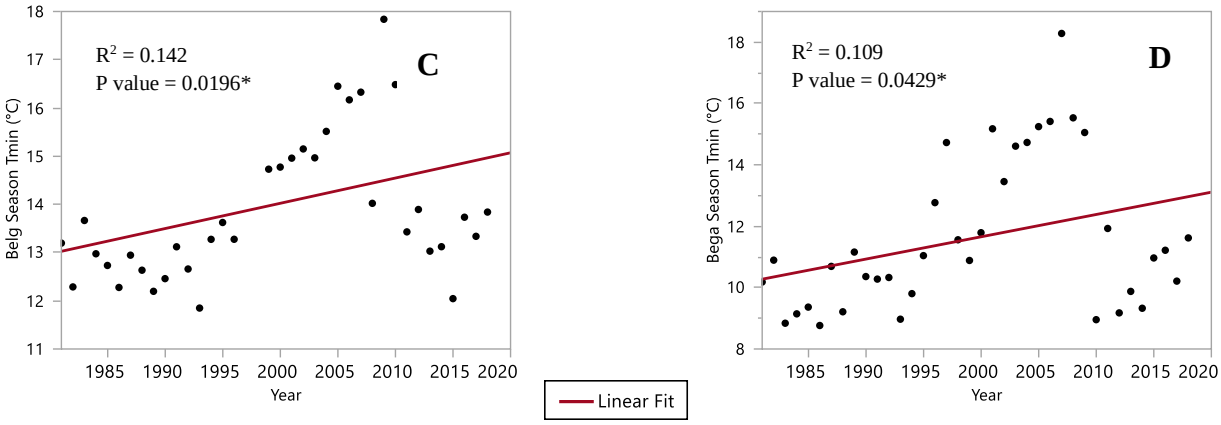

Figure 30: Average maximum and minimum temperature of Annual (A), *Kiremt* (B), *Belg* (C), and *Bega* (D) of Addis Ababa (1981-2018).

4.15. Decadal temperature trend analysis

Table 9 shows the average decadal maximum, minimum, and average temperature of Addis Ababa in the period between 1981 and 2018. As the analysis result underpines that the mean annual maximum temperature from 1981 to 1990 and from 1991 to 2000 were 24.53 °C and 25.33 °C with ± 0.38 and ± 0.31 standard deviation and 1.63 and 1.31 coefficient of variation (Table 8 & Figure 32A, B). The mean annual maximum temperature for the third decade (2001-2010) and the last eight observation years (2011-2018) were 26.71 °C and 27.23 °C with standard deviation of ± 0.73 and ± 1.32 and coefficient of variation of 2.92 and 7.38, respectively. The analysis reflected that in the first two decades (1981-2000) the average maximum temperature rose by 0.8 °C. The difference in temperature between the second (1991-2000) and third (2001-2010) observation period further escalated by 1.38 °C.

The decadal maximum temperature increase over the last eighteen years (2001-2018) was soared by 0.52 °C. Overall, in the study period (1981-2018) the decadal maximum temperature was augmented by 2.7 °C (Figure 32 and Table 8). In this regard, previous studies noted that maximum temperature showed an increasing propensity from the 1980s to 1990s and 2000s in most parts of East Africa with a maximum change observed in Ethiopia (anomalies up to +0.9 °C) (Gebrechorkos et al., 2018). The empirical evidence demonstrated how temperature increases over time in the area of concern. On top of that, as shown in the scatter plot in Figure 31, the area has undergone a significant increase in mean annual maximum temperature during the last 38 years. In this regard, Feyissa et al., (2018) highlighted that over the last decades high temperature were recorded in different parts Ethiopia. Previous research

suggested that Addis Ababa's future maximum temperature will rise by 1-2 degrees Celsius for the whole city and neighboring districts, the greatest change occurring along the Bole, Yeka, and Akaki sub-cities and in the city's east and south (Arsiso et al., 2018). In this regard, the findings of this study are consistent with the reports of the earlier research.

Similarly, the decadal minimum temperature difference in the first two decades (1981-2000) climbed by 1.27 °C (Table 9 and Figure 33). Between the second (1991-2000) and third observation (2001-2010) period accrued by 2.55 °C. In contrast, it abruptly dropped by 3.99 °C during the most recent observation period (2011-2018). Over the study period, it is possible to understand that there was no such significant increment of the decadal minimum temperature. Nevertheless, the decadal maximum temperature was significantly increased across the study period. The mean decadal maximum and minimum temperature ranges between 22.48 °C and 24.36 °C, and 8.91 °C and 10.63 °C, respectively. The long-term average decadal maximum and minimum temperature increased by 1.88 °C and 1.72 °C, consecutively as stipulated in Table 9.

In the first two decades (1981-2000), the average decadal maximum and minimum temperature scaled-up by 0.45 °C and 0.64 °C, respectively (Table 9 and Figures 32 and 33). In the second and third observation the average decadal maximum temperature rose by 1.05 °C. While the average decadal minimum temperature surged by 1.08 °C. By comparison, in this observation period, the temperature difference was much higher than the preceding decade. Between the third and fourth observation, the decadal average maximum temperature escalated by 0.38 °C while the decadal average minimum temperature declined by 0.22 °C. Generally, it is possible to conclude that the average decadal maximum and minimum temperatures progressively increased throughout the study period except for a slight reduction in average decadal minimum temperature in the last observation.

Table 9: Descriptive statistics of decadal, decadal average maximum/minimum temperature along with variance and standard deviation.

	Obervations	Decadal	Mean	Variance	Std.deviation
Maximum temperature (°C)	1981-1990	24.53	22.48	1.63	0.38
	1991-2000	25.33	22.93	1.31	0.31
	2001-2010	26.71	23.98	2.92	0.73
	2011-2018	27.23	24.36	7.38	1.32
Minimum temperature (°C)	1981-1990	11.34	8.91	6.95	0.46
	1991-2000	12.61	9.55	8.89	0.81
	2001-2010	15.16	10.63	6.46	0.78
	2011-2018	11.17	10.41	5.44	0.59

Source: statistical analysis result on ArcGIS

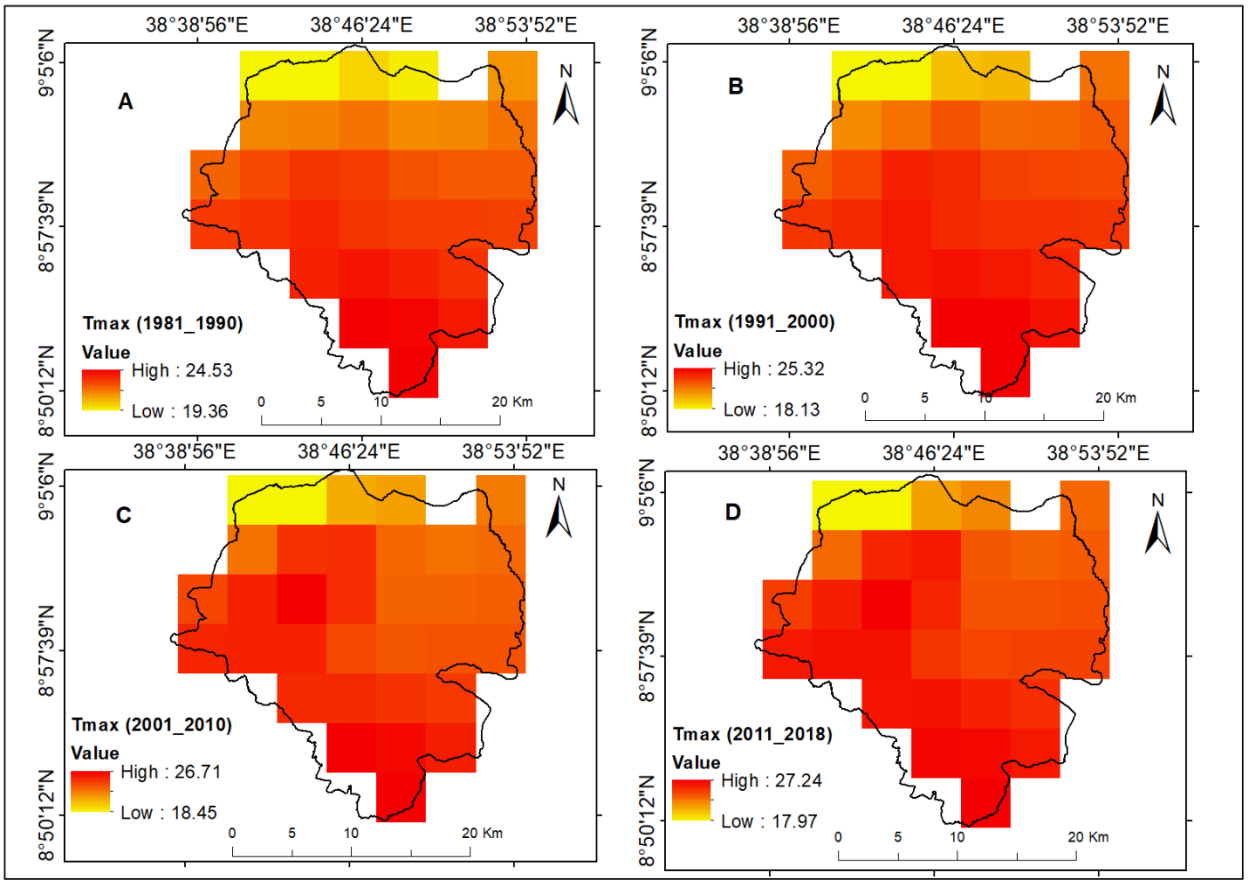

Figure 31: portrays the average decadal maximum temperature of Addis Ababa for the year (A) 1981-1990, (B) 1991-2000, (C) 2001-2010 and (D) 2011-2018.

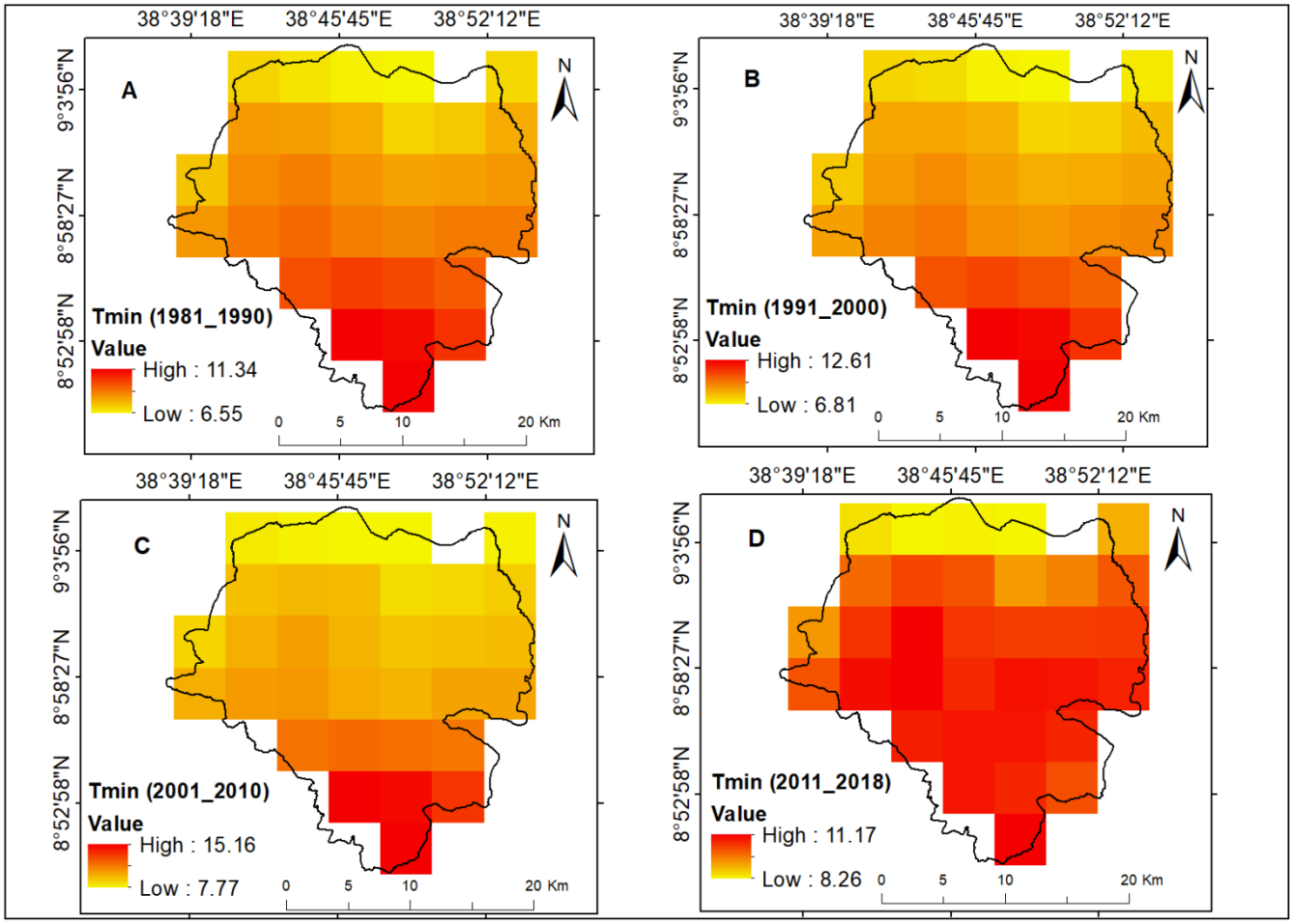

Figure 32: demonstrates the average decadal minimum temperature of Addis Ababa for the year (A) 1981-1990, (B) 1991-2000, (C) 2001-2010 and (D) 2011-2018.

4.16. Mann-Kendall and Sen's slope estimator test result

4.16.1. Long-term monotonic trends of maximum and minimum temperature

Temperature trend analysis for Addis Ababa was performed using 38 years of temperature data (1981-2018). The MK test result stipulated that the Z value for maximum annual and seasonal (*Kiremt, Belg,* and *Bega*) temperature was 6.46, 5.41, 5.76, and 5.85, respectively as shown in (Table 10). The result of the Sen's slope estimator positive value indicated an increasing trend of maximum temperature and statistically significant as the p-value for all the seasons was less than the < 0.05.

Conversely, for the mean annual and seasonal minimum temperature for *Kiremt, Belg,* and *Bega,* the Z value found to be 3.37, 3.17, 2.82 and 2.79, correspondingly. Similarly, the P values for all the seasons were less than the significant value of 0.05, which means the minimum temperature increment was statistically significant. The positive Kendall's tau value (Table 10) elucidated an upward trend for both annual and seasonal maximum and minimum temperature. This implies that an increasing trend of maximum and minimum temperature was observed over the course of the period under investigation (1981-2018). The findings of this research aligned with the earlier studies conducted in Addis Ababa reported that there was a propensity of temperature increase in the study area (Alemu & Dioha, 2020). In addition, another study conducted in South Gonder Zone underline that the maximum temperature showed an increasing trend (Getachew, 2018).

Table 10: MMK trend analysis of average annual and seasonal maximum and minimum temperature (1981-2018) in Addis Ababa.

Seasons	Kendall's Tau	S	P-value	Trend	Significant	Sen's slope (°C/year)	Var(s)	Test statistics (Z)
Annual Tmax	0.73	515	0.0001	Increasing	Significant	0.12	6327	6.46
Annual Tmin	0.38	269	0.0007	Increasing	Significant	0.066	6327	3.37
Kiremt Tmax	0.61	431	0.0001	Increasing	Significant	0.11	6327	5.41
Kiremt Tmin	0.36	223	0.0015	Increasing	Significant	0.060	6327	3.17
Belg Tmax	0.65	459	0.0001	Increasing	Significant	0.14	6327	5.76
Belg Tmin	0.32	225	0.0049	Increasing	Significant	0.052	6327	2.82
Bega Tmax	0.67	448	0.0001	Increasing	Significant	0.13	5846	5.85
Bega Tmin	0.32	214	0.0053	Increasing	Significant	0.094	5846	2.79

Source: Rstudio Menn-Kendell test Significant at α=0.05

4.16.2. Observed monthly maximum and minimum temperature

The results of Sen's slope estimator analysis and the Modified Mann-Kendall (MK) test were shown in Table 11 for the monthly maximum and minimum temperatures of Addis Ababa between 1981 and 2018. The monthly maximum temperature has been considerably increasing throughout all months with P-value of 0.0001 significant level (Table 11). The highest monthly maximum temperatures were recorded in the months of March (27.59 °C), April (27.03 °C), and May (27.52 °C). Similarly, the greatest monthly minimum temperatures were 14.01 °C and 14.33 °C, respectively, recorded in April and May. Except

for January, February, March, and September, the increment of minimum temperature was significant in every month where the calculated P-value was less than 0.05 (Table 11).

Table 11: MMK trend analysis of monthly Tmax and Tmin (1981-2018) in Addis Ababa City.

Month	Mean's value	Kendall's tau	S	P-value	Trend	Significant	Sen's slope (mm/year)	Var(s)	Test statistics (Z)
January Tmax	26.09	0.64	453	0.0001	Increasing	Significant	0.124	6327	5.6825
January Tmin	10.88	0.21	145	0.0702	Increasing	Insignificant	0.061	6327	1.8104
February Tmax	26.79	0.59	421	0.0001	Increasing	Significant	0.152	6327	5.2802
February Tmin	12.14	0.16	111	0.1667	Increasing	Insignificant	0.053	6327	1.3829
March Tmax	27.59	0.59	417	0.0001	Increasing	Significant	0.135	6327	5.2299
March Tmin	13.12	0.20	143	0.0742	Increasing	Insignificant	0.046	6327	1.7852
April Tmax	27.03	0.58	407	0.0001	Increasing	Significant	0.162	6327	5.1042
April Tmin	14.01	0.303	213	0.0076	Increasing	Significant	0.063	6325	2.6657
May Tmax	27.52	0.56	393	0.0001	Increasing	Significant	0.122	6327	4.9282
May Tmin	14.33	0.337	237	0.0030	Increasing	Significant	0.076	6327	2.967
June Tmax	26.11	0.52	367	0.0001	Increasing	Significant	0.108	6327	4.6013
June Tmin	13.53	0.345	243	0.0023	Increasing	Significant	0.066	6327	3.0424
July Tmax	23.79	0.58	411	0.0001	Increasing	Significant	0.113	6327	5.1545
July Tmin	13.39	0.399	281	0.0004	Increasing	Significant	0.067	6327	3.5201
August Tmax	23.37	0.52	365	0.0001	Increasing	Significant	0.082	6325	4.5769
August Tmin	13.36	0.325	229	0.0041	Increasing	Significant	0.049	6327	2.8664
September Tmax	24.65	0.66	469	0.0001	Increasing	Significant	0.119	6327	5.8837

September Tmin	13.06	0.218	153	0.0560	Increasing	Insignificant	0.041	6327	1.9109
October Tmax	25.59	0.65	459	0.0001	Increasing	Significant	0.126	6327	5.7579
October Tmin	11.87	0.277	195	0.0147	Increasing	Significant	0.096	6327	2.4389
November Tmax	25.55	0.65	461	0.0001	Increasing	Significant	0.134	6327	5.7831
November Tmin	11.29	0.323	227	0.0044	Increasing	Significant	0.109	6327	2.8413
December Tma**x**	25.33	0.58	411	0.0001	Increasing	Significant	0.096	6327	5.1545
December Tmin	10.70	0.229	161	0.0442	Increasing	Significant	0.095	6327	20115

Source: Rstudio Menn-Kendell test Significant at α=0.05

4.17. Principal component analysis (PCA)

4.17.1. Annual and seasonal PCA analysis

In this section, time series maximum and minimum temperature were analyzed at monthly, annual, and seasonal (*Kiremt*, Spring, and *Bega*) levels for the period from 1981 to 2018. As suggested by Tadić et al. (2019) PCA analysis is used in order to assess the change in climate in a particular geographic area.

Table 12: Eigen values of the correlation matrix (1981-2018)

Seasons	Annual Tmax	Kiremt Tmax	Belg Tmax	Bega Tmax	Annual Tmin	Kiremt Tmin	Belg Tmin	Bega Tmin
Tmax, Tmin	PC1	PC2	PC3	PC4	PC5	PC6	PC7	PC8
Eigenvalue	5.21	2.03	0.33	0.28	0.08	0.05	0.02	0.01
% Variance	65.14	25.41	4.11	3.45	1.03	0.57	0.24	0.06
% cumulative variance	65.14	90.54	94.65	98.10	99.13	99.70	99.94	100
Standard deviation	2.28	1.43	0.57	0.53	0.29	0.21	0.14	0.07

Source: PCA analysis in R studio

The Eigenvalue matrix correlation result (Table 12) indicated that both the average maximum and minimum temperatures generally show high variation in the maximum and minimum temperatures. The main principal components (PC1, annual Tmax) explain about 65.14% of the total variance. PC2, *Kiremt* (main rainy) Tmax, reveals the second highest variance, explaining 25.41% of the variation. The third principal component explained 4.1% of the variance. The first two components together account for more than 90% of the variance. In this regard, the greater variation in the entire dataset is represented by the first component (Reusch et al., 2005). The result of the PCA eigenvalue matrix exhibited that PC1 is greater than PC2 and PC2 is higher than PC3. The influence of eigenvectors on each principal component and the percentage of variance are well explained by the first three principal components, as depicted in the table: PC1 (65.14%), PC2 (25.41%), and PC3 (4.11%). It is important to denote that most of the variation in annual and seasonal maximum and minimum temperature results due to PC1 and PC2.

Comparatively, the annual and seasonal minimum temperatures have shown low variance. Based on the analysis, the first two principal components were the dominant variables that considerably contributed to the increase in temperature in Addis Ababa city. In relation to this, literature noted that the first PC is linked with land heat, the second with sea heat, and the third associated with air

(Pandžić & Kisegi, 1990). Based on this assumption, the PCA analysis result of this study reflected the susceptibility of the city for urban heat island effect.

The analysis result of the cumulative principal components varies from season to season (Table 12). PC1 demonstrated the annual maximum temperature, which has an impact explaining 65.14% of the total variance. PC2 represents the *Kiremt* season maximum temperature, revealing a total variance of 90.54%. The third principal component, *Belg* Tmax, explained 94.65% of the total variance. In contrast, the analysis result of the principal components of the minimum temperature for *Kiremt* (main rainy), *Belg* (Spring), and *Bega* (dry) showed a cumulative variance of almost 100%. Thus, it is possible to conclude that the combination of the first two PCs highly influenced the change in temperature in Addis Ababa city.

As shown in Table 13, in PC4, the effect of the annual maximum and minimum temperature was dominant, while in PC3, the *Kiremt* (main rainy) temperature maximum and minimum had a strong impact. In PC2, *Belg* (spring) and *Bega* (dry season) temperatures had a moderate impact. Both the annual and seasonal maximum and minimum temperatures have a low impact on PC1.

Table 13: The principal components elements of annual and seasonal (1981-2018).

Annual/seasonal Tmax	PC1	PC2	PC3	PC4
Annual Tmax	0.52	0.06	-0.00	**0.85**
Kiremt Tmax	0.51	-0.07	**0.80**	-0.31
Belg Tmax	0.48	**0.70**	-0.38	-0.35
Bega Tmax	0.48	**-0.70**	-0.47	-0.25
Annual/seasonal Tmin	PC1	PC2	PC3	PC4
Annual Tmin	0.52	-0.04	0.10	**0.85**
Kiremt Tmin	0.52	0.03	**0.75**	-0.40

Belg Tmin	0.48	**0.71**	-0.47	-0.21
Bega Tmin	0.48	**-0.71**	-0.44	-0.28

Source: PCA analysis result in R studio. Bold values indicate statistically significance: no impact (0.0-0.2); low impact (0.2-0.4); moderate (0.4-0.7); strong (0.7-0.9); very strong (0.9-1.0) (Richman, 1981).

Figure 34 revealed the percentage of each dimension's (PCs) contribution to variance of both maximum and minimum temperature. As the scree plot depicted, there are eight dimensions that represent both the maximum and minimum temperature of both annual and seasonal. Dim-1 and Dim-5 represented annual Tmax and Tmin; Dim-2 and Dim-6 indicated *Kiremt* season Tmax and Tmin; Dim-3 and Dim-7 reflect *Belg* season Tmax and Tmin; Dim-4 and Dim-8 are attributed to *Bega* season Tmax and Tmin, respectively. Dim-1 (annual Tmax) and Dim-2 (*Kiremt* Tmax) explained a variance of 65.1% and 25.4%, respectively. While the least contribution was attributed to *Bega* (dry season) Tmin (0.1%). In this case, the scree plot analysis result is consistent with the eigenvalue matrix result displayed in table shown (Table 13).

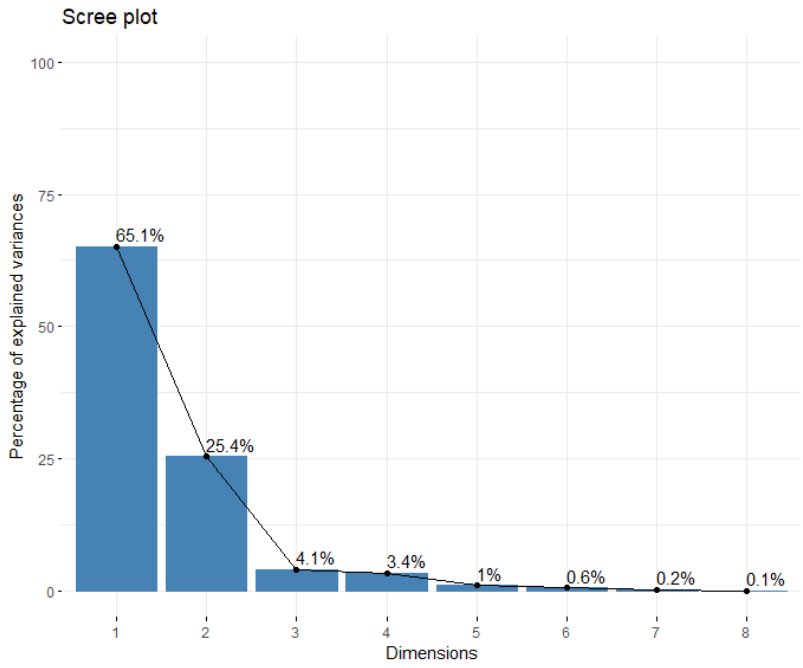

Figure 33: portrays the percentage of each dimension contribution for the variance.

The variable graph 35 demonstrated the correlation between the maximum and minimum temperature on the principal components, PC1 and PC2. Generally, the result implies that there was a positive correlation among the different variables. Both plots illustrated that Dim-1 (PC1) has 65.1% variation, whereas Dim-2 (PC2) contains 25.4% variation. In addition, the analysis results further exhibited that the annual Tmax and annual Tmin (green color) are highly correlated. While *Kiremt* Tmax and Tmin (light gray color) were moderately correlated, a negative correlation (red color) was found between *Belg* Tmax and *Belg* Tmin; the same is true for *Bega* Tmax and *Bega* Tmin. This implies that the average annual maximum and minimum temperature played a significant role in the increase of Addis Ababa City's temperature.

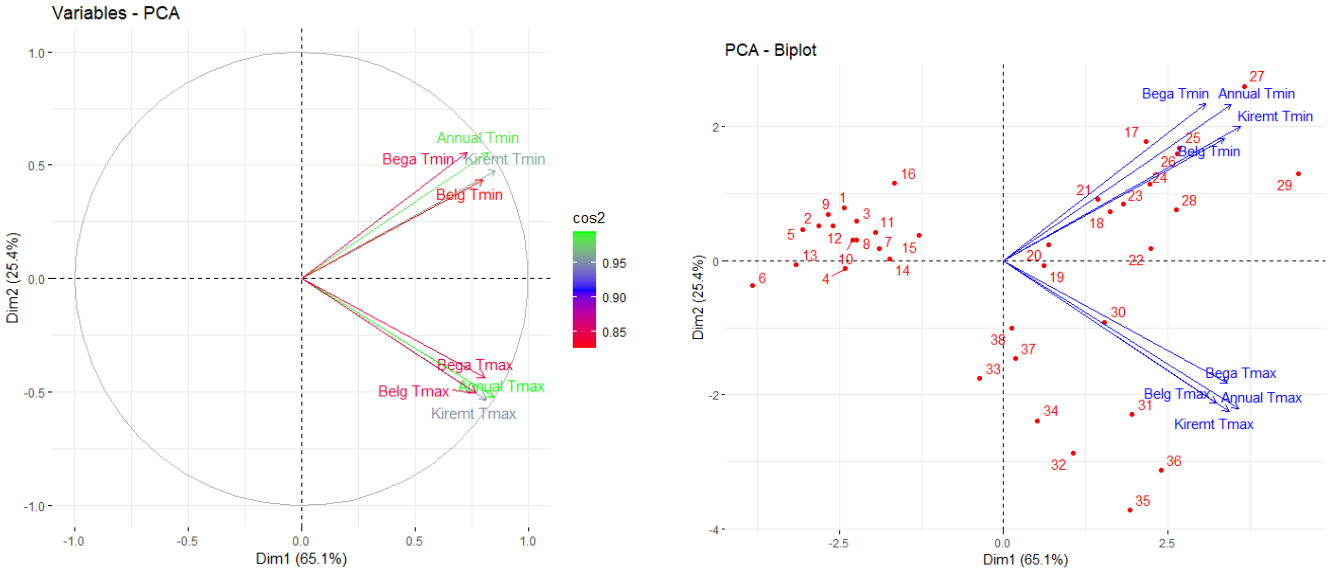

Figure 34: illustrates the correlation of variable to PCA (left) and PCA-Biplot (right).

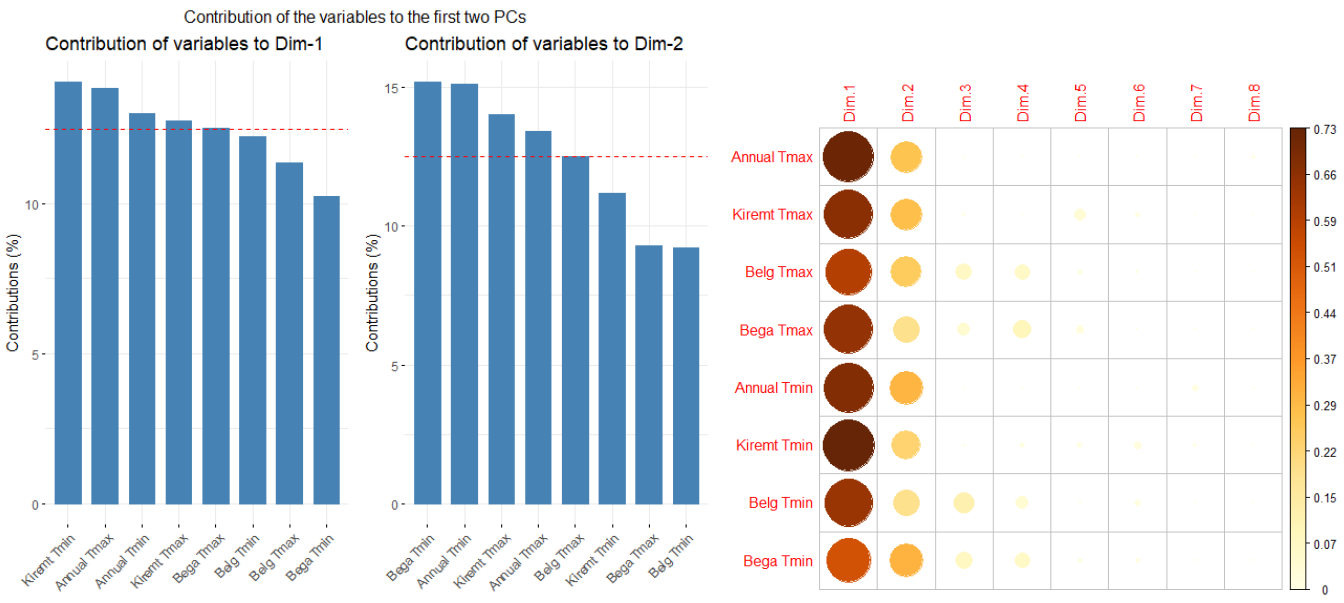

Figure 35: shows the contribution of each variable for the different PCs.

Source: analysis result in "R" studio

The graph 36 reveals the contribution of each variable for the first two dimensions (PCs). Among the various seasons, *Kiremt* Tmin, Annual Tmax, Annual Tmin, and *Kiremt* Tmax contributions were the highest. Particularly, *Kiremt* and Annual Tmax played the significant contributors for both dimensions. On the other hand, the contribution of variables to dimension 2 was *Bega* Tmin, Annual Tmin, *Kiremt* Tmax, and Annual Tmax. *Bega* Tmin and Annual Tmin were the greatest compared to others. Similarly, the figure on the right side also explains the contribution of each variable to each dimension (PCs). As it is shown figure on the right, all the variables contribute to dimension 1 (PC1) in different degrees. Annual Tmax and *Kiremt* Tmax contributed the most which is >0.7%. It was followed by *Kiremt* and *Bega* Tmax, annual Tmin, and *Belg* Tmin. The least contribution comes from *Bega* Tmin. Similarly, all the different variables at varying degrees contributed to dimension 2 (PC2). However, the greatest contribution came from annual Tmax, *Kiremt* Tmax, Annual Tmin, and *Bega* Tmin. For the remaining dimensions, the contribution of each variable was insignificant.

4.17.2. Monthly PCA analysis result

Table 14: The monthly principal component elements of (1981-2018).

Monthly	PC1	PC2	PC3
Tmax	-0.70	0.04	0.71
Tmin	-0.12	-0.10	-0.06
Average	-0.70	0.13	-0.70

Source: analysis result in R studio

Table 15: Eigen values of monthly the correlation matrix (1981-2018)

Components	PC1	PC2	PC3
Eigenvalue	2.00	0.99	0.01
% variance	0.67	0.33	0.00
% cumulative variance	0.67	0.10	1.00
Standard deviation	1.42	0.99	0.10

Source: analysis result in R studio

Table 14 and 15 highlight the monthly correlation matrix results of the three PCs. The eigenvalue matrix stipulated that the first two principal components (PC1 and PC2) account for 100% of the total data variance (Figure 37-right). especially, PC1 immensely contributed (66.8%) to the variance of monthly temperature. While PC3 has insignificant contribution (0.3%). When examining the individual contribution (Figure 37-right) for Dim-1-2 (PC1 and PC2), the months of August, May, July, and March are the largest contributors that highly influence the variability of monthly temperature in the period of concern over the study area.

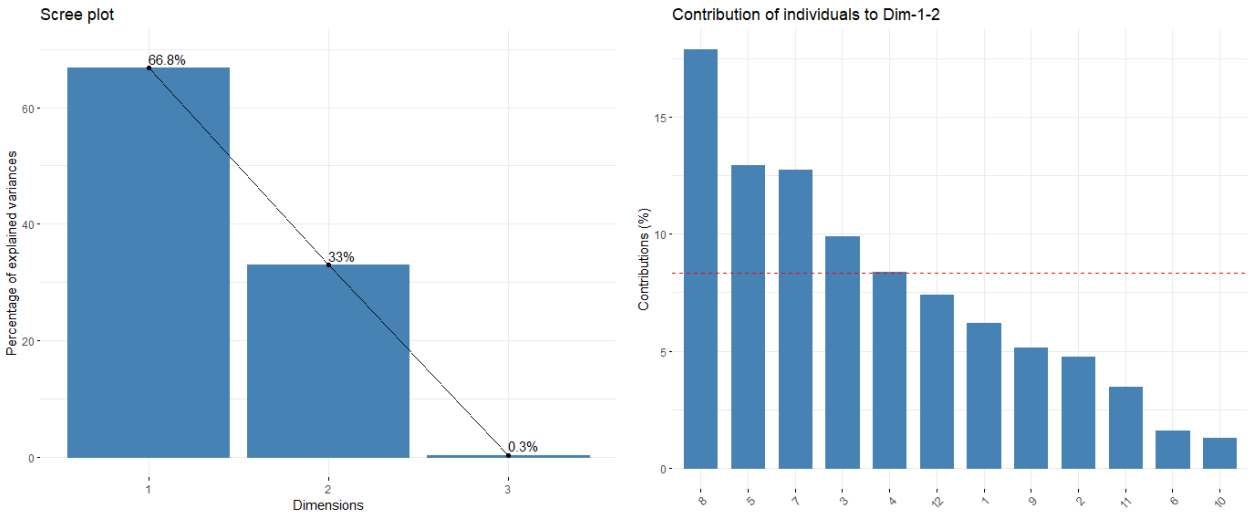

Figure 36: depicts the percentage of explained variance (left) and contribution of individuals to Dim-1-2 (right).

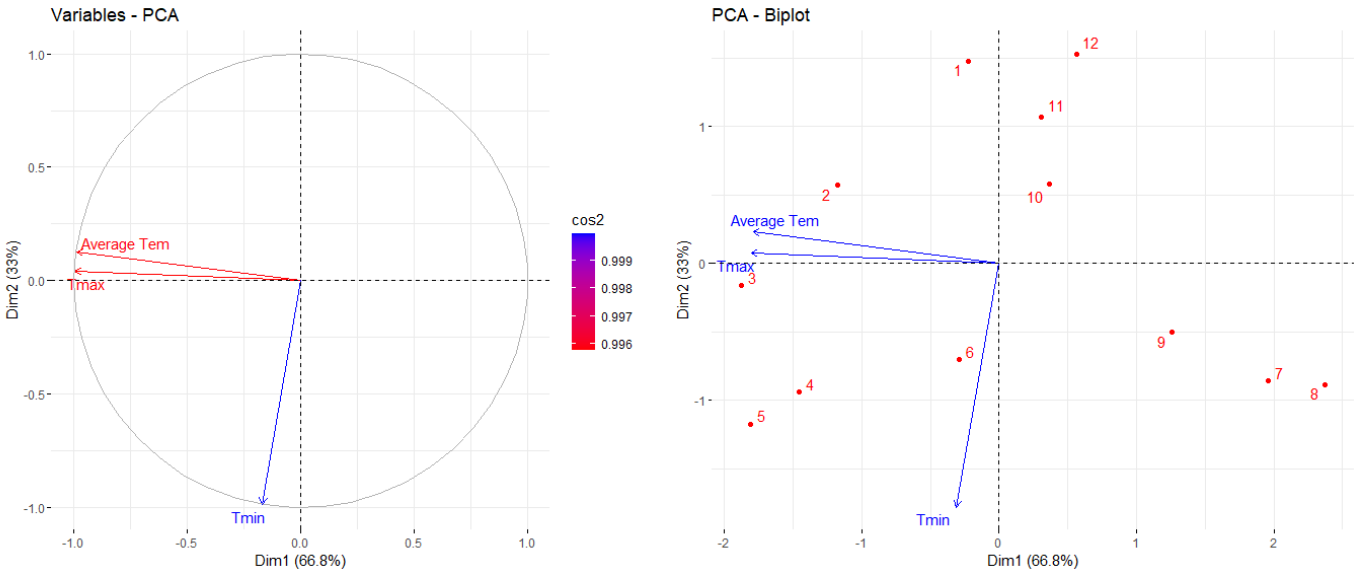

Figure 37: portrays correlation circles of monthly Tmax, Tmin, and Average (left) and Biplot of the same variables (right).

Evidently, as the correlation matrix (Figure 38) depicts the average and maximum temperature have a strong influence on the variables related to monthly temperature and it is also highly correlated. Contrary to this, the influence of the minimum temperature was insignificant. As the correlation result displays, the level of variation of Dim-1 (PC1) and Dim-2 (PC2) was 66.8% and 33%, respectively. It is important

to note that PC1 is higher than PC2. This signifies that 99.8% of the variation in monthly maximum and minimum temperature was due to PC1 and PC2.

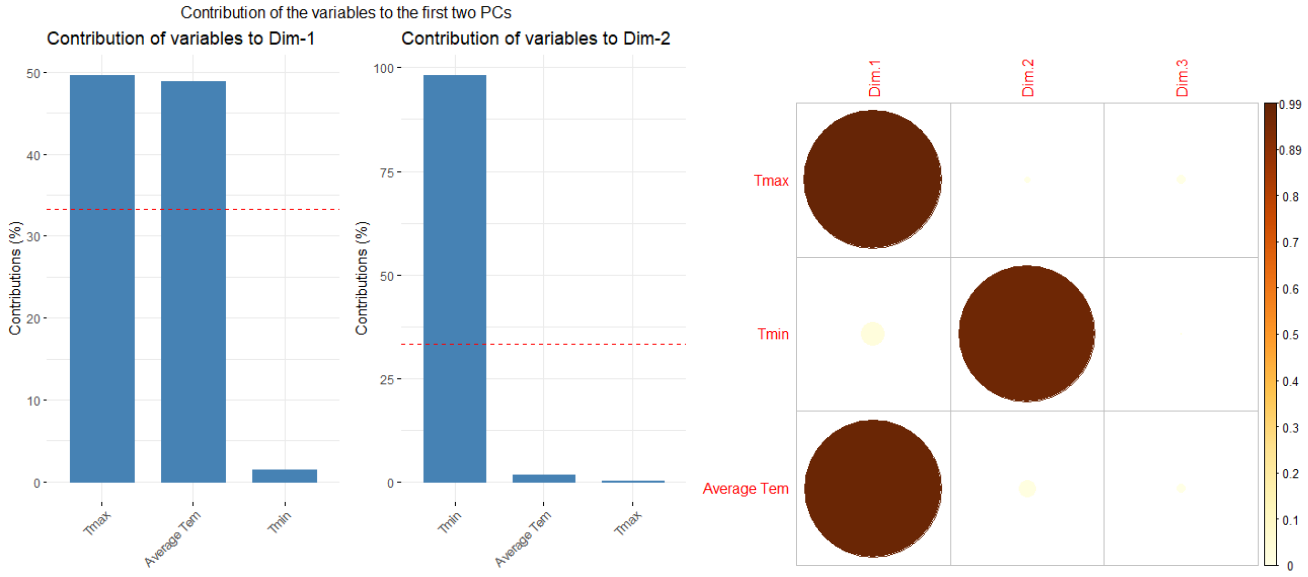

Figure 38: illustrates the contribution of each variable for the first two PCs (left and right).

Figure 39 shows the analysis result of the monthly contributions for Dim-1 and Dim-2, revealing that the maximum and average temperature were by far the largest contributors for Dim-1 (PC1). While monthly Tmin is the single most important contributor for Dim-2 (PC2). This is also supported by the analysis results under Table 12, which reveal that Tmax and the monthly average were the principal components of PC1 and PC2.

4.18. T-test analysis of Tmax and Tmin

Table 16 and 17 show the t.test analysis result for maximum and minimum temperature of the study period. The mean annual max temperature (M=26.16, SD=1.499, n=38) was hypothesized to be greater than the mean annual min temperature (M=12.767, SD=1.787, n=38). The difference was significant t (74) =1.99, p = 0.000 (1 tail). This means a highly statistically significant result. Since our p-value is far less than (1.94 x 10^-48), it was possible to state that our results are significant.

Table 16: T-test for annual maximum and minimum temperature (1981-2018).

		Average Annual Tmax	Average Annual Tmin
Mean	26.164231	Mean	12.7671173
Standard Error	0.2432331	Standard Error	0.289887436
Median	26.505108	Median	12.06654
Mode	#N/A	Mode	#N/A
Standard Deviation	1.4993893	Standard Deviation	1.786986171
Sample Variance	2.2481684	Sample Variance	3.193319576
Kurtosis	-0.857854	Kurtosis	-0.555415339
Skewness	0.3116161	Skewness	0.828831386
Range	5.1177	Range	6.655266667
Minimum	24.228525	Minimum	10.0909
Maximum	29.346225	Maximum	16.74616667
Sum	994.24078	Sum	485.1504575
Count	38	Count	38

Table 17: T-test: Two-Sample Assuming Equal Variances

	Average Annual Tmax	Average Annual Tmin
Mean	26.16423	12.7671173
Variance	2.248168	3.193319576
Observations	38	38
Pooled Variance	2.720744	
Hypothesized Mean Difference	0	
Df	74	
t Stat	35.40334	
P(T<=t) one-tail	1.94E-48	
t Critical one-tail	1.665707	
P(T<=t) two-tail	3.88E-48	
t Critical two-tail	1.992543	

4.19. Spatial distribution of LST

The analysis results, which are presented in Figure 40 and Table 18, illustrated that in the first observation year (1985), higher land surface temperatures (LST) were observed in the sub-cities of Akaki Kality, Bole, Lemi-Kura, and Nifasilk-Lafto. In the second observation year (2020), the dominant part of the city experienced a higher LST. This is largely attributable to the city's diminishing vegetation cover and the large expansion of industries and built-up areas. Milstein & Hart (1999) underscore that high-density residential areas and central business districts experience high temperatures. As cities grow, more vegetation is lost, and more surfaces are covered by buildings. In this regard, Tariq & Shu (2020) pointed out that as cities expand, the proportion of greenery coverage that protects the environment diminishes due to the replacement of impermeable surfaces with high rise buildings.

Previous study has revealed that high surface temperature are related with places with little vegetation cover, while low surface temperature are linked with areas with high vegetation cover (Weng & Lo, 2001;Yuan & Bauer, 2007). Gulele and Yeka sub-cities in the northern part of the city had the lowest LST, as seen in Figures 40 and 41. This is largely related to the presence of forest coverage and high-altitude location, which is a favorable condition for vegetation growth. In relation to this, literature underpin that areas covered with vegetation assumed to have lower concentration of LST (Moisa et al., 2022).

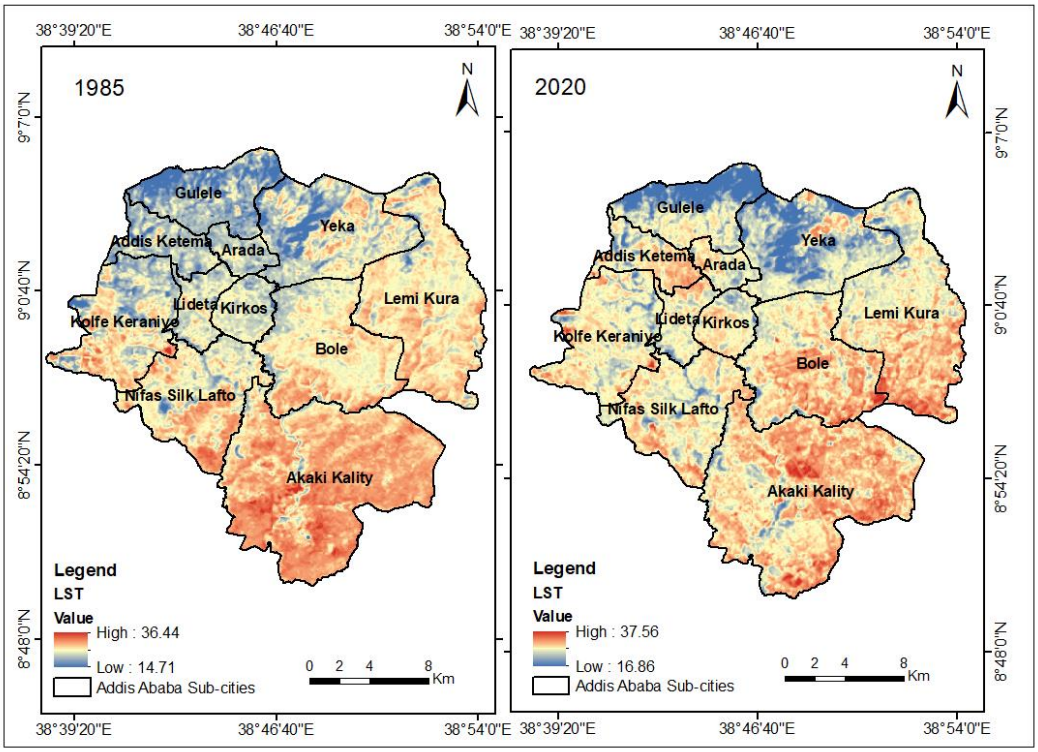

Figure 39: LST map of Addis Ababa in 1985 (left) and in 2020 (right).

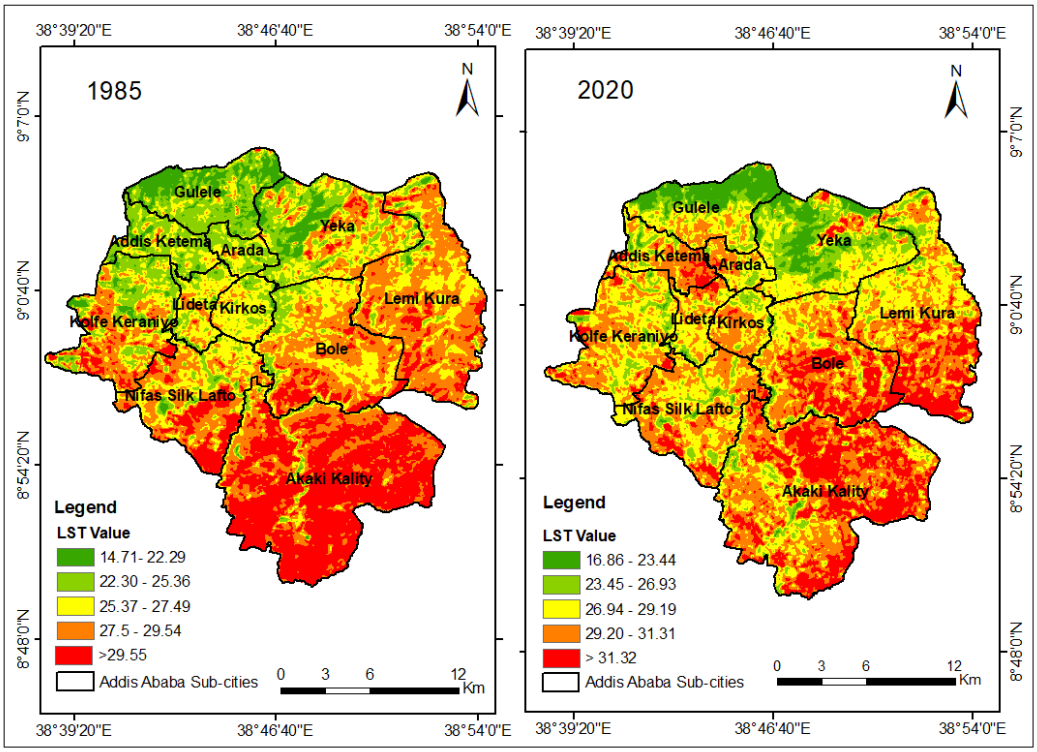

Figure 40: LST classified map of Addis Ababa in 1985 (left) and in 2020 (right).

Referring to Figure 41 and Table 18, the LST significantly rose between 1985 and 2020 because of the decreased vegetation cover in Addis Ketema, Arada, Kirkos, and Lideta sub-cities. Other factors such as the dynamics of the LULC and the presence of high impervious surface coverage in the area would also largely contributed for the escalation of LST in the city (Stemn & Kumi-Boateng, 2020). Studies also indicated that the LST over Addis Ababa sub-cities have significantly amplified over the observation period due to the rapid change in land use land cover. Additionally, studies have shown that changes in land-use-land-cover (LULC) have a substantial impact on the anomalies of land surface temperature (Barbieri et al., 2018; Choudhury et al., 2019; Sekertekin & Bonafoni, 2020). Moreover, rapid rate of urbanization is primarily responsible for the observed change in high heat concentration in cities (Dissanayake et al., 2019; Priyankara et al., 2019).

In the last one-decade (2010 onwards) Addis Ababa city witnessed that an overwhelming number of populations migrated from different parts of the country to the city due to economic and political reasons. In this regard, World Bank Group (2020) denoted that migration is the major factor for city's population growth. As a result, the city's population has increased significantly which subsequently would have an impact on the rise of LST of the city. Therefore, it is imperative to have an urban land use information which is critical to monitor city's population growth, government policy making, and most importantly for urban land management (Tariq & Mumtaz, 2023b).

Table 18: LU/LC with the corresponding mean LST

No.	LU/LC types	LST mean (°C)	
		1985	2020
1.	Bare land	28.2	30.8
2.	Built-up area	26.5	29.2
3.	Cultivated land	29.6	28.4
4.	Forest	23.1	22.2
5.	Water body	24.4	25.5

Source: analysis result in ArcGIS environs.

The analysis's findings showed that the average minimum LST in 1985 was 14.7 °C, while the mean maximum LST for the same year was 27.2 °C and the extreme maximum LST was 36.4 °C (Figure 41). With an average LST of 29 °C in 2020, the minimum and maximum LST grew to 16.86 °C and 37.5 °C, respectively. This implied that the mean, maximum, and minimum LST over Addis Ababa city have increased by 1.8 °C, 1.1 °C and 2.16 °C respectively, over the past 35 years (1985 - 2020). The surface temperature of the earth in the first twenty years (2001-2020) of 21st century was 0.99 °C higher than 1850-1900 (IPCC, 2023b). A more recent study conducted by Moisa et al. (2022) reported that the mean LTS in Addis Ababa city increased by 8.3 °C between 1991 and 2021. From this it is possible to comprehend that the result was a bit overstated. Similar researches indicated that the city temperature as compared with the surrounding countryside warmer by annually average of 2.5 °C (Sidiropoulos, 2023). On top of that, Mulatu & Desta (2023) denoted that Addis Ababa experienced a higher land surface temperature increase of 2.2 °C between 2006 and 2016.

4.19.1. Land surface temperature gradient across Addis Ababa Sub-cities

In this section, the pattern, relationship, and comparison among LST, NDVI, NDBI and elevation values were analyzed and presented. In all the observed 11 sub-cities (Table 19), the land surface temperature increased between 1985 and 2020. In these sub-cities, the mean land surface temperature ranged from 22.9 to 29.8 °C in 1985 and 25.1 to 30.6 °C in 2020. According to the statistical findings, the four sub-cities of Lideta, Kirkos, Arada, Addis Ketema, and the highest increases in land surface temperature during the study's years, with values ranging from 2.79 to 4.72 °C (Table 19). This is largely attributed to several factors. A study on highly urbanized cities in Africa demonstrated that cities with large proportion of impervious surfaces were warmer by 3-4 °C (Simwanda et al., 2019). In this regard, studies divulge that there is a variation in the impacts of UHI within a city the stronger impact would be felt in city center than that of the peri-urban area (Li et al., 2019). Similar studies conducted in Lahore City of Pakistan underscores that temperature rises were more pronounced in the built-up city center than the periphery (Tariq & Mumtaz, 2023b).

In the city's low-NDVI sub-cities were Arada, Lideta, Kirkos, and Addis Ketema, the land surface temperature was significantly higher, this can be used as a reliable predictor of the presence of

urban heat islands (UHI). Land surface temperature was discovered to have a negative correlation with elevation values in every sub-city. For instance, the sub-city of Akaki Kality, which is at the lowest altitude with an elevation of 2162 m, is one of the highest average land surface temperatures for the years 1985 and 2020, with values of 29.84 °C and 30.55 °C, respectively. It is important to note that the low elevated area of the sub-cities such as Akaki Kality and Nifas-silk Lafto there was no significant temperature increase over the study period as compared the urban core sub-cities of Addis Ketema, Arada, Kirkos, and Lideta. On the other hand, Yeka and Akaki Kality are situated at an altitude of 2583 and 2162 meters above sea level, respectively. However, in contrast to the other sub-cities, the land surface temperature was the lowest increment (Table 19). This is largely because Yeka sub-city is dominantly covered by natural forests which is a contributing factor for low increment of temperature in the area. While Akaki-kality because it is largely covered by urban agriculture.

Emissivity is a spectrally changing attribute of a material that describes the efficiency with which an object emits electromagnetic radiation as a function of temperature at any given wavelength (Malik et al., 2019; Langsdale et al., 2020). Land surface emissivity (LSE) influences satellite measurements in three ways: (1) it reduces surface-emitted radiance, (2) non-black surfaces reflect more radiance, and (3) the anisotropy of reflectivity and emissivity can reduce or increase total radiance from the surface (Prata, 1994).

In Addis Ababa sub-cities, the spatial relationship among land surface temperature and land surface emissivity was studied. Consequently, a strong upward relationship between LST and land surface emissivity was discovered in all the sub-cities. Similarly, how topography (elevation) affects the fluctuation of land surface temperature across sub-cities was explored (Table 19). Based on the findings of the investigation, land surface temperature has a weak downward relationship with elevation in almost all the sub-cities. In contrast to the correlations reported for NDVI and land surface emissivity, a weak and irregular relationship between land surface temperature and elevation was revealed (Table 19).

Table 19: LST, NDVI, LSE, and elevation mean values in Addis Ababa's sub-cities.

Sub-cities	LST(°C)		NDVI		LSE		Mean elevation (m)	LST Difference (1985 & 2020)
	1985	2020	1985	2020	1985	2020		
Yeka	25.39	25.94	0.21	0.17	0.9874	0.9869	2583	0.55
Nifas Silk Lafto	27.79	29.15	0.14	0.12	0.987	0.9867	2240	1.36
Lideta	25.94	28.73	0.09	0.11	0.9868	0.9867	2332	2.79
Lemi Kura	27.80	29.71	0.13	0.14	0.987	0.9868	2374	1.91
Kolfe Keraniyo	26.47	28.85	0.20	0.12	0.9873	0.9867	2396	2.39
Kirkos	25.81	28.84	0.10	0.09	0.9868	0.9866	2329	3.03
Gulele	22.85	25.05	0.25	0.17	0.9876	0.9869	2674	2.20
Bole	27.60	30.11	0.11	0.13	0.9869	0.9868	2282	2.51
Arada	24.99	28.80	0.10	0.10	0.9869	0.9866	2447	3.81
Akaki Kality	29.84	30.55	0.08	0.15	0.9867	0.9868	2162	0.71
Addis Ketema	24.45	29.17	0.14	0.10	0.987	0.9866	2476	4.72

Source: ArcGIS zonal statistics result

4.19.2. NDVI and LST analysis result

The scatter plot analysis result (Figure 42) indicated that between 1985 and 2020, there was NDVI value change. NDVI and LST typically have an inverse relationship; areas with low NDVI values have high LST (Ullah et al., 2023). The highest NDVI value in 1985 was 0.57 and the lowest was -0.29 with a mean of 0.14. Previous studies noted that the greater the NDVI value, the lower the LST, and the lower the NDVI, the higher the LST (Balew & Korme, 2020b). Related studies have also found a negative relationship between LST and NDVI (Hua et al., 2020; Zare et al., 2020; Merga et al., 2022). The highest, lowest, and mean NDVI readings for the year 2020 were 0.56, -0.16, and 0.13, respectively. In comparison, the NDVI rating for 2020 was lower. These clearly indicated that a decline of vegetation coverage in the study area. In addition, the scatter plot

statistical analysis result (Figure 42) demonstrated a negative association between NDVI and LST with an R^2 value of 0.39 in 1985 and 0.21 in 2020.

In Gulele and Kolfe Keraniyo sub-cities, the normalized difference vegetation index (NDVI) was significantly reduced, according to the analysis of its distribution (Figure 43 and Table 19). The calculated NDVI value in Gulele and Kolfe Keraniyo was 0.25 and 0.20 in 1985, but it fell to 0.17 and 0.12 in 2020, respectively. In comparison, the share of NDVI value in the Akaki Kality sub-city increased from 0.08 in 1985 to 0.15 in 2020. While in Arada sub-city, it remained constant. In terms of geographic distribution, the northern part of the city (Gulele and Yeka sub-cities) has the highest NDVI value. While in the central Addis Ababa City, including Addis Ketema, Arada, Kirkose, and Lideta sub-cities, vegetation coverage has decreased over the last 35 years (1985-2020). This was mainly attributed to factors such as accelerated expansion of built-up areas across the city. In relation to this, Tafesse & Suryabhagavan (2019) described that the decrease in NDVI values is a sign of a typical determinantal effect of urban expansion on the natural ecosystem. In addition, Lu et al. (2008) explained that one of the most significant changes caused by urban expansion is the alteration of natural surfaces into artificial built-up surfaces.

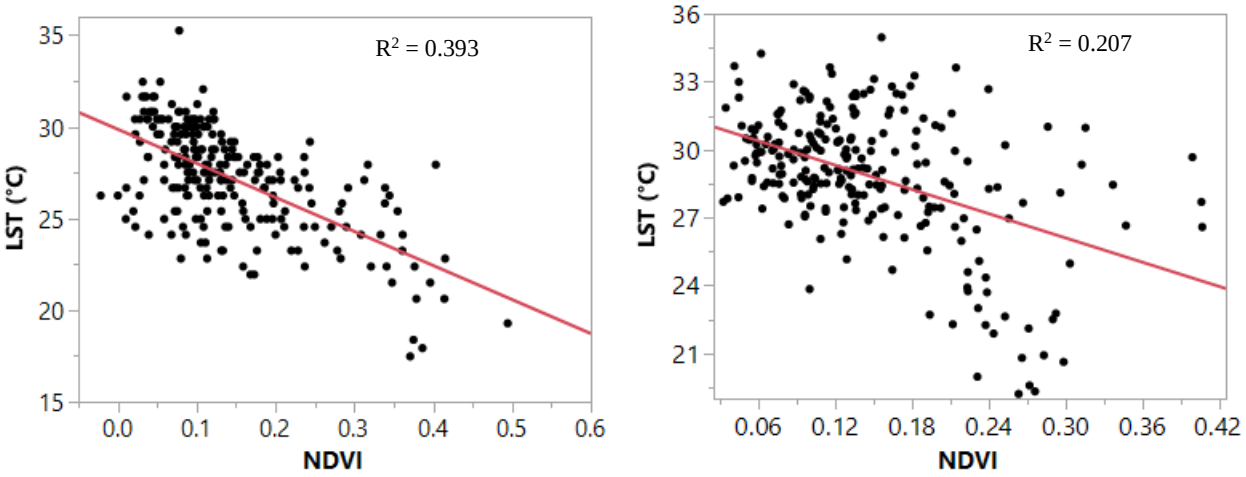

Figure 41: correlation between LST and NDVI for 1985 (left side) and 2020 (right side).

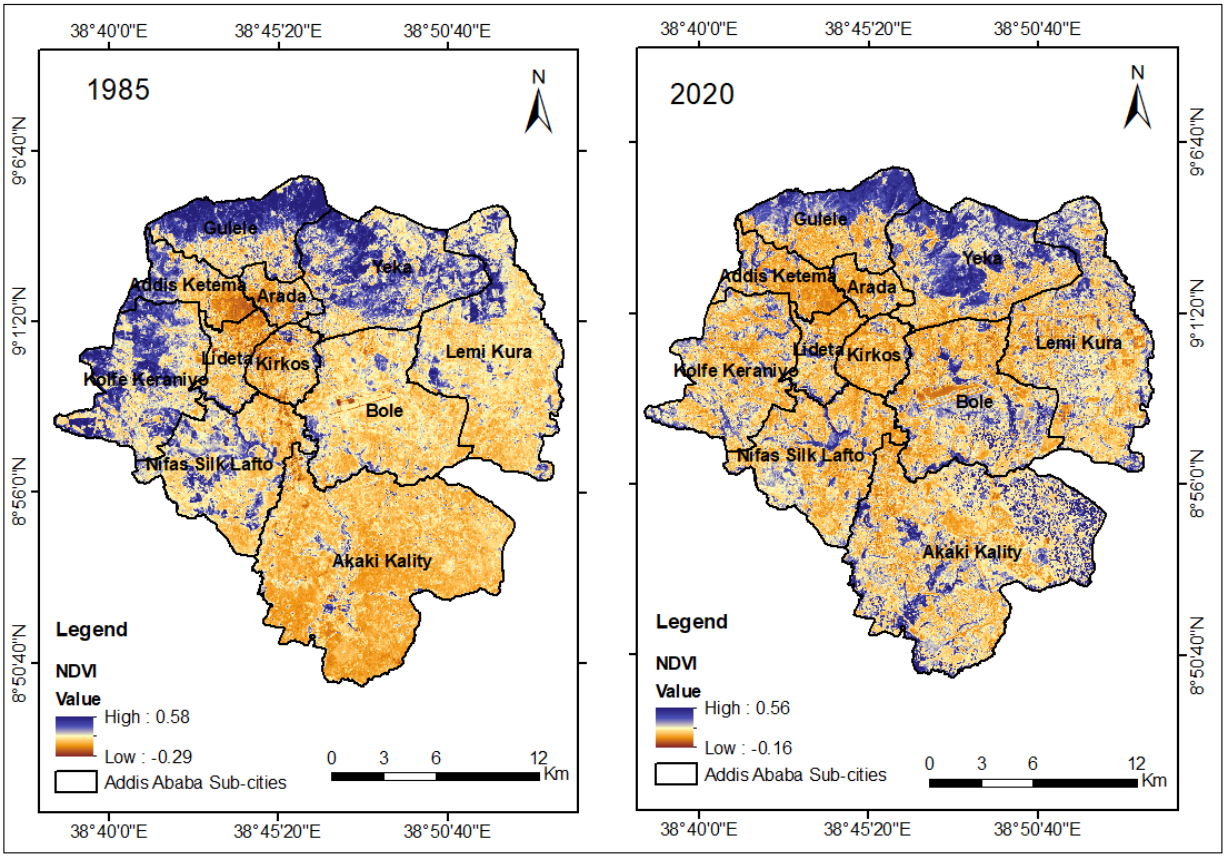

Figure 42: NDVI map of Addis Ababa City for the year 1985 (left side) and 2020 (right side).

4.19.3. NDBI and LST relationship

Figures 44 and 45 demonstrate the spatial distribution and correlation of the NDBI with LST between 1985 and 2020. The correlation between NDBI and LST was found to be positive over the study period, as indicated by the scatter plot (Figure 45). In connection to this, Pandey et al. (2022) underline that NDBI is considered as the most reliable variable index as compared with other indices. In 1985, greater NDBI values were detected throughout the city except the northernmost, north-west, and north-east areas of the city, as spatially depicted in Figure 44. On the other hand, for the later year (2020), comparatively greater NDBI values were observed all over the city apart from the areas along the northern perimeter of the city, which is predominately covered by forest plantation.

As shown in the scatter plot in Figure 45, there was a positive association between LST and NDBI during the study period, with R^2 values of 0.36 and 0.32 for the years 1985 and 2020, respectively. Similarly, studies conducted in Raipur city of India observed that LST builds positive correlation with NDBI (Guha & Govil, 2022). Given that NDBI and LST have an upward and positive association, it is likely that the built-up area is the main contributor for the increase in land surface temperature and urban heat islands. Pertaining with this, as literature revealed that the highest NDBI values were associated with areas where there is high density of built-up areas (Alexander, 2020; Sarif et al., 2020).

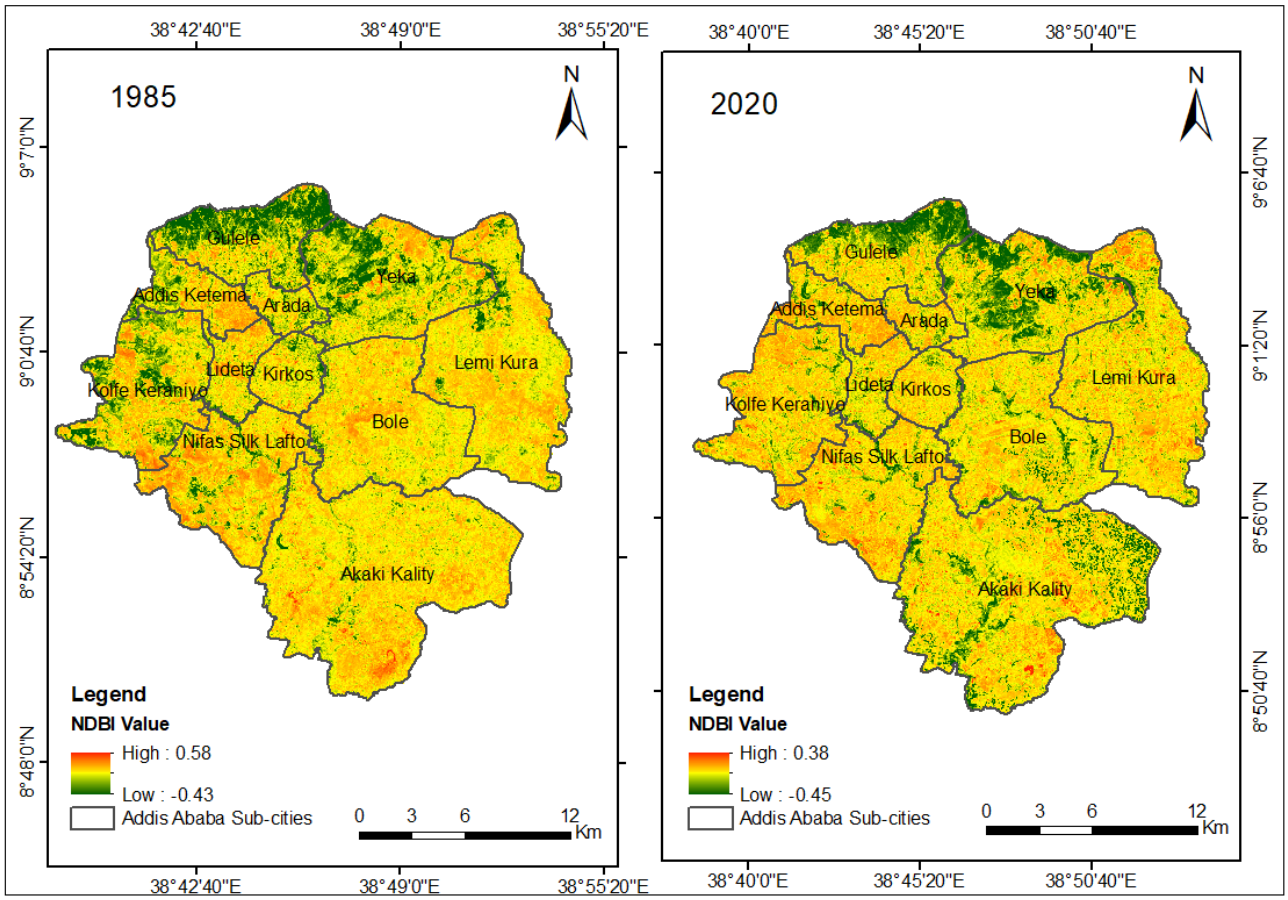

Figure 43: spatial NDBI dynamics in Addis Ababa city in 1985 (left side) and 2020 (right side).

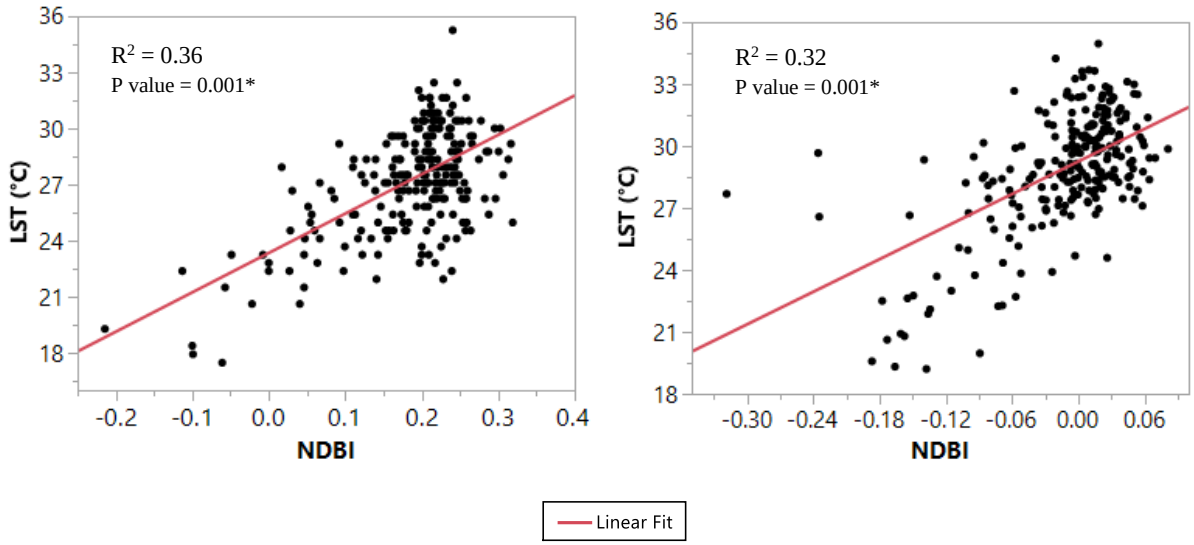

Figure 44: Correlation between LST and NDBI for the year 1985 (left side) and 2020 (right side).

4.19.4. NDBI and NDVI analysis result

The NDBI analyzes the quantity of built-up area in a certain geographic arena, while the NDVI assesses the distribution of vegetation (Shahfahad et al., 2020). The values of NDVI and NDBI both fall between -1 and +1 (Kshetri, 2018). A negative value signifies that there is no vegetation or built-up area, while a positive value implies that there is vegetation or built-up area present (Malik et al., 2019). During the research period, a relationship between NDVI and NDBI was also developed (Figure 46). Based on the analysis result, the NDVI and NDBI values of Addis Ababa ranged between 0.0-0.5 and -0.2 - 0.3 for the year 1985 and 0.07 - 0.42 and -0.32 – 0.08 in 2020, respectively, over the observation period. The scatter plot in Figure 48 shows a strong negative correlation between NDVI and NDBI, with an R^2 value of 0.66 in 1985 and 0.58 in 2020. Studies exhibited that NDVI can be employed to symbolize the progress and expansion of built-up land (Chen et al., 2013).

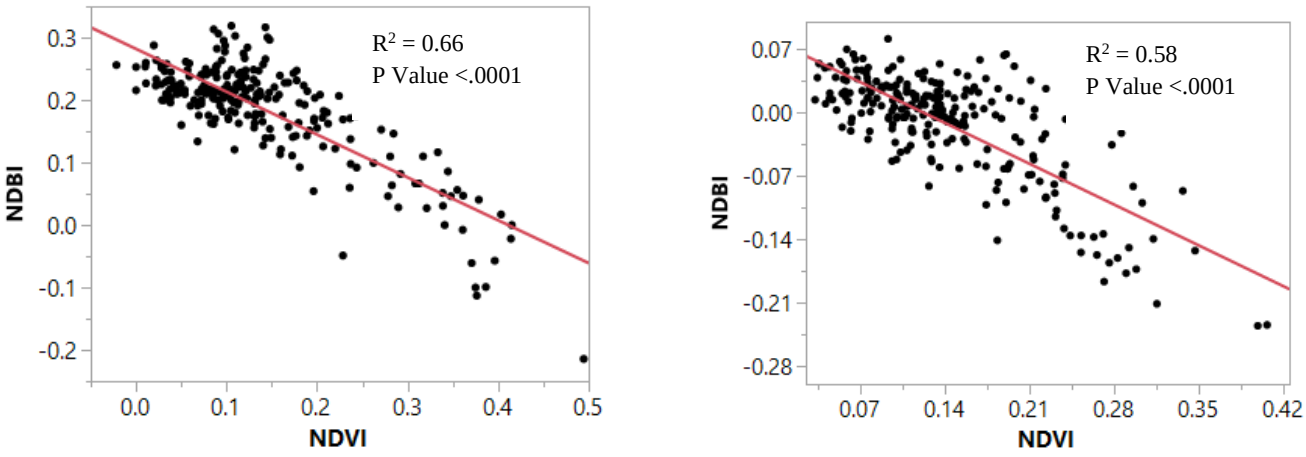

Figure 45: correlation between NDBI and NDVI for the year 1985 (left side) and 2020 (right side).

4.19.5. LST vs Elevation interplay

The proximity of Ethiopia to the equator, as well as the intricacy of the country's topography, have an indispensable role in maintaining Ethiopia's climate, particularly the temperature (Kshetri, 2018; Asefa et al., 2020). The comparison of LST and elevation revealed an inverse association with R^2 values of 0.434 and 0.314 for the years 1985 and 2020, respectively (Figure 47). The diagrams provided in Figures 47 and 48 made it very evident that LST rises as elevation falls across Addis Ababa city. Firozjaei et al. (2020) provided evidence that topographic and biophysical features have a role in the inverse association between LST and elevation. Consistently, Jin et al. (2005) discovered an inverse association among the LST and altitude. The main reason for influence on the LST is caused by air temperature, and the temperature value normally drops progressively with increasing altitude (Peng et al., 2020).

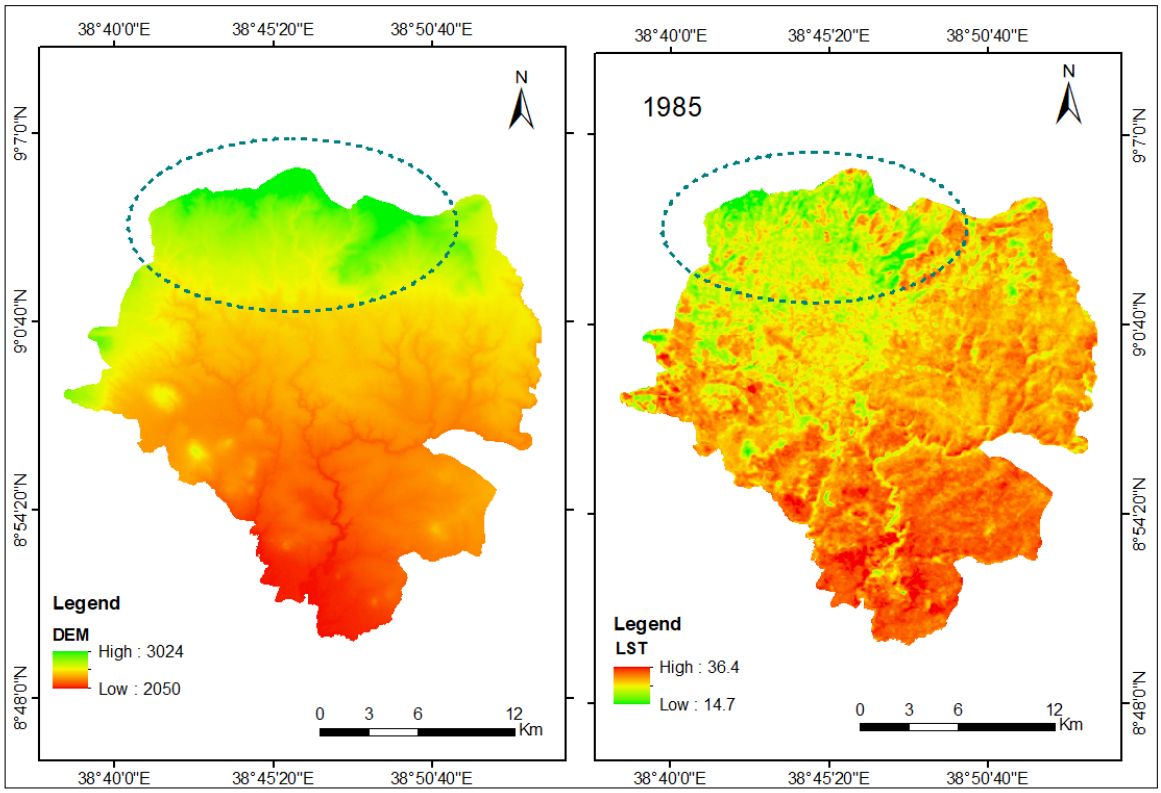

Figure 46: the spatial relationship between DEM (left side) and LST (right side).

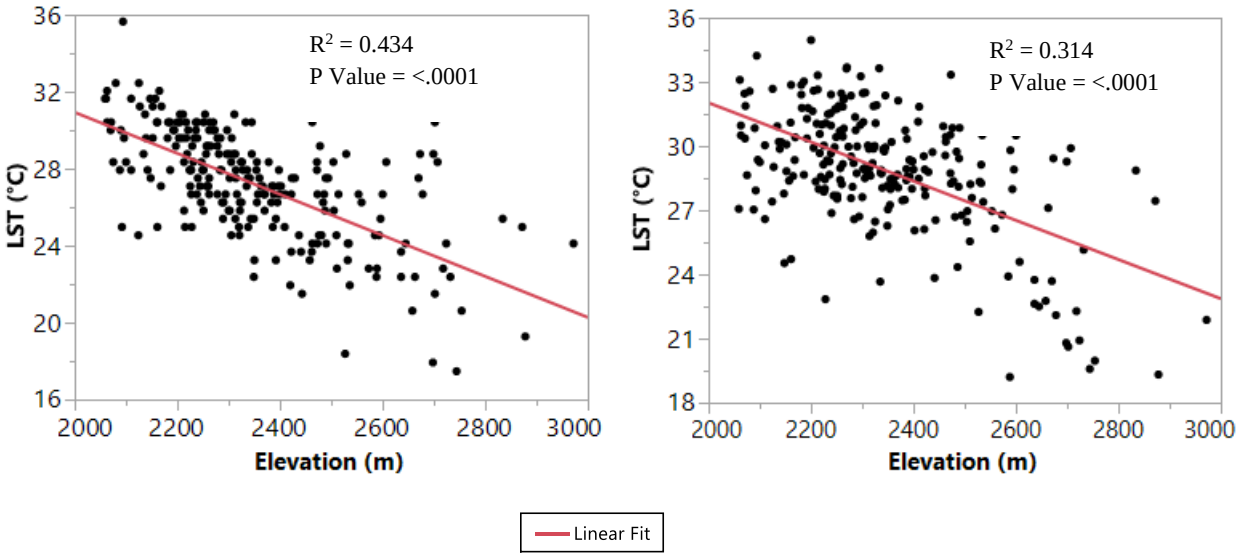

Figure 47: correlation between elevation and LST for 1985 (right side) and 2020 (left side).

4.19.6. LULCC relationship with LST

LST responds differently depending on the land use type. Vegetation and Agricultural land produces low LST while built-up areas and open spaces generate high LST (Pandey et al., 2022) For comparison reasons, the study area was compartmentalized into five land use classes. These are: built-up area, bare land, cultivated land, forest, and water body. From the results of the land use/land cover change analysis (Table 20 and Figure 49), the main land use land cover classes in the research area for the year 1985 were built-up area, which made up 195 km^2 (37.5%), and bare land, which comprised 147.3 km^2 (28.4%). The water body occupied the least area in this category, with 115.6 km2 (22.2%) of cultivated land. However, the LULC study result for 2020 shows that built-up area, which made up 326.3 km^2 (62.8%) of the total land area, is the largest land use class. Bare land, which accounts 118.3 km^2 (22.7%), is in second position. The water body once again constituted the smallest percentage.

Over the course of the study period, the LULC patterns in the study area showed considerable change. Apart from the waterbody, all the five LULC classes underwent significant alterations. The LULC classification result for 1985 and 2020, built-up area was the dominant land use class, with an area of 195 km^2 (37.5%) and 326.3 km^2 (62.8%), respectively (Table 19 and Figure 49). The bare land was the second largest with an area of 147.4 km^2 (28.4%) and 118.3 km^2 (22.8%) for the year 1985 and 2020. In contrast to the built-up area, the bare land was considerably reduced during the study period.

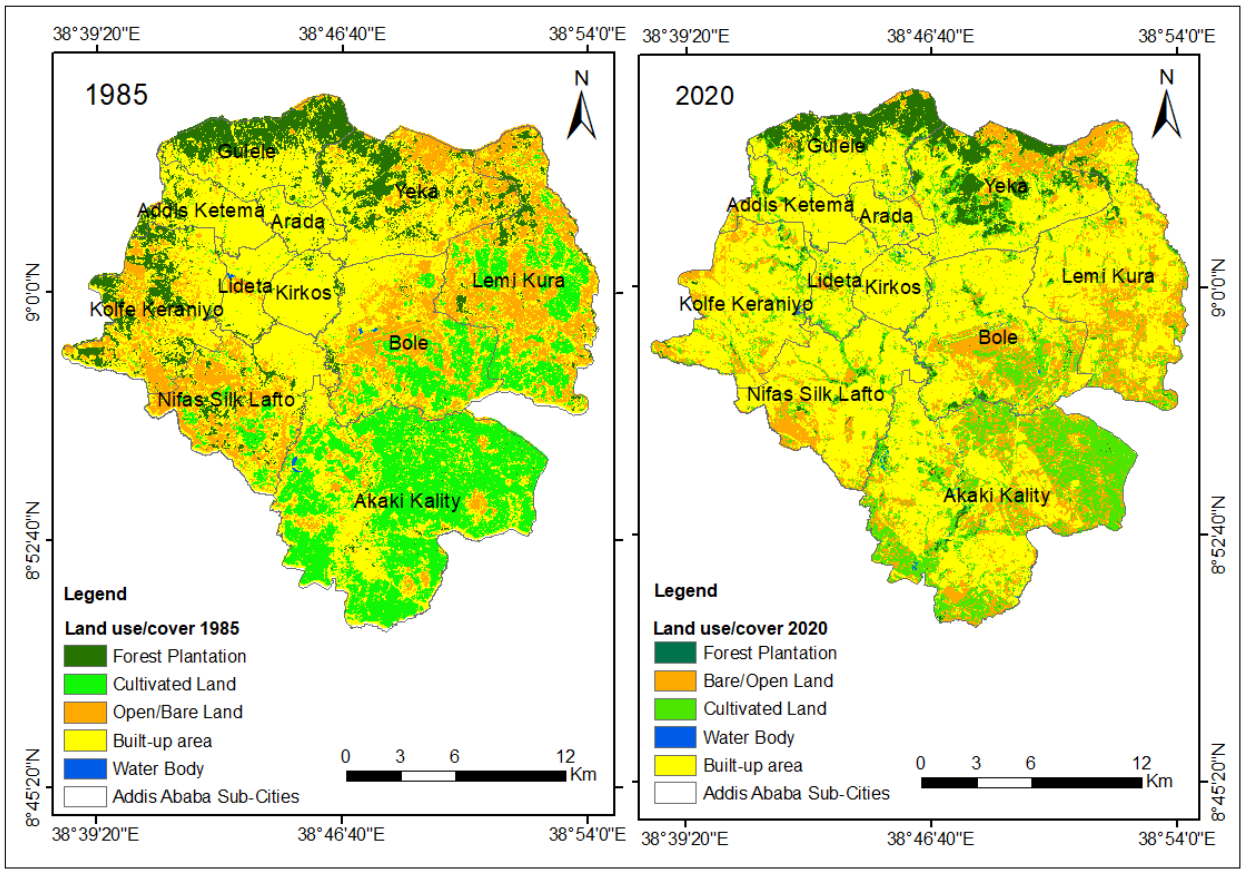

Figure 48: Map of LULC types over Addis Ababa, 1985 (left) and 2020 (right).

This study's findings were consistent with the previous LST related studies revealed that the built-up areas of Addis Ababa rose from 19.20% in 1986 to 34.45% in 2011 (Teferi & Abraha, 2017a). The built-up area in Addis Ababa metropolis is expanding at an unprecedented rate (Worku et al., 2021). In addition, Hua et al. (2020) and Kafy et al. (2021) designated that a growth in urbanization and impermeable surfaces led to an increasing trend of LST. Conversely, the area of forest, cultivated land, and bare land were drastically reduced from 61 km^2 (11.7%), 115.6 km^2 (22.2%), 147.3 km^2 (28.4%) in 1985 to 33.1 km^2 (6.4%), 38.5 km^2 (7.4%), 118.1km^2 (22.7%) in 2020, respectively (Figure 50 and Table 20). This was a major factor for the increase of the built-up land use class. For instance, a total of 87.2 km^2 (16.8%) of bare land, 26.1 km^2 (5%) of Forest, and 57.5 km^2 (11.1 %) of cultivated land were transformed into built-up area. This reflects how the built-up area has grown substantially during the last 35 years, having an enormous effect in the increase of LST in the city. Pertaining with this, studies reported that LULC change have a significant impact on the fluctuation of LST (Guha et al., 2020).

Figure 50 exemplified that a large expansion of built-up areas occurred towards Addis Ababa sub-cities of Akaki Kality, Bole, Lemi Kura, Nefas Silk Lafto, and Kolfe Keranyo. However, the expansion of built-up area was largely limited around the northern parts of Gulele and Yeka sub-cities. This is due to the fact that since the two sub-cities are situated in high elevated area of Addis Ababa City, where it is mostly covered by forest combined with the nature of topography, and the city administration's land use policies which made the area uninhabitable (Worku et al., 2021).

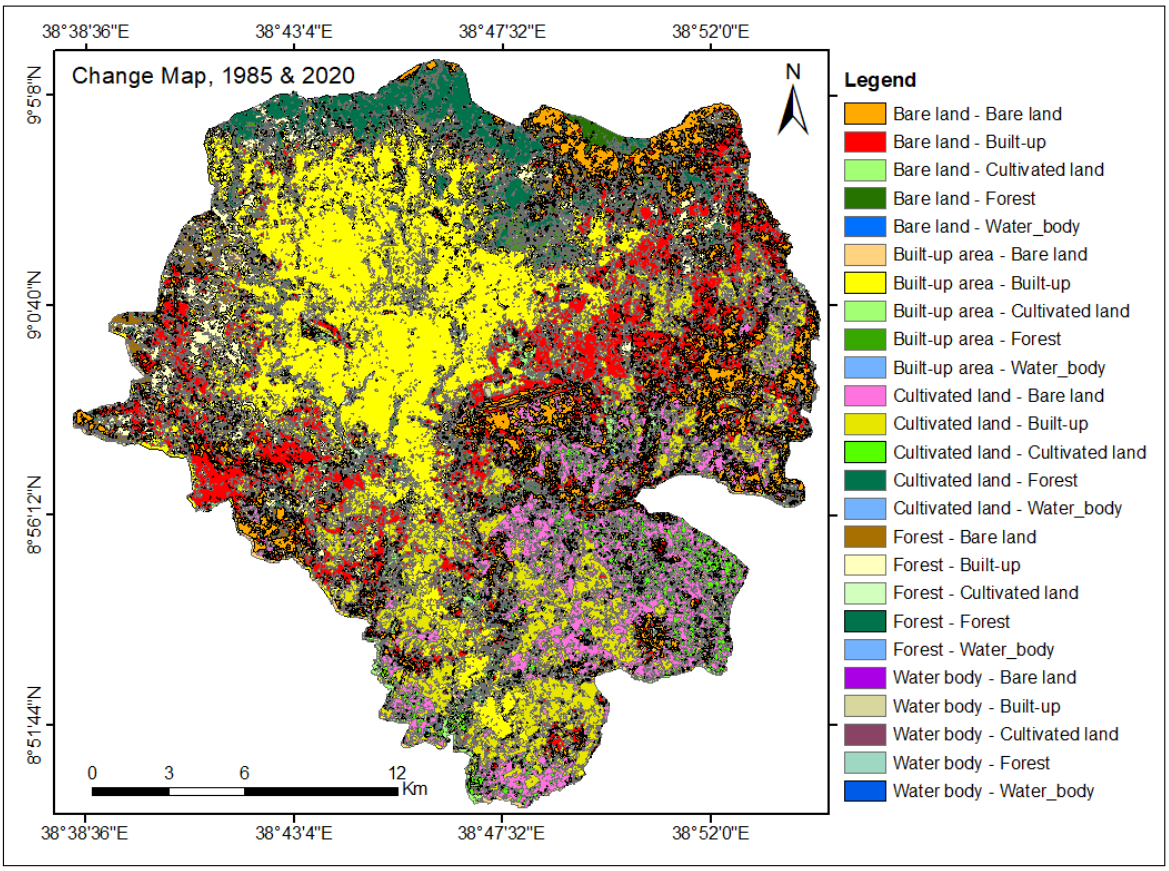

Figure 49: LULC change detection matrix between 1985 and 2020 in Addis Ababa city.

Table 20: Land use land cover change detection matrix in Addis Ababa city between 1985 and 2020.

Year	Land use land cover class for 2020											
Land use land cover class for 1985	LULC classes	Forest		Built-up area		Cultivated land		Water body		Bare land		Class total	
		Sq.km	%	Sq.km	%	Sq.km	%	Sq.km	%	Sq.km	%	Sq.km	%
	Forest	22.1	4.3	26.1	5.0	4.7	0.9	0.8	0.2	7.3	1.4	61.0	11.7
	Built-up area	7.0	1.3	155.0	29.8	11.4	2.2	1.6	0.3	19.8	3.8	195	37.5
	Cultivated land	0.3	0.1	57.5	11.1	13.1	2.5	0.5	0.1	44.1	8.5	115.6	22.2
	Water body	0.0	0	0.5	0.1	0.1	0.0	0.1	0.0	0.0	0	0.6	0.1
	Bare land	3.7	0.7	87.2	16.8	9.2	1.8	0.3	0.1	46.9	9.0	147.3	28.4
	Class total	33.1	6.4	326.3	62.8	38.5	7.4	3.3	0.6	118.1	22.7	519.3	100
	Image anomaly	-27.9	-5.3	131.5	25.3	-77.1	-14.8	2.7	0.5	-29.2	-5.7		

Source: ArcGIS confusion matrix result.

The average and highest LST distribution for each LU/LC class was calculated (Table 21). It was found that in 1985, the mean LST for cultivated land was 29.52 ℃, followed bare land and built-up area, which were 28.15 ℃ and 26.47 ℃, correspondingly. In contrast, the analysis results for 2020 exhibited that the highest mean LST was assumed to be in bare land, with an average value of 30.79 ℃. Built-up and cultivated land had the second and third highest LST values, 29.15 ℃ and 28.22 ℃, respectively. Water body found to have the lowest mean LST change across the observation period.

Generally, the built-up and bare land had the maximum LST and highest rate of change in the mean LST values of 2.68 ˚C and 2.64 ˚C between 1985 and 2020, respectively (Table 21). In relation to this, a study reported that a larger increase in land surface temperature is expected in Addis Ababa city following the elimination of vegetation and expansion of built-up area (Worku et al., 2021). Similarly, a recent study reported a high LST over densely populated areas and places with little vegetative cover. Furthermore, the urban core parts of Addis Ababa were more affected by UHI than the outskirts (Moisa et al., 2022).

Table 21: the rate of mean and maximum LST over each LU/LC class in Addis Ababa between 1985 and 2020.

No.	LU/LC types	LST Mean & Max (^{0}C)				
		1985		2020		1985-2020 change in Mean (^{0}C)
		Mean	Max	Mean	Max	
3.	Bare land	28.15	36.05	30.79	37.56	2.64
4.	Built-up area	26.47	36.44	29.15	37.54	2.68
5.	Cultivated land	29.52	35.65	28.22	34.94	-1.30
6.	Forest	23.27	32.05	22.26	33.40	-1.01
7.	Water body	26.28	31.65	26.28	35.42	0.00

Source: ArcGIS zonal statistics result.

4.20. Accuracy Assessment

The total classification accuracy in 1985 and 2020 was 81% and 85%, respectively, with Kappa of 0.81 and 0.85. An error matrix (Tables 22 and 23) was used to evaluate the relationships between the reference data with the corresponding classification results. The matrix exhibits the kappa statistics, as well as the accuracy of users and producers.

Table 22: Accuracy assessment result, 1985

Reference data								
Classified data	Forest	Cultivated land	Bare land	Built-up area	Water body	Total	UA (%)	Kappa statistics
Forest	58	1	1	0	0	60	0.97	0
Cultivated land	0	60	0	0	0	60	1	0
Bare land	3	5	51	1	0	60	0.85	0
Built-up area	1	7	7	45	0	60	0.75	0
Water body	1	1	11	7	40	60	0.67	0
Total	63	74	70	53	40	300	0	0
PA (%)	0.92	0.81	0.73	0.85	1	0	0.85	0
Kappa statistics	0	0	0	0	0	0	0	0.81

Source: ArcGIS confusion matrix analysis result.

Table 23: Accuracy assessment result, 2020

Reference data								
Classified data	Forest	Built-up area	Cultivated land	Bare land	Water body	Total	UA (%)	Kappa statistics
Forest	60	0	0	0	0	60	1	0
Built-up	0	55	2	3	0	60	0.92	0
Cultivated land	6	1	51	2	0	60	0.85	0
Bare land	0	1	5	54	0	60	0.90	0
Water body	7	6	0	3	44	60	0.73	0
Total	73	63	58	62	44	300	0	0
PA (%)	0.82	0.87	0.88	0.87	1	0	0.88	0
Kappa statistics	0	0	0	0	0	0	0	0.85

Source: ArcGIS confusion matrix analysis result.

CHAPTER FIVE: CONCLUSION AND RECOMMENDATIONS

5.1. Conclusions

The study conducted an in-depth investigation of climate variability in Addis Ababa, Ethiopia, over a 38-year time from 1981 to 2018. Precipitation, temperature, and urban heat island effect trend analysis were conducted across space and time. The study provided valuable information about the city's climate trend and magnitude of change over the past four decades. The investigation covered various aspects, including monthly fluctuations, annual, seasonal, and decadal patterns. The coefficient of variation, standardized anomaly index, Mann-Kendall, Modified Mann-Kendall test, principal component analysis, and t-test were used to analyze and detect the trend, anomalies, and magnitude of change using geospatial technologies, "R" programming, and statistical software such as JMP and Origin. In addition, the study also examined how the land use dynamics interplay with the rate of change on surface temperature in Addis Ababa sub-cities, Ethiopia.

The key findings and implications of this comprehensive analysis revealed significant spatial and temporal variations both in temperature, precipitation, and LST within Addis Ababa as a whole. The result showed that the mean annual rainfall in the area ranges between 943 and 1150 mm, indicating relatively low variability. The highest rainfall was observed in the western, central, and northern parts of Addis Ababa, with an expected increase in rainfall over time. Conversely, the southern and south-eastern parts of the city receive the lowest rainfall.

The spatial distribution of rainfall and temperature across seasons shows distinct patterns. In relative terms, the north-western parts of Addis Ababa city receive the maximum rainfall during the *Kiremt* (main rainy) season, while the central parts experience the highest rainfall during the *Belg* (spring) season. The *Bega* season, characterized as the dry season, but the south-western and central parts of the city (Kirkos, Arada, parts of Kolfe Keraniyo and Nifasilk Lafto) received a small amount of rainfall. During *Belg* (Spring) season the amount and distribution of precipitation have significantly diminished across the observation period. Regarding temperature, among the seasons, *Belg* (March - May) was the hottest, where the highest maximum temperature was recorded, consistent with previous research. Regional and temporal variability of temperature was

also noted in line with earlier studies, indicating the need for localized climate monitoring and adaptation strategies. The analysis designated that a strong positive correlation between rainfall and elevation was observed, with an elevated areas on the northern edge of the city receiving more precipitation, while the less elevated areas of the city comparatively received the smallest amount of rainfall. The analysis of inter-annual and seasonal fluctuations in rainfall anomalies highlights varying patterns over the study period. The standardized rainfall anomalies show a decreasing trend in both annual and *Kiremt* season rainfall after 2001, while the *Belg* season experiences significant inter-annual fluctuation and drier conditions in certain years.

The coefficient of variation (CV) analysis reveals that the edge areas of the south-western and north-eastern parts of Addis Ababa experience the highest inter-annual rainfall variability. Furthermore, the CV of seasonal rainfall indicates high inter-annual variability during the *Bega* season, while the *Kiremt* season demonstrates relatively stable rainfall. As opposed to this, temperature variations exhibited relatively low coefficients of variation (CV) for both maximum and minimum temperatures, with the lowest variability observed during the *Belg* season. These findings were consistent with previous studies, which reported minimal temperature variability over time. Significant variations in monthly temperatures were observed, with March being the hottest and December the coolest. For all months, the coefficient of variations for maximum temperatures was less than 20%, while in November, December, and January, the variability of minimum was slightly higher. The study identified a warming trend in maximum temperatures across all seasons from 2011 to 2018. This warming effect was statistically significant, with strong correlations observed between time and increasing maximum temperature anomalies. This trend aligned with previous research, suggesting a long-term, multi-decadal warming pattern in the region.

The Sen's slope estimator for the mean annual and seasonal rainfall shows a negative downward trajectory, except for the *Kiremt* season, which exhibits a positive trend. The long-term monotonic trend analysis of Mann-Kendall and Sen's slope tests suggests a decreasing trend of rainfall for several months except for October, November, May, and June. However, these trends are not statistically significant. Contrarily, trend analysis exhibited a positive trend in both annual and seasonal maximum and minimum temperatures over the study period (1981-2018). The maximum

temperature demonstrated a more pronounced increase, with statistical significance (P<0.05). The increase in maximum temperatures was particularly notable during the *Belg* season. This is further attested by the t-test analysis, which reveals that there was a significant increase in the annual and seasonal maximum and minimum temperatures.

On the other hand, the decadal rainfall substantially diminished across the study period (1981–2018), although it was not statistically significant, whereas a steady rise in maximum temperature was observed throughout the study period, with an overall increase of 2.7 °C. In contrast, minimum temperatures did not exhibit a significant upward trend. In addition, the annual and seasonal minimum temperatures showed low variation. The findings concurred with previous research indicating an increasing maximum temperatures trend in the region. The Mann-Kendall and Sen's slope estimator tests provided further evidence of an upward trend in both maximum and minimum temperatures, affirming the statistical significance of the temperature increases. Moreover, based on the results of the principal component analysis (PCA) analysis, it was determined that PC1 (mean annual Tmax) and PC2 (mean *Kiremt* Tmax) accounted for almost 90% of the variation in temperature in the study areas. Thus, it is possible to conclude that the combination of the first two PCs highly influenced the change in temperature in Addis Ababa city.

Regarding the LST, the analysis results revealed that the built-up area significantly increased from 195 km^2 (37.5%) in 1985 to 326.3 km^2 (62.8%) in 2020. It was augmented by 131.5 km^2 (25.3%) over the study period. The bare land, the cultivated land, and the forest land all declined as the built-up area increased. The results of the study also revealed that a large proportion of natural vegetation, forest land, and cultivated land were converted into built-up areas, which significantly influenced the upward trend in LST. Between 1985 and 2020, the mean LST over the built-up area increased by 2.68 °C, from 26.47 °C to 29.15 °C. The change is largely attributed to the replacement of cultivated land, forest, and bare land with impervious surfaces. Overall, the mean LST of Addis Ababa City between 1985 and 2020 augmented by about 1.8 °C. Moreover, among the different LULC classes, the built-up areas and bare land experienced the highest LST in comparison to other land use classes. Furthermore, a higher land surface temperature was observed in the inner sub-cities of Kirkos, Arada, Addis Ketema, and Lideta, while a drastic change in the LST was exhibited as compared with the peri urban areas. The LST was exacerbated because of

the increased pavement materials used in the city that absorb and store more heat (such as asphalt, concrete, bricks, buildings, vehicles etc.).

5.1. Recommendations

The findings of this study provided a valuable insight into the variability, distribution, pattern, and intensity of rainfall and temperature as well as the magnitude of changes in surface temperature, over time in Addis Ababa, Ethiopia, across the study period.

The study recommends mitigation and adaptation measures in order to cope with the warming effect and variability of precipitation in Addid Ababa, Ethiopia. Literature suggests urban climate resilience needs to be integrative, location-based, focused on long-term changes, and require the cooperation of versatile actors (Davidson et al., 2016; Meerow et al., 2016). In this regard, for the effective implementation of policies, regulations, and directives; cooperation, collaboration, and integration of the different actors/institutions working in the areas of climate change, forestry, environmental protection, and preservation, natural disaster management etc. would be imperative to effectively monitor the environment and realize a sustainable, healthy, livable, and resilient urban environment.

As part of city's urban planning packages, initiating measures such as the city-wide green space initiative must be practiced in the major corridors of the city, including at the neighborhood, village level, and private houses. This can be put into practice with the support of local/indigenous knowledge in identifying, selecting, and planting fast growing trees/seeds that are suitable for the local weather conditions, soil type, and minimal environmental risk. In this regard, the local communities need to have the mandate and ownership to cultivate, monitor, and manage the plated seeds/trees in their immediate surrounding environment.

5.1.1. Ameliorating city's climate change resilience

To enhance Addis Ababa climate resilience, urban systems are a conglomeration of technical components (buildings, roads, and infrastructures, etc.), social aspects, and ecological aspects. These components have to be built in a way that can withstand natural disasters and adapt to changes. As the literature suggests, the pathways to urban climate resilience are: persistence, transition, and transformation (Matyas et al., 2014; Chelleri et al., 2015). Perseverance reflects the engineering (physical) component, it underlines that the various buildings constructed in the city must be well planned, properly designed, and constructed in such a way that can resist natural hazards caused by climate change such as flooding, storms, intensified temperatures, and the urban

heat island effect (UHI). While transition implies maintaining the status quo of urban systems such as ecosystem services (benefits people obtain from nature such as ecological and economic development), settlements, infrastructure development like telecommunications and electric power etc. functions and adapts itself to the environmental changes in the city.

5.1.2. Role of parks in climate mitigation

As literature pointed out at micro scale that is in cities and regions the extensive utilization of green spaces (creation of parks, planting trees, grasses, and green roofs) and water bodies would be crucial in lowering atmospheric temperatures and urban heat island effect. In relation to this, a review by Bowler et al. (2010) suggested that on average parks temperature is lower than its surroundings by 1 °C. Urban park's contribute highly to decreasing the ambient temperatures (Zoulia et al., 2009). The presence of parks would create a pressure difference with the adjacent urban areas, this in turn would permit the transfer of cool air from parks to the urban centers (Akbari et al., 2016). Therefore, urban greenery can regulate microclimate through shading, evapotranspiration, allowing air movement, and heat exchange (Dimoudi & Nikolopoulou, 2003). In addition, parks provide an indispensable mitigating capacity in cities. The contribution of parks on the climate quality of a city is largely determined by factors such as the size and structure of the park, the presence of trees, the local weather and soil conditions, wind direction, the nature of plants used, the watering of plants, and the thermal characteristics of the city (Skoulika et al., 2014).

Experimental studies conducted on the National Garden of Athens reported that the distance of parks from areas affected by urban heat has to be in a range of 200 to 1000m from the parks boundaries, considering the wind direction and speed as a means of thermal balance (Zoulia et al., 2009). With respect to Addis Ababa, as literature suggests, the large expansion of parks in major climate hotspot sub-cities of Addis Ababa is essential as it would help in fighting against temperature rise in the different sub-cities. Despite the rapid population growth of Addis Ababa city, there are only 23 public parks which are unevenly distributed across the city (Seifu & Stellmacher, 2021). The number of parks in the city is very small compared with the city's population. Therefore, the study recommended that the city administration along with the concerned stakeholders and most importantly with the public need to establish new parks in the city with fair distribution across the different sub-cities to intercede the growing urban heat island

effect and minimize the temperature rise. This has to be integrated with the city's structural plan and proper follow-up and supervision has been carried out in a sustainable manner for the effective implementation.

5.1.3. Shading of outdoor spaces as a mitigation measure

Designing and applying appropriate shading mechanisms would contribute substantially to lowering the radiative temperature. In relation to this, Akbari et al. (2016) explain that the use of suitable permeable materials in open spaces can offer a significant reduction of both ambient and radiative temperature, allowing the air to flow freely through these materials. Extensive practice and implementation of shading outdoor spaces in the major climate hotspot sub-cities of Addis Ketema, Arada, Kirkos, and Lideta where the highest increase of urban heat island was detected would help to improve the urban microclimate. Shading is used for things like pergolas, canopies, etc. because shaded urban surfaces receive smaller amounts of solar radiation, thus having lower temperatures. This results in lowering the surrounding atmospheric temperatures.

5.1.4. Strengthening institutions capacity in disaster management as a mitigation measure

During the rainy season (*Kiremt*), it is very common to observe that the urban systems of the city are largely affected by flash floods, heavy winds, and storms. It is a common phenomenon that the city's most neighborhoods were inundated after heavy rain with strong winds. In recent years, it is witnessed that natural disasters caused by heavy rainfall costing the lives of dozens of people in the city, particularly those who reside in the river neighborhoods of Addis Ababa city largely affected by the incident, it has also destroyed the urban spaces, roads submerged, extensive property damages including buildings, and infrastructures. Although, it requires further investigation on the extent of the damage that it had caused both on human and material (World Bank Group, 2019). Therefore, as part of city resilience, the recovery of these facilities back to pre-disaster level is one of form of resilience. The notion of urban resilience is the ability of social-ecological system to absorb, adapt, and respond to changes in the urban system (Desouza & Flanery, 2013). On top of that, Wardekker (2021) noted that urban resilience is framed into two: on the one hand it considers the system and people, and on the other end the communities. There is a need for strengthening community resilience by backstopping the capacity of the local community through mobilizing resources and enhancing their adaptability to resist natural shocks caused by climate change and variability.

5.1.5. Observed Gaps in the working Master Plan of Addis Ababa and recommendations.

Based on the proposed structural plan of Addis Ababa (2017-2027), the proportion of built-up area constituted 40%, the street network accounts for 30%, and green area, open space, and plaza comprised the remaining, 30% (Addis Ababa City Planning Project Office, 2017). As one of the components of the structural plan, the environment was discussed in detail in the report, which includes green infrastructure, waste and natural resource management, and urban agriculture. It is astonishing that the report well addressed the issue of urban agriculture while leaving the concern of climate change aside. From this, we can learn that the report did not explicitly discuss the issue of climate change, the existing condition, future scenarios, and the potential climate change impacts that would pose on the residents of the city. Given the dynamic nature of climate change and variability, that largely shape the environment (weather, fauna, and flora), however, limited emphasis was given by the report. Therefore, this study recommended that there should be a room to incorporate relevant issues pertaining to climate change and variability on the already implemented structural plan as the issue of climate change is very sensitive and immensely influences the design and planning practice of the city.

The structural plan report of Addis Ababa indicated that the green area coverage accounts for 30% of the total landmass area coverage of the city. However, the green areas are not well protected from any environmental hazards and human intrusions. As a result, from time to time, it has been significantly diminishing. This is largely attributed to violations by the public in converting the green spaces into waste disposals areas, the other factor is proliferating urban expansion in the city, and lack of proper urban green space in the city. Consequently, urban green spaces are degraded and in some cases also inaccessible for city residents (Azagew & Worku, 2020). In this regard, the presence of parks would provide an important benefit for the environment, the vegetations would help to combat global warming and climate change impacts through carbon sequestration as the plants, forests, and soil absorb carbon dioxide for photosynthesis and release it over respiration. In addition, plants and gardens could play a pivotal role in moderating local climate. Therefore, raising awareness of the local communities about the ecological and economic benefits of preserving and protecting parks would be one important aspect that needs to be extensively addressed with the active participation of different stakeholders and city's residents.

5.1.6. Observed gaps on Policies and recommendations.

In Ethiopia, there are several environmental proclamations, policy directives, and strategies developed at macro and micro level pertaining with climate change. However, the problem lies in the effective implementation of these strategies and policies at different hierarchy levels. Enhancing the adaptation and mitigation measures of the city is the utmost importance as the report of Ethiopia's Climate Resilient Green Economy National Adaptation Plan (CRGE, 2019) revealed that the country has low adaptive capacity to climate change and variability. This can be realized by integrating climate science research findings in the planning, decision-making process, and prioritizing largely on mechanisms of urban climate resilient programs and initiatives. Specially, climate change and variability are a pressing issue in cities like Addis Ababa. Given the hostile nature of problem, establishing a climate research resilience center by allocating the required resources and facilities, and encouraging research that could potentially contribute a viable solution to environmental related problems has to be encouraged and promoted.

5.1.7. Green infrastructure to mitigate climate change.

Green infrastructure (GI) is a prominent nature-based solution for climate change adaptation and mitigation. It is the interconnected network of natural and semi-natural elements within urban areas at all scales, providing multiple functions and ecosystem services, encompassing positive ecological, economic, and social benefits for humans and other species (Staddon et al., 2018).

GI encompasses a broad range of green and blue spaces such as parks, woods, vegetation, waterbodies, green roofs, vertical greenery, permeable pavements, and bioretention (Koc et al., 2017). The multiple benefits of GI among others, includes reduced air and surface temperatures through shading and evapotranspiration of vegetation, increased CO_2 sequestration, improved water and air quality, more recreation and tourism opportunities.

As literature noted, planting diverse and larger native species of trees in Addis Ababa would improve biodiversity benefits and ecosystem resilience to climate change impacts (Choi et al., 2021). Therefore, GI is a crucial tool for boosting urban resilience, fending off environmental stresses and climate change in urban settings (Pozoukidou, 2020). Pertaining with this, the literature underline that GI is at the early stage of development in Ethiopian cities, and there is no comprehensive GI policy that can offer a strategic roadmap for integrating into spatial designs (Ayele et al., 2022). Therefore, the city administration has to give priority to the integration of GI

into the existing environmental proclamations, policies, and directions as it is very important to combat climate change impacts. The effective implementation of GI is imperative since it uses nature-based solutions against climate change induced afflicts. A new planning perspective would be appropriate to integrate GI into planning and design processes considering the current urban realities and future planning perspectives.

5.1.8. Climate change and UHI implications on urban planning

Climate change and variability is a critical issue that affect largely developing countries such as Ethiopia. Literature underpin that urban planning and climate change are two important fields of research very much interconnected (Fallmann & Emeis, 2020). The same source further explained that the alteration of the local climate had been a major concern for city planners in antiquity, however, in the course of time, climate adapted city planning evolved and largely practiced in most parts of the world. In countries like Ethiopia, the implementation of climate friendly urban planning would be imperative as it plays an indispensable role in climate mitigation and adaptation measures, in a way it will ascertain a sustainable environmental condition. The urban design and planning developed at city scale has to take into consideration the dynamic nature of climate change and the growing concern of urban heat island effects. The city infrastructures and buildings constructed in the city has to be resilient to environmental changes mainly caused by climate change and variability.

In addition, concerted efforts are required to realize a resilient Addis Ababa city. This can be achieved with the implementation of various adaptation and mitigation measures such as the application of urban blue: the notion is that the presence of waterbodies such as small ponds in core urban environment, where there is high UHI intensity, is considered as an important temperature regulator as water surfaces have high thermal storage capacity and would ultimately sink the urban heat intensity in the inner city. In addition, the water surfaces influence the ambient environment through cooling effect and evapotranspiration. On top of that, the small ponds can be used as a potential recreational spot for cities residents and visitors. Nevertheless, its implementation depends on the availability of adequate freshwater supply. Otherwise, due to the rising temperature, the water quality would degrade through thermal pollution consequently it would be a breeding area for insects which could serve as vectors for diseases. Therefore, to curb the rising temperature and the potential impacts of urban heat island effect, the integration of urban

blue concept with the urban design and planning practices would be indispensable.

Designing fresh air corridor in the planning and design: the presence of high-rise buildings in cities substantially influence the air movement as the buildings obstruct the flow of air from sub-urban to city centers, which would have a cooling effect and lower the ambient temperature (Schau-Noppel et al., 2020).

Advocating urban green space and integrating with city urban planning: in Addis Ababa there are 23 public parks throughout the city which is very small as compared with the rapidly growing of city's population (Seifu & Stellmacher, 2021). Literature indicated that the high rate of population growth accompanied by accelerated land use land cover change and more urban infrastructures such as concrete, asphalt, buildings, bricks dominated the city which resulted in increase of UHI density. One mitigation measure is the expansion of parks in city centers and integrating with the urban design. Oke (1982) underscore that the temperature difference between central areas of large city and the surrounding sub-urban areas ranges from 1 °C to 3 °C. Pertaining to this, a study carried out in the German Stuttgart city demonstrated that by applying urban planning measures of high reflective roof paints and replacing impervious surfaces (heat absorbing buildings and pavements) by green infrastructures such as natural vegetation and trees it is possible to lower the intensity of UHI by up to 2 °C and 1 °C, respectively (Fallmann et al., 2013). By taking the experience of Stuttgart and others, in cities like Addis Ababa, specific urban planning strategies such as green roofs, or facades, parks, small ponds, and greenery of buildings able to reduce the UHI (Taha, 1997).

Use of natural materials: construction of buildings in a city center could be done partly using natural materials such as wood which helps to reduce the proportion of CO2 concentration in the atmosphere as the woods has the natural capacity to store carbon for a long period of time. This would have a multifarious benefit in regulating both the atmospheric and surface temperature. It can minimize the effect that would be caused by the greenhouse effect as it extracted CO2 from the atmosphere. It can also reduce the urban heat intensity as it is replacing the impervious surfaces with pervious materials (Buffi & Angelini, 2019; Tupėnaitė et al., 2020).

Urban gardening: greening the city is one form of mitigation in response to urban climate change. Urban gardening not only can be used as mitigation measure to growing urban climate dynamics but also can contribute to the attractiveness of the city and this can open doors for tourism (Lindemann-Matthies & Brieger, 2016).

Figure 51: illustrates the interconnected nature of urban climate change and mitigation measures.

5.2. Future research direction

Climate change and variability impacts are highly proliferating from time to time in an unrestrained manner affecting both urban and rural settings of the country. However, the concern of climate variability and change in the urban context is still not adequately researched in the Ethiopian urban context. Thus, this study identified a number of potential research areas that could be of interest for future researchers.

A. Peoples' perception on climate change and variability over the past decades and its associated impacts on the Addis Ababa city residents.
B. The nexus between air temperature and land surface temperature change across different time span in Addis Ababa.
C. Prediction of Addis Ababa's land use land cover change using Markov of chains approach by taking satellite images of different points of time.

References

AACPPO. (2017). Addis Ababa City Structure Plan. *Aacppo*, 1–10.

Abdullah, H., Darvishzadeh, R., Skidmore, A. K., & Heurich, M. (2019). Sensitivity of Landsat-8 OLI and TIRS Data to Foliar Properties of Early Stage Bark Beetle (Ips typographus, L.) Infestation. *Remote Sensing*, *11*(4). https://doi.org/10.3390/rs11040398

Abebe, B. A., Grum, B., Degu, A. M., & Goitom, H. (2022). Spatio-temporal rainfall variability and trend analysis in the Tekeze-Atbara river basin, northwestern Ethiopia. *Meteorological Applications*, *29*(2), 1–17. https://doi.org/10.1002/met.2059

Abebe, M. (2006). *The Onset , Cessation and Dry Spells of the Small Rainy Season (Belg) of Ethiopia. National Meteorological Agency of Ethiopia, Addis Ababa*. 1–41.

Abebe, M. S., Derebew, K. T., & Gemeda, D. O. (2019). Exploiting temporal-spatial patterns of informal settlements using GIS and remote sensing technique: a case study of Jimma city, Southwestern Ethiopia. *Environmental Systems Research*, *8*(1). https://doi.org/10.1186/s40068-019-0133-5

Abera, D., Kibret, K., & Beyene, S. (2018). *spatial land use / cover change in Zeway , Ketar and basins , Central Rift Valley of Ethiopia*. *January 2018*, 76–92. https://doi.org/10.1111/lre.12240

Adaptation Partnership. (2012). Review of Current and Planned Adaptation Action: East Africa. *Jurnal Penelitian Pendidikan Guru Sekolah Dasar*, *6*(August), 128.

Addis Ababa City Administration and C40 Cities. (2020). *Addis Ababa City 2016 Greenhouse Gas Emissions Inventory Report:Version v8.0*. 1–47.

Addis Ababa City Planning Project Office. (2017). Addis Ababa City Structure Plan. *Aacppo*, 1–317. https://c40-production-images.s3.amazonaws.com

Addis, T. L., Birhanu, B. S., & Italemahu, T. Z. (2023). *Factors Affecting Climate Change Governance in Addis Ababa*.

Addisu, S., Selassie, Y. G., Fissha, G., & Gedif, B. (2015). Time series trend analysis of

temperature and rainfall in lake Tana Sub-basin, Ethiopia. *Environmental Systems Research*, *4*(1). https://doi.org/10.1186/s40068-015-0051-0

Adedoyin, F. F., Alola, A. A., & Bekun, F. V. (2020). An assessment of environmental sustainability corridor: The role of economic expansion and research and development in EU countries. *Science of the Total Environment*, *713*, 136726. https://doi.org/10.1016/j.scitotenv.2020.136726

Adeniyi, P. A. (2016). Climate change induced hunger and poverty in Africa. *Journal of Global Biosciences*, *5*(3), 3711–3724. https://www.mutagens.co.in/jgb/vol.05/3/050302.pdf

Adenle, A. A., Ford, J. D., Morton, J., Twomlow, S., Alverson, K., Cattaneo, A., Cervigni, R., Kurukulasuriya, P., Huq, S., Helfgott, A., & Ebinger, J. O. (2017). Managing Climate Change Risks in Africa - A Global Perspective. *Ecological Economics*, *141*, 190–201. https://doi.org/10.1016/j.ecolecon.2017.06.004

ADF-VII. (2010). *"Acting on Climate Change for Sustainable Development in Africa."*

Adger, W. N., Huq, S., Brown, K., Declan, C., & Mike, H. (2003). Adaptation to climate change in the developing world. *Progress in Development Studies*, *3*(3), 179–195. https://doi.org/10.1191/1464993403ps060oa

Admassu, H., Getinet, M., & Kirub, A. (2010). *Impacts of Climate Variability and Change in Agricultural Systems of Semi-Arid Areas of Ethiopia*.

Agarwal, S., Suchithra, A. S., & Singh, S. P. (2021). Analysis and interpretation of rainfall trend using Mann-Kendall's and Sen's slope Method. *Indian Journal of Ecology*, *48*(2), 453–457.

Agnew, C. T., & Chappell, A. (2000). Drought in the Sahel. *Black Scholar*, *5*(10), 37–42. https://doi.org/10.1080/00064246.1974.11431441

Ahmed, K., Shahid, S., Wang, X., Nawaz, N., & Najeebullah, K. (2019). Evaluation of gridded precipitation datasets over arid regions of Pakistan. *Water (Switzerland)*, *11*(2). https://doi.org/10.3390/w11020210

Ahmed, S. I., Rudra, R., Dickinson, T., & Ahmed, M. (2014). Trend and Periodicity of

Temperature Time Series in Ontario. *American Journal of Climate Change*, *03*(03), 272–288. https://doi.org/10.4236/ajcc.2014.33026

Akbari, H., Cartalis, C., Kolokotsa, D., & Muscio, A. (2016). *Local climate change and urban heat island mitigation techniques - The state of the art Local Climate Change and Urban Heat Island Mitigation Techniques – The State of the Art*. *February*. https://doi.org/10.3846/13923730.2015.1111934

Akponikpe, I., Johnston, P., & Agbossou, E. K. (2010). *An investigation into climate knowledge and perception of climate variability and change amongst farmers along the West African climate gradient*. 1–31.

Al-hasani, A. A. J. (2020). Trend analysis and abrupt change detection of streamflow variations in the lower Tigris River. *Intl. J. River Basin Management*, *0*(0), 1–12. https://doi.org/10.1080/15715124.2020.1723603

Alemayehu, A., & Bewket, W. (2017). Local spatiotemporal variability and trends in rainfall and temperature in the central highlands of Ethiopia. *Geografiska Annaler, Series A: Physical Geography*, *99*(2), 85–101. https://doi.org/10.1080/04353676.2017.1289460

Alemayehu, A., Maru, M., Bewket, W., & Assen, M. (2020). Spatiotemporal variability and trends in rainfall and temperature in Alwero watershed, western Ethiopia. *Environmental Systems Research*, *9*(1). https://doi.org/10.1186/s40068-020-00184-3

Alemu, M. M., & Bawoke, G. T. (2020). Analysis of spatial variability and temporal trends of rainfall in Amhara Region, Ethiopia. *Journal of Water and Climate Change*, *11*(4), 1505–1520. https://doi.org/10.2166/wcc.2019.084

Alemu, Z. A., & Dioha, M. O. (2020a). Climate change and trend analysis of temperature: the case of Addis Ababa, Ethiopia. *Environmental Systems Research*, *9*(1). https://doi.org/10.1186/s40068-020-00190-5

Alemu, Z. A., & Dioha, M. O. (2020b). Climate change and trend analysis of temperature: the case of Addis Ababa, Ethiopia. *Environmental Systems Research*, *9*(1). https://doi.org/10.1186/s40068-020-00190-5

Alexander, C. (2020). Normalised difference spectral indices and urban land cover as indicators of land surface temperature (LST). *International Journal of Applied Earth Observation and Geoinformation*, *86*(October 2019), 102013. https://doi.org/10.1016/j.jag.2019.102013

Ali-Toudert, F., & Mayer, H. (2007). Effects of asymmetry, galleries, overhanging façades and vegetation on thermal comfort in urban street canyons. *Solar Energy*, *81*(6), 742–754. https://doi.org/10.1016/j.solener.2006.10.007

AMCEN. (2011). Adressing Climate Change Challenges in Africa;A Pratical Guide Towards Sustainable Development. *African Union*, 272.

Aming, P., Awange, J. L., Forootan, E., Ogallo, A., Girmaw, B., Fesseha, I., Kululetera, V., Mbati, M., Kilavi, M., King, M., Adek, P., Njogu, A., Badr, M., Musa, A., & Muchiri, P. (2014). *Changes in temperature and precipitation extremes over the Greater Horn of Africa region from 1961 to 2010*. *1277*(June 2013), 1262–1277. https://doi.org/10.1002/joc.3763

Amorim, M. C. de C. T. (2020). Daily evolution of urban heat islands in a Brazilian tropical continental climate during dry and rainy periods. *Urban Climate*, *34*(September), 100715. https://doi.org/10.1016/j.uclim.2020.100715

Anderson, J. W. (1998). The Kyoto Protocol on Climate Change and next steps. *Weathervane*, *January*, 1–21.

Anose, F. A., Beketie, K. T., Terefe Zeleke, T., Yayeh Ayal, D., & Legese Feyisa, G. (2021). Spatio-temporal hydro-climate variability in Omo-Gibe river Basin, Ethiopia. *Climate Services*, *24*, 100277. https://doi.org/10.1016/j.cliser.2021.100277

Apaydin, H., Kemal Sonmez, F., & Yildirim, Y. E. (2013). Spatial interpolation techniques for climate data in the GAP region in Turkey. *Climate Research*, *28*(1), 31–40. https://doi.org/10.3354/cr028031

Arsiso, B. K., Mengistu Tsidu, G., & Stoffberg, G. H. (2018). Signature of present and projected climate change at an urban scale: The case of Addis Ababa. *Physics and Chemistry of the Earth*, *105*, 104–114. https://doi.org/10.1016/j.pce.2018.03.008

Arsiso, B. K., Mengistu Tsidu, G., Stoffberg, G. H., & Tadesse, T. (2018). Influence of

urbanization-driven land use/cover change on climate: The case of Addis Ababa, Ethiopia. *Physics and Chemistry of the Earth*, *105*, 212–223. https://doi.org/10.1016/j.pce.2018.02.009

Arsiso, B. K., Tsidu, G. M., & Stoffberg, G. H. (2018). *Signature of present and projected climate change at an urban scale : The case of Addis Ababa*. *May 2017*. https://doi.org/10.1016/j.pce.2018.03.008

Arsiso, B. K., Tsidu, G. M., Stoffberg, G. H., & Tadesse, T. (2017a). "Climate change and population growth impacts on surface water supply and demand of Addis Ababa, Ethiopia" (2017). Drought Mitigation Center Faculty Publications. 130. https://digitalcommons.unl.edu/droughtfacpub/130. *Climate Risk Management*, *18*, 21–33.

Arsiso, B. K., Tsidu, G. M., Stoffberg, G. H., & Tadesse, T. (2017b). *Climate change and population growth impacts on surface water supply and demand of Addis Ababa ,*.

Arsiso, B. K., Tsidu, G. M., Stoffberg, G. H., & Tadesse, T. (2018). *In fl uence of urbanization-driven land use / cover change on climate : The case of Addis Ababa , Ethiopia*. *105*(May 2017), 212–223. https://doi.org/10.1016/j.pce.2018.02.009

Asaminew, E. (2013). Climate Change, Growth , and Poverty in Ethiopia. *Working Paper No.3*, *June*.

Asefa, M., Cao, M., He, Y., Mekonnen, E., Song, X., & Yang, J. (2020a). Ethiopian vegetation types, climate and topography. *Plant Diversity*, *42*(4), 302–311. https://doi.org/10.1016/j.pld.2020.04.004

Asefa, M., Cao, M., He, Y., Mekonnen, E., Song, X., & Yang, J. (2020b). Ethiopian vegetation types, climate and topography. *Plant Diversity*, *42*(4), 302–311. https://doi.org/10.1016/j.pld.2020.04.004

Asfaw, A., Simane, B., Hassen, A., & Bantider, A. (2018a). Variability and time series trend analysis of rainfall and temperature in northcentral Ethiopia: A case study in Woleka sub-basin. *Weather and Climate Extremes*, *19*(December), 29–41. https://doi.org/10.1016/j.wace.2017.12.002

Asfaw, A., Simane, B., Hassen, A., & Bantider, A. (2018b). Variability and time series trend analysis of rainfall and temperature in northcentral Ethiopia: A case study in Woleka sub-basin. *Weather and Climate Extremes*, *19*(December 2017), 29–41. https://doi.org/10.1016/j.wace.2017.12.002

Ashraf, M., Loftis, J. C., & Hubbard, K. G. (1997). *Application of geostatistics to evaluate partial weather station networks*. *1923*(1973).

Aswad, F., Yousif, A., & Ibrahim, S. (2020). Trend Analysis Using Mann-kendall And Sen's Slope Estimator Test for Annual And Monthly Rainfall for Sinjar District, Iraq. *The Journal of the University of Duhok*, *23*(2), 501–508. https://doi.org/10.26682/csjuod.2020.23.2.41

Ayalew, D., Tesfaye, K., Mamo, G., Yitaferu, B., & Bayu, W. (2012). *Variability of rainfall and its current trend in Amhara region , Ethiopia*. *7*(10), 1475–1486. https://doi.org/10.5897/AJAR11.698

Ayele, B. Y., Megento, T. L., & Habetemariam, K. Y. (2022). Assessing green infrastructure spatial plans in Addis Ababa, Ethiopia. *Socio-Ecological Practice Research*, *4*(2), 85–101. https://doi.org/10.1007/s42532-022-00115-9

Ayele, H. S., Li, M.-H., Tung, C.-P., & Liu, T.-M. (2016). *Impact of Climate Change on Runoff in the Gilgel Abbay Watershed, the Upper Blue Nile Basin, Ethiopia*. https://doi.org/10.3390/w8090380

Azagew, S., & Worku, H. (2020). Accessibility of urban green infrastructure in Addis-Ababa city, Ethiopia: current status and future challenge. *Environmental Systems Research*, *9*(1). https://doi.org/10.1186/s40068-020-00187-0

Babazadeh, M., & Kumar, P. (2015). *Estimation of the Urban Heat Island in Local Climate Change and Vulnerability Assessment for Air Quality in Delhi*. *7881*(Jdune), 55–65.

Badasa, M., Indale, M., Dejene, N., & Reta, Z. (2022). Impact of urban land use and land cover change on urban heat island and urban thermal comfort level : a case study of Addis Ababa City , Ethiopia. *Environmental Monitoring and Assessment*. https://doi.org/10.1007/s10661-022-10414-z

Balding, D. J., Cressie, N. A. C., Garrett M. Fitzmaurice, H. G., Johnstone, I. M., Molenberghs, G., Scott, D. W., Smith, A. F. M., Tsay, R. S., & Weisberg, S. (2012). *Geostatistics Modeling Spatial Uncertainity*.

Balew, A., & Korme, T. (2020a). Monitoring land surface temperature in Bahir Dar city and its surrounding using Landsat images. *Egyptian Journal of Remote Sensing and Space Science*, *23*(3), 371–386. https://doi.org/10.1016/j.ejrs.2020.02.001

Barbieri, T., Despini, F., & Teggi, S. (2018). A multi-temporal analyses of Land Surface Temperature using Landsat-8 data and open source software: The case study of Modena, Italy. *Sustainability (Switzerland)*, *10*(5). https://doi.org/10.3390/su10051678

Bartesaghi Koc, C., Osmond, P., & Peters, A. (2017). Towards a comprehensive green infrastructure typology: a systematic review of approaches, methods and typologies. *Urban Ecosystems*, *20*(1), 15–35. https://doi.org/10.1007/s11252-016-0578-5

Bast, J. L. (2010). *Seven Theories of Climate Change*.

Bayable, G., Amare, G., Alemu, G., & Gashaw, T. (2021). Spatiotemporal variability and trends of rainfall and its association with Pacific Ocean Sea surface temperature in West Harerge Zone, Eastern Ethiopia. *Environmental Systems Research*, *10*(1). https://doi.org/10.1186/s40068-020-00216-y

Bekalo, M. T. (2009). *Spatial metrics and landsat data for urban landuse change detection in Addis Ababa, Ethiopia*. 89.

Belay, A., Demissie, T., Recha, J. W., Oludhe, C., Osano, P. M., Olaka, L. A., Solomon, D., & Berhane, Z. (2021). Analysis of climate variability and trends in Southern Ethiopia. *Climate*, *9*(6), 1–17. https://doi.org/10.3390/cli9060096

Belay, A. S., Fenta, A. A., Yenehun, A., Nigate, F., Tilahun, S. A., Moges, M. M., Dessie, M., Adgo, E., Nyssen, J., Chen, M., Van Griensven, A., & Walraevens, K. (2019). Evaluation and application of multi-source satellite rainfall product CHIRPS to assess spatio-temporal rainfall variability on data-sparse western margins of Ethiopian highlands. *Remote Sensing*, *11*(22), 1–22. https://doi.org/10.3390/rs11222688

Belay, F. (2016). Households' Vulnerability to Climate Change and Adaptation Strategies: The Case of Choke Mountain Watershed, Eastern Gojjam Zone, Ethiopia. *Core.Ac.Uk*, *6*(3), 109–152. www.iiste.org

Beltrando, G., & Camberlin, P. (1993). Interannual variability of rainfall in the eastern horn of Africa and indicators of atmospheric circulation. *International Journal of Climatology*, *13*(5), 533–546. https://doi.org/10.1002/joc.3370130505

Benti, F., & Abara, M. (2019). Trend Analyses of Temperature and Rainfall and Their Response to Global CO2 Emission in Masha, Southern Ethiopia. *Caraka Tani: Journal of Sustainable Agriculture*, *34*(1), 67. https://doi.org/10.20961/carakatani.v34i1.28022

Berhane, A., Hadgu, G., Worku, W., & Abrha, B. (2020). Trends in extreme temperature and rainfall indices in the semi-arid areas of Western Tigray, Ethiopia. *Environmental Systems Research*, *9*(1). https://doi.org/10.1186/s40068-020-00165-6

Berhe, A. G., Erena, D. B., Hassen, I. M., Mamaru, T. L., & Soressa, Y. A. (2017). City Profile: Addis Ababa. *World Literature Today*, *96*(3), 5. https://doi.org/10.1353/wlt.2022.0101

Berhe, A. G., Erena, D. B., Hassen, I. M., Mamaru, T. L., Soressa, Y. A., Hassen, I. M., & Mamaru, T. L. (2017). *City Profile of Addis Ababa*.

Bewket, W., & Conway, D. (2007). A note on the temporal and spatial variability of rainfall in the drought-prone Amhara region of Ethiopia. *International Journal of Climatology*, *2029*(March 2008), 2011–2029. https://doi.org/10.1002/joc

Bewket, W., Radeny, M., & Mungai, C. (2015). *Agricultural Adaptation and Institutional Responses to Climate Change Vulnerability in Ethiopia*. *July*. https://doi.org/10.13140/RG.2.1.2106.7362

Biddlestone, M., Azevedo, F., & van der Linden, S. (2022). Climate of conspiracy: A meta-analysis of the consequences of belief in conspiracy theories about climate change. *Current Opinion in Psychology*, *46*, 101390. https://doi.org/10.1016/j.copsyc.2022.101390

Biernacik, P., Kazimierski, W., & Włodarczyk-Sielicka, M. (2023). Comparative Analysis of Selected Geostatistical Methods for Bottom Surface Modeling. *Sensors*, *23*(8).

https://doi.org/10.3390/s23083941

Bindi, M., Brandani, G., Dibari, C., Dessi, A., Ferrise, R., Moriondo, M., & Trombi, G. (2009). Proceedings e report 43. In *Society*.

Birhanu, D., Kim, H., Jang, C., & Park, S. (2016). Flood Risk and Vulnerability of Addis Ababa City Due to Climate Change and Urbanization. *Procedia Engineering*, *154*, 696–702. https://doi.org/10.1016/j.proeng.2016.07.571

Blanco G., R. Gerlagh, S. Suh, J. Barrett, H. C. de Coninck, C. F. Diaz Morejon, R. Mathur, N. Nakicenovic, A. Ofosu Ahenkora, J. Pan, H. Pathak, J. Rice, R. Richels, S. J. Smith, D. I. Stern, F. L. Toth, and P. Zhou, 2014: (2014). *Drivers, Trends and Mitigation*. 351–412.

Borga, M., & Vizzaccaro, A. (1997). On the interpolation of hydrologic variables: Formal equivalence of multiquadratic surface fitting and kriging. *Journal of Hydrology*, *195*(1–4), 160–171. https://doi.org/10.1016/S0022-1694(96)03250-7

Bouza-Deaño, R., Ternero-Rodríguez, M., & Fernández-Espinosa, A. J. (2008). Trend study and assessment of surface water quality in the Ebro River (Spain). *Journal of Hydrology*, *361*(3–4), 227–239. https://doi.org/10.1016/j.jhydrol.2008.07.048

Bowler, D. E., Buyung-Ali, L., Knight, T. M., & Pullin, A. S. (2010). Urban greening to cool towns and cities: A systematic review of the empirical evidence. *Landscape and Urban Planning*, *97*(3), 147–155. https://doi.org/10.1016/j.landurbplan.2010.05.006

Brien, K. L. O., & Leichenko, R. M. (2000). Double exposure: assessing the impacts of climate change within the context of economic globalization. *Global Environmental Change*, *52*(11), 6487–6496. https://doi.org/10.1021/acs.est.7b05861

Buffi, A., & Angelini, G. M. (2019). *Adaptive Timber Towers . An Evolutionary Prototype for the 21st Century Skyscraper*. Springer International Publishing. https://doi.org/10.1007/978-3-030-03676-8

McSweeney, M. N. and G. L. (2012). *General Climate*. 1–27.

Cardoso, R. dos S., Dorigon, L. P., Teixeira, D. C. F., & Amorim, M. C. de C. T. (2017).

Assessment of urban heat Islands in small- and mid-sized cities in Brazil. *Climate*, *5*(1). https://doi.org/10.3390/cli5010014

Carlson, T. N., & Ripley, D. A. (1997). On the relation between NDVI, fractional vegetation cover, and leaf area index. *Remote Sensing of Environment*, *62*(3), 241–252. https://doi.org/10.1016/S0034-4257(97)00104-1

Chan, H., Liou, Y., Analyzing, T. W., Changes, L., Chan, H., Wang, T., & Wang, H. C. Y. L. T. (2013). *Analyzing LULC Changes with Remote Sensing Data in Taoyuan , Taiwan*. *September 2018*. https://doi.org/10.13140/RG.2.2.11176.42248

Chander, G., Markham, B. L., Helder, D. L., & Ali, E.-. (2009). Remote Sensing of Environment Summary of current radiometric calibration coef fi cients for Landsat MSS , TM , ETM + , and EO-1 ALI sensors. *Remote Sensing of Environment*, *113*(5), 893–903. https://doi.org/10.1016/j.rse.2009.01.007

Chao, Z., van Dijk, A. I. J. M., Wang, L., Che, M., & Hou, S. (2020). Effects of different urbanization levels on land surface temperature change: Taking Tokyo and shanghai for example. *Remote Sensing*, *12*(12). https://doi.org/10.3390/rs12122022

Chelleri, L., Waters, J. J., Olazabal, M., & Minucci, G. (2015). Resilience trade-offs: addressing multiple scales and temporal aspects of urban resilience. *Environment and Urbanization*, *27*(1), 181–198. https://doi.org/10.1177/0956247814550780

Chen, G., Hay, G. J., Carvalho, L. M. T., & Wulder, M. A. (2012). *International Journal of Remote Object-based change detection*. *January 2012*, 37–41.

Chen, H., Guo, S., Xu, C. yu, & Singh, V. P. (2007). Historical temporal trends of hydro-climatic variables and runoff response to climate variability and their relevance in water resource management in the Hanjiang basin. *Journal of Hydrology*, *344*(3–4), 171–184. https://doi.org/10.1016/j.jhydrol.2007.06.034

Chen, L., Li, M., Huang, F., & Xu, S. (2013). Relationships of LST to NDBI and NDVI in Changsha-Zhuzhou-Xiangtan area based on MODIS data. *6th International Congress on Image and Signal Processing (CISP 2013)*, *Cisp*, 840–845.

http://en.cnki.com.cn/Article_en/CJFDTOTAL-DLKX200902018.htm

Chen, S., Yang, Y., Deng, F., Zhang, Y., Liu, D., Liu, C., & Gao, Z. (2022). A high-resolution monitoring approach of canopy urban heat island using a random forest model and multi-platform observations. *Atmospheric Measurement Techniques*, *15*(3), 735–756. https://doi.org/10.5194/amt-15-735-2022

Chibuike, E. M., Ibukun, A. O., Abbas, A., & Kunda, J. J. (2018). Assessment of green parks cooling effect on Abuja urban microclimate using geospatial techniques. *Remote Sensing Applications: Society and Environment*, *11*(March), 11–21. https://doi.org/10.1016/j.rsase.2018.04.006

Choi, C., Berry, P., & Smith, A. (2021). The climate benefits, co-benefits, and trade-offs of green infrastructure: A systematic literature review. *Journal of Environmental Management*, *291*(June). https://doi.org/10.1016/j.jenvman.2021.112583

Choudhury, D., Das, K., & Das, A. (2019). Assessment of land use land cover changes and its impact on variations of land surface temperature in Asansol-Durgapur Development Region. *Egyptian Journal of Remote Sensing and Space Science*, *22*(2), 203–218. https://doi.org/10.1016/j.ejrs.2018.05.004

Chuanyan, Z., Zhongren, N., & Guodong, C. (2005). *Methods for modelling of temporal and spatial distribution of air temperature at landscape scale in the southern Qilian mountains , China*. *189*, 209–220. https://doi.org/10.1016/j.ecolmodel.2005.03.016

Clark, P. U., Shakun, J. D., Marcott, S. A., Mix, A. C., Eby, M., Kulp, S., Levermann, A., Milne, G. A., Pfister, P. L., Santer, B. D., Schrag, D. P., Solomon, S., Stocker, T. F., Strauss, B. H., Weaver, A. J., Winkelmann, R., Archer, D., Bard, E., Goldner, A., … Plattner, G. K. (2016). Consequences of twenty-first-century policy for multi-millennial climate and sea-level change. *Nature Climate Change*, *6*(4), 360–369. https://doi.org/10.1038/nclimate2923

Cochrane, L., & Costolansk, P. (2013). Climate change vulnerability and adaptability in an urban context: A case study of Addis Ababa, Ethiopia. *International Journal of Sociology and Anthropology*, *5*(6), 192–204. https://doi.org/10.5897/ijsa2013.0459

Cochrane, L., & Costolanski, P. (2013). Climate change vulnerability and adaptability in an urban context: A case study of Addis Ababa, Ethiopia. *International Journal of Sociology and Anthropology*, *5*(6), 192–204. https://doi.org/10.5897/ijsa2013.0459

Collier, P., Conway, G., & Venables, T. (2008). Climate change and Africa. *Oxford Review of Economic Policy*, *24*(2), 337–353. https://doi.org/10.1093/oxrep/grn019

Collins, J. M. (2011). Temperature variability over Africa. *Journal of Climate*, *24*(14), 3649–3666. https://doi.org/10.1175/2011JCLI3753.1

Congalton, R. G. (1991). A Review of Assessing the Accuracy of Classifications of Remotely Sensed Data. *Epilepsy Currents*, *16*(3), 198–205. https://doi.org/10.5698/1535-7511-16.3.198

Conway, D., & Schipper, E. L. F. (2011). Adaptation to climate change in Africa: Challenges and opportunities identified from Ethiopia. *Global Environmental Change*, *21*(1), 227–237. https://doi.org/10.1016/j.gloenvcha.2010.07.013

Conway, G. (2009). *The science of climate change in Africa : impacts and adaptation*. *1*, 1–24.

Cook, J., Nuccitelli, D., Green, S. A., Richardson, M., Winkler, B., Painting, R., Way, R., Jacobs, P., & Skuce, A. (2013). Quantifying the consensus on anthropogenic global warming in the scientific literature. *Environmental Research Letters*, *8*(2). https://doi.org/10.1088/1748-9326/8/2/024024

Corburn, J. (2009). Cities, climate change and urban heat island mitigation: Localising global environmental science. *Urban Studies*, *46*(2), 413–427. https://doi.org/10.1177/0042098008099361

CRGE. (2019). Ethiopia's Climate Resilient Green Economy Strategy. National Adaptation Plan. *Federal Democratic Republic of Ethiopia. National Adaptation Plan.*, *May*, 1–147.

Dale, V. H. (1997). The relationship between land-use change and climate change. *Ecological Applications*, *7*(3), 753–769. https://doi.org/10.1890/1051-0761(1997)007[0753:TRBLUC]2.0.CO;2

Daron, J. (2014). *Regional Climate Messages for East Africa*. 1–29.

Dastagir, M. R. (2015). Modeling recent climate change induced extreme events in Bangladesh : A review. *Weather and Climate Extremes*, *7*, 49–60. https://doi.org/10.1016/j.wace.2014.10.003

Davidson, J. L., Jacobson, C., Lyth, A., Dedekorkut-Howes, A., Baldwin, C. L., Ellison, J. C., Holbrook, N. J., Howes, M. J., Serrao-Neumann, S., Singh-Peterson, L., & Smith, T. F. (2016). Interrogating resilience: Toward a typology to improve its operationalization. *Ecology and Society*, *21*(2). https://doi.org/10.5751/ES-08450-210227

Croix, D., & Gobbi, P. E. (2022). Population homeostasis in sub-Saharan Africa. *Economics and Human Biology*, *45*(January), 101102. https://doi.org/10.1016/j.ehb.2021.101102

Defries, R. S., Rudel, T., Uriarte, M., & Hansen, M. (2010). Deforestation driven by urban population growth and agricultural trade in the twenty-first century. *Nature Geoscience*, *3*(3), 1–4. https://doi.org/10.1038/ngeo756

Desouza, K. C., & Flanery, T. H. (2013). Designing, planning, and managing resilient cities: A conceptual framework. *Cities*, *35*, 89–99. https://doi.org/10.1016/j.cities.2013.06.003

Dia, K. B., & Wadjamsse Beaudelaire, D. (2021). *Bringing Rigour and Evidence to Economic Policy Making in Africa Climate Variability and Urbanization in sub-Saharan Africa: Mitigating the Effects on Economic Growth*.

Dickinson, R. E. (1991). Global change and terrestrial hydrology-a review. *Tellus A: Dynamic Meteorology and Oceanography*, *43*(4), 176. https://doi.org/10.3402/tellusa.v43i4.11946

Dimoudi, A., & Nikolopoulou, M. (2003). *Vegetation in the urban environment : microclimatic analysis and bene ® ts*. *35*, 69–76.

Dinku, T., Asefa, K., Hilemariam, K., Grimes, D., & Connor, S. (2011). *Improving availability , access and use of climate information*. *60*(2), 80–86.

Dinku, T., Ceccato, P., Grover-Kopec, E., Lemma, M., Corner, S. J., & Ropelewski, C. F. (2007). *Validation of satellite rainfall products over East Africa ' s complex topography*.

28(7), 1503–1526. https://doi.org/10.1080/01431160600954688

Dinku, T., Hailemariam, K., Maidment, R., & Connor, S. (2014). *Combined use of satellite estimates and rain gauge observations to generate high-quality historical rainfall time series over Ethiopia*. *2504*(November 2013), 2489–2504. https://doi.org/10.1002/joc.3855

Dissanayake, D. M. S. L. B., Morimoto, T., Ranagalage, M., & Murayama, Y. (2019). Land-use/land-cover changes and their impact on surface urban heat islands: Case study of Kandy City, Sri Lanka. *Climate*, *7*(8). https://doi.org/10.3390/cli7080099

Dissanayake, D., Morimoto, T., Murayama, Y., Ranagalage, M., & Handayani, H. H. (2019). Impact of urban surface characteristics and socio-economic variables on the spatial variation of land surface temperature in Lagos City, Nigeria. *Sustainability (Switzerland)*, *11*(1). https://doi.org/10.3390/su11010025

Duhan, D., Pandey, A., Gahalaut, K. P. S., & Pandey, R. P. (2013). Spatial and temporal variability in maximum, minimum and mean air temperatures at Madhya Pradesh in central India. *Comptes Rendus - Geoscience*, *345*(1), 3–21. https://doi.org/10.1016/j.crte.2012.10.016

Duren, R. M., & Miller, C. E. (2012). Measuring the carbon emissions of megacities. *Nature Climate Change*, *2*(8), 560–562. https://doi.org/10.1038/nclimate1629

EFDR, MoH. (2015). *Federal Democratic Republic of Ethiopia Ministry of Health Vulnerability and Adaptation Assessment of Health to Climate Change in Ethiopia Final Report*. *September*.

Elias, E., Seifu, W., Tesfaye, B., & Girmay, W. (2019). Impact of land use/cover changes on lake ecosystem of Ethiopia central rift valley. *Cogent Food & Agriculture*, *5*(1). https://doi.org/10.1080/23311932.2019.1595876

Eshetu, M. (2021). Hydro-climatic Variability and Trend Analysis of Modjo River Watershed, Awash River Basin of Ethiopia. *Journal of Environment and Earth Science*, *11*(Figure 1), 1–8. https://doi.org/10.7176/jees/11-9-04

Estoque, R. C., Murayama, Y., & Myint, S. W. (2017). Effects of landscape composition and

pattern on land surface temperature: An urban heat island study in the megacities of Southeast Asia. *Science of the Total Environment*, *577*, 349–359. https://doi.org/10.1016/j.scitotenv.2016.10.195

Ethiopian Central Statistical Agency (CSA). (2013). *Population Projections for Ethiopia Population Census Commission*. *July*.

Fahey, D.W., S.J. Doherty, K.A. Hibbard, A. Romanou, and P. C. T. (2017). *Physical Drivers of Climate Change*. *I*, 73–113. https://doi.org/10.7930/J0513WCR.U.S.

Fallmann, J., & Emeis, S. (2020). How to bring urban and global climate studies together with urban planning and architecture? *Developments in the Built Environment*, *4*(August), 100023. https://doi.org/10.1016/j.dibe.2020.100023

Fallmann, J., Emeis, S., & Suppan, P. (2013). Mitigation of urban heat stress -a modelling case study for the area of Stuttgart. *Erde*, *144*(3–4), 202–216. https://doi.org/10.12854/erde-144-15

FAO. (2011). *The State of the World'S Land and Water Resources for Food and Agriculture*.

FDRE-NAP. (2019). Ethiopia's Climate Resilient Green Economy Strategy. National Adaptation Plan. *Federal Democratic Republic of Ethiopia. National Adaptation Plan.*, 147.

FDRE. (2023). *Ethiopia's long-term low emission and climate resilient development strategy (2020-2050)*. 108. https://unfccc.int/documents/630312

FDRE Ministry of Transport. (2017). *Ethiopia : Transport Sector GHG Emissions*.

Feng, G., Cobb, S., Abdo, Z., Fisher, D. K., Ouyang, Y., Adeli, A., & Jenkins, J. N. (2016). Trend analysis and forecast of precipitation, reference evapotranspiration, and rainfall deficit in the blackland prairie of eastern Mississippi. *Journal of Applied Meteorology and Climatology*, *55*(7), 1425–1439. https://doi.org/10.1175/JAMC-D-15-0265.1

Fernando, H. J. S. (2015). Urban heat islands. *Environmental Indicators*, 67–75. https://doi.org/10.1007/978-94-017-9499-2_5

Feyisa, G. L., Dons, K., & Meilby, H. (2014). Efficiency of parks in mitigating urban heat island

effect: An example from Addis Ababa. *Landscape and Urban Planning*, *123*, 87–95. https://doi.org/10.1016/j.landurbplan.2013.12.008

Feyissa, G., & Gebremariam, E. (2018). Mapping of landscape structure and forest cover change detection in the mountain chains around Addis Ababa: The case of Wechecha Mountain, Ethiopia. *Remote Sensing Applications: Society and Environment*, *11*, 254–264. https://doi.org/10.1016/j.rsase.2018.07.008

Feyissa, G., Zeleke, G., Bewket, W., & Gebremariam, E. (2018a). Downscaling of future temperature and precipitation extremes in Addis Ababa under climate change. *Climate*, *6*(3). https://doi.org/10.3390/cli6030058

Feyissa, G., Zeleke, G., Bewket, W., & Gebremariam, E. (2018b). *Downscaling of Future Temperature and Precipitation Extremes in Addis Ababa under Climate Change*. https://doi.org/10.3390/cli6030058

Feyissa, G., Zeleke, G., Gebremariam, E., & Bewket, W. (2018a). GIS based quantification and mapping of climate change vulnerability hotspots in Addis Ababa. *Geoenvironmental Disasters*, *5*(1). https://doi.org/10.1186/s40677-018-0106-4

Firozjaei, M. K., Fathololoumi, S., Alavipanah, S. K., Kiavarz, M., Vaezi, A. R., & Biswas, A. (2020). A new approach for modeling near surface temperature lapse rate based on normalized land surface temperature data. *Remote Sensing of Environment*, *242*(March), 111746. https://doi.org/10.1016/j.rse.2020.111746

Forster, P., Ramaswamy, V., Artaxo, P., Berntsen, T., Betts, R., Fahey, D. W., Haywood, J., Lean, J., Lowe, D. C., Myhre, G., Nganga, J., Prinn, R., Raga, G., Schulz, M., & Dorland, R. Van. (2007). *Changes in Atmospheric Constituents and in Radiative Forcing*. *15*(3), 228–237. https://doi.org/10.20892/j.issn.2095-3941.2017.0150

Frimpong, B. F., Koranteng, A., & Molkenthin, F. (2022). Analysis of temperature variability utilising Mann–Kendall and Sen's slope estimator tests in the Accra and Kumasi Metropolises in Ghana. *Environmental Systems Research*, *11*(1), 1–13. https://doi.org/10.1186/s40068-022-00269-1

Funk, C., Peterson, P., Landsfeld, M., Pedreros, D., Verdin, J., Shukla, S., Husak, G., Rowland, J., Harrison, L., Hoell, A., & Michaelsen, J. (2015). The climate hazards infrared precipitation with stations - A new environmental record for monitoring extremes. *Scientific Data*, *2*, 1–21. https://doi.org/10.1038/sdata.2015.66

Gabriel, K. R. (1971). The Biplot display of multivariate matrices with application to principal components analysis. *Biometrika*, *58*, 453–467.

Gatarić, D., Belij, M., Đerčan, B., & Filipović, D. (2019). The origin and development of Garden cities: An overview. *Zbornik Radova - Geografski Fakultet Univerziteta u Beogradu*, *67–1*, 33–43. https://doi.org/10.5937/zrgfub1901033g

Gebrechorkos, S. H., Hülsmann, S., & Bernhofer, C. (2018). Changes in temperature and precipitation extremes in Ethiopia, Kenya, and Tanzania. *International Journal of Climatology*, *39*(1), 18–30. https://doi.org/10.1002/joc.5777

Gebreegziabher, Z., Stage, J., Mekonnen, A., & Alemu, A. (2011). Climate Change and the Ethiopian Economy [Elektronisk resurs] : A Computable General Equilibrium Analysis. *Discussion Papers*, *October*.

Gebremicael, T. G., Mohamed, Y. A., Zaag, P. V., & Hagos, E. Y. (2017). Temporal and spatial changes of rainfall and streamflow in the Upper Tekezē-Atbara river basin, Ethiopia. *Hydrology and Earth System Sciences*, *21*(4), 2127–2142. https://doi.org/10.5194/hess-21-2127-2017

Gelata, F. T., Jiqin, H., & Chaka Gemeda, S. (2023). Application of MK trend and test of Sen's slope estimator to measure impact of climate change on the adoption of conservation agriculture in Ethiopia. *Journal of Water and Climate Change*, *14*(3), 977–988. https://doi.org/10.2166/wcc.2023.508

Gerace, A., & Montanaro, M. (2017). Remote Sensing of Environment Derivation and validation of the stray light correction algorithm for the thermal infrared sensor onboard Landsat 8. *Remote Sensing of Environment*, *191*, 246–257. https://doi.org/10.1016/j.rse.2017.01.029

Getachew, B. (2018). Trend analysis of temperature and rainfall in south gonder zone, anhara

ethiopia. *Journal of Degraded and Mining Lands Management*, *5*(2), 1111–1125. https://doi.org/10.15243/jdmlm.2018.052.1111

Gleixner, S., Luttringhaus, S., Kaufmann, J., Smytzek, P., & Gornott, C. (2022). *Assessment of Climatic Impact Drivers in Ethiopia*.

Gocic, M., & Trajkovic, S. (2013). Analysis of changes in meteorological variables using Mann-Kendall and Sen's slope estimator statistical tests in Serbia. *Global and Planetary Change*, *100*, 172–182. https://doi.org/10.1016/j.gloplacha.2012.10.014

Goosse H., P.Y. Barriat, W. Lefebvre, M.F. Loutre and V. Zunz, (2008-2010). (2008). *Chapter 1 . Description of the climate system and its components*. *2007*, 1–24.

Goovaerts, P. (1999). *Geostatistics in soil science : state-of-the-art and perspectives*. 1–45.

Goovaerts, P. (2000). Determining molecular weight distribution index from flow curves for polypropylene. *Journal of Hydrology*, *228*(3), 113–129.

Griggs, D., Stafford-Smith, M., Gaffney, O., Rockstrom, J., Ohman, M. C., Shyamsundar, P., Steffen, W., Glaser, G., Kanie, N., & Noble, I. (2013). *Sustainable development goals for people and planet*. 5–7.

Grimmond, C. S. B. (2006). *Progress in measuring and observing the urban atmosphere*. *22*, 3–22. https://doi.org/10.1007/s00704-005-0140-5

Grujić, K. (2023). A Review of Thermal Spectral Imaging Methods for Monitoring High-Temperature Molten Material Streams. *Sensors*, *23*(3). https://doi.org/10.3390/s23031130

Guha, S., & Govil, H. (2022). Annual assessment on the relationship between land surface temperature and six remote sensing indices using landsat data from 1988 to 2019. *Geocarto International*, *37*(15), 4292–4311. https://doi.org/10.1080/10106049.2021.1886339

Guha, S., Govil, H., Dey, A., & Gill, N. (2018). Analytical study of land surface temperature with NDVI and NDBI using Landsat 8 OLI and TIRS data in Florence and Naples city, Italy. *European Journal of Remote Sensing*, *51*(1), 667–678. https://doi.org/10.1080/22797254.2018.1474494

Guha, S., Govil, H., Dey, A., & Gill, N. (2020). A case study on the relationship between land surface temperature and land surface indices in Raipur City, India. *Geografisk Tidsskrift - Danish Journal of Geography* , *120*(1), 35–50. https://doi.org/10.1080/00167223.2020.1752272

Guptha, G. C., Swain, S., Al-Ansari, N., Taloor, A. K., & Dayal, D. (2021). Evaluation of an urban drainage system and its resilience using remote sensing and GIS. *Remote Sensing Applications: Society and Environment*, *23*(May), 100601. https://doi.org/10.1016/j.rsase.2021.100601

Hadgu, G., Tesfaye, K., Mamo, G., & Kassa, B. (2015). *Farmers ' climate change adaptation options and their determinants in Tigray Region , Northern Ethiopia*. *10*(9), 956–964. https://doi.org/10.5897/AJAR2014.9146

Hailemariam, S. N., Soromessa, T., & Teketay, D. (2016). *Land Use and Land Cover Change in the Bale*. https://doi.org/10.3390/land5040041

Haines, A., Kovats, R. S., & Corvalan, C. (2006). *Harben Lecture Climate change and human health : impacts , vulnerability ,*. https://doi.org/10.1016/j.puhe.2006.01.002

Haining, R. P., Kerry, R., & Oliver, M. A. (2010). *Geography , Spatial Data Analysis , and Geostatistics : An Overview*. *42*, 7–31.

Hale, R. C., Gallo, K. P., Owen, T. W., & Loveland, T. R. (2006). Land use/land cover change effects on temperature trends at U.S. Climate Normals stations. *Geophysical Research Letters*, *33*(11), 2–5. https://doi.org/10.1029/2006GL026358

Hallegatte, S., Henriet, F., & Corfee-Morlot, J. (2011). The economics of climate change impacts and policy benefits at city scale: A conceptual framework. *Climatic Change*, *104*(1), 51–87. https://doi.org/10.1007/s10584-010-9976-5

Hamed, K. H., & Rao, A. R. (1998). A modified Mann-Kendall trend test for autocorrelated data. *Journal of Hydrology*, *36*(15_suppl), 522–522. https://doi.org/10.1200/jco.2018.36.15_suppl.522

Hare, W. (2003). Assessment of Knowledge on Impacts of Climate Change – Contribution to the

Specification of Art. 2 of the UNFCCC. In *Wissenschaftliche Beirat der Bundesregierung Globale Umweltveränderungen* (Issue 1). http://www.wbgu.de/wbgu_sn2003_ex01.pdf

Hassaan, M. A., Abdrabo, M. A., & Masabarakiza, P. (2017). GIS-Based Model for Mapping Malaria Risk under Climate Change Case Study: Burundi. *Journal of Geoscience and Environment Protection*, *05*(11), 102–117. https://doi.org/10.4236/gep.2017.511008

Hegerl, G. C., Zwiers, F. W., Braconnot, P., Gillett, N. P., Luo, Y., Orsini, J. A. M., Nicholls, N., Penner, J. E., & Stott, P. A. (2007). Understanding and Attributing Climate Change. In: Climate Change 2007: The Physical Science Basis. Contribution of Working Group I to the Fourth Assessment Report of the Intergovernmental Panel on Climate Change. *Cambridge University Press*, *80*(3–4), 213–238. https://www.ipcc.ch/pdf/assessment-report/ar4/wg1/ar4-wg1-chapter9.pdf

Herold, M., Goldstein, N. C., & Clarke, K. C. (2003). *The spatiotemporal form of urban growth : measurement , analysis and modeling*. *86*, 286–302. https://doi.org/10.1016/S0034-4257(03)00075-0

Hofierka, J., Mitasova, H., Parajka, J., & Mitas, L. (2002). *Multivariate Interpolation of Precipitation Using Regularized Spline with Tension*. *6*(2).

Hopkins, F. M., Ehleringer, J. R., Bush, S. E., Duren, R. M., Miller, C. E., Lai, C. T., Hsu, Y. K., Carranza, V., & Randerson, J. T. (2016). Mitigation of methane emissions in cities: How new measurements and partnerships can contribute to emissions reduction strategies. *Earth's Future*, *4*(9), 408–425. https://doi.org/10.1002/2016EF000381

Hou, Y., Huang, X., & Zhao, L. (2022). Point-to-Surface Upscaling Algorithms for Snow Depth Ground Observations. *Remote Sensing*, *14*(19). https://doi.org/10.3390/rs14194840

Hu, Z., Liu, S., Zhong, G., Lin, H., & Zhou, Z. (2020). Modified Mann-Kendall trend test for hydrological time series under the scaling hypothesis and its application. *Hydrological Sciences Journal*, *65*(14), 2419–2438. https://doi.org/10.1080/02626667.2020.1810253

Hua, L., Zhang, X., Nie, Q., Sun, F., & Tang, L. (2020). The impacts of the expansion of urban impervious surfaces on urban heat islands in a coastal city in China. *Sustainability*

(Switzerland), *12*(2). https://doi.org/10.3390/su12020475

Huang, S., Tang, L., Hupy, J. P., Wang, Y., & Shao, G. (2021). A commentary review on the use of normalized difference vegetation index (NDVI) in the era of popular remote sensing. *Journal of Forestry Research*, *32*(1), 1–6. https://doi.org/10.1007/s11676-020-01155-1

Hughes, D. A. (2006). *Comparison of satellite rainfall data with observations from gauging station networks*. 399–410. https://doi.org/10.1016/j.jhydrol.2005.11.041

Huisman, O., & By, R. A. de. (2009). Principles of Geographic Information Systems: An introductory textbook. *Journal of Multivariate Analysis*, *127*, 98–111. https://doi.org/10.1016/j.jmva.2014.02.006

Hulme, M. (2017). Climate Change, Concept of. *International Encyclopedia of Geography: People, the Earth, Environment and Technology*, 1–6. https://doi.org/10.1002/9781118786352.wbieg0343

Huq, S., Kovats, S., Reid, H., & Satterthwaite, D. (2007). Editorial: Reducing risks to cities from disasters and climate change. *Environment and Urbanization*, *19*(1), 3–15. https://doi.org/10.1177/0956247807078058

Hussain, F., Boota, M. W., & Nabi, G. (2015). *Rainfall Trend Analysis by Using the Mann-Kendall Test & Sen'S Slope Estimates : A Case Study of District Chakwal Rain Gauge, Barani Area, Northern Punjab Province, Pakistan*. *January*.

Hussain, M., Chen, D., Cheng, A., Wei, H., & Stanley, D. (2013). Change detection from remotely sensed images: From pixel-based to object-based approaches. *ISPRS Journal of Photogrammetry and Remote Sensing*, *80*, 91–106. https://doi.org/10.1016/j.isprsjprs.2013.03.006

IPCC. (2000). Land use, land-use change and forestry. *Land Use, Land-Use Change and Forestry*, 1–160. https://doi.org/10.4337/9781849805834.00023

IPCC. (2001a). Climate Change 2001: The Scientific Basis. *Journal of Shoulder and Elbow Surgery*, *12*(3), 302–305. https://doi.org/10.1016/S1058-2746(02)86826-4

IPCC. (2001b). Climate Change 2001. Synthesis Report. IPCC Third Assessment Report (TAR):A Contribution of Working Groups I, II, and III to the Third Assessment Report of the Integovernmental Panel on Climate Change. *Ipcc*, 409. http://www.ipcc.ch/ipccreports/tar/

IPCC. (2001c). Contribution of Working Group I to the Third Assessment Report of the Intergovernmental Panel on Climate Change [Houghton, J.T. Ding, Y. Griggs, D.J. Noguer, M. Linden, P.J. van der Dai, X. Maskell, K. Johnson, C.A.]. *Cambridge University Press*, 94.

IPCC. (2002). Climate change and biodiversity. *Bioresources and Bioprocess in Biotechnology*, *1*, 99–124. https://doi.org/10.1007/978-981-10-3573-9_5

IPCC. (2007a). Climate Change 2007 Impacts, Adaptation and Vulnerability. In *International Encyclopedia of Human Geography*. https://doi.org/10.1016/B978-008044910-4.00250-9

IPCC. (2007b). Climate change 2007 The Physical Science Basis. In *Weather* (Vol. 59, Issue 8). https://doi.org/10.1256/wea.58.04

IPCC. (2012a). IPCC Special Report on Managing the Risks of Extreme Events and Disasters to Advance Climate Change Adaptation (SREX). In *Journal of Epidemiology and Community Health* (Vol. 66, Issue 9). https://doi.org/10.1136/jech-2012-201045

IPCC. (2012b). Managing the Risks of Extreme Events and Disasters to Advance Climate Change Adaptation. In *Managing the Risks of Extreme Events and Disasters to Advance Climate Change Adaptation*. https://doi.org/10.1017/cbo9781139177245

IPCC. (2013a). *Climate Change 2013 The Physical Science Basis*.

IPCC. (2013b). Climate Change 2021—The Physical Science Basis. In *Chemistry International* (Vol. 43, Issue 4). https://doi.org/10.1515/ci-2021-0407

IPCC. (2013c). Summary for Policymakers. In: Climate Change 2013: The Physical Science Basis. *Energy and Environment*, *18*(3–4), 433–440. https://doi.org/10.1260/095830507781076194

IPCC. (2014a). Climate Change 2014 Impacts, Adaptation, and Vulnerability. *Sustainaspeak*, 153–154. https://doi.org/10.4324/9781315270326-109

IPCC. (2014b). *Climate Change 2014 Impacts, Adaptation, and Vulnerability*.

IPCC. (2014c). *Climate Change 2014 Synthesis Report*.

IPCC. (2014d). Climate Change 2014 Synthesis Report. In *Managing the Risks of Extreme Events and Disasters to Advance Climate Change Adaptation: Special Report of the Intergovernmental Panel on Climate Change* (Vol. 9781107025). https://doi.org/10.1017/CBO9781139177245.003

IPCC. (2014e). Intergovernmental Panel on Climate Change. *Sustainaspeak*, 153–154. https://doi.org/10.4324/9781315270326-109

IPCC. (2014f). Part A: Global and Sectoral Aspects. (Contribution of Working Group II to the Fifth Assessment Report of the Intergovernmental Panel on Climate Change). *Climate Change 2014: Impacts, Adaptation, and Vulnerability.*, 1132. https://www.ipcc.ch/pdf/assessment-report/ar5/wg2/WGIIAR5-FrontMatterA_FINAL.pdf

IPCC. (2014g). *The IPCC's Fifth Assessment Report What's in it for Africa?*

IPCC. (2018). Summary for Policymakers. In: Global Warming of 1.5°C: An IPCC Special Report on Impacts of Global Warming of 1.5°C above Pre-industrial Levels in Context of Strengthening Response to Climate Change, Sustainable Development, and Efforts to Eradicate Pover. *Global Warming of 1.5°C*, 1–24. https://www.cambridge.org/core/product/identifier/9781009157940%23prf2/type/book_part

IPCC. (2021a). Climate Change 2021: Summary for all. *Cambridge University Press*, *In Press*, In Press.

IPCC. (2021b). *Climate Change 2021 The Physical Science Basis Summary for Policymakers*.

IPCC. (2021c). Summary for policymakers. In *Managing the Risks of Extreme Events and Disasters to Advance Climate Change Adaptation: Special Report of the Intergovernmental Panel on Climate Change* (Vol. 9781107025).

https://doi.org/10.1017/CBO9781139177245.003

IPCC. (2022a). Climate Change 2022 - Mitigation of Climate Change - Full Report. In *Cambridge University Press* (Issue 1).

IPCC. (2022b). Climate Change 2022 Impacts, Adaptation and Vulnerability Summary for policymakers. *Implementing a US Carbon Tax: Challenges and Debates*, xxiii–xxxiii. https://doi.org/10.4324/9781315071961-11

IPCC. (2023a). *Climate Change 2023: Synthesis Report: Summary for Policy Makers*. https://www.unep.org/resources/report/climate-change-2023-synthesis-report

IPCC. (2023b). Summary for Policymakers. In: Climate Change 2023: Synthesis Report. *Journal of Crystal Growth*, *218*(2), 259–264.

Jain, S. K., & Kumar, V. (2012). Trend analysis of rainfall and temperature data for India. *Current Science*, *102*(1), 37–49.

Jemberie, M. A., & Melesse, A. M. (2021). *Urban Flood Management through Urban Land Use*.

Jimenez-Munoz, J. C., Cristobal, J., Sobrino, J. A., Sòria, G., Ninyerola, M., & Pons, X. (2009). Revision of the single-channel algorithm for land surface temperature retrieval from landsat thermal-infrared data. *IEEE Transactions on Geoscience and Remote Sensing*, *47*(1), 339–349. https://doi.org/10.1109/TGRS.2008.2007125

Jin, M., Li, J., Wang, C., & Shang, R. (2015). A practical split-window algorithm for retrieving land surface temperature from Landsat-8 data and a case study of an urban area in China. *Remote Sensing*, *7*(4), 4371–4390. https://doi.org/10.3390/rs70404371

Jin, X., Wang, K., Wen, Z., & Zhang, W. (2005). Effect of rail corrugation on vertical dynamics of railway vehicle coupled with a track. *Acta Mechanica Sinica/Lixue Xuebao*, *21*(1), 95–102. https://doi.org/10.1007/s10409-004-0010-x

Jollife, I. T., & Cadima, J. (2016). Principal component analysis: A review and recent developments. *Philosophical Transactions of the Royal Society A: Mathematical, Physical and Engineering Sciences*, *374*(2065). https://doi.org/10.1098/rsta.2015.0202

Joseph, J. E., Akinrotimi, O. O., Rao, K. P. C., Ramaraj, A. P., Traore, P. S. C., Sujatha, P., & Whitbread, A. M. (2020). *The Usefulness of Gridded Climate Data Products in Characterizing Climate Variability and Assessing Crop Production The Usefulness of Gridded Climate Data Products in Characterizing Climate Variability and Assessing Crop Production*.

Jury, M. R., & Funk, C. (2013). Climatic trends over Ethiopia: Regional signals and drivers. *International Journal of Climatology*, *33*(8), 1924–1935. https://doi.org/10.1002/joc.3560

Kabir, M., Habiba, U. E., Khan, W., Shah, A., Rahim, S., Rios-Escalante, P. R. D. los, Farooqi, Z. U. R., & Ali, L. (2023). Climate change due to increasing concentration of carbon dioxide and its impacts on environment in 21st century; a mini review. *Journal of King Saud University - Science*, *35*(5), 102693. https://doi.org/10.1016/j.jksus.2023.102693

Kafy, A.- Al, Faisal, A. Al, Al Rakib, A., Roy, S., Ferdousi, J., Raikwar, V., Kona, M. A., & Fatin, S. M. A. Al. (2021). Predicting changes in land use/land cover and seasonal land surface temperature using multi-temporal landsat images in the northwest region of Bangladesh. *Heliyon*, *7*(7). https://doi.org/10.1016/j.heliyon.2021.e07623

Kalnay, E., & Cai, M. (2003). Erratum: Impact of urbanization and land-use change on climate (Nature (2003) 423 (528-531)). *Nature*, *425*(6953), 102. https://doi.org/10.1038/nature01952

Kamal, A., Mahfouz, A., Sezer, N., Hassan, I. G., Wang, L. L., & Rahman, M. A. (2023). Investigation of urban heat island and climate change and their combined impact on building cooling demand in the hot and humid climate of Qatar. *Urban Climate*, *52*(November 2022), 101704. https://doi.org/10.1016/j.uclim.2023.101704

Kassa, L., Zeleke, G., Alemu, D., Hagos, F., & Heinimann, A. (2012). Impact of urbanization of addis abeba city on peri-urban environment and livelihoods. *The Tenth Conference on Ethiopian Economy, January 2015*, 1–30.

Kelman, I. (2017). Linking disaster risk reduction, climate change, and the sustainable development goals. *Disaster Prevention and Management*, *26*(3), 254–258. https://doi.org/10.1108/DPM-02-2017-0043

Khan, T. U., Mannan, A., Hacker, C. E., Ahmad, S., Siddique, M. A., Khan, B. U., Din, E. U., Chen, M., Zhang, C., Nizami, M., & Luan, X. (2021). *Use of GIS and Remote Sensing Data to Understand the Impacts of Land Use / Land Cover Changes (LULCC) on Snow Leopard (Panthera uncia) Habitat in Pakistan*.

Kifle, B. (2003). Urban Health Island and its feature in Addis Ababa (A case study). *Fifth International Conference on Urban Climate*.

Kilmer, P. D. (2010). Review Article: Review Article. *Journalism*, *11*(3), 369–373. https://doi.org/10.1177/1461444810365020

Kindu, M., Schneider, T., Teketay, D., & Knoke, T. (2013). *Land Use / Land Cover Change Analysis Using Object-Based Classification Approach in Munessa-Shashemene Landscape of*. 2411–2435. https://doi.org/10.3390/rs5052411

Kiros, G., Shetty, A., & Nandagiri, L. (2016). Analysis of variability and trends in rainfall over northern Ethiopia. *Arabian Journal of Geosciences*, *9*(6). https://doi.org/10.1007/s12517-016-2471-1

Kisaka, M. O., Mucheru-Muna, M., Ngetich, F. K., Mugwe, J. N., Mugendi, D., & Mairura, F. (2015). Rainfall variability, drought characterization, and efficacy of rainfall data reconstruction: Case of Eastern Kenya. *Advances in Meteorology*, *2015*. https://doi.org/10.1155/2015/380404

Kocabas, A., Gibson, M. S., & Diren, M. (2015). Climate change mitigation: From carbon-intensive sprawl toward low carbon urbanization: Progress and prospects for istanbul. In *Handbook of Climate Change Adaptation*. https://doi.org/10.1007/978-3-642-38670-1_35

Koroso, N. H., Lengoiboni, M., & Zevenbergen, J. A. (2021). Urbanization and urban land use efficiency: Evidence from regional and Addis Ababa satellite cities, Ethiopia. *Habitat International*, *117*(July), 102437. https://doi.org/10.1016/j.habitatint.2021.102437

Kotharkar, R., Bagade, A., & Ramesh, A. (2019). Assessing urban drivers of canopy layer urban heat island: A numerical modeling approach. *Landscape and Urban Planning*, *190*(January), 103586. https://doi.org/10.1016/j.landurbplan.2019.05.017

Kotharkar, R., Bagade, A., & Singh, P. R. (2020). A systematic approach for urban heat island mitigation strategies in critical local climate zones of an Indian city. *Urban Climate*, *34*(February), 100701. https://doi.org/10.1016/j.uclim.2020.100701

Krauer, J., Gaemperli, U., Hurni, K., Fries, M., Wuersch, L., Kassawmar, T., Zeleke, G., & Aragie, Y. (2019). *EthioGIS-3 Data Catalog: National Geospatial Database System Ethiopia*. *41*(0), 1–21. http://data.worldbank.org/data-catalog

Krissansen-Totton, J., & Davies, R. (2013). Investigation of cosmic ray-cloud connections using MISR. *Geophysical Research Letters*, *40*(19), 5240–5245. https://doi.org/10.1002/grl.50996

Kron, W., Löw, P., & Kundzewicz, Z. W. (2019). Changes in risk of extreme weather events in Europe. *Environmental Science and Policy*, *100*(June), 74–83. https://doi.org/10.1016/j.envsci.2019.06.007

Kshetri, T. B. (2018). NDVI, NDBI & NDWI Calculation Using Landsat 7,8. *Https://Www.Linkedin.Com/*, *September 2018*, 8. https://www.linkedin.com/pulse/ndvi-ndbi-ndwi-calculation-using-landsat-7-8-tek-bahadur-kshetri/%0Ahttps://www.linkedin.com/pulse/ndvi-ndbi-ndwi-calculation-using-landsat-7-8-tek-bahadur-kshetri

Kumar, P. (2021). Climate Change and Cities: Challenges Ahead. *Frontiers in Sustainable Cities*, *3*(February), 1–8. https://doi.org/10.3389/frsc.2021.645613

Kumar, V., Jain, S. K., & Singh, Y. (2010). Analyse des tendances pluviométriques de long terme en Inde. *Hydrological Sciences Journal*, *55*(4), 484–496. https://doi.org/10.1080/02626667.2010.481373

Kumari, B., Tayyab, M., Shahfahad, Salman, Mallick, J., Khan, M. F., & Rahman, A. (2018). Satellite-Driven Land Surface Temperature (LST) Using Landsat 5, 7 (TM/ETM+ SLC) and Landsat 8 (OLI/TIRS) Data and Its Association with Built-Up and Green Cover Over Urban Delhi, India. *Remote Sensing in Earth Systems Sciences*, *1*(3–4), 63–78. https://doi.org/10.1007/s41976-018-0004-2

Kundzewicz, Z. W., & Radziejewski, M. (2006). *Methodologies for trend detection*. *November*,

538–550.

Kupika, O. L., Gandiwa, E., Kativu, S., & Nhamo, G. (2018). Impacts of Climate Change and Climate Variability on Wildlife Resources in Southern Africa: Experience from Selected Protected Areas in Zimbabwe. *Selected Studies in Biodiversity*, 1–24. https://doi.org/10.5772/intechopen.70470

Kuttler, W., Weber, S., Schonnefeld, J., & Hesselschwerdt, A. (2007). *Urban/rural atmospheric water vapour pressure differences and urabn moisture excess in Krefeld, Germany*.

Lambin, E. F., & Geist, H. (2006). Land-Use and Land-Cover Change. In *PhD Proposal* (Vol. 1, Issue October). https://doi.org/10.1017/CBO9781107415324.004

Lambin, E. F., Turner, B. L., Geist, H. J., Agbola, S. B., Angelsen, A., Folke, C., Bruce, J. W., Coomes, O. T., Dirzo, R., George, P. S., Homewood, K., Imbernon, J., Leemans, R., Li, X., Moran, E. F., Mortimore, M., Ramakrishnan, P. S., Richards, J. F., Steffen, W., … Veldkamp, T. A. (2001). *The causes of land-use and land-cover change : moving beyond the myths*. *11*, 261–269.

Langsdale, M. F., Dowling, T. P. F., Wooster, M., Johnson, J., Grosvenor, M. J., de Jong, M. C., Johnson, W. R., Hook, S. J., & Rivera, G. (2020). Inter-comparison of field-and laboratory-derived surface emissivities of natural and manmade materials in support of land surface temperature (Lst) remote sensing. *Remote Sensing*, *12*(24), 1–30. https://doi.org/10.3390/rs12244127

Legese, W., D, K., & K, T. (2018). Perception of Farmers on Climate Change and their Adaptive Strategies over Bale Highlands, Southeastern Ethiopia. *Journal of Earth Science & Climatic Change*, *09*(09). https://doi.org/10.4172/2157-7617.1000491

Lettenmaier, D. P., Wood, E. F., & Walls, J. R. (1994). *Hydro-Climatological Trends in the Continental United States, 1948-88*.

Li, J., & Heap, A. D. (2008). A Review of Spatial Interpolation Methods for Environmental Scientists. *Australian Geological Survey Organisation*, *GeoCat# 68*(2008/23), 154. https://doi.org/http://www.ga.gov.au/image_cache/GA12526.pdf

Li, L., Zha, Y., & Wang, R. (2020). Relationship of surface urban heat island with air temperature and precipitation in global large cities. *Ecological Indicators*, *117*(June), 106683. https://doi.org/10.1016/j.ecolind.2020.106683

Li, X., Zhou, Y., Asrar, G. R., Imhoff, M., & Li, X. (2017). The surface urban heat island response to urban expansion: A panel analysis for the conterminous United States. *Science of the Total Environment*, *605–606*, 426–435. https://doi.org/10.1016/j.scitotenv.2017.06.229

Li, X., Zhou, Y., Yu, S., Jia, G., Li, H., & Li, W. (2019). Urban heat island impacts on building energy consumption: a review of approaches and findings. *Energy*. https://doi.org/10.1016/j.energy.2019.02.183

Li, Z.-L., Tang, B. H., Wu, H., Ren, H., Yan, G., Wan, Z., Trigo, I. F., & Sobrino, J. A. (2013). Satellite-derived land surface temperature: Current status and perspectives. *Remote Sensing of Environment*, *131*, 14–37. https://doi.org/10.1016/j.rse.2012.12.008

Lillo, M. De, & Ferguson, H. J. (2018). Why conspiracy theories matter: A social psychological analysis. *European Journal of Social Psychology*, *40*(2), 366–374.

Lindemann-Matthies, P., & Brieger, H. (2016). Does urban gardening increase aesthetic quality of urban areas? A case study from Germany. *Urban Forestry and Urban Greening*, *17*, 33–41. https://doi.org/10.1016/j.ufug.2016.03.010

Ling, Z., Gao, Y., & Chen, Q. (2021). Application of principal component analysis in meteorological forecast. *IOP Conference Series: Earth and Environmental Science*, *631*(1). https://doi.org/10.1088/1755-1315/631/1/012019

Liu, H., Zhan, Q., Gao, S., & Yang, C. (2019). Seasonal variation of the spatially non-stationary association between land surface temperature and urban landscape. *Remote Sensing*, *11*(9), 1–20. https://doi.org/10.3390/rs11091016

Liu, Y., Zhuo, L., Pregnolato, M., & Han, D. (2022). An assessment of statistical interpolation methods suited for gridded rainfall datasets. *International Journal of Climatology*, *42*(5), 2754–2772. https://doi.org/10.1002/joc.7389

Lu, D., Song, K., Zeng, L., Liu, D., Khan, S., Zhang, B., Wang, Z., & Jin, C. (2008). Estimating impervious surface for the urban area expansion: Examples from Changchun, Northeast China. *International Archives of the Photogrammetry, Remote Sensing and Spatial Information Sciences - ISPRS Archives*, *37*(1), 385–392.

Malik, M. S., Shukla, J. P., & Mishra, S. (2019). Relationship of LST, NDBI and NDVI using landsat-8 data in Kandaihimmat watershed, Hoshangabad, India. *Indian Journal of Geo-Marine Sciences*, *48*(1), 25–31.

Manatsa, D., Chingombe, W., & Matarira, C. H. (2008). The impact of the positive Indian Ocean dipole on Zimbabwe droughts Tropical climate is understood to be dominated by. *International Journal of Climatology*, *2029*(March 2008), 2011–2029. https://doi.org/10.1002/joc

Mandale, V. P., Mahale, D. M., Nandgude, S. B., Gharde, K. D., & Thokal, R. T. (2017). Spatio-Temporal Rainfall Trends in Konkan Region of Maharashtra State. *Advanced Agricultural Research & Technology Journal*, *1*(1), 61–69.

Mann, H. B. (1945). Non-Parametric Test Against Trend. *Econometrica*, *13*(3), 245–259. http://www.economist.com/node/18330371?story%7B_%7Did=18330371

Mantyka-Pringle, C. S., Martin, T. G., & Rhodes, J. R. (2012). *Interactions between climate and habitat loss effects on biodiversity : a systematic review and meta-analysis*. 1239–1252. https://doi.org/10.1111/j.1365-2486.2011.02593.x

Marchant, R., Richer, S., Boles, O., Capitani, C., Courtney-Mustaphi, C. J., Lane, P., Prendergast, M. E., Stump, D., De Cort, G., Kaplan, J. O., Phelps, L., Kay, A., Olago, D., Petek, N., Platts, P. J., Punwong, P., Widgren, M., Wynne-Jones, S., Ferro-Vázquez, C., … Wright, D. (2018). Drivers and trajectories of land cover change in East Africa: Human and environmental interactions from 6000 years ago to present. *Earth-Science Reviews*, *178*, 322–378. https://doi.org/10.1016/j.earscirev.2017.12.010

Mariye, M., Mariyo, M., Changming, Y., Teffera, Z. L., & Weldegebrial, B. (2022). Effects of land use and land cover change on soil erosion potential in Berhe district: a case study of Legedadi watershed, Ethiopia. *International Journal of River Basin Management*, *20*(1),

79–91. https://doi.org/10.1080/15715124.2020.1767636

Matewos, T. (2019). Climate change-induced impacts on smallholder farmers in selected districts of Sidama, Southern Ethiopia. *Climate*, *7*(5). https://doi.org/10.3390/cli7050070

Matthews, H. D., Zickfeld, K., Knutti, R., & Allen, M. R. (2018). Focus on cumulative emissions, global carbon budgets and the implications for climate mitigation targets. *Environmental Research Letters*, *13*(1). https://doi.org/10.1088/1748-9326/aa98c9

Matyas, D., Regional, S., Adviser, R., Pelling, M., & Kingdom, U. (2014). Positioning resilience for 2015: the role of resistance, incremental adjustment and transformation in disaster risk management policy - 2835bdba742e7d837e2dfeaa3206f3727880f95d95105276f5261c2595a71028.pdf. *Disasters*, *39*, 1–19. https://onlinelibrary.wiley.com/doi/abs/10.1111/disa.12107

Mayewski, P. A., Meeker, L. D., Twickler, M. S., Whitlow, S., Yang, Q., Lyons, W. B., & Prentice, M. (1997). Major features and forcing of high-latitude northern hemisphere atmospheric circulation using a 110,000-year-long glaciochemical series. *Journal of Geophysical Research: Oceans*, *102*(C12), 26345–26366. https://doi.org/10.1029/96JC03365

Mcmillin, L. M. (1975). *Estimation of Sea Surface Temperatures From Two Infrared Window Measurements With Different Absorption*. *80*(36), 5113–5117.

Mcphillips, L. E., Chang, H., Chester, M. V, Depietri, Y., Friedman, E., Grimm, N. B., Kominoski, J. S., Mcphearson, T., Méndez-lázaro, P., Rosi, E. J., & Shiva, J. S. (2018). *Earth ' s Future Defining Extreme Events : A Cross-Disciplinary Review Earth ' s Future*. 441–455. https://doi.org/10.1002/2017EF000686

Meerow, S., Newell, J. P., & Stults, M. (2016). Defining urban resilience: A review. *Landscape and Urban Planning*, *147*, 38–49. https://doi.org/10.1016/j.landurbplan.2015.11.011

Mekonen, A. A., Berlie, A. B., & Ferede, M. B. (2020). Spatial and temporal drought incidence analysis in the northeastern highlands of Ethiopia. *Geoenvironmental Disasters*, *7*(1). https://doi.org/10.1186/s40677-020-0146-4

Mekonnen, E. N., Damene, S., Gebremariam, E., & Nebebe, A. (2022). Geospatially-Based Land Use/Land Cover Dynamics Detection, Central Ethiopian Rift Valley. *GeoJournal*, *0123456789*. https://doi.org/10.1007/s10708-022-10815-0

Mengistu, D., Bewket, W., & Lal, R. (2014). Recent spatiotemporal temperature and rainfall variability and trends over the Upper Blue Nile River Basin, Ethiopia. *International Journal of Climatology*, *34*(7), 2278–2292. https://doi.org/10.1002/joc.3837

Mensah, C., Atayi, J., Kabo-Bah, A. T., Švik, M., Acheampong, D., Kyere-Boateng, R., Prempeh, N. A., & Marek, M. V. (2020). Impact of urban land cover change on the garden city status and land surface temperature of Kumasi. *Cogent Environmental Science*, *6*(1), 1–16. https://doi.org/10.1080/23311843.2020.1787738

Mera, G. A. (2018). Drought and its impacts in Ethiopia. *Weather and Climate Extremes*, *22*(October 2018), 24–35. https://doi.org/10.1016/j.wace.2018.10.002

Merga, B. B., Moisa, M. B., Negash, D. A., Ahmed, Z., & Gemeda, D. O. (2022). Land Surface Temperature Variation in Response to Land-Use and Land-Cover Dynamics: A Case of Didessa River Sub-basin in Western Ethiopia. *Earth Systems and Environment*, *April*. https://doi.org/10.1007/s41748-022-00303-3

Michaud, J. D. (1995). *Spatial and Elevational Variations of Summer Rainfall in the Southwestern United Stated*.

Mills, G., Cleugh, H., Emmanuel, R., Endlicher, W., Erell, E., McGranahan, G., Ng, E., Nickson, A., Rosenthal, J., & Steemer, K. (2010). Climate information for improved planning and management of mega cities (Needs Perspective). *Procedia Environmental Sciences*, *1*(1), 228–246. https://doi.org/10.1016/j.proenv.2010.09.015

Milstein, M. B., & Hart, S. L. (1999). Global Sustainability and the Creative Destruction of Industries. *Sloan Management Review*, *41*(1), 23–33.

Ministry of Environment and Forest. (2015). Ethiopia's Second National Communication to the United Nations Framework Convention on Climate Change (UNFCC). *Social Welfare in Africa*, 1–358. https://doi.org/10.4324/9781315670546

Mishra, P. K., Rai, A., & Rai, S. C. (2019). Land use and land cover change detection using geospatial techniques in the The Egyptian Journal of Remote Sensing and Space Sciences Land use and land cover change detection using geospatial techniques in the Sikkim Himalaya , India. *The Egyptian Journal of Remote Sensing and Space Sciences*, *March*. https://doi.org/10.1016/j.ejrs.2019.02.001

Moges, S. A., Taye, M. T., Willems, P., & Gebremichael, M. (2013). *Exceptional pattern of extreme rainfall variability at urban centre of Addis Ababa , Ethiopia*. *October 2013*, 37–41. https://doi.org/10.1080/1573062X.2013.831914

Moges, S. A., Taye, M. T., Willems, P., & Gebremichael, M. (2014). Exceptional pattern of extreme rainfall variability at urban centre of Addis Ababa, Ethiopia. *Urban Water Journal*, *11*(7), 596–604. https://doi.org/10.1080/1573062X.2013.831914

Moges, S., Raschid-sally, L., & Gebremichael, M. (2013). Is Climate Chang Responsible to Recent Urban Flooding in Devloping Cities in Africa? A Case study of Addis Ababa City, Ethiopia. *Geophysical Research Abstracts*, *15*, 9417. https://meetingorganizer.copernicus.org/EGU2013/EGU2013-9417.pdf

Mohammed, Y., Yimer, F., Tadesse, M., & Tesfaye, K. (2018). Variability and trends of rainfall extreme events in north east highlands of Ethiopia. *International Journal of Hydrology*, *2*(5), 594–605. https://doi.org/10.15406/ijh.2018.02.00131

Mohan, M., Kikegawa, Y., Gurjar, B. R., Bhati, S., Kandya, A., & Ogawa, K. (2012). Urban Heat Island Assessment for a Tropical Urban Airshed in India. *Atmospheric and Climate Sciences*, *02*(02), 127–138. https://doi.org/10.4236/acs.2012.22014

Moisa, M. B., Dejene, I. N., Roba, Z. R., & Gemeda, D. O. (2022). Impact of urban land use and land cover change on urban heat island and urban thermal comfort level: a case study of Addis Ababa City, Ethiopia. *Environmental Monitoring and Assessment*, *194*(10). https://doi.org/10.1007/s10661-022-10414-z

Moisa, M. B., & Gemeda, D. O. (2021a). Analysis of urban expansion and land use/land cover changes using geospatial techniques: a case of Addis Ababa City, Ethiopia. *Applied Geomatics*, *13*(4), 853–861. https://doi.org/10.1007/s12518-021-00397-w

Moisa, M. B., & Gemeda, D. O. (2022). Assessment of urban thermal field variance index and thermal comfort level of Addis Ababa metropolitan city, Ethiopia. *Heliyon*, *8*(8), e10185. https://doi.org/10.1016/j.heliyon.2022.e10185

Moisa, M. B., Merga, B. B., & Gemeda, D. O. (2022). Urban heat island dynamics in response to land use land cover change: a case of Jimma city, southwestern Ethiopia. *Theoretical and Applied Climatology*, *0123456789*. https://doi.org/10.1007/s00704-022-04055-y

Montanaro, M., Gerace, A., Lunsford, A., & Reuter, D. (2014). Stray light artifacts in imagery from the landsat 8 thermal infrared sensor. *Remote Sensing*, *6*(11), 10435–10456. https://doi.org/10.3390/rs61110435

Morris, C. J. G., & Simmonds, I. (2001). Quantification of the influence of wind and cloud on the nocturnal urban heat island of a large city. *Journal of Applied Meteorology*, *40*(2), 169–182. https://doi.org/10.1175/1520-0450(2001)040<0169:QOTIOW>2.0.CO;2

Mosha, A. C. (2011). Climate change and sustainable urban development in Africa and Asia. In *Climate Change and Sustainable Urban Development in Africa and Asia*. https://doi.org/10.1007/978-90-481-9867-2

Mukheibir, P., & Ziervogel, G. (2007). Developing a Municipal Adaptation Plan (MAP) for climate change: The city of Cape Town. *Adapting Cities to Climate Change: Understanding and Addressing the Development Challenges*, *19*(1), 271–289. https://doi.org/10.4324/9781849770361

Mulatu, T., & Desta, H. (2023). Surface temperature variation among traditional and modern residential forms in Addis Ababa, Ethiopia: Implications for land use planning. *City and Environment Interactions*, *20*(August), 100126. https://doi.org/10.1016/j.cacint.2023.100126

Mulugeta, S., Fedler, C., & Ayana, M. (2019). Analysis of long-term trends of annual and seasonal rainfall in the Awash River Basin, Ethiopia. *Water (Switzerland)*, *11*(7). https://doi.org/10.3390/w11071498

Mulusew, A., & Hong, M. (2024). A dynamic linkage between greenhouse gas (GHG) emissions

and agricultural productivity: evidence from Ethiopia. *Humanities and Social Sciences Communications*, *11*(1), 1–17. https://doi.org/10.1057/s41599-023-02437-9

Muthoni, F. K., Odongo, V. O., Ochieng, J., Mugalavai, E. M., Mourice, S. K., Hoesche-Zeledon, I., Mwila, M., & Bekunda, M. (2019). Long-term spatial-temporal trends and variability of rainfall over Eastern and Southern Africa. *Theoretical and Applied Climatology*, *137*(3–4), 1869–1882. https://doi.org/10.1007/s00704-018-2712-1

Mwangi, K. K., & Mutua, F. (2015). *Modeling Kenya ' s Vulnerability to Climate Change – A Multifactor Approach*. *4*(6), 12–19.

Mwangi, K., & Mutua, F. (2015). Modeling Kenya's Vulnerability to Climate Change – A Multifactor Approach (PDF Download Available). *Thesis for: MSc. Geosptatial Information System and Remote Sensing, , 4*(6), 12–19. https://www.researchgate.net/publication/279885203_Modeling_Kenya's_Vulnerability_to_Climate_Change_-_A_Multifactor_Approach

Naeem, S., Cao, C., Qazi, W. A., Zamani, M., Wei, C., Acharya, B. K., & Rehman, A. U. (2018). Studying the association between green space characteristics and land surface temperature for sustainable urban environments: An analysis of Beijing and Islamabad. *ISPRS International Journal of Geo-Information*, *7*(2), 1–24. https://doi.org/10.3390/ijgi7020038

NAPA. (2007). *Climate Change National Adaptation Programme of Action (NAPA) of Ethiopia*. *June*, 73. https://doi.org/10.1007/s10113-011-0244-7

National Meteorological Agency [NMA], 2007. (2007). *The Federal Democratic Republic of Ethiopia Climate Change National Adaptation Programme of Action (NAPA) of Ethiopia Climate Change National Adaptation Programme of Action (Napa) of Ethiopia*. *June*, 85. https://unfccc.int/resource/docs/napa/eth01.pdf

Ndossi, M. I., & Avdan, U. (2016). Application of open source coding technologies in the production of Land Surface Temperature (LST) maps from Landsat: A PyQGIS plugin. *Remote Sensing*, *8*(5). https://doi.org/10.3390/rs8050413

Ngarambe, J., Oh, J. W., Su, M. A., Santamouris, M., & Yun, G. Y. (2021). Influences of wind

speed, sky conditions, land use and land cover characteristics on the magnitude of the urban heat island in Seoul: An exploratory analysis. *Sustainable Cities and Society*, *71*(December 2020), 102953. https://doi.org/10.1016/j.scs.2021.102953

Ngongondo, C., Xu, C. Y., Gottschalk, L., & Alemaw, B. (2011). Evaluation of spatial and temporal characteristics of rainfall in Malawi: A case of data scarce region. *Theoretical and Applied Climatology*, *106*(1–2), 79–93. https://doi.org/10.1007/s00704-011-0413-0

Nguyen, T. P., Tran, T. N., Dinh, T. T. H., Hoang, T. M., & Duong Thi Thuy, T. (2022). Drivers of climate change in selected emerging countries: the ecological effects of monetary restrictions and expansions. *Cogent Economics and Finance*, *10*(1). https://doi.org/10.1080/23322039.2022.2114658

Niang, A., Becker, M., Ewert, F., Dieng, I., Gaiser, T., Tanaka, A., Senthilkumar, K., Rodenburg, J., Johnson, J., Akakpo, C., Segda, Z., Gbakatchetche, H., Jaiteh, F., Bam, R. K., Dogbe, W., Keita, S., Kamissoko, N., Maïga, I., Bakare, O. S., … Saito, K. (2017). Field Crops Research Variability and determinants of yields in rice production systems of West Africa. *Field Crops Research*, *207*, 1–12. https://doi.org/10.1016/j.fcr.2017.02.014

Njoh, A. J. (2003). Urbanization and development in sub-Saharan Africa. *Cities*, *20*(3), 167–174. https://doi.org/10.1016/S0264-2751(03)00010-6

NMSA. (2001a). *Federal Democratic Republic of Ethiopia*. *June*.

NMSA. (2001b). *Intial National Communication of Ethiopia to the United Nations Framework Convention on Climate Change*. *June*.

NOAA. (2018). Climate Variability vs . Climate Change. *National Oceanic and Atmospheric Administration*, *July*, 2. https://www.weather.gov/media/climateservices/VariabilityAndChange.pdf

Norman, J. M., & Becker, F. (1995). Terminology in thermal infrared remote sensing of natural surfaces. *Agricultural and Forest Meteorology*, *77*(3–4), 153–166. https://doi.org/10.1016/0168-1923(95)02259-Z

Nunes, L. J. R. (2023). The Rising Threat of Atmospheric CO2: A Review on the Causes,

Impacts, and Mitigation Strategies. *Environments - MDPI*, *10*(4). https://doi.org/10.3390/environments10040066

Oke, T. R. (1982). The energetic basis of the urban heat island. *Quarterly Journal of the Royal Meteorological Society*, *108*(455), 1–24. https://doi.org/10.1002/qj.49710845502

Oliver, M. A., & Webster, R. (1990). Kriging: A method of interpolation for geographical information systems. *International Journal of Geographical Information Systems*, *4*(3), 313–332. https://doi.org/10.1080/02693799008941549

Orke, Y. A., & Li, M. H. (2021). Hydroclimatic variability in the bilate watershed, ethiopia. *Climate*, *9*(6). https://doi.org/10.3390/cli9060098

Oxfam. (2017). A climate in crisis. *How Climate Change Is Making Droughty and Humanitarian Disaster Worse in East Africa*, *April*, 12.

Ozturk, D., & Kilic, F. (2016). *Geostatistical Approach for Spatial Interpolation of Meteorological Data*. *88*, 2121–2136.

Pacillo, G., Achicanoy, H., Ramirez-Villegas, J., Craparo, A., Basel, A., Villa, V., Schapendonk, F., Carneiro, B., Resce, G., Ruscica, G., Liebig, T., & Läderach, P. (2021). *Factsheet Climate Security in Ethiopia Is climate a "risk multiplier" in Ethiopia?*

Pandey, A., Mondal, A., Guha, S., Upadhyay, P. K., & Rashmi. (2022). A Seasonal Investigation on Land Surface Temperature and Spectral Indices in Imphal City, India. *Journal of Landscape Ecology(Czech Republic)*, *15*(3), 1–18. https://doi.org/10.2478/jlecol-2022-0015

Pandey, A., Mondal, A., Guha, S., Upadhyay, P. K., & Singh, D. (2022). Land use status and its impact on land surface temperature in Imphal city, India. *Geology, Ecology, and Landscapes*, *00*(00), 1–15. https://doi.org/10.1080/24749508.2022.2131962

Pandžić, K., & Kisegi, M. (1990). Principal Component analysis of a local temperature field within the global circulation. *Theoretical and Applied Climatology*, *41*(4), 177–200. https://doi.org/10.1007/BF00866450

Parikh, J., Sandal, G., & Jindal, P. (2014). *Asian Cities Climate Resilience Vulnerability profiling*

of cities A framework for climate-resilient urban development in India.

Patz, J. A., Engelberg, D., & Last, J. (2000). *The Effects of Changing Weather on Public Health*. 271–307.

Pauleit, S., Coly, A., Fohlmeister, S., Gasparini, P., Jørgensen, G., Kabisch, S., Kombe, W. J., Lindley, S., Simonis, I., & Yeshitela, K. (2015). *Urban Vulnerability and Climate Change in Africa: A Multidisciplinary Approach* (Vol. 4). http://www.springer.com/de/book/9783319039848

Peng, X., Wu, W., Zheng, Y., Sun, J., Hu, T., & Wang, P. (2020). Correlation analysis of land surface temperature and topographic elements in Hangzhou, China. *Scientific Reports*, *10*(1), 1–16. https://doi.org/10.1038/s41598-020-67423-6

Phillips, D. L., Dolph, J., & Marks, D. (1992). *A comparison of geostatistical procedures for spatial analysis of precipitation in mountainous terrain *. 58*, 119–141.

Pielke, R. A., Adegoke, J., Beltrán-Przekurat, A., Hiemstra, C. A., Lin, J., Nair, U. S., Niyogi, D., & Nobis, T. E. (2007). An overview of regional land-use and land-cover impacts on rainfall. *Tellus, Series B: Chemical and Physical Meteorology*, *59*(3), 587–601. https://doi.org/10.1111/j.1600-0889.2007.00251.x

Pielke, R. A., Marland, G., Betts, R. A., Chase, T. N., Eastman, J. L., Niles, J. O., Niyogi, D. D. S., & Running, S. W. (2002). The influence of land-use change and landscape dynamics on the climate system: Relevance to climate-change policy beyond the radiative effect of greenhouse gases. *Philosophical Transactions of the Royal Society A: Mathematical, Physical and Engineering Sciences*, *360*(1797), 1705–1719. https://doi.org/10.1098/rsta.2002.1027

Pingale, S. M., Khare, D., Jat, M. K., & Adamowski, J. (2016). Trend analysis of climatic variables in an arid and semi-arid region of the Ajmer District, Rajasthan, India. *Journal of Water and Land Development*, *28*(1), 3–18. https://doi.org/10.1515/jwld-2016-0001

Piri, I., KHanamani, A., SHojaei, S., & FAthizad, H. (2016). *Determination of the best geostatistical method for climatic zoning in Iran Determination of the Best Geostatistical*

Method for Climatic Zoning in Iran. *November*. https://doi.org/10.15666/aeer/1501

Pongracz, R., Bartholy, J., & Dezso, Z. (2006). *Remotely sensed thermal information applied to urban climate analysis*. *37*, 2191–2196. https://doi.org/10.1016/j.asr.2005.06.069

Porter, J. R., Uk, D., & Uk, J. J. (2014). *Coordinating Lead Authors : Lead Authors : Contributing Authors : Review Editors : Volunteer Chapter Scientist :* 485–533.

Poudel, S., & Shaw, R. (2016). The relationships between climate variability and crop yield in a mountainous environment: A case study in Lamjung District, Nepal. *Climate*, *4*(1). https://doi.org/10.3390/cli4010013

Pozoukidou, G. (2020). Designing a green infrastructure network for metropolitan areas: a spatial planning approach. *Euro-Mediterranean Journal for Environmental Integration*, *5*(2), 1–15. https://doi.org/10.1007/s41207-020-00178-8

Prakasam, C. (2010). Land use and land cover change detection through remote sensing approach: A case study of Kodaikanal taluk, Tamil Nadu. *International Journal of Geomatics and Geosciences*, *1*(2), 150–158. https://doi.org/10.3390/vaccines6030051

Prata, A. J. (1994). Land surface temperatures derived from the advanced very high resolution radiometer and the along-track scanning radiometer 2. Experimental results and validation of AVHRR algorithms. *Journal of Geophysical Research*, *99*(D6). https://doi.org/10.1029/94jd00409

Priyankara, P., Ranagalage, M., Dissanayake, D. M. S. L. B., Morimoto, T., & Murayama, Y. (2019). Spatial process of surface urban heat island in rapidly growing seoul metropolitan area for sustainable urban planning using landsat data (1996-2017). *Climate*, *7*(9). https://doi.org/10.3390/cli7090110

Qin, Z., Karnieli, A., & Berliner, P. (2001). A mono-window algorithm for retrieving land surface temperature from Landsat TM data and its application to the Israel-Egypt border region. *International Journal of Remote Sensing*, *22*(18), 3719–3746. https://doi.org/10.1080/01431160010006971

Qin, Z., Li, W., Gao, M., & Zhang, H. (2006). Estimation of land surface emissivity for Landsat

TM6 and its application to Lingxian Region in north China. *Remote Sensing for Environmental Monitoring, GIS Applications, and Geology VI*, *6366*, 636618. https://doi.org/10.1117/12.689310

Quintano, C., Fernández-Manso, A., Calvo, L., Marcos, E., & Valbuena, L. (2015). Land surface temperature as potential indicator of burn severity in forest Mediterranean ecosystems. *International Journal of Applied Earth Observation and Geoinformation*, *36*, 1–12. https://doi.org/10.1016/j.jag.2014.10.015

Ranagalage, M., Estoque, R. C., & Murayama, Y. (2017). An urban heat island study of the Colombo Metropolitan Area, Sri Lanka, based on Landsat data (1997-2017). *ISPRS International Journal of Geo-Information*, *6*(7). https://doi.org/10.3390/ijgi6070189

Ranagalage, M., Estoque, R. C., Zhang, X., & Murayama, Y. (2018). Spatial changes of urban heat island formation in the Colombo District, Sri Lanka: Implications for sustainability planning. *Sustainability (Switzerland)*, *10*(5). https://doi.org/10.3390/su10051367

Reacher, M., McKenzie, K., Lane, C., Nichols, T., Kedge, I., Iversen, A., Hepple, P., Walter, T., Laxton, C., & Simpson, J. (2004). Health impacts of flooding in Lewes: a comparison of reported gastrointestinal and other illness and mental health in flooded and non-flooded households. *Communicable Disease and Public Health / PHLS*, *7*(1), 39–46.

Regasa, M. S., Nones, M., & Adeba, D. (2021). Ethiopian Basins. *Land*, *10*(585), 1–18.

Rehman, A., Ma, H., Radulescu, M., Sinisi, C. I., Paunescu, L. M., Alam, S., & Alvarado, R. (2021). The Energy Mix Dilemma and Environmental Sustainability : *Energies*, *14*(7703), 1–21.

Reusch, D. B., Alley, R. B., & Hewitson, B. C. (2005). Relative performance of self-organizing maps and principal component analysis in pattern extraction from synthetic climatological data. *Polar Geography*, *29*(3), 188–212. https://doi.org/10.1080/789610199

Richman, M. B. (1981). *Obliquely Rotatted Principal Components: An Improved Meteorological Map Typing Technique?*

Richman, M. B., & Lamb, P. J. (1985). Climatic pattern analysis of three- and seven-day summer

rainfall in the central United States: some methodological considerations and a regionalization. *Journal of Climate & Applied Meteorology*, *24*(12), 1325–1343. https://doi.org/10.1175/1520-0450(1985)024<1325:CPAOTA>2.0.CO;2

Rogelj, J., & Schleussner, C. F. (2019). Reply to Comment on "Unintentional unfairness when applying new greenhouse gas emissions metrics at country level." *Environmental Research Letters*, *16*(6). https://doi.org/10.1088/1748-9326/ac02ec

Rolkier, G. G., & Worku, H. (2015). *The International Journal of Science & Technoledge Climate Change Mitigation and Adaptation Planning in Addis Ababa City*. *3*(9), 1–8.

Romero, P. (2008). *Urban Areas and Climate Change: Review of Current Issues and Trends*. *11*(2), 10–14. https://doi.org/10.16194/j.cnki.31-1059/g4.2011.07.016

Romero, P. (2011). *Urban Areas and Climate Change: Review of Current Issues and Trends*. *December 2008*.

Rosell, S. (2011). Regional perspective on rainfall change and variability in the central highlands of Ethiopia, 1978-2007. *Applied Geography*, *31*(1), 329–338. https://doi.org/10.1016/j.apgeog.2010.07.005

Rosenzweig, C., Hammer, S. A., Solecki, W. D., & Mehrotra, S. (2011a). Climate change and cities. *Built Environment*, *33*(1), 5–9. https://doi.org/10.2148/benv.33.1.5

Rosenzweig, C., Hammer, S. A., Solecki, W. D., & Mehrotra, S. (2011b). *Climate Change and Cities First Assessment Report of the Urban Climate Change Research Network*.

Rousta, I., Sarif, M. O., Gupta, R. D., Olafsson, H., Ranagalage, M., Murayama, Y., Zhang, H., & Mushore, T. D. (2018). Spatiotemporal analysis of land use/land cover and its effects on surface urban heat Island using landsat data: A case study of Metropolitan City Tehran (1988-2018). *Sustainability (Switzerland)*, *10*(12). https://doi.org/10.3390/su10124433

Rushayati, S. B., Prasetyo, L. B., Puspaningsih, N., & Rachmawati, E. (2016). Adaptation Strategy Toward Urban Heat Island at Tropical Urban Area. *Procedia Environmental Sciences*, *33*(in 1997), 221–229. https://doi.org/10.1016/j.proenv.2016.03.073

Ryu, J., Kim, M., Cha, K.-J., Lee, T. H., & Choi, D.-H. (2002). *Kriging Interpolation Methods in Geostatistics and DACE Model*. *16*(5), 619–632.

Sahana, M., Hong, H., & Sajjad, H. (2018). Analyzing urban spatial patterns and trend of urban growth using urban sprawl matrix: A study on Kolkata urban agglomeration, India. *Science of the Total Environment*, *628–629*, 1557–1566. https://doi.org/10.1016/j.scitotenv.2018.02.170

Sahoo, S., Swain, S., Goswami, A., Sharma, R., & Pateriya, B. (2021). Assessment of trends and multi-decadal changes in groundwater level in parts of the Malwa region, Punjab, India. *Groundwater for Sustainable Development*, *14*(October 2020), 100644. https://doi.org/10.1016/j.gsd.2021.100644

Samson Warkaye, K.V. Suryabhagavan, B. S. (2018). Urban Green Areas to Mitigate Urban Heat Island Effect: The Case of Addis Ababa, Ethiopia. *International Journal of Ecology and Environmental Sciences*, *44*(4), 353−367.

Sang, Y. F., Wang, Z., & Liu, C. (2014). Comparison of the MK test and EMD method for trend identification in hydrological time series. *Journal of Hydrology*, *510*, 293–298. https://doi.org/10.1016/j.jhydrol.2013.12.039

Santamouris, M. (2015). Analyzing the heat island magnitude and characteristics in one hundred Asian and Australian cities and regions. *Science of the Total Environment*, *512–513*, 582–598. https://doi.org/10.1016/j.scitotenv.2015.01.060

Sari, D. P. (2021). A Review of How Building Mitigates the Urban Heat Island in Indonesia and Tropical Cities. *Earth (Switzerland)*, *2*(3), 653–666. https://doi.org/10.3390/earth2030038

Sarif, M. O., Rimal, B., & Stork, N. E. (2020). Assessment of changes in land use/land cover and land surface temperatures and their impact on surface Urban heat Island phenomena in the Kathmandu Valley (1988–2018). *ISPRS International Journal of Geo-Information*, *9*(12). https://doi.org/10.3390/ijgi9120726

Sarkodie, S. A., & Strezov, V. (2019). Effect of foreign direct investments, economic development and energy consumption on greenhouse gas emissions in developing countries.

Science of the Total Environment, *646*, 862–871. https://doi.org/10.1016/j.scitotenv.2018.07.365

Satterthwaite, D. (2008a). Cities' contribution to global warming: Notes on the allocation of greenhouse gas emissions. *Environment and Urbanization*, *20*(2), 539–549. https://doi.org/10.1177/0956247808096127

Satterthwaite, D. (2008b). Climate Change and Urbanization: Effects and Impliactions for Urban Governance. *United Nations Expert Group Meeting on Population Distribution, Urbanization, Internatl Migration and Development. New York , 21-23 January 2008.*, *December 2007*, 29. http://www.un.org/esa/population/meetings/EGM_PopDist/P16_Satterthwaite.pdf

Satterthwaite, D. (2017). The impact of urban development on risk in sub-Saharan Africa's cities with a focus on small and intermediate urban centres. *International Journal of Disaster Risk Reduction*, *26*(September), 16–23. https://doi.org/10.1016/j.ijdrr.2017.09.025

Schau-Noppel, H., Kossmann, M., & Buchholz, S. (2020). Meteorological information for climate-proof urban planning - The example of KLIMPRAX. *Urban Climate*, *32*(April 2019), 100614. https://doi.org/10.1016/j.uclim.2020.100614

Seifu, S., & Stellmacher, T. (2021). Accessibility of public recreational parks in Addis Ababa, Ethiopia: A GIS based analysis at sub-city level. *Urban Forestry and Urban Greening*, *57*(March 2020), 126916. https://doi.org/10.1016/j.ufug.2020.126916

Sekertekin, A., & Bonafoni, S. (2020). Land surface temperature retrieval from Landsat 5, 7, and 8 over rural areas: Assessment of different retrieval algorithms and emissivity models and toolbox implementation. *Remote Sensing*, *12*(2). https://doi.org/10.3390/rs12020294

Seleshi, Y., & Camberlin, P. (2006). Recent changes in dry spell and extreme rainfall events in Ethiopia. *Theoretical and Applied Climatology*, *83*(1–4), 181–191. https://doi.org/10.1007/s00704-005-0134-3

Seleshi, Y., & Zanke, U. (2004). Recent changes in rainfall and rainy days in Ethiopia. *International Journal of Climatology*, *24*(8), 973–983. https://doi.org/10.1002/joc.1052

Sen, P. K. (1968). Estimates of the Regression Coefficient Based on Kendall's Tau. *Journal of the American Statistical Association*, *63*(324), 1379–1389. https://doi.org/10.1080/01621459.1968.10480934

Seto, K. C., Güneralp, B., & Hutyra, L. R. (2012). *Global forecasts of urban expansion to 2030 and direct impacts on biodiversity and carbon pools*. https://doi.org/10.1073/pnas.1211658109

Shadmani, M., Marofi, S., & Roknian, M. (2012). Trend Analysis in Reference Evapotranspiration Using Mann-Kendall and Spearman's Rho Tests in Arid Regions of Iran. *Water Resources Management*, *26*(1), 211–224. https://doi.org/10.1007/s11269-011-9913-z

Shahfahad, Kumari, B., Tayyab, M., Ahmed, I. A., Razi, M., & Baig, I. (2020). *Longitudinal study of land surface temperature (LST) using mono- and split-window algorithms and its relationship with NDVI and NDBI over selected metro cities of India*.

Shen, X., Wang, X., Zhang, Z., Lu, Z., & Lv, T. (2019). Evaluating the effectiveness of land use plans in containing urban expansion: An integrated view. *Land Use Policy*, *80*(September 2018), 205–213. https://doi.org/10.1016/j.landusepol.2018.10.001

Short, J. R., & Farmer, A. (2021). Cities and Climate Change. *Earth (Switzerland)*, *2*(4), 1038–1045. https://doi.org/10.3390/earth2040061

Sibiya, N., Sithole, M., Mudau, L., & Simatele, M. D. (2022). *Empowering the Voiceless : Securing the Participation of Marginalised Groups in Climate Change Governance in South Africa*.

Sidiropoulos, M. (2023). *Ten theories of climate change*. *November*.

Signorino, C. S., & Ritter, J. M. (1999). Tau-b or not Tau-b: Measuring the similarity of foreign policy positions. *International Studies Quarterly*, *43*(1), 115–144. https://doi.org/10.1111/0020-8833.00113

Simone, G. De, Janeiro, R. De, Toronto, T. D., Jack, D., York, N., Toronto, J. P., & Rahman, M. (2011). Climate change and human health in cities Coordinating Lead Authors : Lead

Authors : *Cities And Climate Change - First Assessment Report of the Urban Climate Change Research Network*, 179–213.

Simwanda, M., & Murayama, Y. (2018). Spatiotemporal patterns of urban land use change in the rapidly growing city of Lusaka, Zambia: Implications for sustainable urban development. *Sustainable Cities and Society*, *39*, 262–274. https://doi.org/10.1016/j.scs.2018.01.039

Simwanda, M., Ranagalage, M., Estoque, R. C., & Murayama, Y. (2019). Spatial analysis of surface urban heat Islands in four rapidly growing african cities. *Remote Sensing*, *11*(14), 1–20. https://doi.org/10.3390/rs11141645

Skinner, B. J., & Murck, B. W. (2011). *The Blue Planet An Introduction to Earth System Science*.

Skoulika, F., Santamouris, M., Kolokotsa, D., & Boemi, N. (2014). Landscape and Urban Planning On the thermal characteristics and the mitigation potential of a medium size urban park in Athens , Greece. *Landscape and Urban Planning*, *123*, 73–86. https://doi.org/10.1016/j.landurbplan.2013.11.002

Sluiter, R. (2009). Interpolation methods for climate data literature review. *Intern*, *August*, 2009–4.

Sobrino, J. A., Jimenez-Munoz, J. C., & Paolini, L. (2004). Land surface temperature retrieval from LANDSAT TM 5. *Remote Sensing of Environment*, *90*(4), 434–440. https://doi.org/10.1016/j.rse.2004.02.003

Sobrino, J. A., Raissouni, N., & Li, Z. L. (2001). A comparative study of land surface emissivity retrieval from NOAA data. *Remote Sensing of Environment*, *75*(2), 256–266. https://doi.org/10.1016/S0034-4257(00)00171-1

Sonali, P., & Nagesh Kumar, D. (2013). Review of trend detection methods and their application to detect temperature changes in India. *Journal of Hydrology*, *476*, 212–227. https://doi.org/10.1016/j.jhydrol.2012.10.034

Staddon, C., Ward, S., De Vito, L., Zuniga-Teran, A., Gerlak, A. K., Schoeman, Y., Hart, A., & Booth, G. (2018). Contributions of green infrastructure to enhancing urban resilience.

Environment Systems and Decisions, *38*(3), 330–338. https://doi.org/10.1007/s10669-018-9702-9

Stein, A., & Moser, C. (2014). *Asset planning for climate change adaptation : Lessons from Cartagena , Asset planning for climate change adaptation : lessons from Cartagena , Colombia*. *January 2016*. https://doi.org/10.1177/0956247813519046

Stemn, E., & Kumi-Boateng, B. (2020). Modelling of land surface temperature changes as determinant of urban heat island and risk of heat-related conditions in the Wassa West Mining Area of Ghana. *Modeling Earth Systems and Environment*, *6*(3), 1727–1740. https://doi.org/10.1007/s40808-020-00786-x

Stern, N. (2007). The economics of climate change: The stern review. *The Economics of Climate Change: The Stern Review*, *9780521877*, 1–692. https://doi.org/10.1017/CBO9780511817434

Sun, Q., Wu, Z., & Tan, J. (2012). The relationship between land surface temperature and land use/land cover in Guangzhou, China. *Environmental Earth Sciences*, *65*(6), 1687–1694. https://doi.org/10.1007/s12665-011-1145-2

Suryavanshi, S., Pandey, A., Chaube, U. C., & Joshi, N. (2014). Long-term historic changes in climatic variables of Betwa Basin, India. *Theoretical and Applied Climatology*, *117*(3–4), 403–418. https://doi.org/10.1007/s00704-013-1013-y

Swain, S., Mishra, S. K., & Pandey, A. (2021). A detailed assessment of meteorological drought characteristics using simplified rainfall index over Narmada River Basin, India. *Environmental Earth Sciences*, *80*(6), 1–15. https://doi.org/10.1007/s12665-021-09523-8

Swain, S., Mishra, S. K., & Pandey, A. (2022). Assessing spatiotemporal variation in drought characteristics and their dependence on timescales over Vidarbha Region, India. *Geocarto International*, *37*(27), 17971–17993. https://doi.org/10.1080/10106049.2022.2136260

Swain, S., Mishra, S. K., Pandey, A., & Dayal, D. (2022a). Assessment of drought trends and variabilities over the agriculture-dominated Marathwada Region, India. *Environmental Monitoring and Assessment*, *194*(12). https://doi.org/10.1007/s10661-022-10532-8

Swain, S., Mishra, S. K., Pandey, A., & Dayal, D. (2022b). Spatiotemporal assessment of precipitation variability, seasonality, and extreme characteristics over a Himalayan catchment. *Theoretical and Applied Climatology*, *147*(1–2), 817–833. https://doi.org/10.1007/s00704-021-03861-0

Tabios, G. Q., & Salas, J. D. (1986). *A Comparative Analysis of Techniques for Spatial Interpolation of Precipitation ’*. *21*(3).

Tadić, L., Bonacci, O., & Brleković, T. (2019). An example of principal component analysis application on climate change assessment. *Theoretical and Applied Climatology*, *138*(1–2), 1049–1062. https://doi.org/10.1007/s00704-019-02887-9

Tafesse, B., & Suryabhagavan, K. V. (2019). Systematic modeling of impacts of land-use and land-cover changes on land surface temperature in Adama Zuria District, Ethiopia. *Modeling Earth Systems and Environment*, *5*(3), 805–817. https://doi.org/10.1007/s40808-018-0567-1

Taha, H. (1997). Urban climates and heat islands: Albedo, evapotranspiration, and anthropogenic heat. *Energy and Buildings*, *25*(2), 99–103. https://doi.org/10.1016/s0378-7788(96)00999-1

Tan, K. C., Lim, H. S., MatJafri, M. Z., & Abdullah, K. (2010). Landsat data to evaluate urban expansion and determine land use/land cover changes in Penang Island, Malaysia. *Environmental Earth Sciences*, *60*(7), 1509–1521. https://doi.org/10.1007/s12665-009-0286-z

Tariq, A., & Mumtaz, F. (2023a). A series of spatio-temporal analyses and predicting modeling of land use and land cover changes using an integrated Markov chain and cellular automata models. *Environmental Science and Pollution Research*, *30*(16), 47470–47484. https://doi.org/10.1007/s11356-023-25722-1

Tariq, A., & Mumtaz, F. (2023b). Modeling spatio-temporal assessment of land use land cover of Lahore and its impact on land surface temperature using multi-spectral remote sensing data. *Environmental Science and Pollution Research*, *30*(9), 23908–23924. https://doi.org/10.1007/s11356-022-23928-3

Tariq, A., & Shu, H. (2020). CA-Markov chain analysis of seasonal land surface temperature and land use landcover change using optical multi-temporal satellite data of Faisalabad, Pakistan. *Remote Sensing*, *12*(20), 1–23. https://doi.org/10.3390/rs12203402

Taylor, P. C., Fahey, D., & Doherty, S. (2020). *DigitalCommons @ University of Nebraska - Lincoln Physical drivers of climate change*. *January 2017*.

Teferi, E., & Abraha, H. (2017a). Urban Heat Island Effect of Addis Ababa City: Implications of Urban Green Spaces for Climate Change Adaptation. *Climate Change Management*, *January*, 539–552. https://doi.org/10.1007/978-3-319-49520-0_33

Teferi, E., & Abraha, H. (2017b). Urban Heat Island Effect of Addis Ababa City: Implications of Urban Green Spaces for Climate Change Adaptation. *Climate Change Adaptation in Africa*, 205–215. https://doi.org/10.1007/978-3-319-49520-0

Terfa, B. K., Chen, N., Liu, D., Zhang, X., & Niyogi, D. (2019). Urban expansion in Ethiopia from 1987 to 2017: Characteristics, spatial patterns, and driving forces. *Sustainability (Switzerland)*, *11*(10), 1–21. https://doi.org/10.3390/su11102973

Tessema, Y. A., Aweke, C. S., & Endris, G. S. (2013). *Understanding the process of adaptation to climate change by small-holder farmers : the case of east Hararghe Zone , Ethiopia*. *May 2016*, 1. https://doi.org/10.1186/2193-7532-1-13

The World Bank Group. (2015). *Shock waves: Managing the Impacts of Climate Change on Poverty*.

Thornton, P., Jones, P., Owiyo, T., Kruska, R., Herrero, M., Kristjanson, P., Notenbaert, a, Bekele, N., & Omolo, a. (2006). Mapping climate vulnerability and poverty in Africa. *Report to the Department for International Development ILRI PO Box*, *30709*(January 2014), 171. http://0-search.ebscohost.com.catalog.library.colostate.edu/login.aspx?direct=true&AuthType=cookie,ip,url,cpid&custid=s4640792&db=lah&AN=20073285958&site=ehost-live

Trisos, C. H., Adelekan, I. O., Totin, E., Ayanlade, A., Efitre, J., Gemeda, A., Kalaba, K., Lennard, C., Masao, C., Mgaya, Y., Ngaruiya, G., Olago, D., Simpson, N. P., & Zakieldeen,

S. (2022). *Climate Change 2022: Impacts, Adaptation and Vulnerability* (Vol. 01). https://doi.org/10.1017/9781009325844.011.1286

Tsidu, G. M. (2012). High-resolution monthly rainfall database for Ethiopia: Homogenization, reconstruction, and gridding. *Journal of Climate*, *25*(24), 8422–8443. https://doi.org/10.1175/JCLI-D-12-00027.1

Tsutsumida, N., & Comber, A. J. (2015). Measures of spatio-temporal accuracy for time series land cover data. *International Journal of Applied Earth Observation and Geoinformation*, *41*(February), 46–55. https://doi.org/10.1016/j.jag.2015.04.018

Tupėnaitė, L., Žilėnaitė, V., Kanapeckienė, L., Sajjadian, S. M., Gečys, T., Sakalauskienė, L., & Naimavičienė, J. (2020). *Multiple Criteria Assessment of High-Rise Timber Buildings*. *11*(3), 87–94.

Tyfield, D., & Yuille, A. (2022). *Introduction to the Special Issue " Bringing Governance Back Home : Lessons for Local Government Regarding Rapid Climate Action ."*

Ullah, M., Li, J., & Wadood, B. (2020). Analysis of Urban Expansion and its Impacts on Land Surface Temperature and Vegetation Using RS and GIS, A Case Study in Xi'an City, China. *Earth Systems and Environment*, *4*(3), 583–597. https://doi.org/10.1007/s41748-020-00166-6

Ullah, W., Ahmad, K., Ullah, S., Tahir, A. A., Javed, M. F., Nazir, A., Abbasi, A. M., Aziz, M., & Mohamed, A. (2023). Analysis of the relationship among land surface temperature (LST), land use land cover (LULC), and normalized difference vegetation index (NDVI) with topographic elements in the lower Himalayan region. *Heliyon*, *9*(2), e13322. https://doi.org/10.1016/j.heliyon.2023.e13322

UN-Habitat. (2011a). Cities and Climate Change: Global Report on Human Settlements 2011. In *The Town Planning Review* (Vol. 83, Issue 4). http://search.proquest.com/docview/1024808703?accountid=6802%5Cnhttp://sfx-82snu.hosted.exlibrisgroup.com/sfxsnu?url_ver=Z39.88-2004&rft_val_fmt=info:ofi/fmt:kev:mtx:journal&genre=unknown&sid=ProQ:ProQ:abiglobal&atitle=Cities+and+Climate+Change+(Global+

UN-Habitat. (2011b). *Cities and Climate Change: PoliCy direCtions*.

UN-Habitat. (2022). *Envisaging the Future of Cities*.

UN-Habitate. (2011). *Cities and Climate Change: Policy Directions Global Report on Human Settlements 2011*.

UN. (2014). Cities and climate change: national governments enabling local action. *Change*, 276. https://www.oecd.org/env/cc/Cities-and-climate-change-2014-Policy-Perspectives-Final-web.pdf%5Cn

UNECA. (2022). *Africa ' s Urbanisation Dynamics 2022 The Economic Power of Africa's Cities*.

UNEP. (2013). *Africa 's Adaptation Gap: Technical Report*. *November*, 58. http://wedocs.unep.org/handle/20.500.11822/8376

UNFCCC. (2007). *Climate Change: Impacts, Vulnerabilities and Adaptation in Developing Countries*.

Unger, J. (2004). Intra-urban relationship between surface geometry and urban heat island: Review and new approach. *Climate Research*, *27*(3), 253–264. https://doi.org/10.3354/cr027253

United Nations. (2009). The impact of climate change on the development prospects of the least developed countries and small island developing states. *Un-Ohrlls*, *116*(3), 1–51. http://www.itc.nl/library/Papers/msc_2002/ereg/tang_yanli.pdf%5Cnhttp://www.victoria.ac.nz/sgees/research-centres/documents/vulnerability-and-adaptation-to-sea-level-rise-in-auckland-new-zealand.pdf%5Cnhttp://eprints.soton.ac.uk/53242/%5Cnhttp://essential

United Nations. (2014). *World Urbanization Prospects: The 2014 Revision*.

United Nations. (2017). World Populatio Prospects: The 2017 Revision, Key Findings and Advance Tables. In *Jurnal Penelitian Pendidikan Guru Sekolah Dasar* (Vol. 6, Issue August, p. 128).

United Nations. (2022). The Sustainable Development Goals Report 2019. *United Nations*

Publication Issued by the Department of Economic and Social Affairs, 64. https://unstats.un.org/sdgs/report/2022/%0Ahttps://www.un-ilibrary.org/content/books/9789210018098%0Ahttps://www.un-ilibrary.org/content/books/9789210478878

USAID. (2016). *Climate change risk profile Ethiopia - Fact Sheet*. *July*, 5. https://www.climatelinks.org/sites/default/files/asset/document/2016 CRM Factsheet - Ethiopia_use this.pdf

USGS. (2015). LANDSAT 8 (L8) DATA USERS HANDBOOK Version 1.0 June 2015. *United States Geological Survey*, *1*(June), 1–106.

USGS. (2019). Landsat 8 Data Users Handbook. *Nasa*, *8*(November), 114.

van der Linden, S., Panagopoulos, C., Azevedo, F., & Jost, J. T. (2021). The Paranoid Style in American Politics Revisited: An Ideological Asymmetry in Conspiratorial Thinking. *Political Psychology*, *42*(1), 23–51. https://doi.org/10.1111/pops.12681

Verburg, P. H., Crossman, N., Ellis, E. C., Heinimann, A., Hostert, P., Mertz, O., Nagendra, H., Sikor, T., Erb, K., Golubiewski, N., Grau, R., Grove, M., Konaté, S., Meyfroidt, P., Parker, D. C., Roy, R., Shibata, H., Thomson, A., & Zhen, L. (2015). Anthropocene Land system science and sustainable development of the earth system : A global land project perspective. *Biochemical Pharmacology*, *12*, 29–41. https://doi.org/10.1016/j.ancene.2015.09.004

Verma, P. A., Shankar, H., & Saran, S. (2019). Comparison of Geostatistical and Deterministic Interpolation to Derive Climatic Surfaces for Mountain Ecosystem. *Remote Sensing of Northwest Himalayan Ecosystems*, 537–547. https://doi.org/10.1007/978-981-13-2128-3_24

Vose, R. S., Arndt, D., Banzon, V. F., Easterling, D. R., Gleason, B., Huang, B., Kearns, E., Lawrimore, J. H., Menne, M. J., Peterson, T. C., Reynolds, R. W., Smith, T. M., Jr, C. N. W., & Wuertz, D. B. (2012). *NOAA's merged land-ocean surface temperature analysis*. *November*, 1677–1686.

Wackernagel, H. (2003). *Multivariate Geostatistics: An Introduction with Applications*. https://www.ptonline.com/articles/how-to-get-better-mfi-results

Wagesho, N., Goel, N. K., & Jain, M. K. (2013). Variabilité temporelle et spatiale des précipitations annuelles et saisonnières sur l'Ethiopie. *Hydrological Sciences Journal*, *58*(2), 354–373. https://doi.org/10.1080/02626667.2012.754543

Walsh, J. E. (1978). *Temporal and Spatial Scales of the Arctic Circulation*.

Wang, F., Qin, Z., Song, C., Tu, L., Karnieli, A., & Zhao, S. (2015). An improved mono-window algorithm for land surface temperature retrieval from landsat 8 thermal infrared sensor data. *Remote Sensing*, *7*(4), 4268–4289. https://doi.org/10.3390/rs70404268

Wang, F., Shao, W., Yu, H., Kan, G., He, X., Zhang, D., Ren, M., & Wang, G. (2020). Re-evaluation of the Power of the Mann-Kendall Test for Detecting Monotonic Trends in Hydrometeorological Time Series. *Frontiers in Earth Science*, *8*(February), 1–12. https://doi.org/10.3389/feart.2020.00014

Wang, S., Zuo, H., Yin, Y., Hu, C., Yin, J., Ma, X., & Wang, J. (2019). Interpreting Rainfall Anomalies Using Rainfall's Nonnegative Nature. *Geophysical Research Letters*, *46*(1), 426–434. https://doi.org/10.1029/2018GL081190

Wang, W., Zhang, Y., & Tang, Q. (2020). Impact assessment of climate change and human activities on streamflow signatures in the Yellow River Basin using the Budyko hypothesis and derived differential equation. *Journal of Hydrology*, *591*(June), 125460. https://doi.org/10.1016/j.jhydrol.2020.125460

Wanyama, D. (2017). *A Spatial Analysis of Climate Change Effects on Maize Productivity in Kenya*. https://ir.una.edu/gmt/1

Wardekker, A. (2021). Contrasting the framing of urban climate resilience. *Sustainable Cities and Society*, *75*(August), 103258. https://doi.org/10.1016/j.scs.2021.103258

Warkaye, S., Suryabhagavan, K. V., & Satishkumar, B. (2018). Urban Green Areas to Mitigate Urban Heat Island Effect: The Case of Addis Ababa, Ethiopia. *International Journal of Ecology and Environmental Sciences*, *44*(4), 353−367.

Wasserstein, R. L., Schirm, A. L., & Lazar, N. A. (2019). Moving to a World Beyond "p < 0.05." *American Statistician*, *73*(sup1), 1–19.

https://doi.org/10.1080/00031305.2019.1583913

Watson, R. T., Albritton, D. L., Barker, T., Bashmakov, I. A., Canziani, O., Christ, R., Cubasch, U., Davidson, O., Gitay, H., Griggs, D., Houghton, J., House, J., Kundzewicz, Z., Lal, M., Leary, N., Mccarthy, J. J., Mitchell, J. F. B., Moreira, J. R., Munasinghe, M., … Zhou, D. (2001). *Climate Change 2001 : Synthesis Report Climate Change 2001 : Synthesis Report*.

Webster, R., & Oliver, M. A. (2007). *Geostatistics for Environmental Scientists*.

Weldegerima, T. M., Zeleke, T. T., Birhanu, B. S., Zaitchik, B. F., & Fetene, Z. A. (2018). *Analysis of Rainfall Trends and Its Relationship with SST Signals in the Lake Tana Basin , Ethiopia*. *2018*.

Weng, Q., & Lo, C. P. (2001). Spatial analysis of urban growth impacts on vegetative greenness with Landsat TM data. *Geocarto International*, *16*(4), 19–28. https://doi.org/10.1080/10106040108542211

Weng, Q., Lu, D., & Schubring, J. (2004). Estimation of land surface temperature-vegetation abundance relationship for urban heat island studies. *Remote Sensing of Environment*, *89*(4), 467–483. https://doi.org/10.1016/j.rse.2003.11.005

West, T. O., & Marland, G. (2002). A synthesis of carbon sequestration, carbon emissions, and net carbon flux in agriculture: Comparing tillage practices in the United States. *Agriculture, Ecosystems and Environment*, *91*(1–3), 217–232. https://doi.org/10.1016/S0167-8809(01)00233-X

WHO. (2013). *Protecting Health from Climate Change*.

Wicaksana, A., & Rachman, T. (1979). Anthropogenic Albedo Chnages and the Earth's Climate. *Angewandte Chemie International Edition, 6(11), 951–952.*, *3*(1), 10–27. https://medium.com/@arifwicaksanaa/pengertian-use-case-a7e576e1b6bf

Wigginton, B. N. S., Fahrenkamp-uppenbrink, J., Wible, B., & Malakoff, D. (2016). *Cities are the Future*. *352*(6288), 904–906.

Wilby, R. L., & Dawson, C. W. (2013). *The Statistical DownScaling Model : insights from one*

decade. *1719*(July 2012), 1707–1719. https://doi.org/10.1002/joc.3544

Williams, A. P., Funk, C., Michaelsen, J., Rauscher, S. A., Robertson, I., Wils, T. H. G., Koprowski, M., Eshetu, Z., & Loader, N. J. (2012). Recent summer precipitation trends in the Greater Horn of Africa and the emerging role of Indian Ocean sea surface temperature. *Climate Dynamics*, *39*(9–10), 2307–2328. https://doi.org/10.1007/s00382-011-1222-y

WMO. (2023). Guidelines on the Defintion and Characterization of Extreme Weather and Climate Events. In *Wmo* (Issue 1310).

Woldegerima, T., Yeshitela, K., & Lindley, S. (2016). Characterizing the urban environment through urban morphology types (UMTs) mapping and land surface cover analysis : the case of Addis Ababa , Ethiopia. *Urban Ecosystems*. https://doi.org/10.1007/s11252-016-0590-9

Wolfram, M., Heijden, J. Van Der, Juhola, S., & Patterson, J. (2019). *Learning in urban climate governance : concepts , key issues and challenges*. *7200*. https://doi.org/10.1080/1523908X.2018.1558848

Worku, G., Teferi, E., & Bantider, A. (2021a). Assessing the effects of vegetation change on urban land surface temperature using remote sensing data: The case of Addis Ababa city, Ethiopia. *Remote Sensing Applications: Society and Environment*, *22*(September 2020), 100520. https://doi.org/10.1016/j.rsase.2021.100520

Worku, G., Teferi, E., & Bantider, A. (2021b). Remote Sensing Applications : Society and Environment Assessing the effects of vegetation change on urban land surface temperature using remote sensing data : The case of Addis Ababa city , Ethiopia. *Remote Sensing Applications: Society and Environment*, *22*(May), 100520. https://doi.org/10.1016/j.rsase.2021.100520

Worku, H. (2017). *Integrating climate change adaptation strategies in urban planning and landscape design of Addis Ababa City , Ethiopia Using urban planning and landscape design to mitigate flooding , drought , and urban heat island effects*. 5–21. https://doi.org/10.1002/tqem.21514

World Bank. (2009). Making Development Climate Resilient. A World Bank Strategy for Sub-Saharan Africa. *Report No. 46947-AFR*, *46947*, 144. https://doi.org/10.1007/s12010-014-1375-3

World Bank. (2010). *Economics of Adaptation to Climate Change Ethiopia.* 1–124. http://documents.worldbank.org/curated/en/2010/01/16279299/economics-adaptation-climate-change-ethiopia

World Bank. (2011). Guide to Climate Change Adaptation in Cities. *Guide to Climate Change Adaptation in Cities*. https://doi.org/10.1596/27396

World Bank Group. (2015). *Enhancing Urban Resilience*. *July*.

World Bank Group. (2017). *Atlas of Sustainable Development Goals*.

World Bank Group. (2019). *Disaster Risk Profile for Ethiopia*.

World Bank Group. (2020). *Demographic trends and urbanization*.

World Bank Group. (2021a). Climate Risk country profile: Ethiopia. *World Bank Group*, *3*(4), 1–32. www.worldbank.org

World Bank Group. (2021b). Climate Risk Country Profile: Uganda. *The World Bank Group*, 36. www.worldbank.org

World Meteorological Organization. (1966). *Climate Change*.

Xie, B., Brewer, M. B., Hayes, B. K., McDonald, R. I., & Newell, B. R. (2019). Predicting climate change risk perception and willingness to act. *Journal of Environmental Psychology*, *65*, 101331. https://doi.org/10.1016/j.jenvp.2019.101331

Yadav, R., S.K.Tripathi, G.Pranuthi, & S.K.Dubey. (2014). Trend analysis by Mann-Kendall test for precipitation and temperature for thirteen districts of Uttarakhand. *Journal of Agrometeorology*, *16*(2), 164–171. https://doi.org/10.54386/jam.v16i2.1507

Yang, D., Dong, Z., Lim, L. H. I., & Liu, L. (2017). Analyzing big time series data in solar engineering using features and PCA. *Solar Energy*, *153*, 317–328.

https://doi.org/10.1016/j.solener.2017.05.072

Yang, J. S., Wang, Y. Q., & August, P. V. (2004). *Estimation of Land Surface Temperature Using Spatial Interpolation and Satellite-Derived Surface Emissivity*. 89–96.

Yeneneh, N., Elias, E., & Feyisa, G. L. (2022). Detection of land use/land cover and land surface temperature change in the Suha Watershed, North-Western highlands of Ethiopia. *Environmental Challenges*, *7*(April), 100523. https://doi.org/10.1016/j.envc.2022.100523

Yuan, F., & Bauer, M. E. (2007). Comparison of impervious surface area and normalized difference vegetation index as indicators of surface urban heat island effects in Landsat imagery. *Remote Sensing of Environment*, *106*(3), 375–386. https://doi.org/10.1016/j.rse.2006.09.003

Yuan, Y., Yang, K., Cheng, L., Bai, Y., Wang, Y., Hou, Y., & Ding, A. (2022). Effect of Normalization Methods on Accuracy of Estimating Low- and High-Molecular Weight PAHs Distribution in the Soils of a Coking Plant. *International Journal of Environmental Research and Public Health*, *19*(23). https://doi.org/10.3390/ijerph192315470

Yue, S., Pilon, P., & Cavadias, G. (2002). *Power of the Mann ± Kendall and Spearman ' s rho tests for detecting monotonic trends in hydrological series*. *259*, 254–271.

Zare, M., Drastig, K., & Zude-Sasse, M. (2020). Tree water status in apple orchards measured by means of land surface temperature and vegetation index (LST-NDVI) trapezoidal space derived from landsat 8 satellite images. *Sustainability (Switzerland)*, *12*(1), 1–19. https://doi.org/10.3390/SU12010070

Zegeye, M. K., Bekitie, K. T., & Hailu, D. N. (2022). Spatio - temporal variability and trends of hydroclimatic variables at Zarima Sub - Basin North Western Ethiopia. *Environmental Systems Research*, *5*. https://doi.org/10.1186/s40068-022-00273-5

Zgłobicki, W., Telecka, M., Skupiński, S., Pasierbińska, A., & Kozieł, M. (2018). Assessment of heavy metal contamination levels of street dust in the city of Lublin, E Poland. *Environmental Earth Sciences*, *77*(23), 1–11. https://doi.org/10.1007/s12665-018-7969-2

Zha, Y., Gao, J., & Ni, S. (2003). Use of normalized difference built-up index in automatically

mapping urban areas from TM imagery. *International Journal of Remote Sensing*, *24*(3), 583–594. https://doi.org/10.1080/01431160304987

Zhang, B., Yao, Y., Cheng, W., Zhou, C., Lu, Z., Chen, X., Alshir, K., ErDowlet, I., Zhang, L., & Shi, Q. (2019). *Human-Induced Changes to Biodiversity and Alpine Pastureland in the Bayanbulak Region of the East Tienshan Mountains*. *22*(4), 383–389.

Zhang, Q., Li, J., Chen, Y. D., & Chen, X. (2011). Observed changes of temperature extremes during 1960-2005 in China: Natural or human-induced variations? *Theoretical and Applied Climatology*, *106*(3–4), 417–431. https://doi.org/10.1007/s00704-011-0447-3

Zhou, D., Zhao, S., Liu, S., Zhang, L., & Zhu, C. (2014). Surface urban heat island in China's 32 major cities: Spatial patterns and drivers. *Remote Sensing of Environment*, *152*, 51–61. https://doi.org/10.1016/j.rse.2014.05.017

Zhou, X., & Wang, Y.-C. (2010a). *Dynamics of Land Surface Temperature in Response to Land-Use / Cover Change*. 23–36. https://doi.org/10.1111/j.1745-5871.2010.00686.x

Zhou, X., & Wang, Y. C. (2010b). Dynamics of Land Surface Temperature in Response to Land-Use/Cover Change. *Geographical Research*, *49*(1), 23–36. https://doi.org/10.1111/j.1745-5871.2010.00686.x

Zoulia, I., Santamouris, M., & Dimoudi, A. (2009). *Monitoring the effect of urban green areas on the heat island in Athens*. 275–292. https://doi.org/10.1007/s10661-008-0483-3

Zuśka, Z., Kopcińska, J., Dacewicz, E., Skowera, B., Wojkowski, J., & Ziernicka-Wojtaszek, A. (2019). Application of the principal component analysis (PCA) method to assess the impact of meteorological elements on concentrations of particulate matter (PM10): A case study of the mountain valley (the Sacz Basin, Poland). *Sustainability (Switzerland)*, *11*(23), 1–12. https://doi.org/10.3390/su11236740

Supplementary: list of publications

Appendix

Test result for seasonal (*Kiremt*, *Belg* and *Bega*) Tmax and Tmin

Average Kiremt Tmax		Average Kiremt Tmin	
Mean	24.84476	Mean	13.44264
Standard Error	0.236631	Standard Error	0.237959
Median	25.04986	Median	12.88525
Mode	#N/A	Mode	#N/A
Standard Deviation	1.458689	Standard Deviation	1.466879
Sample Variance	2.127773	Sample Variance	2.151734
Kurtosis	-0.39291	Kurtosis	0.010015
Skewness	0.430457	Skewness	0.622513
Range	5.378825	Range	6.5296
Minimum	22.8528	Minimum	10.3286
Maximum	28.23163	Maximum	16.8582
Sum	944.1008	Sum	510.8202
Count	38	Count	38

T-test: Two-Sample Assuming Equal Variances	*Kiremt* Tmax	*Kiremt* Tmin
Mean	24.84476	13.44264
Variance	2.127773	2.151734
Observations	38	38
Pooled Variance	2.139754	
Hypothesized Mean Difference	0	
df	74	
t Stat	33.97665	
P(T<=t) one-tail	3.42E-47	

t Critical one-tail	1.665707	
P(T<=t) two-tail	6.84E-47	
t Critical two-tail	1.992543	

The mean *kiremt* (main rainy season) max temperature (M=24.84, SD=1.459, n=38) was hypothesized to be greater than the mean *kiremt* min temperature (M=13.443, SD=1.467, n=38). The difference was significant *t* (74) =1.99, *p*=0.000 (1 tail). This means a highly statistically significant result. Since our p-value is far less than (3.42 x 10^-47), We can say our results are significant.

	Belg Tmax		*Belg* Tmin
Mean	27.82124	Mean	13.99515
Standard Error	0.298321	Standard Error	0.250468
Median	27.79788	Median	13.5262
Mode	#N/A	Mode	#N/A
Standard Deviation	1.838974	Standard Deviation	1.543991
Sample Variance	3.381825	Sample Variance	2.38391
Kurtosis	0.13223	Kurtosis	-0.39964
Skewness	0.502616	Skewness	0.751916
Range	7.910233	Range	5.9894
Minimum	25.0114	Minimum	11.8487
Maximum	32.92163	Maximum	17.8381
Sum	1057.207	Sum	531.8157
Count	38	Count	38

T-test: Two-Sample Assuming Equal Variances		
	Belg Tmax	*Belg* Tmin
Mean	27.82124	13.99515
Variance	3.381825	2.38391
Observations	38	38
Pooled Variance	2.882867	
Hypothesized Mean Difference	0	
df	74	
t Stat	35.49472	
P(T<=t) one-tail	1.62E-48	
t Critical one-tail	1.665707	
P(T<=t) two-tail	3.24E-48	
t Critical two-tail	1.992543	

The mean *Belg* (spring) max temperature (M=27.82, SD=1.839, n=38) was hypothesized to be greater than the mean *Belg* min temperature (M=13.995, SD=1.544, n=38). The difference was significant *t* (74) =1.99, *p*=0.000 (1 tail). This means a highly statistically significant result. Since our p-value is far less than (1.62 x 10^-48), We can say our results are significant.

Bega Tmax		*Bega* Tmin	
Mean	26.22857	Mean	11.62821
Standard Error	0.24994	Standard Error	0.397048
Median	26.45516	Median	10.9308
Mode	#N/A	Mode	11.928
Standard Deviation	1.540732	Standard Deviation	2.447569
Sample Variance	2.373855	Sample Variance	5.990593
Kurtosis	-0.74352	Kurtosis	-0.09224

Skewness	0.195408	Skewness	0.890426
Range	5.81296	Range	9.51799
Minimum	23.8077	Minimum	8.76551
Maximum	29.62066	Maximum	18.2835
Sum	996.6858	Sum	441.8719
Count	38	Count	38

T-test: Two-Sample Assuming Equal Variances			
	Bega Tmax	*Bega* Tmin	
Mean	26.22857	**11.62821**	
Variance	2.373855	5.990593	
Observations	38	**38**	
Pooled Variance	4.182224		
Hypothesized Mean Difference	0		
df	74		
t Stat	31.11981		
P(T<=t) one-tail	1.49E-44		
t Critical one-tail	1.665707		
P(T<=t) two-tail	2.99E-44		
t Critical two-tail	1.992543		

The mean *Bega* (dry season) max temperature (M=26.22, SD=1.541, n=38) was hypothesized to be greater than the mean *Bega* min temperature (M=13.995, SD=1.544, n=38). The difference was significant *t* (74) =1.99, *p*=0.000 (1 tail). This means a highly statistically significant result. Since our p-value is far less than (1.49 x 10^-44), We can say our results are significant.

Autocorrelation Result

The autocorrelation result was generated in R studio using modified mann-kandall package. The result revealed that there was a significant autocorrelation for all the monthly, annual, and seasonal time series maximum and minimum tempertaures except for March minimum temperature. The graph below and tables demonstrated that.

Annual and seasonal autocorrelation Tmax and Tmin

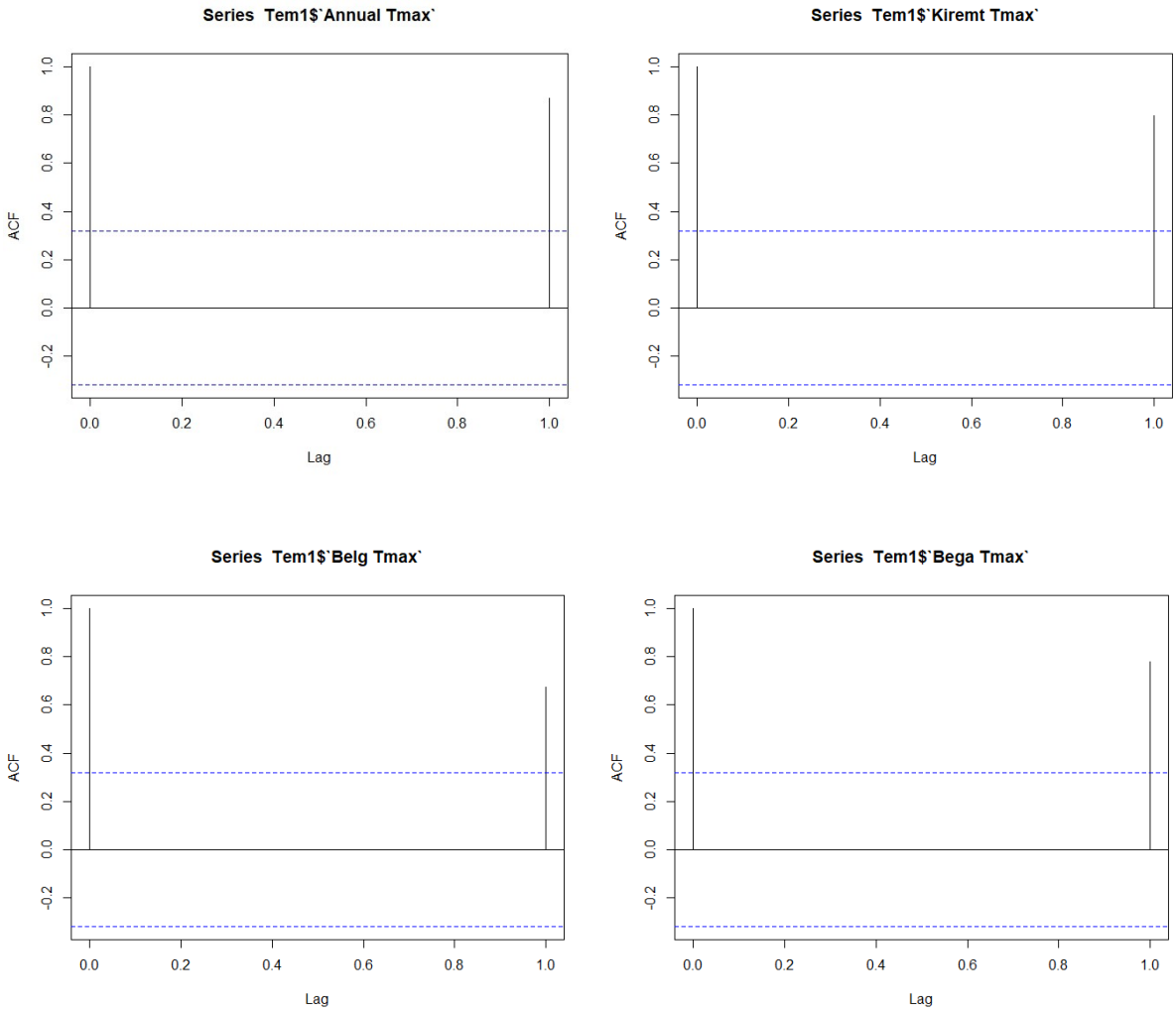

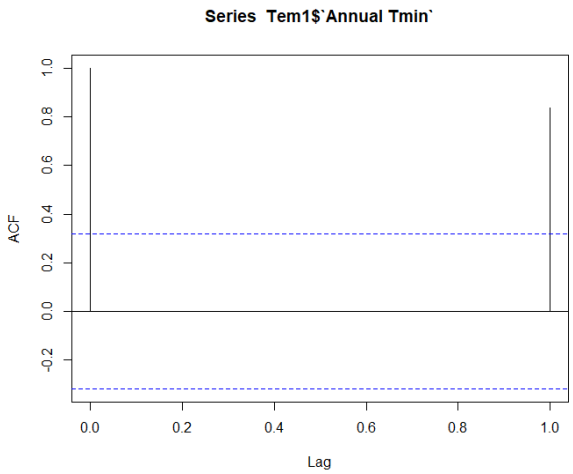

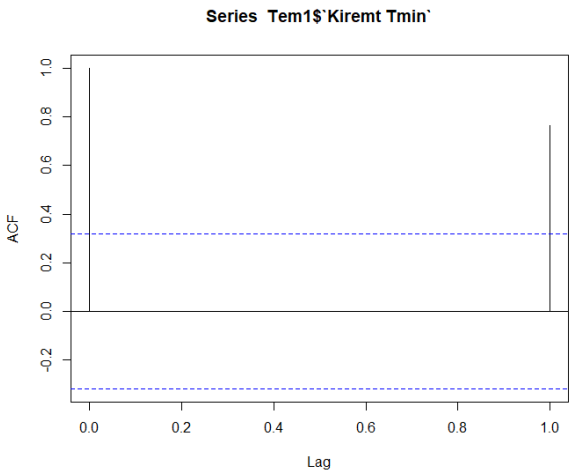

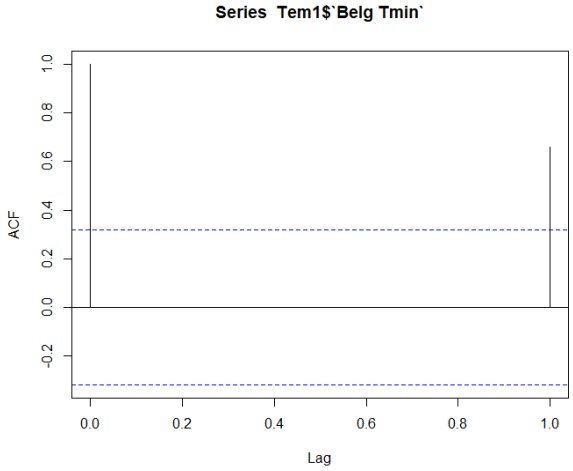

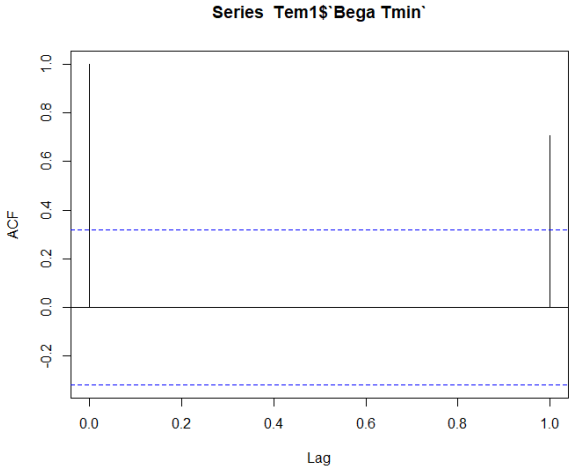

Autocorrelation result	Lag max 1
Annual Tmax	0.8692628
Annual Tmin	0.8366763
Kiremt Tmax	0.7975074
Kiremt Tmin	0.7636759

Belg Tmax	0.6729579
Belg Tmin	0.6591596
Bega Tmax	0.7802847
Bega Tmin	0.7051057

Monthly Autocorrelation result for Tmax

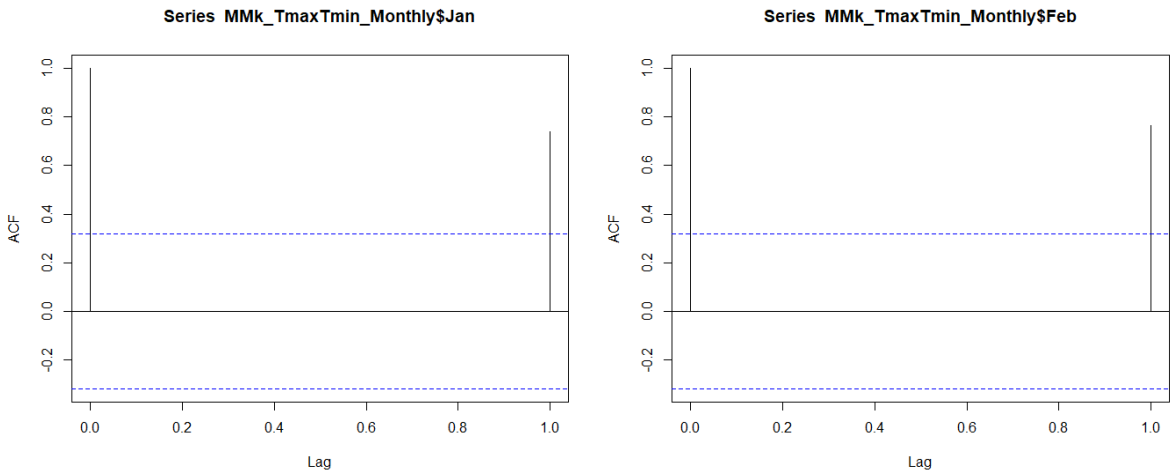

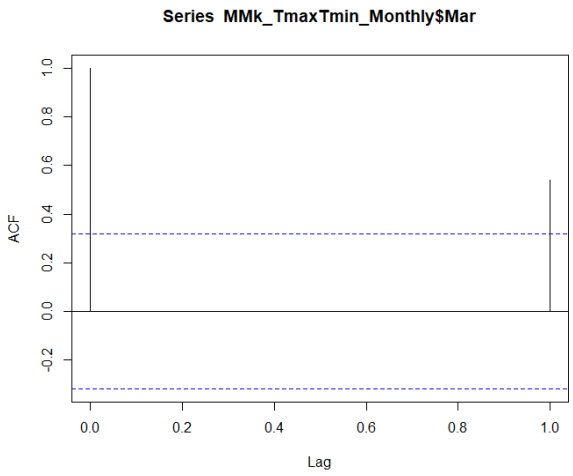
Series MMk_TmaxTmin_Monthly$Mar
ACF
Lag

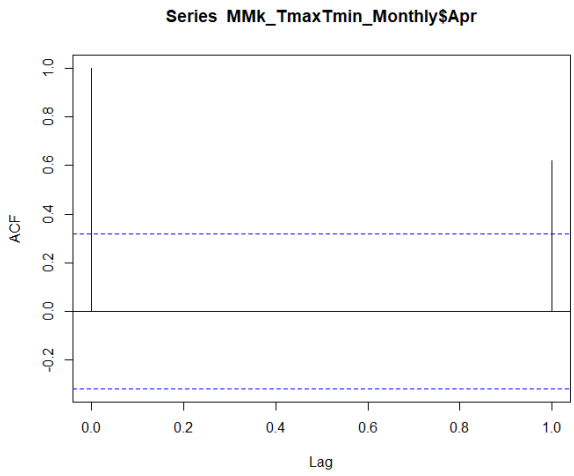
Series MMk_TmaxTmin_Monthly$Apr
ACF
Lag

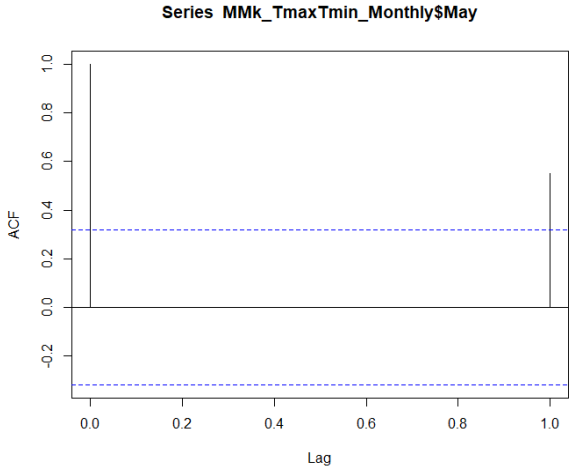
Series MMk_TmaxTmin_Monthly$May
ACF
Lag

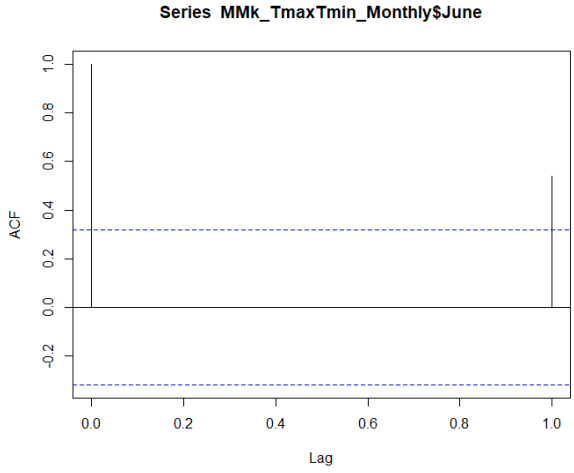
Series MMk_TmaxTmin_Monthly$June
ACF
Lag

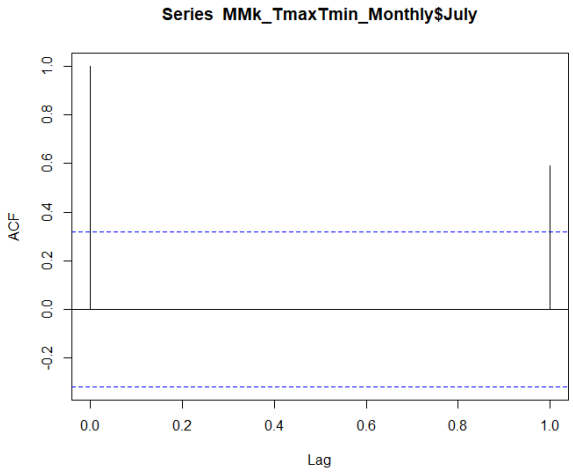
Series MMk_TmaxTmin_Monthly$July
ACF
Lag

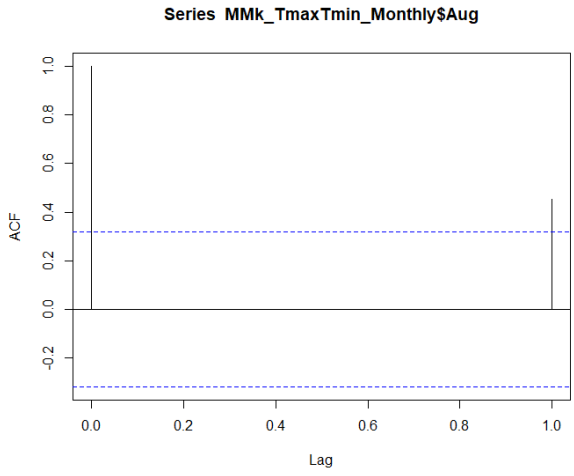
Series MMk_TmaxTmin_Monthly$Aug
ACF
Lag

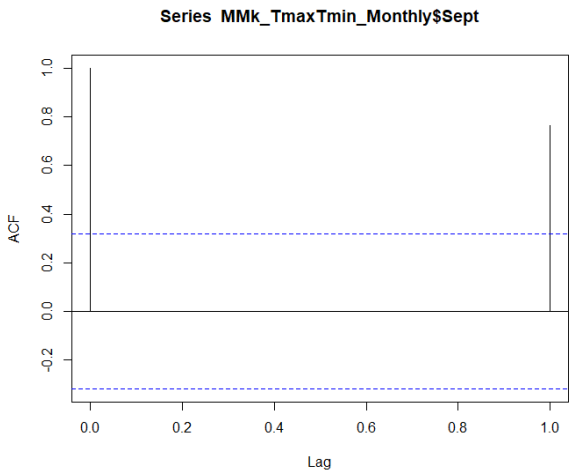

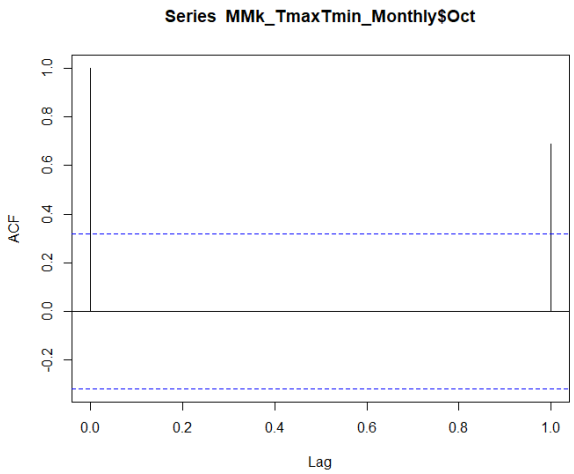

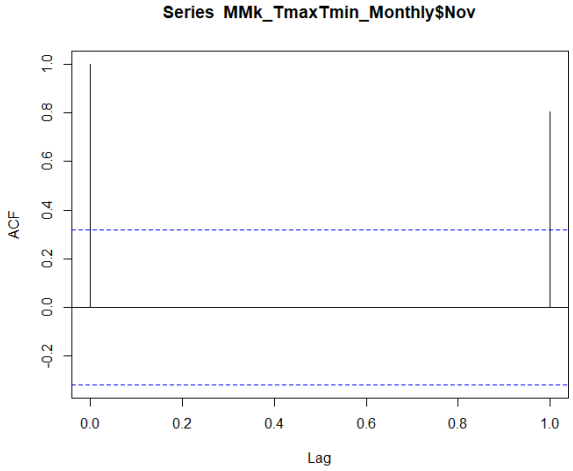

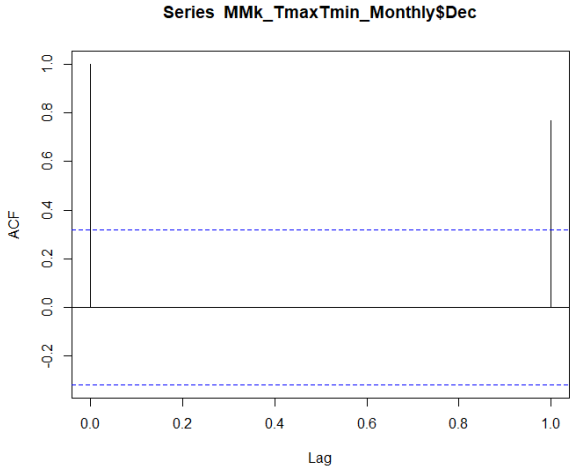

Autocorrelation result Tmax	Lag max 1
January	0.7401821
February	0.7630121
March	0.5393618
April	0.6190608
May	0.5496412

June	0.5410589
July	0.5887482
August	0.4527299
September	0.7654036
October	0.6894417
November	0.8040311
December	0.7685531

Monthly autocorrelation result for Tmin

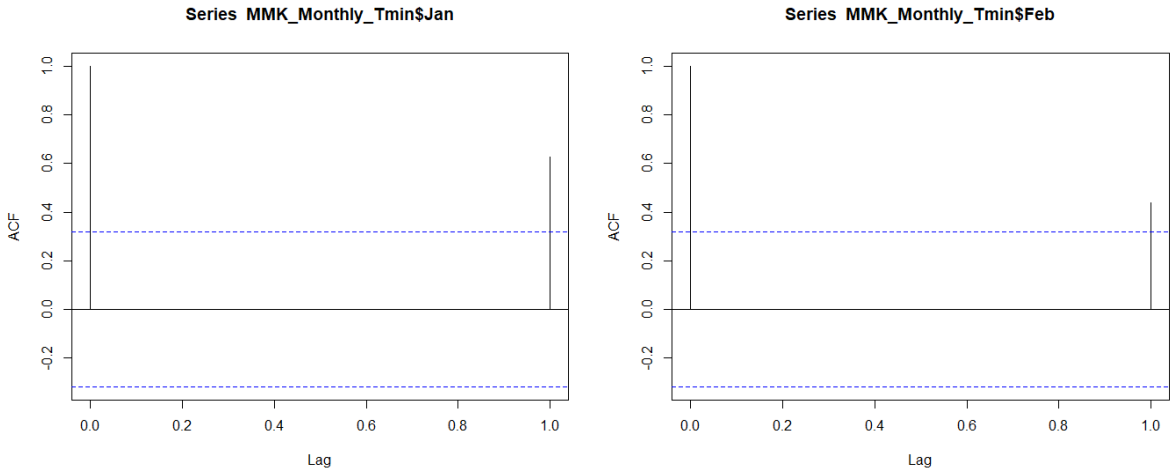

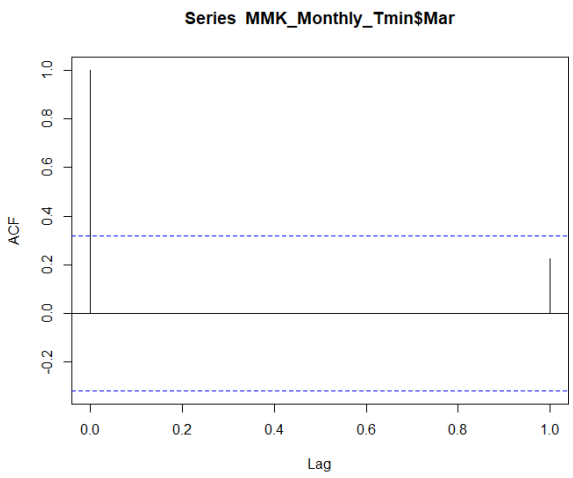
Series MMK_Monthly_Tmin$Mar
ACF
Lag

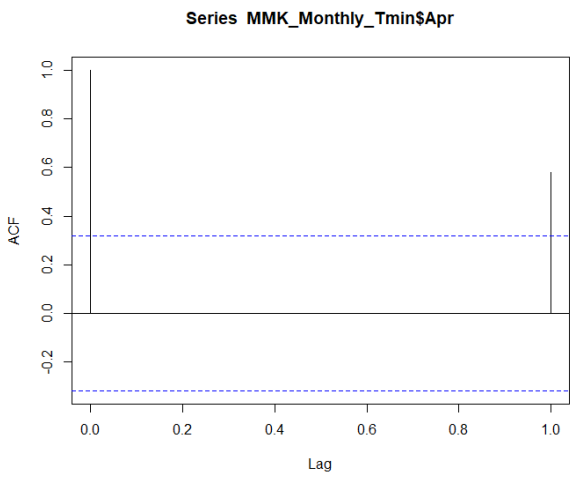
Series MMK_Monthly_Tmin$Apr
ACF
Lag

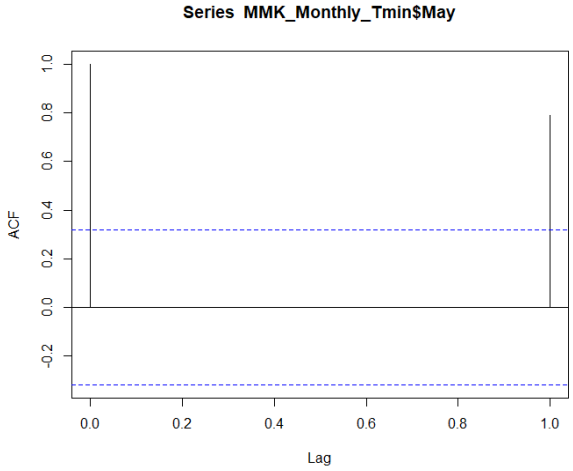
Series MMK_Monthly_Tmin$May
ACF
Lag

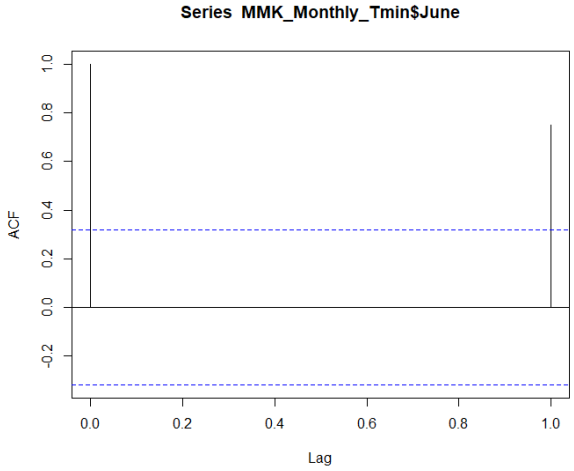
Series MMK_Monthly_Tmin$June
ACF
Lag

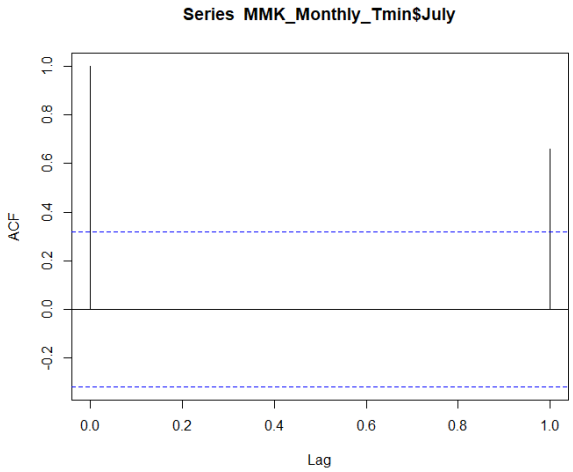
Series MMK_Monthly_Tmin$July
ACF
Lag

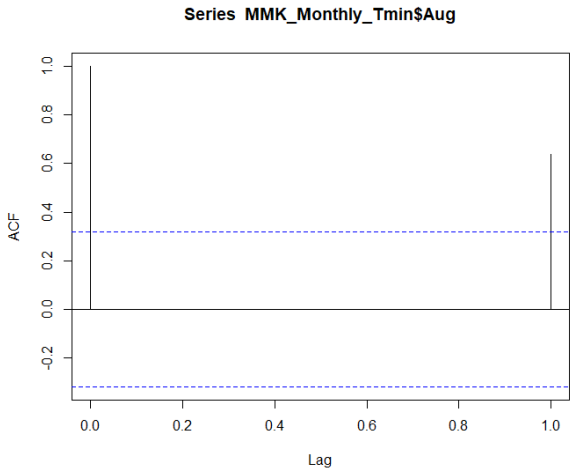
Series MMK_Monthly_Tmin$Aug
ACF
Lag

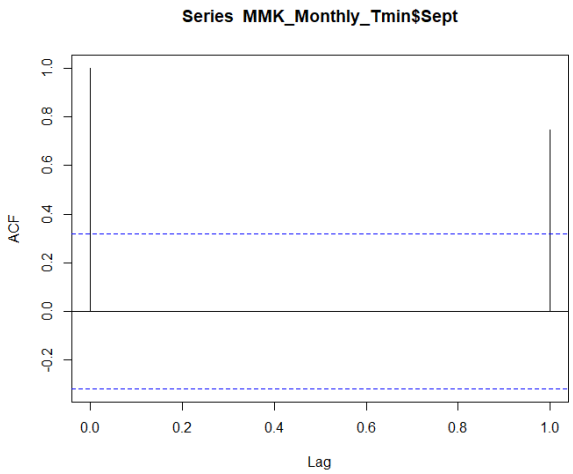
Series MMK_Monthly_Tmin$Sept
ACF
Lag
1.0
0.8
0.6
0.4
0.2
0.0
-0.2
0.0
0.2
0.4
0.6
0.8
1.0

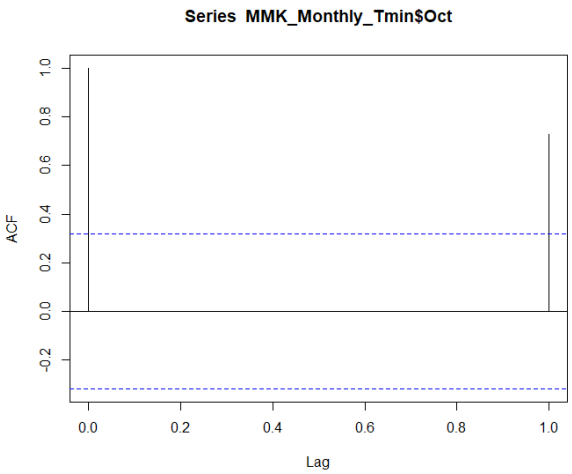
Series MMK_Monthly_Tmin$Oct
ACF
Lag
1.0
0.8
0.6
0.4
0.2
0.0
-0.2
0.0
0.2
0.4
0.6
0.8
1.0

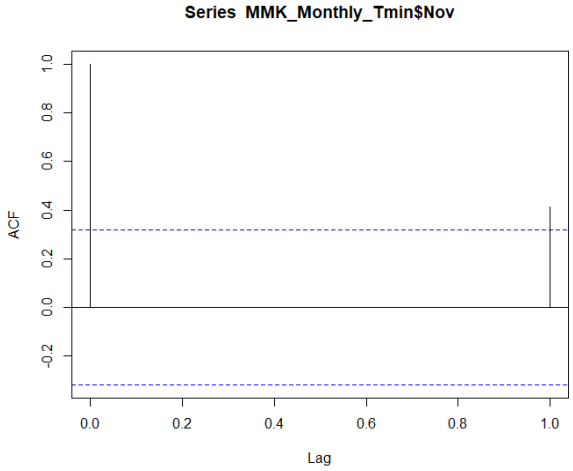
Series MMK_Monthly_Tmin$Nov
ACF
Lag
1.0
0.8
0.6
0.4
0.2
0.0
-0.2
0.0
0.2
0.4
0.6
0.8
1.0

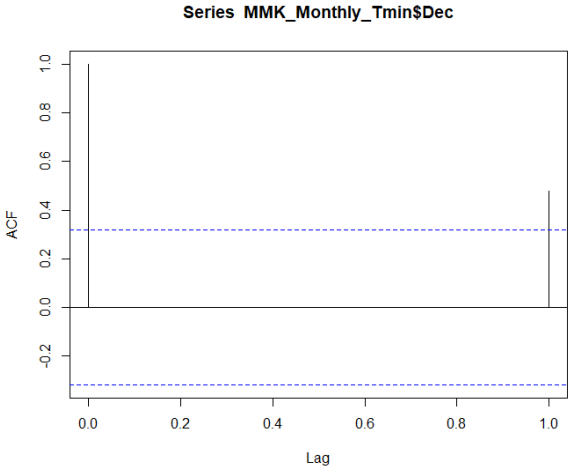
Series MMK_Monthly_Tmin$Dec
ACF
Lag
1.0
0.8
0.6
0.4
0.2
0.0
-0.2
0.0
0.2
0.4
0.6
0.8
1.0

Autocorrelation result Tmin	Lag max 1
January	0.6258401
February	0.4366391
March	0.2255791
April	0.5790147
May	0.7903521
June	0.7493728
July	0.6597823
August	0.6361264
September	0.7469719
October	0.7264999
November	0.4132188
December	0.4776027